GLASS SAND CONCRETE AND “SANDLESS CONCRETE”

DU HONGJIAN

NATIONAL UNIVERSITY OF SINGAPORE

2011

GLASS SAND CONCRETE AND “SANDLESS CONCRETE”

DU HONGJIAN

(B.Eng.), SJTU

A THESIS SUBMITTED

FOR THE DEGREE OF DOCTOR OF PHILOSOPHY

DEPARTMENT OF CIVIL AND ENVIRONMENTAL ENGINEERING

National University of Singapore

2011

Acknowledgement

To my supervisor Professor Tan Kiang Hwee, I express my deepest gratitude for his continuous guidance, suggestions and discussions all along my graduate study. Without his help, I would have been lost in the sea of endless experiments and analyses of data.

I gratefully acknowledge that this work was made possible by the full support from Structural and Concrete Laboratory at National University of Singapore and all the technicians.

Great appreciation goes to my thesis committee members (Professor Zhang Min-Hong and Dr. Tam Chat Tim) for their constructive advices along my research.

I am also grateful to all of my teachers and colleagues at National University of Singapore and Shanghai Jiao Tong University. Here, I must thank Dr. Zhang Zhen and Dr. Ye Feijian, from whom I have learnt a lot, not only in research.

The scholarship provided by National University of Singapore is sincerely acknowledged.

Finally, this work is dedicated to my family.

Contents

Acknowledgement ..... **I**

Summary ..... **V**

List of Tables ..... **VII**

List of Figures ..... **IX**

List of Notations ..... **XIII**

Chapter 1. Introduction **1**

1.1 Sustainable Concrete 3

1.2 Alternative Materials for Natural Sand 4

1.2.1 Manufactured Sand 4

1.2.2 Recycled Concrete Sand 5

1.2.3 By-Product Sand 5

1.2.4 Recycled Solid Waste Sand 6

1.3 Research Objectives and Scope of Work 6

1.3.1 Cementitious Composites Containing Waste Glass Sand 6

1.3.2 Alkali-Silica Reaction of Glass Sand 7

1.3.3 Viability of "Sandless Concrete" 7

1.4 Thesis Structure 8

Chapter 2. Literature Review **9**

2.1 General 9

2.2 Glass Concrete 9

2.2.1 Crushed Glass Particles 10

2.2.2 Fresh Properties 10

2.2.3 Mechanical Properties 13

2.2.4 Alkali-Silica Reaction 18

2.2.5 Other Durability Properties 37

2.3 Role of Sand in Concrete 40

2.3.1 Sand in Plastic Concrete 40
2.3.2 Sand in Hardened Concrete: Mechanical Properties 41
2.3.3 Sand in Hardened Concrete: Durability Properties 43
2.4 Concrete without Sand (No-Fines Concrete) 43
2.4.1 Mix Proportion 44
2.4.2 Fresh Properties 46
2.4.3 Mechanical Properties 46
2.4.4 Durability 48
2.5 Summary 48

Chapter 3. Glass Sand Cementitious Composites 59
3.1 General 59
3.2 Processing of Recycled Glass and Properties 59
3.2.1 Collection and Crushing 59
3.3 Recycled Glass in Mortar 61
3.3.1 Test Program 61
3.3.2 Test Results and Discussion 63
3.3.3 Alkali-Silica Reaction in Glass Mortar 69
3.3.4 Summary 79
3.4 Recycled Glass in Concrete 81
3.4.1 Test Program 81
3.4.2 Test Results and Discussion 82
3.4.3 Summary 90
3.5 Comparison of Effect of Glass Sand in Mortar and Concrete 91
3.6 Expanded Study on ASR in Mortars with Glass Sand 92
3.6.1 Comparison of ASR in Green and Brown Glass Mortars 92
3.6.2 Effect of Glass Particle Size on ASR Expansion 94
3.6.3 Optimal Content of ASR Mitigation Methods 96
3.6.4 Summary 102
3.7 Summary 103

Chapter 4. Sandless Concrete 154
4.1 General 154
4.2 Methodology 154
4.3 Approach 1: Extension of No-Fines Concrete 156
4.3.1 Test Program 156
4.3.2 Test Results and Discussion 159
4.3.3 Summary 167
4.4 Approach 2: Aggregates Packing and Excess Paste Theory 169
4.4.1 Test Program 169
4.4.2 Test Results and Discussion 171
4.4.3 Summary 180
4.5 Comparison of Mix Design Approaches 181
4.6 Summary 182

Chapter 5. Conclusions and Recommendations 198
5.1 Review of Work 198
5.2 Summary of Main Findings 199
5.3 Limitations of Study and Suggestions for Future Research 202

References…. 206

Summary

Concrete is one of the most widely used construction materials, with annual global consumption exceeding one cubic meter per capita. Recently, there has been an increasing motivation in the study of sustainable concrete, as a result of awareness of environmental degradation, resource depletion and global warming.

This research work examines two types of sustainable concrete, that is, glass sand concrete and "sandless concrete", aimed at increasing concrete sustainability with respect to the use of fine aggregates. In glass sand concrete, the natural sand is replaced by recycled waste glass sand. Major properties were investigated for cement-based mortar and concrete containing glass sand. All the mortar and concrete properties were found to be not harmfully affected, even at 100 % sand replacement. Instead, finer glass particles could enhance the concrete properties, such as strength and impermeability, due to pozzolanic reaction. Emphasis is on alkali-silica reaction (ASR) in glass sand mortar and concrete. The influence of glass color, content and particle size on ASR was thoroughly examined. It was found that glass sand with a size between 1.18 and 2.36 mm, regardless of color, would exhibit the highest ASR expansion. Different ASR mitigation methods, including cement replacement by supplementary cementitious materials (SCM), and addition of fiber reinforcement and lithium compounds, have also been examined. It is recommended that the combined use of fly ash or slag would significantly restrain ASR expansion.

In “sandless concrete”, the sand is totally eliminated and replaced by the other ingredients, that is, coarse aggregates, cement and water. Fly ash, up to 50% replacement, is used as cement alternative to avoid the high cement content in “sandless concrete”. Mix design is achieved by two different approaches: (a) based on mix design of no-fines concrete; and (b) based on coarse aggregate packing and excess paste theory. Diverse properties, in both plastic and hardened states, were studied. From the results, “sandless concrete” was found to show comparable characteristics as normal concrete, while its workability could be further improved. In addition, the durability of “sandless concrete” with fly ash is substantially improved because of the densified micro-structure. Also, the mix design for “sandless concrete” could be further optimized.

Overall, this research work provides guidance for the practical application of glass sand concrete and “sandless concrete”, from the perspective of mix design, mechanical properties and durability. Both glass sand concrete and “sandless concrete” could be new options for construction industry, in view of sustainability issues.

Keywords: Alkali-silica reaction, Concrete, Durability, Mortar, Mechanical properties, Microstructure, Recycling, Sand, Sustainability, Waste glass.

List of Tables

Table 2-1: Chemical compositions of commercial glasses [McLellan and Shand, 1984]..... 49

Table 2-2: Summary of effect of glass sand on fresh density of concrete..... 49

Table 2-3: Summary of test methods for ASR expansion for aggregates [Zhu et al., 2009]..... 50

Table 2-4: Influence of sand on plastic properties of concrete [Alexander and Mindess, 2005] . 51

Table 3-1: Chemical compositions of green, brown and clear glass, and natural sand 104

Table 3-2: Chemical compositions of cement, fly ash, GGBS and silica fume..... 104

Table 3-3: Physical properties of cement, fly ash, GGBS and silica fume..... 104

Table 3-4: Test properties, specimen numbers, test age and dimensions, and standard methods for glass mortar and concrete..... 105

Table 3-5: Grading requirement of sand by ASTM C 1260 105

Table 3-6: Mix proportions of glass mortar for ASR study..... 106

Table 3-7: ASR expansion (%) of mortar with green glass sand..... 107

Table 3-8: ASR expansion (%) of mortar with brown glass sand 108

Table 3-9: ASR expansion (%) of mortar with clear glass sand..... 109

Table 3-10: Mix proportions of glass concrete..... 110

Table 3-11: Mix proportions of ASTM standard mortar and screened mortar from concrete (by mass)..... 110

Table 3-12: Amounts of each ASR mitigation method 111

Table 3-13: Effect of different methods on expansion of mortar with 100% green 1.18-mm glass sand..... 111

Table 3-14: Mortar compressive strength and relative strength of each method at 28 days 112

Table 3-15: Effect of 30% fly ash or 60% GGBS on ASR expansion of C45 green glass sand mortar 113

Table 4-1: Mix proportions for “sandless concrete” by Approach 1 183

Table 4-2: Properties of “sandless concrete” by Approach 1 183

Table 4-3: Mix proportions for “sandless concrete” by Approach 2 183

Table 5-1: Overview of the main contributions from the study..... 205

List of Figures

Figure 2-1: Mechanism of ASR [Thomas et al., 2007a]. 52

Figure 2-2: Loss in engineering properties of concrete due to ASR [Swamy and Al-Asali, 1989]. 53

Figure 2-3: Double layer theory [Prezzi et al., 1997]. 54

Figure 2-4: Literature review of effect of glass sand content on ASR expansion. 54

Figure 2-5: Illustration of pessimum effect of glass particle size by Jin et al. [2000]. 55

Figure 2-6: Leaching and dissolution of a particle of glass according to Dhir et al. [2009]. 55

Figure 2-7: SEM image of mortar with brown glass sand [Rajabipour et al., 2010]. 56

Figure 2-8: Literature review of influence of glass sand size on ASR expansion. 56

Figure 2-9: Relationship between paste and void content for No. 8 aggregate size designations [ACI 522R]. 57

Figure 2-10: Illustration of excess paste theory [Kennedy, 1940]. 57

Figure 2-11: Void ratio as functions of the proportion of coarse aggregate [Powers, 1968]. 58

Figure 2-12: Relationship between air content and compressive strength for no-fines concrete [ACI 522R]. 58

Figure 3-1: Processing of recycled waste glass sand. 114

Figure 3-2: Grading curve of crushed glass sand and natural aggregates. 115

Figure 3-3: Test program for recycled glass sand in (a) mortar, and (b) concrete. 115

Figure 3-4: Fresh properties of glass mortar: (a) density, (b) air content, and (c) flowability. .. 116

Figure 3-5: Compressive strength of glass mortar. 117

Figure 3-6: Flexural strength of glass mortar. 118

Figure 3-7: Splitting tensile strength of glass mortar. 119

Figure 3-8: Static and dynamic modulus of elasticity of glass mortar. 119

Figure 3-9: Drying shrinkage of mixed color glass mortar..... 120

Figure 3-10: RCPT results of glass mortar at 28-day. 120

Figure 3-11: Sulfate attack test results of glass mortar: (a) weight loss, (b) compressive strength, and (c) flexural strength. 121

Figure 3-12: Picture of mortar specimens with (a) green, (b) brown, (c) clear, and (d) mixed color glass sand after sulfate attack tests. 122

Figure 3-13: ASR expansion of mortar with different colored glass sands. 123

Figure 3-14: Effect of glass sand content on ASR expansion at 14 days. 125

Figure 3-15: Effect of glass particle size on ASR expansion (glass content of 25%). 126

Figure 3-16: Comparison of effect of glass particle size on ASR expansion. 127

Figure 3-17: SEM micrographs of glass mortar. 128

Figure 3-18: Comparison of different mitigation methods on ASR expansion of mortar with (a) green, (b) brown, and (c) clear glass sand. 129

Figure 3-19: Fresh density of glass concrete. 130

Figure 3-20: Air content of fresh glass concrete..... 130

Figure 3-21: Slump of glass concrete. 131

Figure 3-22: Compressive strength of glass concrete. 131

Figure 3-23: Compressive strength of glass concrete with 30% fly ash or 60% GGBS. 132

Figure 3-24: Flexural strength of glass concrete..... 132

Figure 3-25: Splitting tensile strength of glass concrete. 133

Figure 3-26: Static and dynamic modulus of elasticity of glass concrete..... 133

Figure 3-27: Drying shrinkage of glass concrete. 134

Figure 3-28: RCPT results of glass concrete. 135

Figure 3-29: ASR expansion of concrete with brown glass sand. 136

Figure 3-30: SEM micrographs of brown C45-100 glass mortar after 49 days of ASR testing. 137

Figure 3-31: Effect of *w/c* ratio on ASR expansion..... 138

Figure 3-32: ASR expansions of brown glass concrete C45 with (a) 30% fly ash, and (b) 60% GGBS. 139

Figure 3-33: ASR expansion comparison. 140

Figure 3-34: Four level microstructure of cement-based composite materials [Constantinides and Ulm, 2004; Richardson, 2004]. 141

Figure 3-35: (a) SEM micrograph of higher Portlandite (CH) concentration in the ITZ (wall effect) of mortar [Heukamp et al., 2003]; (b) Diagrammatic representation of the ITZ and bulk cement paste in concrete [Mehta and Monteiro, 2006]. 142

Figure 3-36: ASR expansion of mortar containing brown and green glass sand. 143

Figure 3-37: Pictures of (a) C60 mortars with different green glass sand contents, (b) mortars with 100% 2.36- and 1.18-mm green glass sand, and mortar with 1.18-mm green glass sand mitigated by (c) fly ash, (d) GGBS, (e) silica fume, (f) steel fiber, (g) LiCl, and (h) Li_2CO_3. 145

Figure 3-38: Effect *w/c* ratio on glass sand mortar ASR expansion. 146

Figure 3-39: Effect of glass particle size on ASR expansion. 147

Figure 3-40: SEM pictures of mortar with 1.18-mm green glass sand. 149

Figure3-41: Mechanism for ASR of glass particle. 150

Figure 3-42: ASR expansion of mortar with different mitigation methods. 151

Figure 3-43: ASR expansions of green glass mortar C45 with (a) 30% fly ash and (b) 60% GGBS. 153

Figure 4-1: Aggregate grading curves. 184

Figure 4-2: Photographs of “sandless concrete” cube specimens: 184

Figure 4-3: Compressive strength with different grading of coarse aggregates. 185

Figure 4-4: Compressive strength with different aggregate-cement (*A/C*) ratios. 185

Figure 4-5: Strength development of “sandless concrete”: (a) compressive strength, (b) splitting tensile strength, (c) flexural strength, (d) relation between cylinder and cube strength. 186

Figure 4-6: Relations between compressive strength and (a) splitting tensile strength, (b) flexural strength, and (c) elastic modulus. 187

Figure 4-7: Drying shrinkage of "sandless concrete". 188

Figure 4-8: RCPT results at 28 days. 188

Figure 4-9: Illustration of void content of aggregate particles [Kosmatka et al., 1995]. 189

Figure 4-10: (a) Void content, and (b) grading curve of combined aggregates. 189

Figure 4-11: Steps for mix design Approach 2. 190

Figure 4-12: Test program of the second mix design method. 190

Figure 4-13: Slump of "sandless concrete". 190

Figure 4-14: Compressive strength of "sandless concrete". 191

Figure 4-15: (a) Splitting tensile strength, (b) flexural strength and (c) elastic modulus of "sandless concrete". 192

Figure 4-16: Relation between compressive strength and (a) flexural and splitting tensile strength, and (b) elastic modulus. 193

Figure 4-17: Drying shrinkage of "sandless concrete". 194

Figure 4-18: (a) RCPT result, (b) D_{nssm} of "sandless concrete", and (c) Relation between RCPT and D_{nssm} 195

Figure 4-19: (a) Weight, (b) Dynamic modulus, and (c) Compressive strength loss of "sandless concrete" after sulfate attack. 196

Figure 4-20: Pictures of "sandless concrete" after sulfate attacks with *w/c* ratio of (a) 0.45, and (b) 0.50 197

List of Notations

A/C	aggregate-cement ratio;
A	specific surface area of aggregates, cm^2/cm^3;
AMBT	accelerated mortar-bar test;
ASR	alkali-silica reaction;
ASTM	American Society for Testing and Materials;
BS	British Standard;
C	void ratio of aggregate;
CA	coarse aggregates;
CH	calcium hydroxide, $Ca(OH)_2$;
CSH	calcium silicate hydrate;
D_{nssm}	non-steady-state migration coefficient, $\times 10^{-12}$ m^2/s;
E_c	elastic modulus of concrete, GPa;
EDS	energy dispersive X-ray spectroscopy;
f_c'	cylinder compressive strength of concrete, MPa;
f_{cu}	cube compressive strength of concrete, MPa;
f_r	flexural strength of concrete, MPa;
f_{st}	splitting tensile strength of concrete, MPa;
GGBS	ground granulated blast-furnace slag;
ITZ	interfacial transition zone;
K	consistency factor;

L	thickness of the specimen, mm;
NC	normal concrete;
OD	oven dry;
OPC	ordinary portland cement;
p	paste volume per unit volume of concrete, ;
Q	total charge passed, Coulombs;
RCPT	rapid chloride permeability test;
RH	relative humidity, %;
s/c	sand-cement;
SCM	supplementary cementitious materials;
SEM	scanning electron microscope;
SLC	“sandless concrete”;
SSD	saturated surfaced dry;
t	test duration, h;
T	average value of the initial and final temperatures in the anolyte solution, ˚C;
U	absolute value of the applied voltage, V;
V_a	volume of aggregates per unit volume of concrete;
w/c	water-cement ratio;
x_d	average value of the penetration depth, mm;
XRF	X-ray fluorescence.

Chapter 1. Introduction

Concrete is the most widely used building material in the world, as well as the largest user of natural resources with annual consumption of 12.6 billion tons [Mehta, 2002]. Fundamentally comprised of coarse and fine aggregates, cement and water, concrete in some cases also contains additional chemical or mineral admixtures for specific purposes. Most of the ingredients, produced from virgin resources, are non-renewable, or strictly speaking non-sustainable. Recently, there has been an increasing awareness of environmental protection, resource and energy conservation, and sustainable development globally. Many research works have been initiated and developed to make concrete more sustainable, mainly in reducing its negative impacts on environment and reserve natural raw materials. Higher degree of sustainability of concrete can be achieved by replacing its virgin ingredients, including cement and aggregates, by other materials, such as reclaimed materials from old structures, by-products from industrial process and recycled solid wastes. Apart from saving raw materials and protecting environment, additional benefits are usually accompanied with the production of sustainable concrete, such as reduced landfills and dumping volumes, decreased amount of energy and CO_2 emission, as well as enhanced life cycle performance and lowered cost in maintenance during the whole life of structures.

Quantities of studies have proved the successful substitution of cement in concrete by some pozzolanic by-product materials, like pulverized fly ash and ground granulated blast-furnace slag (GGBS) [Malhotra, 1999; Mehta, 2001]. Besides the reduction in cement content and cost, workability, long term mechanical properties and durability can also be improved for such concrete, resulting in higher sustainability. Also, recycled coarse aggregates and manufactured

coarse aggregates have been widely accepted in construction as alternative virgin coarse aggregates. However, the research and development of fine aggregate (sand) substitution is relatively slow.

The definition of fine aggregate in ASTM C 125 is the aggregate passing the 9.5-mm sieve and almost entirely passing the 4.75-mm sieve and predominantly retained on the 75-μm sieve, either in a natural condition or after processing. Sand refers to fine aggregate resulting from natural disintegration and abrasion of rock or processing of completely friable sandstone, while manufactured sand means fine aggregate produced by crushing rock, gravel, iron blast furnace slag, or hydraulic concrete [ASTM C 125].

Sand consumes around 20~27% of concrete by volume, thus playing an important role in fresh and hardened properties of concrete [Neville, 1995]. The reserve of natural sand is depleting and the conventional sand mining, quarrying and river and ocean dredging is being criticized for their negative influences on environment, such as drinking water degradation, land and coast corrosion, flood and species depletion. Therefore, the necessity to seek sound replacements of natural sand for concrete is compelling to satisfy the sustainable development in concrete. Present alternative fine aggregates includes manufactured sand, recycled concrete sand, by-products sand, and recycled waste sand. However, no perfect substitution has been found. Nevertheless, each sand alternative would also bring in problems to compromise the performance of concrete, limiting the popular application. Under the circumstance of shortage of natural sand, further work should be carried out to study sustainable concrete with certain possible sand substitutions. Moreover, concrete containing no sand has never been studied for structural application. The significance of such concrete will become more prominent in sustainable development of concrete.

Section 1.1 briefly introduces the development of sustainable concrete, followed by a brief introduction of current sand alternatives in Section 1.2. Research objectives, scope and significance are presented in Section 1.3. The most relevant literature will be reviewed in Chapter 2, mainly on glass sand concrete properties, the role of sand in concrete and the application of concrete with no sand.

1.1 Sustainable Concrete

According to the definition by United Nations, sustainable development is development that meets the needs of the present without compromising the ability of future generation to meet their own needs [United Nations, 1987]. As the most widely used construction material after water around the world, concrete plays a leading role in the development of sustainability in construction industry. As recommended by BACSD [2005], sustainable concrete includes the following elements:

- Concrete must be specified, designed, and proportioned for its intended application with mixtures developed for durability (where appropriate), resource conservation, and minimal environmental impact;
- Production of concrete ingredients, production of concrete, and construction practices must be environmentally responsible;
- Concrete, in all applications, must be sustainable and must be viewed as such by owners and the public at large, and
- The concrete industry must remain competitive.

At present, the sustainable strategy varies in different countries, academics and enterprises. Many activities have been involved in improving the sustainability of concrete including

- Reduction in the amount of polluting and greenhouse gases emitted during the creation of concrete, particular the manufacture of cement;
- More efficient use of resources in concrete production, including re-used materials and by-products from other industrial processes;
- Better re-use of waste and other secondary materials such as water, aggregate, fuel or other cementitious materials;
- Lower reliance on quarrying materials or reduce sending construction and demolition waste to landfill by maximizing the use of recycled material where practical;
- Development of low-energy, long-lasting yet flexible buildings and structures;
- Environmental restoration after industrial activity has ceased.

1.2 Alternative Materials for Natural Sand

1.2.1 Manufactured Sand

Manufactured sand, in contrast with the natural sand, comes from the mechanical crushing of virgin rock [Villalobos et al., 2005]. Manufactured sand has been widely used so far [Ahn and Fowler, 2001; CCAA T60, 2008; Wigum and Danielsen, 2009], due to the shortage of natural sand. However, instead of total replacement, manufactured sand must be blended with natural sand due to its angular particle shape, open-void surface texture, high water absorption and high

content of ultra fines (< 75μm). The characteristics of manufactured sand would harmfully affect the fresh, mechanical properties and durability of concrete.

1.2.2 Recycled Concrete Sand

Recycled concrete fine aggregates refer to small particles demolished from old concrete structure or pavement, which generally contain a considerable amount of old cement paste and mortar. This tends to increase the drying shrinkage and creep properties of new concrete, as well as leading to problems with concrete mix stability and strength [Alexander and Mindess, 2005]. Therefore, a RILEM report [Hansen, 1994] recommends that any materials smaller than 2 mm should be discarded. BS 8500-2 [2006] allows the use of clean recycled concrete sand in concrete provided that significant quantities of deleterious materials are not present and the use has been agreed.

1.2.3 By-Product Sand

By-products such as bottom fly ash and un-ground slag have been investigated as sand in concrete, instead of further finely grinding to replace cement. The direct use of as-received by-products would reduce the cost and increase the used volume. However, it was found that the fly ash or slag particles would cause porous structure within concrete and subsequent reduced performances [Yuksel et al., 2006; Yuksel and Genc, 2007]. In some cases, silica fume may be used as sand replacement to improve the durability of concrete [Ghafoori and Diawara, 2007]. However, this kind of sand substitution is only limited in certain conditions and low replacement level, not suitable for high or total replacement of sand.

1.2.4 Recycled Solid Waste Sand

Due to the increasing environmental degradation and waste volumes, some solid wastes have been studied as substitution for natural sand in concrete, such as glass, plastics, rubber tires, and so on [Naik, 2002; Meyer, 2009]. Benefits on both environmental and economical aspects could be obviously obtained from the utilization of solid waste in construction, making this kind of sand alternative promising. However, the waste materials would possess negative influences on the concrete properties, limiting their wide application. Glass sand might cause deleterious ASR expansion in concrete, plastics sand could lead to a very weak ITZ with cement paste, and rubber tires would result in large reduction in concrete mechanical properties because of its low elastic modulus.

1.3 Research Objectives and Scope of Work

As mentioned earlier, concrete sustainability has been rarely improved from the perspective of natural sand alternative. It is worthwhile to study the utilization of waste glass in concrete as sand, particularly at high percentage. The alkali reactivity of glass is still controversial based on the literature. No research has been carried out to investigate the viability of concrete without containing sand in structural application. Therefore, this study was conducted with the following objectives, scope and significance:

1.3.1 Cementitious Composites Containing Waste Glass Sand

The first part of this thesis will present an exploratory study of recycled glass sand in cementitious composites, including mortar and concrete, to study the influences of glass sand on properties of mortar and concrete. The study would provide the guidelines for the reuse of glass

sand in construction, instead of landfills, leading to green and sustainable concrete. The most common properties of mortar and concrete in both plastic and hardened states are examined. Besides ASR, other durability properties, including resistance to chloride ion penetration and sulfate attack, are also tested, which are essential for concrete performance at long term under severe environment.

1.3.2 Alkali-Silica Reaction of Glass Sand

The thesis next will discuss the ASR of mortar and concrete containing glass sand, as well as mitigating methods. The study into ASR can shed light on the practical utilization of waste glass, since it is deemed as the most detrimental mechanism for mortar and concrete. The effects of glass color, content and particle size on ASR are investigated according to accelerated mortar-bar test. Thereafter, various ASR suppressing approaches are examined, including mineral and chemical admixtures as well as fiber reinforcement.

1.3.3 Viability of "Sandless Concrete"

The thesis will finally present the study of viability of concrete without the use of sand, namely "sandless concrete", in structural application. Two different mix design methods are proposed for "sandless concrete". The fresh, mechanical and durability properties are investigated for "sandless concrete" from both design methods. The study thus provides valuable information for the development of sustainable concrete with respect to sand conservation. Nevertheless, only the major properties of "sandless concrete" are studied while some minor characteristics remain to be explored in future research.

1.4 Thesis Structure

Chapter 1 briefly introduces the background of concrete, the efforts taken into sustainable concrete, and the current alternative materials for natural sand in concrete, as well as the disadvantages of incorporating such substitutions. Research objectives, scopes and significance are highlighted.

Chapter 2 reviews the most relevant literature, including recycled waste glass in concrete and the resulted alkali-silica reaction, the significance and role of sand in concrete and the properties of no-fines concrete. Last, the limitations and gaps of previous studies are summarized.

Chapter 3 presents the research into glass sand mortar and concrete, emphasizing on mechanical properties of glass concrete, alkali-silica reaction as well as its mitigation methods and other durability properties.

Chapter 4 introduces the concept of "sandless concrete", describes the mix design approaches, and presents the diverse properties to evaluate the viability of concrete with no sand in structural application.

Chapter 5 summaries the work and draws conclusions based on the experimental tests, and finally offers recommendations for future research.

Chapter 2. Literature Review

2.1 General

This chapter reviews the pertinent literature on the previous studies of glass sand cementitious composites such as mortar and concrete, in fresh and hardened states, with emphasis on alkali-silica reaction (ASR) and its mitigation methods. To better understand the possible influences of eliminating sand from concrete mixtures, the role of sand in concrete will be introduced. Finally, a special type of concrete, no-fines concrete (or pervious concrete) which is mainly used for non-structural applications will be reviewed.

2.2 Glass Concrete

United Nations estimates the volume of yearly disposed solid waste to be 200 million tons, 7% of which is made up of glass the world over [Topcu and Canbaz, 2004]. Glass is a readily recyclable material, in that it can be returned to the glassmaking furnace with minimal reprocessing. However, in many cases quantities of recovered glass can arise which are not recyclable [Dhir et al., 2009]. Only a small fraction of bottles and container glass can be reused directly and there is an upper limit for the recycling of glass cullet from postconsumer waste, due to the technical limitations in how much colored glass cullet can be used [Christensen and Damaggard, 2010; Siddique, 2008]. Alternative uses for the waste glass need to be found. The initial attempt to incorporate waste glass in concrete as aggregates can be traced back to 1960s. Schmidt and Saia [1963], Johnston [1974] and Figg [1981] and studied the use of waste glass as

aggregates and its effect on mechanical properties and ASR. It was found that the concrete with glass aggregates cracked due to ASR. In the past ten years, the use of glass as fine aggregates has again come under investigation due to high disposal costs for waste glasses and environmental regulations [Shi and Zheng, 2007]. Meyer and Baxter [1997, 1998] conducted very extensive laboratory studies on the use of crushed glasses as fine aggregates, emphasizing on ASR and suppressing methods, shedding light on the practical application of recycled waste glass as sand in concrete.

2.2.1 Crushed Glass Particles

Crushed glass particles are usually angular in shape and may contain some elongated and flat particles due to the crushing process, with specific density of 2.53 and negligible water absorption. Internal micro-cracks may exist in the glass particles. The chemical compositions of glass are summarized in the book by McLellan and Shand [1984] and shown in **Table 2.1**. Among those different categories of glasses, soda-lime glasses are the most commonly used and the main interest of research as well.

2.2.2 Fresh Properties

2.2.2.1 Unit Weight

Due to the relatively smaller specific gravity of glass, the fresh density of mortar and concrete would be reduced with natural sand replacement with glass. A number of test results showed this trend [Topcu and Canbaz, 2004; Taha and Nounu, 2008; Ismail and Hashmi, 2009], at various mix proportions of mortar and concrete, as summarized in **Table 2.2**.

2.2.2.2 Air Content

Park et al. [2004] tested concrete containing waste glass sand of diverse colors and the test results showed that air content continuously increased with higher glass sand content, to as high as 41.4% at 70% replacement of natural sand by clear glass sand. They attributed this increase in air content to the irregular shape of glass particles, which resulted in a larger relative surface area that retained more air. Moreover, in their test program, there were more waste glass sands that were larger than 0.6 mm in particle size than natural sand.

Topcu and Canbaz [2004], however, obtained the opposite result that more waste glass sand would unevenly decrease air content, by as much as 27%. The reason was thought to result from the irregular geometry of glass sand, as a result of which water and air voids occurred in particularly lower parts of glass particles. Furthermore, the smooth surface of glass sand also helped decrease porosity between glass sand and cement paste.

2.2.2.3 Slump

Park et al. [2004] studied concrete with waste glass sand and observed a consistent tendency for slump to decrease as the glass sand increased, regardless of the color of glass. At replacement ratio of 70%, concrete showed a decrease of about 38.5-44.3% in slump values. The sharper and more angular grain shapes, as well as more attached cement paste on glass sand, would result in less fluidity.

Taha and Nounu [2008] reported the properties of concrete containing mixed color waste glass sand, at 50% and 100% replacement. The sharp edges and harsh texture of glass sand would lead to reduction in slump, from 120 mm for normal concrete to 95 and 80 mm for concrete with 50% and 100% glass sand, respectively.

Limbachiya [2009] carried out experiments on engineering properties of concrete containing up to 50% of mixed color glass sand. The slump showed a small reduction, 10 mm at 50% of glass sand content, regardless of concrete strength. Concrete mixes with greater than 20% glass sand were found to be somewhat harsher and less cohesive than the corresponding normal concrete, due to inherent smooth surface, sharp edge and harsh texture of waste glass sand.

Inconsistent test result was observed by Terro [2006], who examined the properties of concrete made with glass as fine aggregates at elevated temperature, with natural sand replacement of 0, 10, 25, 50 and 100%. The slump value was 85, 85, 95, 105 and 90 mm for concrete with the above glass sand content. In the test, the slump value seemed to increase with higher percentages of waste glass, attributed to the poorer cohesion between cement paste and glass aggregates which have smooth impermeable surfaces.

2.2.2.4 Setting Time

Terro [2006] conducted tests of concrete with glass as fine aggregates up to 100% replacement of natural aggregates. From the results, both initial and final setting times exhibited an increasing almost-linear relation with more glass sand content. This delay in setting time could be attributed to a number of reasons including the presence of impurities, such as sugar, introduced with waste glass, and the relative increase in water-cement (*w/c*) ratio due to the low absorption of glass aggregates. However, information on the impurities in glass was not reported in his research.

2.2.2.5 Bleeding and Segregation

Taha and Nounu [2008] replaced natural sand with waste glass sand at 0, 50% and 100% in concrete. This is the first study to thoroughly investigate the fresh properties of glass concrete. Based on visual inspection, concrete with glass sand of 50% replacement was homogenous but

less consistent; concrete with 100% of glass sand was harsh, with bleeding and segregation; while the reference concrete without glass sand showed consistency and homogeneity. Severe bleeding and segregation resulted from the inherent smooth surface and very low water absorption of waste glass, both leading to lack in adhesive bond between the components of the concrete mix.

2.2.3 Mechanical Properties

2.2.3.1 Compressive Strength

Park et al. [2004] replaced natural sand with glass sand in concrete at 30, 50 and 70% content. The compressive strength of concrete at 28 days, displayed 99.4, 90.2 and 86.4% of the reference concrete without glass sand. This reduction may be due to the decrease in adhesive strength between the surface of the waste glass sand and the cement paste as well as the increase in fineness modulus of the glass sand and the decrease in compacting factor with increasing glass sand content.

Taha and Nounu [2008] carried out tests on compressive strength of concrete with glass sand at 0, 50% and 100% replacement. There was no clear trend that governed the variation in the compressive strength with the presence of waste glass. They concluded that there should be more than one parameter that could significantly affect the compressive strength of concrete, such as contamination and the organic content in waste glass, the inherent cracks in glass particles due to the crushing process, and bleeding and segregation.

Kou and Poon [2009] investigated the use of waste glass sand in self-compacting concrete, at replacement content of 15%, 30% and 45%. The corresponding reduction in the 28-day strength

was 1.5%, 4.2% and 8.5%, respectively. It may be attributed to the decrease in bond strength between the cement paste and the glass sand, and the increase in fineness modulus of glass sand.

Limbachiya [2009] used waste glass sand to substitute natural sand in concrete up to 50% replacement and reported the compressive strength. Less than 20% glass content had no effect on strength development, but thereafter gradual reduction in strength was apparent with increasing glass content. The possible factors, to explain the strength reduction in concrete with high glass sand proportion, included inherent physical characteristics, a weak bond between aggregate-matrix interface, and inherent cracks in glass particles.

Terro [2006] measured the compressive strength of concrete with glass sand at replacement proportions of 10, 25, 50 and 100%, at temperatures of 20, 60, 150, 300, 500 and 700 ˚C. In general, concrete made with 10% aggregate replacement with waste glass sand possessed a slightly higher compressive strength than normal concrete at temperatures above 150 ºC. However, higher replacement percentage would reduce compressive strength, due to the poorer cohesion between glass sand and cement paste.

Ismail and Hashmi [2009] examined the compressive strength development of concrete with 10, 15 and 20% of glass as fine aggregates. According to the test results, all the waste glass concrete showed compressive strength values that were slightly higher than those of the plain concrete mixes, except for the 14-day results. The low compressive strength of the glass concrete at 14 days could be attributed to the decrease in the adhesive strength between surface of the waste glass aggregates and the cement paste. Pozzolanic reactions appeared to offset this trend at later stage and helped to improve the compressive strength at 28 days.

2.2.3.2 Flexural Strength

Park et al. [2004] tested the flexural strength of concrete, with sand replaced by glass sand in 30, 50 and 70% content. The concrete of 28 days of age containing waste glass sand at 30, 50 and 70% replacement showed a slight decrease in the flexural strength, being 96.8, 88.7 and 81.9% of that of plain concrete. This reducing tendency was repeated in 13-week old concrete, due to the decrease in adhesive strength between the glass sand and cement pate. No obvious difference in the strength depending on color of the waste glass was noticed. The flexural strength was about 1/7 ~ 1/6 of the compressive strength.

Limbachiya [2009] reported the effect of glass sand, up to 50%, on flexural strength of concrete. Negligible difference in flexural strength was noticed in concrete mixes with up to 20% glass sand. Thereafter, reduction occurred with increase in glass sand content. In addition, the effect of glass sand on flexural strength variation tended to become less noticeable with increasing concrete strength.

Topcu and Canbaz [2004] determined the influence of using glass as coarse aggregate in concrete on the flexural strength. Flexural strength was 4.5, 5.27, 3.97 and 3 MPa for concrete containing 0, 15, 30, 45 and 60% of waste glass, respectively. Flexural strength decreased inconsistently with higher proportion of glass content.

Taha and Nounu [2008] studied the flexural strength of concrete with mixed color waste glass as sand replacement at 0, 50 and 100%. The flexural strength was slightly reduced with the presence of glass sand, due to the following hypothesis: (1) lack in compaction due to the inconsistency of concrete; (2) poor concrete quality because of severe bleeding and segregation; (3) inherent cracks in glass particles leading to more fragility; (4) contamination, foreign

materials and organic content which could degrade with time and create voids in concrete microstructure; and (5) inherent smooth and plane surface of large glass particles, weakening the bond between the cement paste and glass sand.

From the above review, the flexural strength seems to be generally reduced by the addition of waste glass sand due to the weakened bond strength between glass particles and cement paste.

2.2.3.3 Splitting Tensile Strength

Park et al. [2004] investigated the possibilities of waste glasses as fine aggregates for concrete with the replacement of 30, 50 and 70%. The splitting tensile strength of glass concrete showed 96.6, 90.8 and 85.0% of that of normal concrete, at 28 days. The reason was due to the decrease in adhesive strength between glass sand surface and cement paste, as well as the increased fineness modulus of glass sand used and the decrease in the compacting factor due to the increase in the glass sand content.

Topcu and Canbaz [2004] examined the change in splitting tensile strength of concrete with glass particles replacing natural coarse aggregates, at the content of 15, 30, 45 and 60%. The addition of waste glass aggregates in concrete reduced the splitting tensile strength by as much as 10, 14, 9 and 37%, for corresponding glass content. The irregular geometry of crushed waste glass particles caused failure in homogenous placing of concrete, resulting in decreased mechanical properties.

Taha and Nounu [2008] used waste glass sand to replace natural sand in concrete, at replacement ratio of 0, 50% and 100%, and presented the test results on splitting tensile strength. At 28 days, the splitting tensile strength decreased from 6.4 MPa to 5.9 and 5.1 MPa, for 50% and 100%

glass concrete respectively. Splitting tensile strength decreased with higher glass sand content, caused by the same reason as for the reduction in flexural strength.

All the test results show that glass sand would decrease the splitting tensile strength of concrete, as a result of the weakened bond. It is interesting to note that no literature observed the beneficial influence of pozzolanic reaction on tensile strength, although it occurred in the development of compressive strength [Ismail and Hashmi, 2009].

2.2.3.4 Elastic Modulus

Topcu and Canbaz [2004] reported the results of dynamic modulus of elasticity of concrete with the use of waste glass as coarse aggregates, at replacement of 15, 30, 45 and 60%. The dynamic modulus of concrete varied between 56.0 and 22.6 GPa. With higher glass addition, the dynamic modulus was observed to decrease. When the amount of waste glass was 60%, the dynamic modulus decreased by as much as 39%.

Limbachiya [2009] produced concrete with recycled waste glass sand up to 50% of natural sand and found the effect on elastic modulus to be negligible. Taha and Nounu [2008] also examined the influence of recycled glass sand on static modulus of concrete, with up to 100% replacement. However, the test results did not show a clear effect of glass sand on modulus.

2.2.3.5 Drying Shrinkage

Insufficient test on drying shrinkage of concrete containing waste glass has been published so far, except the following investigations.

Shayan and Xu [2004] studied the use of waste glass as coarse and fine aggregates. In addition, as value-added utilization, waste glass was incorporated in concrete as partial cement replacement. The drying shrinkage of the concrete with 50% coarse glass aggregates and various

amounts of fine glass aggregates was well below 0.075% at 56 days, specified by the Australian Standard AS 3600 [2001]. However, no clear trend was reported by the researchers on the relation between drying shrinkage and amount of glass sand added. The concrete mixes with glass powder as pozzolan, up to 40% in cement, showed shrinkage values less than 0.075% at 56 days. From the test results, addition of more glass powder would lead to higher drying shrinkage.

Kou and Poon [2009] investigated the drying shrinkage of self-compacting concrete with the use of waste glass sand, at replacement content of 15, 30 and 45%. The drying shrinkage, up to 112 days, decreased with increasing glass sand content, probably due to the lower water absorption characteristics of glass particles (0.36%). The drying shrinkage of all concrete mixes was well below the limit of 0.075% at 56 days, as specified by AS 3600 [2001].

Limbachiya [2009] showed almost identical drying shrinkage values for concrete mixes with different glass sand content, varying from 0 to 50%. The concrete, with designed strength of 30 and 40 MPa, showed drying shrinkage in the range of 775~785 $\times 10^{-6}$ and 805~815 $\times 10^{-6}$, respectively at 90 days.

2.2.4 Alkali-Silica Reaction

2.2.4.1 Mechanism of ASR

Alkali-silica reaction (ASR) is a reaction between the hydroxyl ions in the pore water of a concrete and certain forms of silica, which occasionally occur in significant quantities in the aggregates [Hobbs, 1988]. Due to the amorphous silicate in the glass, ASR is potentially the most detrimental mechanism for glass sand in concrete. However, the mechanism of ASR is not well known, especially for glass sand, and has been inconsistently reported.

Helmuth and Stark [1992] observed that the ASR results in the production of two component gels – one component is a non-swelling calcium-alkali-silicate-hydrate [C-N(K)-S-H] and the other is a swelling alkali-silicate-hydrate [N(K)-S-H]. When the ASR occurs in concrete, some non-swelling C-N(K)-S-H is always formed. The reaction will be safe if this is the only reaction product, but unsafe if both gels form. The key factor appears to be the relative amounts of alkali and reactive silica.

Mindess et al. [2003] and later Thomas et al. [2007a] explained that the overall process proceeds in a series of overlapping steps:

a. In the presence of a pore solution consisting of H_2O and Na^+, K^+, Ca^{2+}, OH^- and $H_3SiO_4^-$ ions (the latter a form of dissolved silica), the reactive silica undergoes depolymerization, dissolution and swelling (**Fig. 2.1a**). The swelling can cause damage to the concrete, but the most significant volume change results from cracking caused by subsequent expansion of reaction products.

b. The alkali and calcium ions diffuse into the aggregates resulting in the formation of a non-swelling C-N(K)-S-H gel, which can therefore be considered as calcium silicate hydrate (CSH) containing some alkali (**Fig. 2.1b**). The calcium content depends on the alkali concentration, since the solubility of $Ca(OH)_2$ is inversely proportional to the alkali concentration.

c. The pore solution diffuses through the rather porous layer of C-N(K)-S-H gel to the silica. Depending on the relative concentration of alkali and the rate of diffusion, the results can be safe or unsafe. If CaO constitutes 53% or more of the C-N(K)-S-H on an anhydrous weight basis of the gel, only a non-swelling gel will form. For high-alkali concentrations,

however, the solubility of calcium hydroxide (CH) is depressed, resulting in the formation of some swelling C-N(K)-S-H gel that contains little or no calcium. The N(K)-S-H gel by itself has a very low viscosity and could easily diffuse away from the aggregate. However, the presence of the C-N(K)-S-H results in the formation of a composite gel with greatly increased viscosity and decreased porosity.

d. The C-N(K)-S-H gel attracts water due to osmosis, which results in an increase in volume, local tensile stresses in the concrete, and eventual cracking (**Fig. 2.1c**). Later, the cracks will be filled with reaction products, which gradually flow under pressure from the point of its initial formation.

The result is that the following three conditions should be satisfied for a traditional ASR to occur in concrete: (1) moisture, (2) alkalis, and (3) alkali-reactive aggregates. Shi [2009] proposed a different mechanism for the ASR in concrete containing glass. In contrast to traditional ASR, the necessary conditions for glass concrete are only moisture and high pH (>12). C-N(K)-S-H will form regardless of the presence of Na^+ ions in cement. Under such conditions, a significant amount of soda-lime glass can dissolve and form swelling gel. The following sections will review pertinent previous work on ASR according to various test parameters, e.g. glass content, color and size.

2.2.4.2 ASR Test Method

Currently, there are a number of test methods to assess the alkali reactivity of aggregates. The test conditions and criteria vary widely from one test to another. This study also provides a critical evaluation of different test methods, which can be mainly divided into two categories:

performance tests, giving information on limiting alkali contents to avoid damaging expansion; and indicator tests to differentiate between potentially reactive and innocuous aggregates.

a. Performance tests

Concrete prism test (CPT) is to determine the potential ASR expansion of cement-aggregate combination for concrete, which is proposed for actual construction. There are several national test methods based on CPT (ASTM C 1293, BS 812-123, RILEM TC 106-3, as compared in **Table 2.3**), however most of them are similar to the extent that elevated temperature and augmented cement alkalis are used to accelerate the reaction [Thomas et al., 2006]. In ASTM C 1293, concrete prism (75 × 75 × 300 mm) is stored over water at 38 ºC. In concrete mix, NaOH is added to the mixing water to increase the alkali content to 1.25% by mass of cement. After 52 weeks of curing, expansion less than 0.05% indicates non-expansive cement and aggregate combination while expansion in the range of 0.05-0.10% or higher than 0.10% implies moderately expansive or expansive combination of cement and aggregate. The effect of ASR expansion on engineering properties of concrete is shown in **Fig. 2. 2**.

It can provide the most reliable and meaningful results than other test methods. It can also be used to evaluate the effectiveness of mineral admixtures. The main disadvantages of CPT for evaluating the efficiency of mineral admixtures in controlling ASR expansion are the long test duration of 2 years.

b. Rapid indicator tests

Mortar Bar Test

ASTM C 227 determines the susceptibility of cement-aggregate combinations to expansive reaction with alkalis. This method uses mortar bar (25 × 25 × 285 mm) with particular sand

grading stored under condition of 38 ºC and high humidity. In this method, cement with equivalent alkali content more than 0.60% should be used. Reactivity is harmful if expansion of mortar bar is larger than 0.05% at 3 months or larger than 0.10% at 6 months. The main drawbacks of this test method include alkali leaching, long test duration (3-12 months), poor correlation with filed performance, and non-feasibility for a numerous rock types such as slowly reacting rock. Because of many shortcomings, ASTM C 227 is not recommended for use as a method either for identifying the reactivity of an aggregate or for evaluating the level of prevention required to suppress ASR expansion [Ranc et al., 1994; Thomas et al, 2006].

Accelerated Mortar-Bar Test

Accelerated mortar-bar test (AMBT) is probably the most common test used worldwide at present for its rapidness [Alexander and Mindess, 2005; Thomas et al., 2006, 2007b]. It has been included in several national test methods such as ASTM C 1260 and BS DD 249, In this test, mortar bar (25 × 25 × 285 mm) comprising susceptible aggregates, with specified grading from 150 μm to 4.75 mm, is stored in 1 N NaOH solution at 80 ºC for 14 days. Aggregates are considered as potentially deleterious if the expansion is higher than 0.20% after 14 days immersion. Expansion below 0.10% is indicative of innocuous behaviors in most cases while expansions between 0.10% and 0.20% require additional expansion values until 28 days.

AMBT is a rapid test useful to slowly reacting aggregates or those producing expansions late in the reaction. AMBT is generally reliable and reproducible [Alexander and Mindess, 2005]. However, the main disadvantage of AMBT is its overly severe curing condition since it identifies many aggregates as reactive despite good performance in the field and in concrete prism tests. As pointed by Thomas et al. [1997], concrete prism test should be used to confirm the results before

an aggregate is rejected if an aggregate fails in AMBT. ASTM C 227 and C 1260 are also compared with CPT in **Table 2.3**.

ASTM approved a modification of the C 1260 AMBT, C 1567, which can be used to evaluate the level of mineral admixture required to control ASR expansion. Expansion more than 0.10% at 14 days is indicative of potentially deleterious expansion for the combination of cement, mineral admixtures and aggregates. The principal ASR mitigation mechanism by mineral admixtures is reducing the quantity of alkali hydroxides in the pore solution. AMBT would however offset this primary function by providing sufficient external source of NaOH. Recently though, some studies have demonstrated that mineral admixtures may still be effective in lowering the pore solution alkalinity during a 14 or 28 day immersion period [Berra et al., 1994; Berube et al., 1995; Thomas and Innis, 1999; Thomas et al., 2007b]. This is the reason why mineral admixtures can still mitigate ASR expansion in AMBT despite the abundant availability of alkalis.

2.2.4.3 Effect of Glass Color

Jin et al. [2000] first reported the effect of glass color on ASR expansion of mortar containing glass particles. From the accelerated mortar-bar tests (AMBT) carried out according to ASTM C 1260, clear glass was found to cause the most expansion at 14 days. Brown glass was considerably less reactive and green glass appeared not only to be non-reactive but also to reduce the expansion due to ASR. The effectiveness of green glass as an ASR suppressant was found to be strongly correlated with the amount of Cr_2O_3 in the glass. The authors used the double-layers hypothesis of Prezzi et al. [1997] to expansion the less expansive characteristics of gel containing Cr^{3+}. As shown in **Fig. 2.3** which illustrates a negatively charged particle suspended in a monovalent electrolytic solution, the charge on the particle selectively attracts the electrolyte

cations and repels its anions. For a symmetrical electrolyte, the resulting double-layer thickness is inversely proportional to the valence of the ions in the double layer. For a given concentration, monovalent ions (Na^+ and K^+) produce larger double-layer thickness and repulsion forces than bivalent ions (Ca^{2+}), meaning that a sodium or potassium gel can generate a larger pressure than that generated by a calcium gel when the expansion is restrained.

Park and Lee [2004] studied the ASR in mortar containing waste glass of green and brown color using AMBT. The ASR expansion of mortar with brown glass was 2.5 to 10.3 times that of reference mortar without glass, while that with green glass was 1.8 to 3.9 times.

Topcu et al. [2008] produced mortar bars with three different colors of glass as fine aggregates in four quantities, that is, 25, 50, 75 and 100%. Based on AMBT, the glass color affected the amount of expansion, and clear color resulted in the greatest expansion. Brown glass contains Fe_2O_3 while green glass contains Cr_2O_3; and both Fe_2O_3 and Cr_2O_3 were probably the reason for reduced expansions, since all glass with different colors had nearly the same chemical compositions except these two components.

Zhu et al. [2009] tested the ASR expansion of mortar with glass sand of different colors, in both short and long terms, according to ASTM C 1260 and C 227, respectively. In the study, different test methods for ASR expansion of concrete, including alkali content in concrete mixture or solution, were compared and discussed, as summarized in **Table 2.3**. Green, brown and clear glass sands showed less than 0.1% expansion up to 14 days, except the very reactive blue glass sand. This implied that the glasses except blue glass should be classified as non-reactive. However, large expansions were observed in all color glass at 133 days and the time to initiate and the rate of ASR reaction varied with glass color. Therefore, the results implied that the

metals used to impart color to glass may affect the ASR reactivity. ASTM C 227 test results showed the same trend that ASR reaction rate varied in the decreasing order of clear, brown and green glass particle.

Dhir et al. [2009], however, found a contradictory trend of ASR expansion, with green glass producing the largest expansion while clear glass producing the least. In their study, the alkali content in cement was adjusted to meet the minimum requirement of 1.00±0.05%, according to BS 812-123. After 3 years, the magnitude of expansion increased in the order of clear, brown and green glass, with the prisms containing clear glass behaving very similar to the control specimens without glass. The writers concluded that chromium did not influence the ASR expansion. Instead, they attributed the effect of different glass color to the nature of the manufacture processes. That is, the chemical composition of colored glasses may not be directly related to the different ASR behavior. In addition, the researchers found that expansion of prisms containing mixed glass as fine aggregates was less than what might be expected if the contribution from each glass color was considered directly proportional to the quantities.

2.2.4.4 Effect of Glass Content

Jin et al. [2000] carried out a comprehensive examination of ASR in concrete to study the effect of glass content on ASR expansion of mortar, as per ASTM C 1260. Clear soda-lime glass was added as natural sand replacement, with replacement ratio increasing from 0% to 100% in steps of 10%. The 14-day expansions of the mortar bars increased consistently with increasing glass content, and no pessimum content was detected. Deleterious expansion, larger than 0.2%, would occur if more than 10% clear glass sand was used as sand. However, the test method was limited to an accelerated condition which therefore over-estimated ASR compared to field conditions.

Park and Lee [2004] also examined the effect of content on ASR expansion of mortar bars with green and brown glass sand according to ASTM C 1260. The natural sand was replaced by glass sand at 0, 10, 20, 30, 50, and 100%. The expansion rates noticeably increased with an increase in glass content, regardless of the glass color. No pessimum was generated as the expansion rate continued to increase along with an increase in the amount of mixing glass sand, due to the unlimited supply of alkali in the 1 N NaOH solution.

Topcu et al. [2008] used three different colors of glass at four different quantities (25, 50, 75 and 100%) as fine aggregates and investigated the effect of glass content on ASR expansion using AMBT. At 14 days, all the mortar mixes showed expansion higher than 0.2%. At 3, 9, 14 and 21 days, the increment in glass sand content resulted in a reduction in the resistance against ASR, regardless of glass color.

Taha and Nounu [2009] utilized mixed-color recycled glass as sand replacement in concrete and carried out ASR tests according to BS 812-123. It was found that the presence of glass sand in concrete resulted in high risk to extensive ASR cracks. No ASR cracks were observed in the control concrete mix without glass sand. The ASR expansion of concrete mix with 50% glass sand exceeded the allowable limit of 0.2% after 52 weeks and considered as a potential risk. The ASR expansion in concrete with 100% glass sand was very high and ASR cracks were clearly identified.

Kou and Poon [2009] investigated the ASR expansion of self-compacting concrete, with mixed color glass as sand, again using AMBT. Although the test results showed that the ASR expansion increased with glass sand content, all the expansions were less than 0.1% within 14 days, up to 45% replacement content. Limbachiya [2009] studied the ASR expansion of mortar bars with

mixed color glass sand at replacement level of 5, 10, 15, and 20%. The test results did not show a clear trend that could identify the effect of glass sand in the first 6 days. Thereafter, expansion appeared to increase progressively with an increase in glass sand content. However, the difference in expansion for mortars prepared with up to 15% glass sand was negligible. The final expansion, at 14 days, was found to be below 0.1%, indicative of innocuous behavior.

Ismail and Hashmi [2009] tested ASR expansion of mortar made of 0, 10, 15 and 20% waste glass as fine aggregates, following ASTM C 1260. There was a clear reduction in the expansion of the specimen, that is, 66%, compared to the control mix. All specimens showed expansions less than 0.1% at 14 days, indicating that no potential deleterious expansion occurred for the waste glass. This is related to the reduction of available alkalis due to the consumption of lime by pozzolanic reaction of fine waste glass particles. However, the sand grading in this study was not strictly following ASTM C 1260 standard, which may result in substantial differences.

The effect of glass sand content on ASR expansion, based on previous research, is summarized in **Fig. 2.4**. The alkali reactivity of glass sand is still controversial and further study is necessary.

2.2.4.5 Effect of Glass Particle Size

Jin et al. [2000] initially reported the effect of glass particle size on ASR expansion of mortar bar with 10% clear glass sand, according to ASTM C 1260. The sizes of glass sand ranged from 4.75 mm to 150 μm. The test results showed that maximum ASR expansion occurred at 1.18 mm. Mortar bars containing glass sand 300 μm in size exhibited approximately the same ASR expansion as the reference bars without glass, while mortar bars with glass sand 150 μm or finer in size showed less expansion. In their paper, they proposed a well-matching model to explain the influence of glass particle size. According to this model, ASR gel formation builds up the

internal pressure, while the gel permeation tends to relieve it. ASR formation, a chemical process, increases with smaller glass particle size since it is considered as a surface reaction. At the same time, gel permeation means a physical process that reacted ASR gel release from the reaction site to cement paste matrix, which can relieve the tensile stress built by ASR formation. The net pressure thus reflects the difference between gel formation and permeation rate. There should be a certain particle size at which the two processes balance each other, since both processes depend on the aggregate surface area. As illustrated in **Fig. 2.5**, the process is reaction dominant for the left branch while the process is transport dominant for the right branch of the curve. In addition, this pessimum size will shift to right as the aggregate reactivity increases and to left as the matrix permeability increases.

However, the pessimum effect was not observed by Zhu and Byars [2004], despite confirming that smaller glass particles results in less ASR expansion. In order to explain the pessimum effect, three different hypotheses have been proposed: (1) using a mathematical model simulating the kinetics of ASR at glass-paste interface associated with diffusion processes [Bazant and Steffens, 2000]. In this model there exists a certain pessimum size for which the pressure is maximum; (2) using a fracture mechanics-based explanation [Bazant et al., 2000] which argues that in addition to the kinetics effects, reducing glass particle size results in a reduction of the stress intensity factor which causes expansions and cracking; and (3) considering that smaller glass aggregates result in a larger volume of ITZ throughout the mortar which provides a porous space into which ASR gel expands freely without causing cracks to the surrounding mortar [Suwito et al., 2002]. According to Rajabipour et al. [2010] and Maraghechi et al. [2012], all these three models have not been evaluated by experiments beyond those performed by Jin et al. [2000], even they offer logical reasons for potential causes of the effect of glass particle size on ASR.

Zhu et al. [2009] tested the effect of clear glass particle size on ASR expansion, as per ASTM C 1260. Mortar bars made with clear glass particles less than 1.18 mm exhibited similar or even less expansion than the control mix without glass, implying that small glass particles (< 1.18 mm) can be considered as an ASR mitigator, while ASR expansion rate increased with particle size larger than 1.18 mm. No pessimum effect was observed.

Shayan and Xu [2004] assessed the reactivity of glass sand with four different size ranges, including powder (<10 μm), very fine sand (0.15 to 0.30 mm) and two coarser sand fractions (0.6 to 1.18 and 2.36 to 4.75 mm) by carrying out AMBT. Glass particles smaller than 0.30 mm would not cause deleterious expansions whereas those larger than 0.60 mm could cause significant deleterious expansion. When the particle size was sufficiently reduced, it could act as a pozzolanic material.

Dhir et al. [2009] tried to explain the effect of glass aggregate size on ASR expansion by a simple mechanism which consisted of simultaneous leaching and dissolution of the glass surface, as illustrated in **Fig. 2.6**. The glass began to leach at its surface and the depth of the leached layer from the original surface increased with time. At the same time, the surface leach layer dissolved. Thus, the quantity of gel will progressively increase until all the glass is converted to gel (that is when $d_L = r$, as shown in **Fig. 2.6**). At this point, there will be a decline in gel as only dissolution could proceed. Also, finer glass particles would reach the state where all glasses were converted to gel more rapidly, meaning that smaller particles would be solely undergoing pozzolanic reaction and thus contributing towards a reduction in gel at relatively early ages. However, this ASR mechanism was oversimplified, since (1) there was no single leached state but an increase in the extent of leaching outwards from the completely unreacted glass to the particle surface; (2)

dissolution of the gel would occur throughout the leached layer, and not solely at the surface; and (3) the model did not consider the actual expansion of the gel.

Rajabipour et al. [2010] investigated the effect of brown color recycled glass particle size on ASR from expansions and observation using scanning electron microscope (SEM). As shown in **Fig. 2.7**, SEM images revealed that ASR did not occur at the glass-paste interface; rather, it occurred inside micro-cracks that existed inside glass particles which were generated during the crushing operations of glass bottles. Larger size glass particles showed larger and more active micro-cracks which rendered their high alkali-silica reactivity. At the interface with cement paste, glass showed evidence of pozzolanic reaction, leading to formation of non-expansive CSH. For particles smaller than 0.6 mm, the intra-particle ASR was minimal and only the pozzolanic reaction was observed to proceed. The findings could have implications on methods such as proper annealing and repeated lime solution saturation and drying to mitigate ASR induced by recycled glass aggregates. However, the mechanism of pozzolanic reaction at the interface remains unexplained. Based the SEM and energy dispersive X-ray spectroscopy (EDS) results, the researchers concluded that all the three proposed explanations [Bazant and Steffens, 2000; Bazant et al., 2000; and Suwito et al., 2002] would be intuitively incorrect, since glass ASR was not surface reactive.

The effect of glass sand size on ASR expansion, from previous test results, is summarized in **Fig. 2.8**. In general, the effects of glass color, size, and content on ASR is not totally understood based on the various test results. Furthermore, the ASR suppressing methods are not fully conducted. A comprehensive study of the above influential factors on ASR in glass sand mortar and concrete is still lacking.

2.2.4.6 ASR Mitigation Methods

Different mitigation methods have been investigated to suppress the ASR expansion for concrete containing glass sand. According to the different ASR mitigation principles, the mainly used methods can be divided into three categories.

a. Cementitious or pozzolanic admixtures

Supplementary cementitious materials such s fly ash, slag, silica fume or metakaolin have been successfully used to prevent or control ASR expansion. As summarized by Xu et al., [1995], the mechanism of ASR control by cementitious materials can be as follows: (1) permeability of cement paste is decreased due to the pozzolanic reaction between cement hydrate products and mineral admixtures, which can consequently reduce the mobility of ions in paste; (2) strength of concrete is also increased by pozzolanic reaction, providing higher resistance to ASR expansive stress; (3) the alkalinity of the pore solution is reduced; (4) calcium hydroxide is depleted by mineral admixtures; and (5) the secondary CSH by pozzolanic reaction can entrap alkali ions. The use of various cementitious materials in ASR mitigation is reviewed as follows.

Fly ash

Topcu et al. [2008] investigated the effect of 10% and 20% fly ash as mineral admixtures on ASR expansion of mortar containing 25, 50, 75 and 100% glass sand of green, brown and clear color. It seemed replacing cement with 10% fly ash did not sufficiently reduce expansion while with 20% fly ash it did. Soluble alkaline concentration could be decreased in concrete by adding fly ash. The pozzolanic reaction between fly ash and $Ca(OH)_2$ decreased the pH value of the pore solution. This reduced the reactivity between the silica of aggregate and the alkalis of cement. The pozzolanic reaction occurring due to fly ash decreased permeability of mortar, leading to

reduced water penetration. Therefore, the gel which occurred in ASR did not swell and expansions could be stopped.

Ground granulated blast-furnace slag

Taha and Nounu [2009] examined the effect of 60% GGBS as ASR suppressant in concrete with glass sand replacing 50 and 100% of cement content. The test was carried out according to BS 812-123. GGBS was proven to be very effective in reducing and eliminating potential ASR risk. Concrete with 60% GGBS exhibited ASR expansion far below 0.2% after 78 weeks, even with 100% glass sand.

Silica fume

Meyer and Baxter [1998] investigated the effectiveness of silica fume as ASR suppressants in mortar bars containing 100% highly reactive mixed-color glass sands as per ASTM C 1260. At content of 20%, silica fume was extremely effective in suppressing ASR, reducing the expansion below 0.1% at 14 days.

Metakaolin

Meyer and Baxter [1998] investigated the effectiveness of two kinds of metakaolin in restraining ASR in mortar with 100% highly reactive mixed-color glass sand. The expansions of the bars containing 20% of either type of metakaolin remained below 0.1% at 14 days.

Taha and Nounu [2009] also examined the effect of 10% metakaolin as ASR suppressant in concrete with glass sand at 50 and 100% replacement content. The test was carried out according to BS 812-123. Metakaolin was proven to be very effective in reducing and eliminating the potential ASR risk. After 78 weeks of measurement, the ASR expansion for concrete with glass sand was well controlled to be significantly less than 0.2%.

Glass powder

Taha and Nounu [2009] also used 20% glass powder as ASR suppressant in concrete containing 50% and 100% glass sand. ASR expansion was tested on concrete prisms according to BS 812-123, till 78 weeks. Very fine glass powder with an average size particle passing 45 μm was used as cement replacement, resulting in significant reduction in ASR expansion. The available alkali in concrete was considered as an alkali activator for the hydration of glass powder and consumed in the chemical reaction of the hydration process to form the microstructure of concrete. The available reactive alkali in glass powder was dissolved during the early stage of hydration and react with other chemical elements to form other reaction products of concrete. Therefore, it would not be free for further ASR at later stages.

Shi et al. [2005] dealt with the fineness and pozzolanic activity of glass powders with four different sizes. Used as cement replacement to reduce ASR expansion, the size distribution of glass powder was almost the same as that of Portland cement. From the ASR expansion results, the replacement of cement with 20% glass powder significantly reduced expansion, from 0.50% to lower than 0.2% at 14 days. The high pozzolanic activity of glass powder may be the main reason for restraining ASR expansion.

Dyer and Dhir [2001] examined the chemical reactions of glass cullet used as cement component. In the ASR test as per modified ASTM C 1260 method, the expansion of all prisms decreased with more glass powder up to 40% of cement, particularly for green and brown glass powder. In chemical terms, the ASR of glass cullet is not different from pozzolanic reaction; both involve alkali reactants and yield an amorphous gel. The main difference between the two reactions is the timescale involved: pozzolanic reaction occurs during the first few months subsequent to mixing, whereas the ASR is generally slower and the detrimental effects only become apparent in the

mature concrete. It has been postulated that the reason for the difference in the nature of the two types of gel formed by the two reactions is the different amounts of calcium ions present in the pore solution during reaction, with high calcium levels leading to the beneficial pozzolanic gel. By reducing the particle size and hence increasing the surface area available for reaction, the material reacts relatively rapidly in an environment in which there is still much calcium available in solution. It is also probable that the greater space available for gel formation in immature concrete and the more uniform distribution of gel that is likely to arise will assist in preventing the deleterious effects encountered in more mature material. Thus, finer particles favor a relatively rapid, beneficial pozzolanic reaction over the slower, deleterious ASR.

Shao et al. [2000] studied the ASR expansion of concrete containing ground waste glass as partial cement replacement. Cement was replaced 30% by volume by 150, 75 and 38 μm glass powder, and tests were carried out according to ASTM C 1260. While both 150 and 75 μm glass batches experienced a similar amount of expansion, the 38 μm glass further reduced the expansion to half of the control specimens. The expansion tests showed that ground glass did not expand and it actually helped suppress the expansion as compared to the control. This was also indicative of pozzolanic activity. According to the test, the finer the particle size, the less the expansion would become.

Shayan and Xu [2004] proposed the value-added utilization of waste glass in concrete as pozzolan instead of as fine aggregates. The glass powder contained particles less than 10 μm. For the ASR expansion test, the control mortar bars were made to contain plain cement and 80% glass sand, and the cement was replaced by 10%, 20% and 30% glass powder. All mortars with glass powder showed less ASR expansion than the one without glass. Furthermore, the long term mortar bar tests, conducted at 38 ˚C and 100% RH, were undertaken in combination with

nonreactive and reactive aggregates and with the same levels of cement replacement. Glass powder itself did not cause any expansion when the aggregate was nonreactive. Moreover, the presence of even 30% glass powder did not release sufficient amount of alkali to trigger the reactivity. Even when used as aggregate rather than cement, the 30% glass powder still did cause deleterious mortar bar expansion. The test results indicated that powder could be used without harmful effects.

Idir et al. [2010] examined both ASR and pozzolanic reaction of glass particles in mortar. The particle sizes ranged from 8 μm to 3.75 mm. Mortars with glass powder and fine glass aggregates, either separately or combined, were monitored for length expansion. They found that only glass particles larger than 1 mm would cause ASR expansion. Therefore, the use of glass fines (<1 mm) led to reduction in ASR expansion. In addition, the glass fines could increase compressive strength as well, as a beneficial result of its pozzolanic reaction.

b. Mechanical confinement

Fiber reinforcement has proved to be also successful in mechanically reducing ASR expansion. Mechanical confinement through either external load application or through fiber reinforcement can reduce expansion caused by ASR [Yi and Ostertag, 2005; Ostertag et al., 2007]. Previous work on suppressing ASR expansion by fiber includes:

Meyer and Baxter [1998] determined the effectiveness of randomly distributed fiber reinforcement in straining ASR expansion of mortar with 10% clear glass sand in accordance with ASTM C 1260, by using hooked steel fibers, deformed steel fibers and polypropylene fibers. The addition of fibers was 1.5% by volume of concrete mixture for each kind of fiber. The addition of the fibers reduced the expansion by up to 60%, due to a multi-directional constraining

effect. Steel fibers were more effective in straining the ASR expansion and reducing the damage due to ASR.

Park and Lee [2004] used steel and polypropylene (PP) fibers to suppress ASR expansion in mortar containing various green and brown glass sands. The internal pressure created by ASR gel caused ASR expansion and cracks in the mortar containing waste glasses. Such internal expansion can be suppressed by randomly distributing discontinuous fibers. ASR expansion decreased with an increase in the contents of both fibers. For 20% brown glass mortar, the relative expansion defined by ASTM C 1260 was suppressed under 0.2% with a steel fiber content of more than 1.0% by volume. The PP fibers did not bring the expansion rate down below 0.2%, which necessitated additional suppressive measures such as adding extra PP fiber. The suppressing effect of both fibers in brown glass was more prominent than in the green glass.

c. Chemical admixtures

The most widely used chemical admixtures in mitigating ASR expansion is lithium salts. McCoy and Caldwell [1951] extensively investigated the effectiveness and dosage influences of versatile chemical admixtures, including lithium salt (1% by mass of cement of LiCl, Li_2CO_3, LiF, $LiNO_3$ and Li_2SO_4). The test results revealed that lithium salts could effectively retrain ASR expansion of sand of Pyres glass. Thereafter, lithium compounds have been extensively studied and confirmed as effective in ASR mitigation [Stark, 1992; Hudec and Banahene, 1993]. However, until now the underlying mechanisms are not yet well understood and different explanations have emerged, although sometimes they seem to contradict each other. For instance, Collins et al. [2004] and Feng et al. [2005] concluded that lithium ion was easy to incorporate into ASR gel product due to its small ionic radius and higher surface charge density, rather than other alkali ions, such as Na^+ and K^+ in concrete. Subsequently, the nature and chemical composition of ASR

gel would be changed. However, Stark et al. [1993] and Prezzi et al. [1998] considered that the Li^+ ions added during mortar preparation were sequestered primarily by cement hydration products and not available to participate in the ASR. As a result, there would be less Li^+ ions to exchange reactions with bivalent cations (Ca^{2+} and Mg^{2+}) which should suppress expansion. Besides, lithium compounds may reduce the solubility of the reactive silica and the ability of any dissolved silica to be repolymerised and form ASR gel particles [Mitchell et al., 2004]. The use of lithium compounds in mitigation of ASR expansion by glass sand in concrete is summarized.

Taha and Nounu [2009] used 1% anhydrous $LiNO_3$ as ASR suppressant in concrete containing 50% and 100% glass sand. ASR expansion was tested on concrete prisms according to BS 812-123, till 78 weeks. $LiNO_3$ was dissolved in water and then added to concrete mix as a chemical admixture. The test results showed that $LiNO_3$ was very effective in reducing ASR expansion to below 0.2%, in the long term.

Topcu et al. [2008] reported the ASR suppressant of Li_2CO_3, at the amount of 1% and 2%, in glass sand mortar. According to the test results of accelerated mortar bars, 2% was sufficient in reducing ASR expansion but 1% Li_2CO_3 was not. However, the effect of Li_2CO_3 on ASR is not yet well understood.

2.2.5 Other Durability Properties

Up to now, tests on durability properties of glass concrete other than ASR have been seldom reported, since ASR has always been of the most concern. However, other durability aspects should be also examined for the practical development of glass sand concrete.

Ozkan and Yuksel [2008] investigated the durability properties of cement mortars with waste glass as pozzolan, at replacement of 10%, 30% and 50%. Resistance to sodium chloride and

sulfates were tested by comparing compressive strength of mortar specimens exposed to these chemicals with the strength of reference specimens. The specimens were immersed in pure water for 7 days and then put in 4% NaCl, 4% Na_2SO_4, or 4% $MgSO_4$ solutions, for the next 21 days. Finally, the compressive strengths of these mortar cubes were measured. It was observed that the residual strength of mortars exposed to chloride attack was reduced as the replacement ratio was increased, except for the case of 10% replacement ratio for which the residual strength was found to be higher than that of control mix. Residual strengths of specimens cured in $MgSO_4$ decreased with increasing replacement ratio. The maximum loss in strength was 8.26% at the replacement ratio of 50%. However, residual strength of mortar with glass powder exposed to sodium sulfate attack was higher than that of reference group at 10% and 30% replacement levels. These results showed that the replacement of cement by glass powder increased durability of mortars to sulfate attack.

In addition to other mechanical properties, Kou and Poon [2009] investigated the chloride ion penetration of self-compacting concrete with the use of waste glass sand, at replacement content of 15%, 30% and 45%. The tests were carried out in accordance with ASTM C 1202 on 28 and 90 days. The chloride ion penetrability decreased with increase in glass content, indicating an increase in resistance to chloride ion penetration. This was due to the lower porosity of glass cullet compared to natural sand. Moreover, the glass sand had a finer particle size distribution than that of natural sand, resulting in a better packing efficiency of the concrete at the fine scales.

Chen et al. [2006] studied the use of waste E-glass particles in concrete, from 0 to 50% replacement of sand, in a step of 10%. Chloride penetration and sulfate attack were tested according to ASTM C 1202 and C 267, respectively. By incorporating E-glass, the total charge passed decreased with higher content. Concretes with E-glass particles have a denser internal

structure providing the specimen with effective barrier against chloride-ion penetration. Such improvement of chloride penetration resistance is more prominent in E-glass concrete with higher *w/c* ratio. The strength and weight loss of specimens, after five cyclic wet-and-dry exposure to sulfate solution, decreased with higher E-glass concrete, particular with lower *w/c* ratio. The surface defects of teste specimens also gave a qualitative evidence of sulfate effect. From the test results, E-glass particles with a size less than 75 μm have three characteristics: high aluminosilicate content, glassy state and finely divided state. Thus, high reactive potential and large specific surface area are provided to activate effective pozzolanic reaction in E-glass concrete mixes, resulting in higher compressive strength, higher resistance of sulfate attack and lower chloride penetration.

Wang [2009] replaced natural sand by LCD glass in concrete, at 0, 20%, 40%, 60% and 80% replacement. The sulfate attack and chloride ion penetration was tested as per ASTM C 1012 and C 1202, at the age of 7 and 28 days, respectively. The concrete weight loss caused by the sulfate attack decreased with increasing glass sand replacement. The charge passed of concrete with glass sand was less than that of control concrete, ranging from 750 to 3250 Coulombs. The optical microscope result indicated that the LCD glass sand could densely integrate with the cement paste. Based on SEM results, the dense CSH gel hydrate was produced in the glass concrete and connected into a continuous matrix, which generated a denser concrete structure, confirming that LCD glass concrete has a better strength and durability.

2.3 Role of Sand in Concrete

2.3.1 Sand in Plastic Concrete

According to Alexander and Mindess [2005], the plastic properties of concrete are more influenced by the characteristics of sand than coarse aggregates. The influence of sand properties or characteristics on the plastic properties of concrete is summarized as follows.

Particle shape

Particle shape has a major influence on workability and water requirement of a concrete mix as it affects particle packing and particle interlocking. Rounded, less angular particles are able to roll or slide over each other in the plastic mix with the minimum resistance. However, flat, elongated or highly angular particles render the concrete harsh, causing voids and honeycombing. Furthermore, sand has greater effect in gap-graded concrete mixes where particle interference or interaction among coarse aggregates is reduced.

Particle surface texture

Surface texture influences the plastic properties of a concrete mix in two ways: the surface area effect and the inter-particle friction effect. Rough particles have a larger surface area than smooth particles of equivalent size and shape. Further, rough particles induce a higher inter-particle friction, requiring greater external effect to move the particles over each other in a mix. These two effects combined to increase the water requirement for rough-textured aggregates. In general, clean natural sand has smoother texture than crushed sand, since the processes of abrasion and attrition generally render them smooth. However, it is possible for natural sands to have rough texture, for example, if they are derived from coarse-grained rocks or where rock minerals weather at varying rates.

Grading

Grading of sand has a very important influence on workability of a mix. It influences the total aggregate surface area and the relative aggregate volume in a concrete mix. In general, workability is best served by conforming to standard grading which ensures that voids of any one particle size are overfilled by particles of the next smaller size. Particular attention should be paid to the quantity and nature of materials small than 300 μm. The finer fractions (less than 150 μm and less than 75 μm) have a greater influence on cohesiveness and bleeding of the mix; quantities required in a mix will depend on the nature of the sand, with higher quantities generally being preferable in crushes sand.

Fines content

Caution should be paid to the nature of the fines (less than 75 μm) and tighter control should be exercised over fines content of natural sand. For crushed fines, improved concrete properties, such as reduced bleeding and increased cohesiveness can result from fines content sometime exceeding 10%. However, free-and-thaw resistance may be decreased by excessive amount of ultra-fines [Neville, 1995].

The relative effects of sand on the plastic properties of concrete are summarized in **Table 2.4**.

2.3.2 Sand in Hardened Concrete: Mechanical Properties

According to Alexander and Mindess [2005], aggregate properties that affect concrete strength are shape, surface texture, stiffness, strength and toughness and grading. Shape, surface texture and grading have direct effects on the stress concentration, the degree of micro-cracking and crack branching before and during failure in the composite material.

Shape

Angular particles improve concrete strength over rounded particles, with flexural strength more enhanced than compressive strength. These improvements are attributed to the greater degree of mechanical interlock, internal friction, and increased surface area associated with angular aggregates [Kaplan, 1959].

Surface texture

Aggregate surface texture significantly affects concrete strength since it improves the bond between paste and aggregate. Flexural strength is obviously increased by a rougher surface texture, although compressive strength is relatively slightly affected. In addition, high strength concrete benefits from a rougher surface texture of aggregate, which produces a superior cement-aggregate bond [Alexander et al., 1995].

Elastic modulus

Aggregate elastic modulus is also important for concrete strength, with continuous increase in strength with increasing aggregate elastic modulus. The possible explanation is that stiffer aggregates attract higher fraction of load in the composite.

Grading

Aggregate grading mainly affects water requirement in concrete and thus *w/c* ratio, which normally determines concrete strength. Sand content can have an indirect influence on strength by affecting the degree of compact of concrete. In addition, a larger amount of very fine material may increase strength by improving the bond at ITZ.

2.3.3 Sand in Hardened Concrete: Durability Properties

The durability of concrete is governed by its transport properties, with a notable exception of alkali-silica reaction (ASR). The incorporation of non-permeable sand into porous and penetrable cement paste would result in both beneficial and negative influences. Within certain amount, the overall penetrability tends to be reduced due to the low permeability of sand and the increased tortuosity. However, with excessive volume of aggregate, a more porous and weak Interface Transition Zone (ITZ) would increase the penetrability and provide pathway for chemical ions. It should be noted that very fine sand will have less effect as the size of these particles approaches that of the ITZ itself. With extreme fineness such particles actually participate in the "fine filler" effect, which generally improves the ITZ properties [Alexander and Mindess, 2005].

2.4 Concrete without Sand (No-Fines Concrete)

According to ACI 522R-10, pervious concrete is a zero-slump, open-graded material consisting of Portland cement, coarse aggregate, little or no fine aggregate, admixtures and water. Pervious concrete is often used as a synonym for no-fines concrete [Ghafoori and Dutta, 1995 a]. No-fines concrete has many different names, such as pervious, porous and permeable concrete. The aggregate is generally of a single size, usually 9.5 or 19 mm, surrounded by a thin layer of hardened cement paste at the points of contact to form a discontinuous system. Thus, the most common application of no-fines concrete is in low traffic volume areas. Although no-fines concrete has been used for paving for more than 20 years in U.S., only a few investigations have been carried out to determine its performance [Ghafoori and Dutta, 1995 b; Haselbach and Freeman, 2006; Schaefer et al., 2006; Bentz, 2008; Mahboub et al., 2009; Haselbach and Liu, 2010; Sumanasooriya et al., 2010].

2.4.1 Mix Proportion

The mix proportion for no-fines concrete depends predominantly on its final application. In pavement application, the concrete strength is critical and aggregate-cement (*A/C*) ratio as low as 4 is used. For previous building application, no-fines wall for example, *A/C* ratio usually ranges from 6 to 10. The leaner mix ensures that the void ratio is high and prevents capillary transport of water. However, low strength must first to be improved to an acceptable level.

The water content is desired for the chemical action of cement so as to provide bond among the aggregates. For a given mix proportion and aggregate size and type, there is a narrow optimum range of water-cement (*w/c*) ratio for a particular *A/C* ratio, usually falling within 0.26 to 0.45 for the needed workability [ACI 522R-10].

The aggregates used in no-fines concrete application are usually uniformly-sized. A 5% oversized and 10% undersized aggregate are acceptable for use but there should be no particles smaller than 5 mm [Neville, 1995], if sufficient voids are required for water flow. This is because small particles will tend to fill the voids, affecting the porosity of the concrete and the associated properties. With more than 30% sand, the concrete started to exhibit properties of normal concrete.

The use of no-fines concrete as a building material has been extremely limited, mainly due to its high interconnectivity and permeability. Normally, 15% or higher void content is required for no-fines concrete for the purpose of rapid percolation of water. At such higher void contents, some critical aspects for the use as structural concrete, such as compressive strength and permeability to chemical substances like chloride ions, might be compromised. Relatively high strength and low permeability of concrete can only be achieved by reducing the air void content

by sand in no-fines concrete mixtures. **Fig. 2.9** is used to estimate the volume of the paste for a mixture using normal weight No. 8 aggregate. It can be clearly seen that approximate 32% of paste (beyond this paste volume, air void content is less than 2%) should be used to fill the voids to achieve a dense concrete.

Excess Paste Theory

A theoretical aspect of mix design for concrete, namely excess paste theory is briefly introduced in this part. Kennedy [1940] advocated methods of concrete mix proportioning based on the assumption that the consistency of concrete depends on two factors: the volume of cement paste in excess of the amount required to fill the voids of the compacted aggregates, and the consistency of the paste itself.

The logical basis of this method is diagrammatically illustrated in **Fig. 2.10**. Diagram A represents a selection of freshly mixed concrete in which the voids in the dry rodded aggregates is filled cement paste, as denoted by the black areas. In this condition, the internal friction between aggregate particles is high and the concrete will be harsh and unworkable. However, if additional amount of cement paste is added to the concrete and assumed uniformly distributed, the individual aggregate particles will be forced apart, filmed by a thin coating with thickness of *t*. Therefore, the cement paste film is proportional to the surface area of the aggregates. To achieve the required workability, the amount of excess paste also depends on *w/c* ratio- lower *w/c* ratio requiring larger excess amounts than higher ratios.

The amount of excess paste is determined by the following formula:

$$p = C + KA \tag{2.1}$$

where *p* represents the volume of paste per unit volume of concrete, *C* is the void ratio of combined fine and coarse aggregates, *K* is the consistency factor and *A* is the specific surface area of combined aggregates.

To apply this method, it is necessary to establish an empirical relationship between the consistency factor and the consistency for each of the *w/c* ratio and for each of the aggregates. Also, it is necessary to establish by experiment a diagram like **Fig. 2.11** for each kind of the coarse and fine aggregates for the least voids ratio. As commented by Powers [1968], the procedure of evaluating *K* is more complicated than can be justified by the degree of accuracy attained from the practical point of view. As a summary for this excess paste theory, experiments must be made with the aggregates alone to obtain a basis for calculating or graphically estimating the optimum ratio of coarse to fine aggregate, and other experiments must be made with concrete mixtures to establish the consistency factor.

2.4.2 Fresh Properties

The void content is dependent on the *A/C* ratio and ranges from 13 to 28% for *A/C* ratio between 4 and 6. It was found that the density of no-fines concrete is generally about 70% of conventional concrete when made with similar components [Malhotra, 1976]. The density of no-fines concrete normally varies from 1600~1900 kg/m^3. Compaction has an influence on the void content and unit weight of no-fines concrete. In a laboratory test [Ghafoori and Dutta, 1995 c], the unit weight varies between 1643 and 1932 kg/m^3, due to different compaction levels.

2.4.3 Mechanical Properties

The various mechanical properties of no-fines concrete depends on cement content, *w/c* ratio, compaction level, and aggregate gradation and quality. The compressive strength is significantly

affected by the mix proportions and compaction efforts. Generally speaking, the compressive strength of no-fines concrete varies between 3.5 and 28 MPa. The relation between compressive strength and void content was determined by Meininger [1998] (see **Fig. 2.12**) in a series of laboratory tests in which a small amount of sand was added to the mixture. The compressive strength increased from 10.3 MPa to 17.2 MPa. The sand added was between 10% and 20% of the aggregates by weight. The increased fines filled some of the voids, reducing the void content from 26% to 17%. A decrease in the voids causes the concrete to bond more effectively, thus increasing the compressive strength. Ghafoori and Dutta [1995 c] determined that strength development of no-fines concrete was independent of the curing condition since there was only a negligible difference in strength between wet and sealed curing. A sealed compressive strength of 20.7 MPa was readily achieved with *A/C* ratio of 4.5 or less. Yang and Jiang [2003] found that a composite consisting of a surface layer and base layer of pervious concrete with different aggregate gradations, and thus pore size, attained a compressive strength of 50 MPa and a flexural strength of 6 MPa. Based on tests, Mahboub et al. [2009] however concluded that compressive strength and permeability were not directly related, at least for the specific type of mixtures used in their study.

The splitting tensile strength of no-fines concrete varied between 1.22 and 2.83 MPa. The greater splitting tensile strength was achieved with a lower *w/c* ratio according to Ghafoori and Dutta [1995 c]. More favorable properties for the lower *A/C* ratio could be attributed to the improved interlocking behavior between the aggregate particles. The relationship between flexural strength and void content was also reported by Meininger [1998]. In his beam specimen tests, the flexural strength increased with the compressive strength, but no regression analysis was presented.

Drying shrinkage in no-fines concrete is usually smaller than conventional concrete [Ghafoori and Dutta, 1995 c] due to its structural characteristics, and decreases as the *A/C* ratio increases. With the reduction in *A/C* ratio, there is more cement paste available to undergo volumetric contraction and axial shrinkage. Moreover, the decrease in *A/C* ratio compromised the contribution of coarse aggregate in restraining drying shrinkage.

2.4.4 Durability

Meininger [1998] reported that a minimum air void content of approximately 15% was required to achieve significant percolation for no-fines concrete. No research has been conducted on the resistance of no-fines concrete to aggressive attack by sulfate-bearing or acidic water. The durability of no-fines concrete under free-and-thawing conditions is also not well documented [ACI 522R-10], which is critical for application in cold weather [Schaefer et al., 2006].

Recently, a successful development of a virtual pervious concrete based on a correlation filter 3D reconstruction algorithm has been demonstrated by Bentz [2008]. In his work, the extensive study of such 3D virtual pervious concrete on exploring durability issues such as freezing-and-thawing resistance and clogging can provide a novel tool to understand the link between durability and the microstructure of pervious concrete.

2.5 Summary

In summary, inconsistent conclusions on diverse properties of glass mortar and concrete, some contradictory findings on ASR and the lack of durability properties of glass concrete will require a comprehensive study into the research of glass cementitious composites. Moreover, concrete with no sand is only limited to pavement or non-structural applications. Further efforts should be put into the structural application.

Table 2-1: Chemical compositions of commercial glasses [McLellan and Shand, 1984]

Glasses and uses	SiO_2	Al_2O_3	B_2O_3	Na_2O	K_2O	MgO	CaO	BaO	PbO	Others
Soda-lime glasses										
Containers	66-75	0.7-7		12-16	0.1-3	0.1-5	6-12			
Float	73-74			13.5-15	0.2	3.6-3.8	8.7-8.9			
Sheet	71-73	0.5-1.5		12-15		1.5-3.5	8-10			
Light bulbs	73	1		17		4	5			
Tempered ovenware	75	1.5		14			9.5			
Borosilicate										
Chemical apparatus	81	2	13	4						
Pharmaceutical	72	6	11	7	1					
Tungsten sealing	74	1	15	4						
Lead glasses										
Color TV funnel	54	2		4	9				23	
Neon tubing	63	1		8	6				22	
Electronic parts	56	2		4	9				29	
Optical dense flint	32			1	2				65	
Barium glasses										
Color TV panel	65	2		7	9	2	2	2	2	10% SrO
Optical dense barium crown	36	4	10						41	9% ZnO
Aluminosilicate glasses										
Combustion tubes	62	17	5	1		7	8			
Fiberglass	64.5	24.5		0.5		10.5				
Resistor substrates	57	16	4			7	10	6		

Table 2-2: Summary of effect of glass sand on fresh density of concrete

Previous study	Glass sand content, %	Fresh density, kg/m^3
Topcu and Canbaz, 2004	0	2340
	15	2335
	35	2340
	45	2330
	60	2335
Taha and Nounu, 2008	0	2440
	50	2430
	100	2390
Ismail and Hashmi, 2009	0	2477
	10	2446
	15	2428
	20	2421

Table 2-3: Summary of test methods for ASR expansion for aggregates [Zhu et al., 2009].

Test method	Comment
ASTM C 227: Standard test method for potential alkali reactivity of cement-aggregate combinations (mortar-bar method)	High alkali cement (Na_2O_{eq} > 0.6%) mortar bar test to determine cement-aggregate reactivity Specimens stored in high-humidity containers at 38 °C Requires one year or even longer if necessary for completion Excessive leaching of alkalis from specimens
ASTM C 1260: Standard test method for potential alkali reactivity of aggregates (mortar-bar method)	Accelerated mortar bar test for aggregate reactivity Bars immersed in 1 N NaOH solution for 14 days at 80 °C Alkali content of the cement is not a significant factor affecting expansion due to the high alkali solution. Suitable for screening to determine alkali-reactive sand. Due to the severe exposure, potentially unsuitable for absolute test. Results of concrete prism test should prevail.
ASTM C 1293: Standard test method for determination of length change of concrete due to alkali-silica reaction	Concrete prism test, regarded as best indicator of field performance, conducted at 38 °C and 100% RH High-alkali cement (1.25% Na_2O_{eq}), with a cement content of 420 kg/m^3 Coarse aggregate test (non-reactive fine aggregate) or vice-versa Requires one year for completion Can be used to test effectiveness of suppressant over 2 years Widely accepted, but lengthy test method
BS 812-123: Testing aggregate: method for determination of alkali-silica reactivity- concrete prism method	Concrete prism test, generally regarded as best indicator of field performance, conducted at 38 °C and 100% RH High-alkali cement (0.8-1.0% Na_2O_{eq}), with a volume fraction of 22.2% in concrete Fine aggregate test (non-reactive coarse aggregate) or vice-versa Requires 52 weeks for completion
RILEM TC 106-3: Detection of potential alkali-reactivity of aggregates- method for aggregate combination using concrete prisms	Concrete prism test, conducted at 38 °C and 100% RH High-alkali cement (raised to 1.25% by adding NaOH to the mixing water), with a cement content of 440 kg/ m^3 in concrete Test requires 52 weeks for completion, mainly used in mainland EU

Na_2O_{eq}=%Na_2O+0.658×%K_2O

Table 2-4: Influence of sand on plastic properties of concrete [Alexander and Mindess, 2005]

Concrete property	Coarser sand (FM*>2.9)	Finer sand (FM<2.0)	Fines content (<75 μm fraction)
Water requirement	Tend to lower the water requirement by reducing overall aggregate specific surface	May increase water requirement; however, a certain amount of fines is required to lubricate a mix, and this will not increase the water requirement	Excessive fines content will increase water requirement
Workability	Tend to increase workability provided particle interference is not included	May reduce workability, but see comment above. Minus 300 μm fraction has relative large influence	This fraction is a portion of the minus 300 μm fraction that is important to workability. Excessive fines will cause mix to be sticky, particularly if cement content is high
Cohesiveness	Will tend to reduce cohesiveness, but coarser sands are suitable in rich mixes	Will influence cohesiveness since they tend to have a larger fines content	Fines content largely governs mix cohesiveness. Type of fines is also important
Segregation	Tend to promote segregation by increasing workability without contaminant increase in cohesiveness	Adequate proportion of minus 300 μm fraction helps control segregation	Helps to control segregation by making mix more cohesive
Bleeding	Tend to increase bleeding by reducing specific surface	Better able to control bleeding provided it has adequate fines content	Bleeding largely controlled by fines content. Inadequate fines lead to bleeding

*FM: Fineness Modulus.

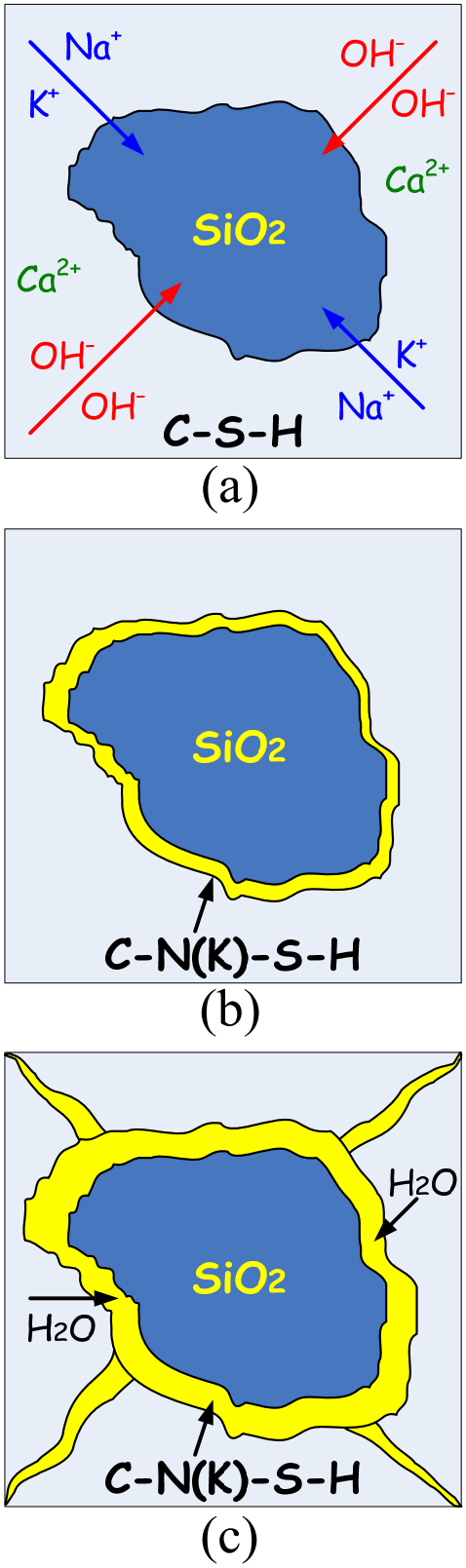

Figure 2-1: Mechanism of ASR [Thomas et al., 2007a].

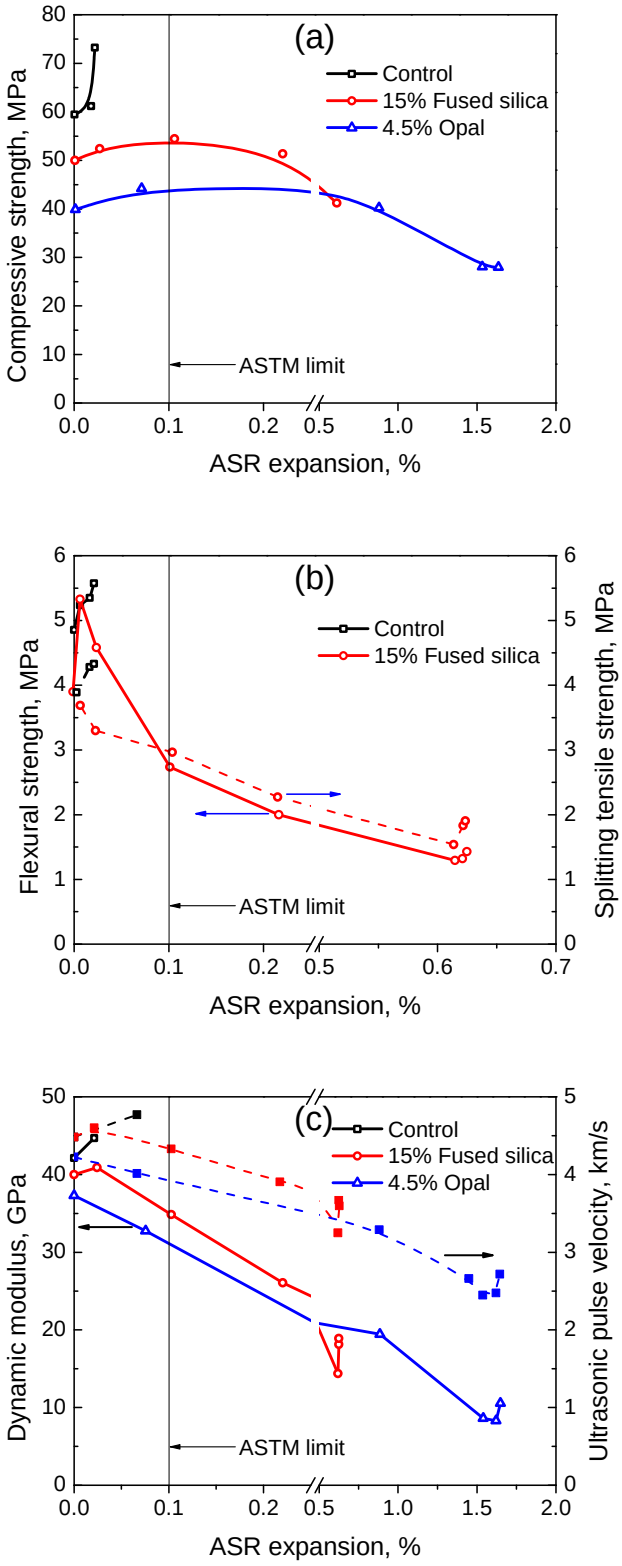

Figure 2-2: Loss in engineering properties of concrete due to ASR [Swamy and Al-Asali, 1989].

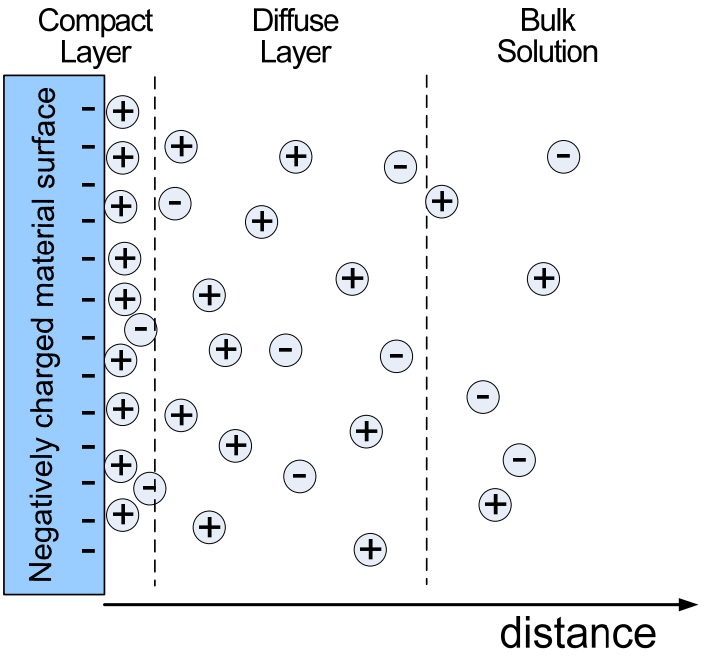

Figure 2-3: Double layer theory [Prezzi et al., 1997].

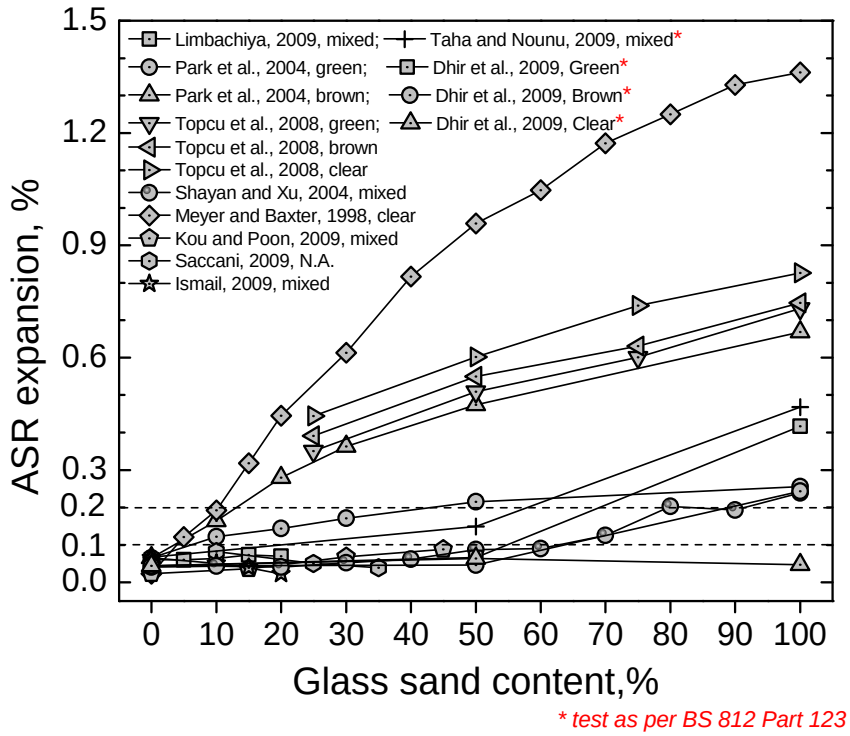

Figure 2-4: Literature review of effect of glass sand content on ASR expansion.

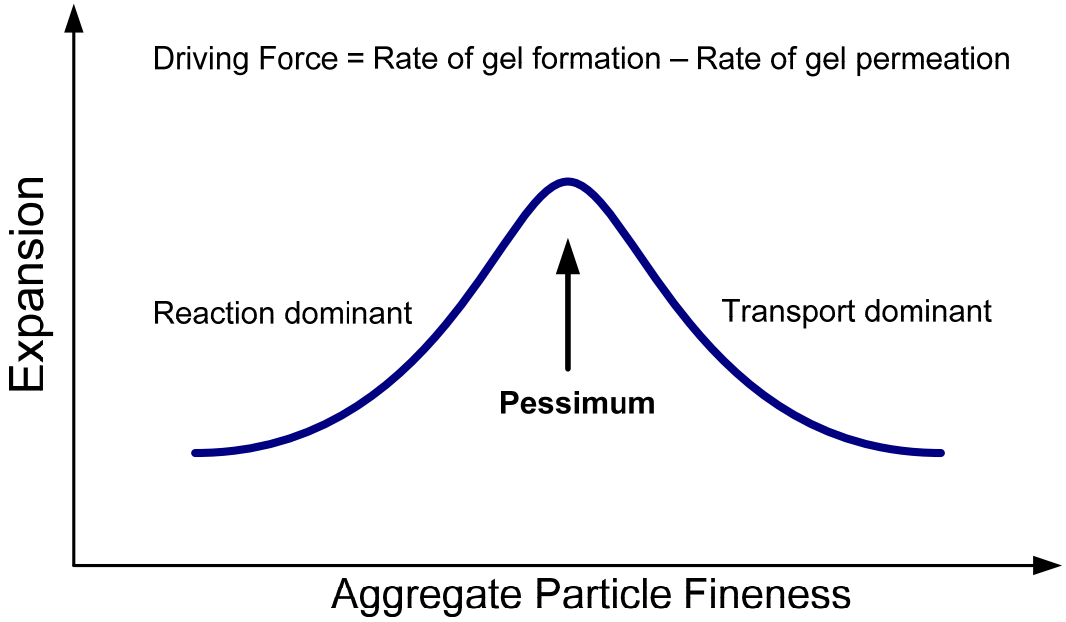

Figure 2-5: Illustration of pessimum effect of glass particle size by Jin et al. [2000].

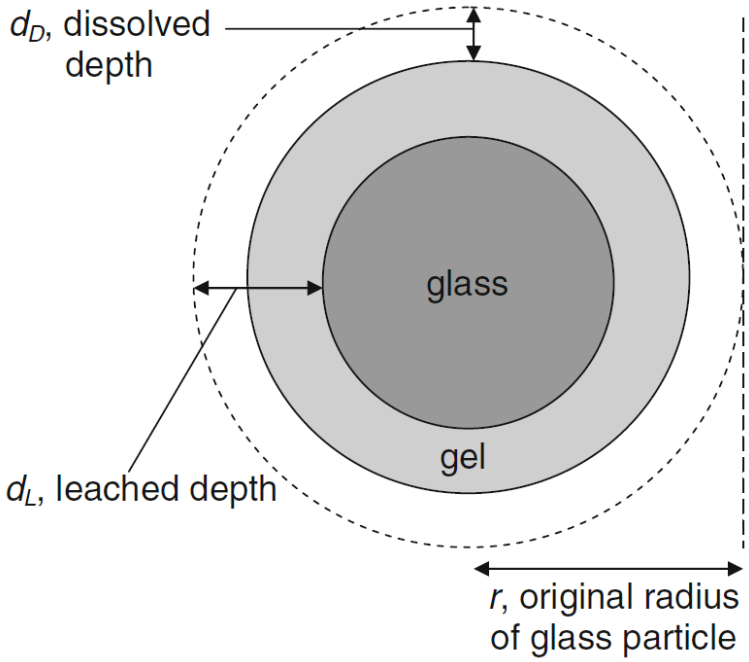

Figure 2-6: Leaching and dissolution of a particle of glass according to Dhir et al. [2009].

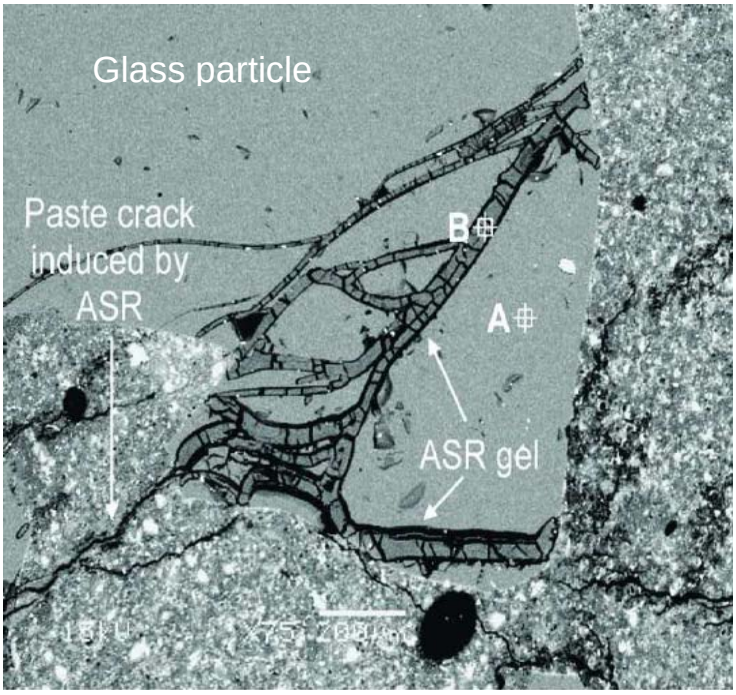

Figure 2-7: SEM image of mortar with brown glass sand [Rajabipour et al., 2010].

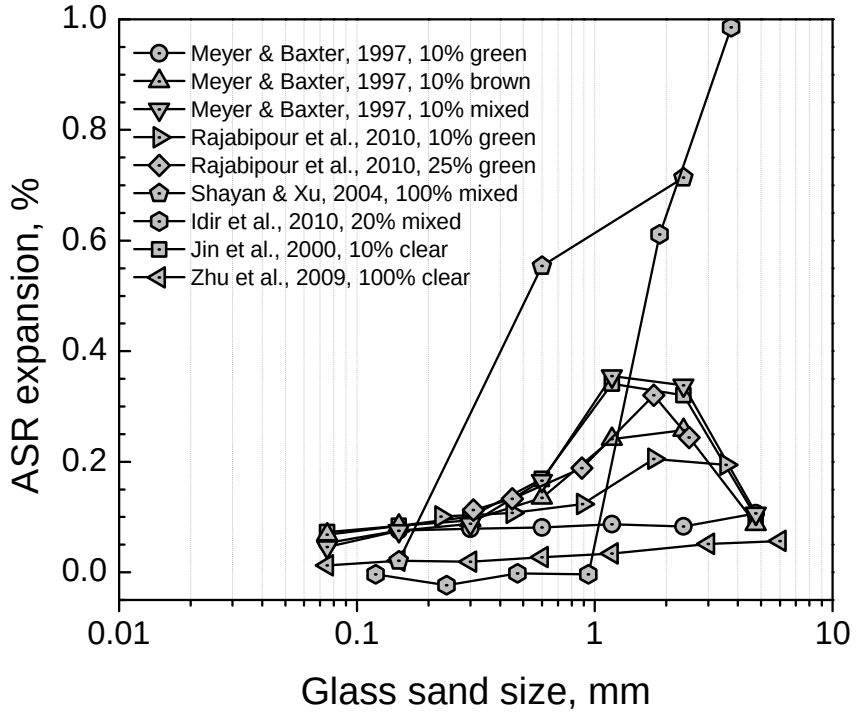

Figure 2-8: Literature review of influence of glass sand size on ASR expansion.

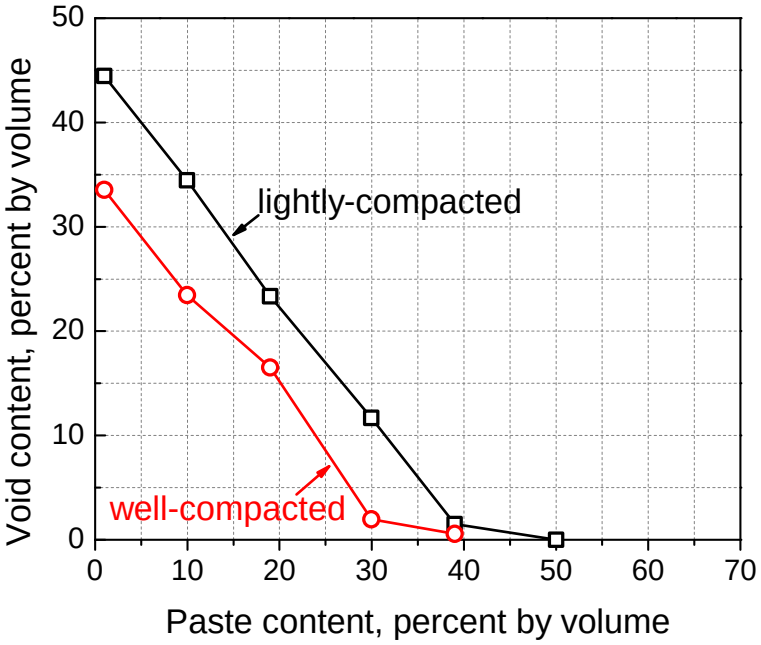

Figure 2-9: Relationship between paste and void content for No. 8 aggregate size designations [ACI 522R].

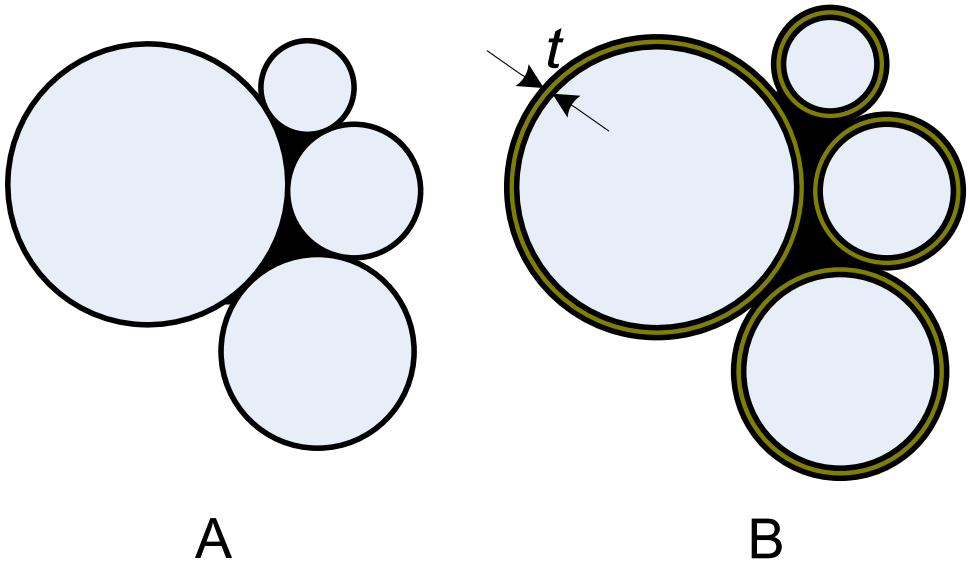

Figure 2-10: Illustration of excess paste theory [Kennedy, 1940].

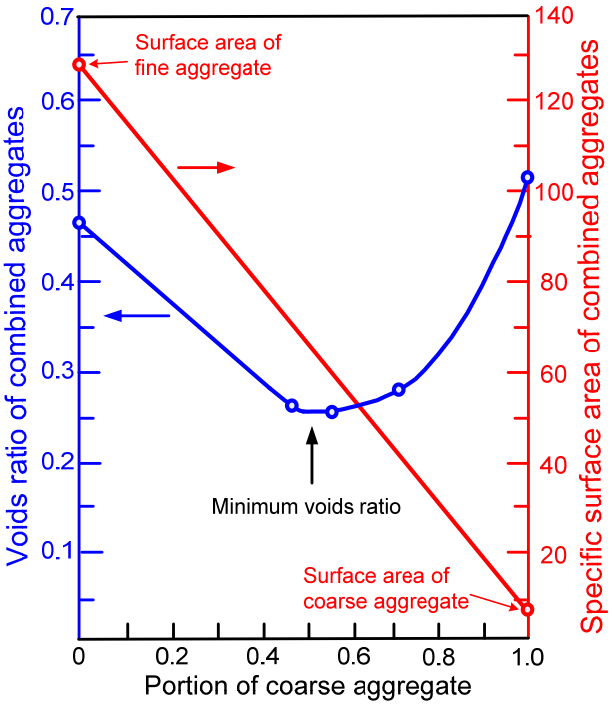

Figure 2-11: Void ratio as functions of the proportion of coarse aggregate [Powers, 1968].

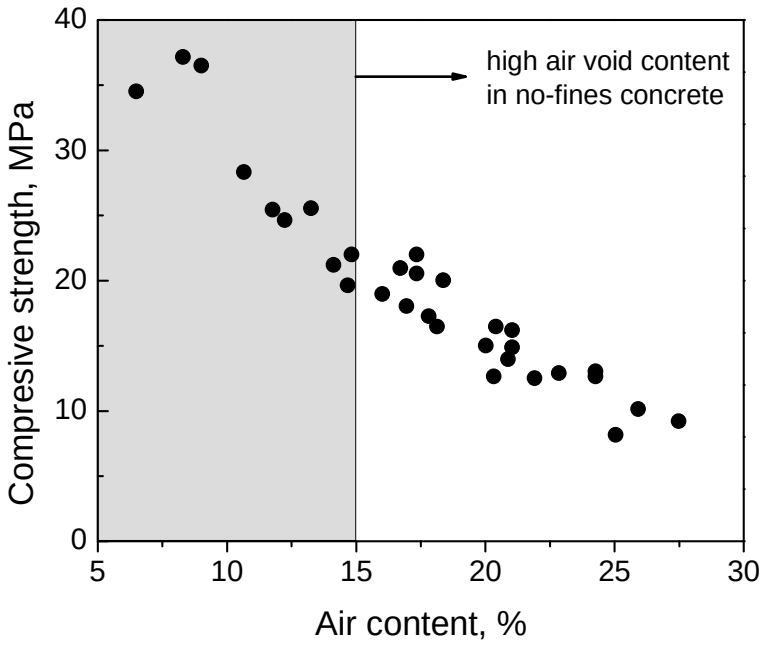

Figure 2-12: Relationship between air content and compressive strength for no-fines concrete [ACI 522R].

Chapter 3. Glass Sand Cementitious Composites

3.1 General

This chapter studies the use of recycled waste glass as sand in both mortar and concrete, starting with the processing of waste glass from as received bottles into purpose-fitted sand. Diverse properties in fresh and hardened states are presented for mortar and concrete. Durability of glass mortar and concrete is also included, with an emphasis on alkali-silica reaction and its mitigation methods. Finally, discussions on the test results are presented.

3.2 Processing of Recycled Glass and Properties

3.2.1 Collection and Crushing

In this study, only soda-lime glasses were used from waste glass bottles, collected from a local recycler. Of all the types of glasses, the soda-lime glass is the only one that matters in the waste due to its popular and large quantities of use. Concerning safety, only unbroken glass bottles were chosen, avoiding broken bottles or debris. Those bottles were originally used for beer, wine, cooking sauces, or other domestic purposes. Glass for these purposes is primarily produced in three colors: clear, green and brown. Clear glass is produced from clean quartz sand with low content of iron oxides, since these may give the glass a vague color. Green glass is colored by oxides of Cr and Co, while brown glass is produced by adding oxides of Mn, Fe, Ni, and Co [Christensen and Damagaard, 2010]. The glasses bottles were exactly the same as what they would be stored in recycling plant before disposal into landfills, with residua, dirt, toxic water or other chemical contaminations from other kinds of wastes (as-received status, see **Fig. 3.1a**).

Before crushing, the glass bottles were cleaned by water by the following steps.

(1) Immerse glass bottles into tap water for 1 day (**Fig. 3.1b**);

(2) Remove metal/plastic caps and neck-caps, wooden corks, as well as plastic/paper labels;

(3) Clean the surface of glass bottles with tap water.

(4) Separate the glass bottles by different colors (**Fig. 3.1c**);

It should be mentioned that dirt and chemical contaminations could be removed, provided that they were water-dissolvable. However, they could retain on the surface if they were not, like glue, oil, cooking sauce, etc, since no detergent was used in this process. In such cases, the properties of glass, mainly the chemical composition, would be affected. The degree of contamination of glass was found to be directly related to its original use. Usually, if the bottle is used for water-dissolved liquid, negligible contaminations would be left after water washing. In the opposite, the glasses would be contaminated to a higher degree if they were used to contain water-indissolvable materials. Considering the local use of glass products, green and brown glass bottles are mainly used for beer and wine, clear glass bottles would be used in versatile ways, such as wine, medicine, oil and cooking sauces. Therefore, clear glass bottles were contaminated glass rather than brown or green glass bottles.

The crushing process was implemented by a jaw crusher (**Fig. 3.1d**), the output size of which could be manually adjusted. Glass bottles were efficiently reduced in size into the required range for sand by ASTM C 33 (see **Fig. 3.1e**). The crushed glass sand fell well into the required ASTM grading range, as shown in **Fig. 3.2**. **Fig. 3.1e** shows the crushed glass sand, which would exhibit angular shape, sharper edge, smooth surface texture and higher aspect ratio than natural sand (**Fig. 3.1f**), because of its brittle characteristics. The saturated surface dry (SSD) specific gravity and water absorption capacity were determined according to ASTM C 128 as 2.53 and 0.07% (compared with 2.65 and 1.0% for natural sand) respectively. Chemical compositions of glasses

with different colors were analyzed by energy dispersive spectrum X-ray spectroscopy (EDS) and are shown in **Table 3.1**.

3.3 Recycled Glass in Mortar

3.3.1 Test Program

In this study, the glass particles were used to replace natural sand as fine aggregates by 0, 25, 50, 75 and 100 percent in mortar. Fresh and mechanical properties, including fresh density, air content and flowability, compressive strength, flexural strength, splitting tensile strength, static and dynamic elastic moduli as well as drying shrinkage were investigated for glass mortar. Durability properties, in terms of resistance to chloride ion penetration, sulfate attack and ASR, were also carried out. All properties were investigated for mortars containing brown, green, clear and mixed-colored (green: brown=2:1 by mass) glasses. The effects of glass color, content and particle size on ASR expansion were examined in this study. To mitigate the ASR expansion, different methods were investigated. The overall test program is summarized in **Fig. 3.3a**.

3.3.1.1 Materials

Natural sand passing a 4.75-mm sieve was used as reference sand for glass sand mortar. The specific gravity and water absorption capacity of natural sand was 2.65 and 1.0% respectively. The grading curves of fine aggregates are shown in **Fig. 3.2**. Type I ordinary Portland cement (OPC) conforming to ASTM C 150 was used in this study, and the chemical compositions are listed in **Table 3.2** (determined by X-ray fluorescence [XRF]). The equivalent sodium alkali content of OPC, calculated as $Na_2O_{eq}=Na_2O+0.658K_2O$, is 0.6%.

The chemical compositions of Class F fly ash, GGBS and silica fume, added as ASR suppressor, were also analyzed by XRF and are included in **Table 3.2**. **Table 3.3** shows the fineness and density of each material. Smooth steel fibers, with length of 5 mm and diameter of 0.16 mm,

were used as reinforcement to reduce ASR expansion. In determination of the potential pozzolanic characteristics of glass, glass particles were further finely ground to less than 75 μm and used as partial cement replacement. Solid lithium chloride (LiCl) and lithium carbonate (Li_2CO_3) were used as additional chemical admixtures for ASR mitigation.

3.3.1.2 Mix Proportions and Test Methods

Except for the ASR tests, mix proportion of mortar was selected in accordance with ASTM C 109, with water: cement: sand = 0.485: 1: 2.75, by mass. The natural sand was replaced by recycled glass particles at 0, 25%, 50%, 75% and 100%, by mass, for each tested property. There were totally five mixtures for each color glass, from which various mortar properties were studied. In addition, mixed color sand (with green-to-brown glass= 2:1 by mass) was also examined as for single color glass. All the tests were carried out as per corresponding ASTM standards (see **Table 3.4**). No superplasticizer was added in mortar mixture.

According to ASTM C 1260, the mortar proportion is as follows, water: cement: sand = 0.47: 1: 2.25, by mass. The grading requirement for sand is shown in **Table 3.5**. For each color, the natural sand was replaced at five levels: 0, 25%, 50%, 75% and 100%. One series of mortar containing 100% glass sand with green-to-brown mixing ratios of 3:1, 2:1, 1:1, 1:2 and 1:3 were also studied. For every ASR mitigating method with single color glass, there were five mixtures with different glass sand content up to 100%. The content of pozzolans used as cement replacement was 30% for fly ash, 60% for GGBS and 10% for silica fume by mass, respectively. Ground glass powder was also used as cement substitution to mitigate ASR, at content of 20%. The added amount of steel fibers used was 1.5% by volume of mortar. The addition of LiCl and Li_2CO_3 compounds was 1% of cement by mass. Regarding LiCl, the content of chloride ion was 0.84% of cement by mass, lower than 1.0%, the limit for reinforced concrete under exposure class of C0 [ACI 318]. The solid lithium compounds were dissolved in the mixing water and thus added to mortar mix. During mixing, the carbonated lithium would not be totally dissolved in the

mixing water due to its low solubility. Therefore, all the solid particles should be poured into the mixer with no residue attached to the container wall. Mix proportions of mortar for ASR expansion study are summarized in **Table 3.5**.

3.3.1.3 Preparation of Mortar Specimens

The dimensions, numbers and tested properties of mortar specimens are summarized in **Table 3.4**. All the mortar specimens were covered with plastic sheets for 24 h after casting, followed by demolding and curing in water until the age of tests, including RCPT and sulfate attack tests. For the drying shrinkage tests, the mortar specimens were cured in water for three days after demolding and then transferred into a controlled room (30 ˚C and 65% RH) for measurements up to 56 days. For the ASR tests, all specimens were put in 80 ˚C water for one day and the initial length taken before transferring to 80 ˚C 1 N NaOH solution for curing. The expanded lengths were subsequently measured after 7, 14, 21 and 28 days. ASR expansion was reported as the average value obtained from three mortar bars.

3.3.2 Test Results and Discussion

Major properties of mortar containing various contents of glass sand are reported and discussed as follows, at both fresh and hardened states.

3.3.2.1 Fresh Properties

a. Fresh density

For all mortar mixes, no segregation or bleeding was observed during mixing and casting. The fresh density decreased with higher content of glass sand, as shown in **Fig. 3.4a**, due to the smaller specific gravity of glass compared to natural sand. The glass color had no effect on the fresh density, especially when the glass content was less than 75%. The fresh density of mortar with 100% brown, green, clear and mixed colored glass sand was 97, 96, 95 and 97% of that of normal mortar, respectively.

b. Air content

The air content of glass sand mortar was between 3 and 3.5%, increasing slightly with higher glass sand content up to 75% (**Fig. 3.4b**). With 100% glass sand, clear glass mortar showed the highest air content of 5.9%, almost twice of that of reference mortar. The results in this study are in agreement with those of Park et al. [2004]. The sharper edge and higher aspect ratio of glass sand enable more air to be retained at the surface of glass particles. It is also noted that the high air content contributed to the low density in mortars with 100% glass sand.

c. Flow

The flowability of glass mortar was reduced, as shown in **Fig. 3.4c**. The flow is defined as the increase in mortar base diameter after 15 times of drop on a flow table (expressed as the percentage of the original base diameter). For glass sand content less than 75%, there was no difference in flow between different colors glass. The flow for complete brown, green, clear and mixed color glass mortar was 75, 90, 60 and 82%, respectively. The sharper edge, angular shape and higher aspect ratio of glass particles reduced the flowability of mortar by hindering the movement of cement paste and the particles. In addition, the increased surface area of glass sand compared to nearly round natural sand would require more paste to coat and lubricate and more water to wet all glass particle surfaces.

3.3.2.2 Mechanical Properties

a. Compressive strength

Fig. 3.5 shows the 7- and 28-day compressive strength of glass mortar. The addition of glass sand led to a decrease in compressive strength due to its smooth surface and sharper edge, which resulted in weaker bond strength at the Interfacial Transition Zone (ITZ) between glass particles and cement paste matrix, which normally dominates the mechanical and durability properties of cementitious compositions. The green glass mortar showed the least reduction in compressive strength at each replacement ratio. Mortar with mixed color glass sand showed comparable

strength as those with brown glass sand. Clear glass sand manifested the most reduction in the compressive strength, perhaps due to a higher degree of chemical contaminations. In addition, the compressive strength was not significantly affected by glass sand if the content was less than 25%. The strength development of mortar with glass sand was slightly higher than that of reference mortar. At 7 days, mortar with 100% brown, green, clear and mixed glass sand showed strength equal to 72%, 75%, 60% and 70% of reference mortar, respectively. At 28 days, this ratio became 78%, 87%, 64% and 76%. The pozzolanic characteristic of fine glass particles (<1.18 mm) might be the reason, which occurs at a later stage and refines the microstructure, thereby reducing the porosity and enhancing the bond strength at the ITZ.

b. Flexural strength

Fig. 3.6 shows the flexural strength of glass mortar at 7 and 28 days. The reduction in flexural strength was obvious for glass sand content exceeding 25%, especially in the case of clear glass. For the other types of glasses, the reduction in 28-day strength was smaller than 10% if the glass content was less than 75%. The flexural strength of complete brown, green, clear and mixed glass sand mortar was 71%, 76%, 64%, 70%; and 76%, 90%, 70%, 76%, respectively, of that of reference mortar at 7 and 28 days. The reduction in flexural strength was similar to that of compressive strength, and was also due to the weakened bond at ITZ. The chemical contaminations in clear glass were expected to further affect the bond strength between clear glass particles and cement paste, resulting in even lower flexural strength.

c. Splitting tensile strength

The splitting tensile strengths of glass mortar at 28 days are shown in **Fig. 3.7**. The waste glass mortar exhibited splitting tensile strength between 2.85 and 3.95 MPa. With 25% of brown, green, clear and mixed glass sand, the splitting tensile strength of mortar showed a slight increase. However, higher percentages of glass sand led to reduced splitting tensile strength regardless of the glass color. For clear glass mortar, the splitting tensile strength decreased

consistently with the glass content. The splitting tensile strength relative to the reference mortar without glass sand was 93%, 92%, 77% and 79%, respectively, for complete brown, green, clear and mixed color glass mortar. Compared to compressive and flexural strength, the reduction in splitting tensile strength was less prominent, probably due to the sharper edge and higher aspect ratio of glass sand associated with higher degree of internal friction [Alexander and Mindess, 2005].

d. Static and dynamic modulus of elasticity

The static and dynamic modulus of elasticity of glass mortar, determined at 28 days, are shown in **Fig. 3.8**. The static and dynamic modulus of mortar varied from 23 to 30 GPa and 27 to 36 GPa, respectively. The glass sand caused an obvious reduction in the modulus of elasticity in the case of clear glass. With other color glass sand, the reduction was less, especially for glass content of up to 50%. At a glass content of 100%, the static elastic modulus of brown, green, clear and mixed glass mortar was 97%, 93%, 80% and 88% of that of reference mortar. For the dynamic modulus, they were 90%, 92%, 77% and 89%, respectively. Although the elastic modulus of glass is higher than sand [Yang et al., 1995], the weaker bond and porous microstructure at ITZ in glass mortar would lead to lower modulus, especially in clear glass mortar. The existence of micro-cracks in clear glass sand particles would further lower the elastic modulus of mortar. Brown, green and mixed glass mortar, on the other hand, only showed slightly reduced modulus. Compared with other mechanical properties, the elastic modulus was the least affected.

e. Drying shrinkage

The drying shrinkages of mortar specimens with mixed color glass are shown in **Fig. 3.9**. All mortar mixes showed stable drying shrinkage after 21 days, indicating that the dimension and surface of mortar specimens were appropriate and accessible for movement and diffusion of moisture to surface and outer environment. All mortar mixes had drying shrinkage less than 700

$\times 10^{-6}$ at 56 days. The reference mortar had the highest drying shrinkage, compared with all glass mortars, suggesting that the replacement of sand by glass particles improve the dimension stability of mortar. The reduced shrinkage could be due to the negligible water absorption capacity of glass particles [Edward, 1966, Alexander and Mindess, 2005; Kou and Poon, 2009; Wang and Huang, 2010; Ling et al., 2011]. The In addition, the relatively higher volume fraction of fine aggregates in glass mortar might also contribute to smaller drying shrinkage. However, mortar with 75% glass sand showed the lowest drying shrinkage while 100% showed intermediate values. The reason might be due to the porous microstructure at ITZ and higher portion of finer particles in glass sand, which incurred the movement of moisture.

3.3.2.3 Durability Properties

a. Rapid chloride permeability test (RCPT)

The RCPT results at 28 days are shown in **Fig. 3.10**. All the mortar specimens showed quite high values of total charge passed, with the reference mortar showing the highest of 6764 (±966) Coulombs, due to the porous structure of cement paste and the lack of coarse aggregates. The total charge passed in 25%, 50%, 75% and 100% brown, green, clear and mixed glass mortar was 94, 93, 85 and 42%; 91, 69, 57 and 42%, 84, 71, 63 and 68%, and 82, 64, 36, and 44%, respectively, of that of reference sand mortar. The resistance of mortar to chloride ion penetration seemed to increase due to the lower porosity and permeability of glass sand [Scholze, 1990], in spite of the more porous ITZ microstructure. Another possible reason is the finer size distribution of crushed glass sand, leading to better packing efficiency of mortar at the fine scales[Kou and Poon, 2009], and pozzolanic reaction which consumed OH^- and improved impermeability. Contrary to mechanical properties, mortar with clear glass sand did not show the poorest performance in RCPT, especially at 25%, 50% and 75% glass content. Instead, brown glass mortar showed the least resistance at such glass contents. Mixed color glass mortar

exhibited the highest resistance while green glass mortar showed intermediate resistance to chloride ion penetration.

According to nordtest method NT build 492, the non-steady-state migration coefficient D_{nssm} of chloride is calculated as

$$D_{nssm} = \frac{0.0239(273+T)L}{(U-2)t}\left(x_d - 0.0238\sqrt{\frac{(273+T)Lx_d}{U-2}} \right) \quad (3.1)$$

where D_{nssm} = non-steady-state migration coefficient, $\times 10^{-12}$ m^2/s;

U = absolute value of the applied voltage, V;

T = average value of the initial and final temperatures in the anolyte solution, ˚C;

L = thickness of the specimen, mm;

x_d = average value of the penetration depth, mm;

t = test duration, h.

In this study, a voltage of 60 V was applied for 6 hours. At the end of the test, the specimens were axially split to measure the depth of chloride penetration, x_d, by spraying with 0.1 N $AgNO_3$ solution. The reported result of non-steady-migration coefficient was the average of three specimens and shown in **Fig. 3.10.** The migration coefficient for brown, green, clear and mixed color glass, at 25, 50, 75 and 100% glass content, was 94, 104, 83 and 68%; 75, 59, 55 and 46%; 88, 73, 52 and 61%; and 80, 59, 37 and 36% of that of the reference sand mortar. The calculated migration coefficients verified the RCPT results that glass sand would increase the resistance to chloride ion penetration. Also, the effect of glass color was confirmed by the values of the migration coefficient. That is, mixed color glass mortar had the lowest chloride migration coefficient while clear glass mortar exhibited intermediate result, at contents of 25, 50 and 75%. The detrimental effect of internal micro-cracks in clear glasses was not obvious. This is because unlike mechanical properties, the chloride conductivity would not be affected if the crack is less than 200 μm wide [Aldea et al., 1999].

b. Sulfate attack

After curing in water for 28 days, three mortar prisms and three cubes were weighed (SSD) before immersion in saturated $MgSO_4$ solution for 24 hours, followed by oven-drying at 105 ˚C for the next 24 hours. The wet-and-dry procedure was repeated for 10 cycles and the weight loss, compressive strength and flexural strength were recorded. The results are shown in **Fig. 3.11**. All glass mortars showed comparable weight loss regardless of glass color. Visual observation (**Fig. 3.12**) of the specimens revealed that the exterior cement paste was dissolved, exposing the glass sands. The compressive strength of brown, green, clear and mixed glass mortar, at the glass content of 25, 50, 75 and 100%, was 106, 100, 93 and 98%; 121, 118, 124 and 115%; 98, 81, 81 and 78%; 115, 104, 113 and 97% of that of control mortar mix. The flexural strength was 103, 88, 88 and 90%; 107, 109, 99 and 92; 90, 75, 79 and 72%; and 98, 89, 98 and 81% of that of reference mortar. Clear glass mortar exhibited the lowest compressive strength and flexural strength after the sulfate attack tests, while green glass mortar exhibited the highest resistance to sulfate attack. It is noted that the glass mortar exhibited higher compressive strength after sulfate attack tests compared to those cured in water for 28 days (see **Section 3.3.2.2a** and b). This is because of the lesser porosity and better packing efficiency at finer scales [Kou and Poon, 2009], as well as pozzolanic reaction of glass particles, leading to reduced permeability of mortar.

3.3.3 Alkali-Silica Reaction in Glass Mortar

3.3.3.1 Effect of Type, Content, and Size of Glass Sand

a. Effect of glass type and content

The ASR expansions of mortar with green, brown, clear and mixed color glass sand are shown in **Figs. 3.13a-c**. At 14 days, mortar containing natural sand showed 0.053% in expansion, mortar with 25%, 50%, 75% and 100% green, brown and clear glass sand showed 0.036, 0.022, 0.012 and 0.005%; 0.032, 0.020, 0.009 and 0.009%; 0.049, 0.065, 0.128 and 0.137%, respectively. With increasing content of glass sand, ASR expansion increased substantially for clear glass

mortar but not so for green and brown glass mortars. At the same replacement content, green and brown glass sand mortar would show similar ASR expansions, indicating that the green and brown color glass had the same reactivity with alkali within 28 days. Some researchers [Jin et al., 2000; Park and Lee, 2004] pointed out that green color glass would be the least reactive in ASR due to its highest content of Cr_2O_3, which is added for greenish color. In this study, this effect was clearly observed, when one compares the results for green and clear glass mortar. In addition, in spite of the less content of Cr_2O_3, brown glass mortar also exhibited similarly small ASR expansion as green glass mortar due to the Fe_2O_3, which is added to give brownish color to the glass. Based on the double-layer theory [Prezzi et al., 1997], the higher valence of Cr^{3+} in green glass and Fe^{3+} in brown glass will lower the double-layer thickness and the repulsion forces, resulting in the much lower ASR expansion than clear glass mortar. However, Dhir et al. [2009] attributed the different alkali resistance of different colored glasses to the manufacturing process, rather than the minor chemical difference, as discussed earlier.

In this study, the results showed that clear glass would accelerate ASR expansion of mortar but remain innocuous (i.e. expansion less than 0.2%) if the total sand replacement content was less than 50%. Green and brown glass would suppress the ASR between glass sand and alkali, indicating that they were non-reactive. At 28 days, the reference mortar showed expansion of 0.149% and mortar with 25%, 50%, 75% and 100% of green, brown and clear glass sand showed expansion of 0.136, 0.074, 0.070 and 0.030%; 0.131, 0.059, 0.026, and 0.012%; and 0.120, 0.212, 0.471 and 0.705%, respectively. This is in contrast to some published results [Shayan and Xu, 2004, Taha and Nounu, 2009; Topcu et al, 2008; Park and Lee, 2004, Meyer and Baxter, 1997; Kou and Poon, 2009; Limbachiya, 2009; Ismail and Al-Hashimi, 2009; Saccani and Bignozzi, 2010; Zhu et al., 2009; Rajabipoour et al., 2010], as shown in **Fig. 3.14**.

Shi [2009] reviewed the ASR in glass concrete and proposed that the mechanism of expansion in concrete caused by glass sand was different from that by traditional ASR expansion

[Rajabipoour et al., 2010]. According to Shi [2009], Na^+ and Ca^{2+} are firstly dissolved from glass when the OH^- in pore solution attacks the glass particle surface, followed by the depolymerization of silicate network. The reaction, as shown in **Eq. (3.2)**, then occurs to form ASR gel of C-N-S-H:

$$Ca^{2+} + Na^+ + \left[SiO(OH)_3\right]^- \rightarrow C-N-S-H \quad (3.2)$$

The swelling capacity of the ASR gel depends on its chemical composition, especially on the ratio of $CaO/(SiO_2+Na_2O)$ [Tang et al., 1987]. It is speculated that in the ASR gel produced in soda-lime glass, the content of calcium is relative higher than other types of glass or natural sand. Therefore, the non-swelling ASR gel in glass mortar would lead to lesser expansion. The same statement was also made by Saccani and Bignozzi [2010].

b. Effect of mixed color glass

To determine the glass color effect, ASR expansion of mixed color glass sand, with green glass: brown glass=2: 1, by mass, was tested at 25, 50, 75 and 100% glass content and the results are shown in **Fig. 3.13d**. The mixed color glass mortar showed similar ASR expansion as single color glass mortar, decreasing with higher glass sand content. The effect of combining two different color glasses, on ASR at different sand replacement content, is in disagreement with previous results [Jin et al., 2000], which stated that the mixed color glass mortar caused larger expansion than single color glass mortar. The effect of mixed color glass sand was also tested at 100% level with green glass: brown glass ratio varying as 3:1, 2:1, 1:1, 1:2 and 1:3, as well as complete green or brown glass sand, as shown in **Fig. 3.13e**. From the test results, it is hard to relate the ASR expansion of mixed color glass mortar from those of single color glass mortars. At early ages less than a week, the mixed color glass mortars showed almost the same expansion, but slightly less than the pure green or brown glass sand mortar. However, this trend reversed as the mixed glass sand mortar expanded more than single glass sand mortar in the following week. The test results for the third week showed no difference between different mix ratios. At the end

of 4th week, the ASR expansion decreased with higher fraction of brown glass sand. At the same time, it should be noted that all the mortars exhibited small expansion, in spite of the inconsistent trend with varying color mix ratios. However, it is interesting to note that a great difference between green and brown glass mortar started emerging at 63 days of testing. A higher fraction of green glass sand could result in a much higher ASR expansion, indicating that brown glass would exhibit less alkali reactivity especially in the long term, which has not been reported before.

c. Effect of glass particle size

The effect of glass particle size on ASR expansion of green, brown and clear glass sand mortars are shown in **Fig. 3.15**. For each color glass, there are in total 5 different single-sized glass sands, including 2.36, 1.18, 0.6, 0.3 and 0.15 mm, to replace 25% of natural sand. All the three colored glass mortars showed the same trend, that is, ASR expansion continuously increased with increasing size of glass sand, at each test age. The maximum and minimum ASR expansion occurred with 2.36 mm and 0.15 mm-size glass sand respectively, regardless of glass color. Mortar with 25% graded glass sand, as specified by ASTM C 1260 for sand grading, showed intermediate expansion (**Figs. 3.13 a-c**) compared to single-size glass sand mortars. From the test results, single-size green and brown glass mortars showed reduced ASR expansion than normal sand mortar (0.053%), while single-size clear glass showed increased ASR expansion if it was larger than 0.6 mm. These can be explained by the alkali non-reactivity of green and brown glass and alkali reactivity of larger particles of clear glass. Once again, brown glass, particularly of larger sizes, showed less ASR expansion than green glass at any age, as previously noted on the effect of glass content on ASR expansion.

It is expected that the finer the glass sand, the higher the ASR expansion because of increasing surface area of sand particles. However, the experimental results showed the opposite trend. Moreover, there was no pessimum effect of glass sand size on ASR expansion, which is different

from previous findings by Jin et al. [2000]. This can be attributed to the pozzolanic reaction between silica in glass sand and cement hydration product, $Ca(OH)_2$ [Dyer and Dhir, 2001; Shi, 2009]. However, the pozzolanic reaction would not occur if the glass sand was too large. In this study, it can be noted that if glass sand was smaller than 2.36 mm, pozzolanic reaction would occur since the ASR expansion started decreasing from 2.36 mm till 0.15 mm. Without pozzolanic reaction, the ASR expansion should be higher with decreasing particle size due to larger surface area. This critical particle size for pozzolanic reaction to occur was differently observed as 0.6-1.18 mm by Idir et al. [2010], Jin et al. [2000] and Xie et al. [2003]; or 0.15-0.30 mm by Yamada and Ishiyama [2005]. Test results in this study as well as results from literature are summarized in **Fig. 3.16**.

Recently, Rajabipour et al. [2010] and Maraghechi et al. [2012] have stated that the glass ASR is actually not a surface reaction, but a pozzolanic reaction, regardless of glass size. It was found that ASR expansion resulted from internal cracks was more prominent for brown glass. The product of the pozzolanic reaction at glass particle surface is non-swelling due to the low SiO_2/CaO ratio, while the ASR expansion occurs inside glass particles, with OH^- ions penetrating through the cracks in the glass particles where the SiO_2/CaO ratio is higher. This conclusion is confirmed from expansion tests and SEM observations.

In this study, internal cracks were clearly observed in clear glass sand (**Fig. 3.17a**). No crack was found for green or brown glass sand mortar, especially at 100% content (**Fig. 3.17b**). In summary, the influence of clear glass particle size would be attributed to the following reasons: (1) pozzolanic reaction occurs more easily with finer particles; and (2) larger glass particles exhibit more inherent cracks which initiate expansive ASR gel. In contrast, for green and brown glass, only the first was true since no inherent crack was observed in the glass particles.

The relation between ASR expansion and glass sand size is significant for the study of ASR expansion with random size distribution of crushed glass sand. Based on the results, it can be concluded that ASR expansion decreases with smaller glass particles, provided that it is finer than 2.36 mm. Therefore, an effective method to mitigate ASR expansion of glass concrete is to control the crushing process to ensure the size of glass particles is less than 2.36 mm. The relation of ASR expansion between multiple-size glass mortar and single-size glass mortar could be assumed to be proportional to the individual mass fraction. From the ASR expansions of single sizes of different color glass, the brown color glass sand would exhibit the least expansion than green glass and clear glass. This was consistent with the ASR expansion of multiple-size glass sand mortar, as discussed earlier regarding color effect. With more fine glass particles at the surface of mortar bar specimens, more pores would be refined by pozzolanic reaction. The permeability of mortar would be decreased, resulting in less supply of alkalis to mortar specimens in the tests.

3.3.3.2 Mitigation Methods

To suppress the potential ASR in mortar containing glass sand, different mitigation methods are investigated, including mineral admixtures, chemical admixtures and additional reinforcements. For each mitigation method, the amount was selected according to its common use as in normal concrete. In this study, the content of cement replacement by mass was 30%, 60% and 10% for fly ash, GGBS and silica fume, respectively. The addition of LiCl and Li_2CO_3 was 1% of cement by mass. The amount of steel fibers was 1.5% by volume of total mortar mixture.

a. Fly ash

The effect of replacing 30% of cement by class F fly ash on ASR expansion of green, brown and clear glass sand mortar at different contents are shown in **Tables 3.7-9**. The suppressing effect of fly ash on ASR expansion is so obvious that the expansion at 14 days was less than 0.02% for all mixtures, significantly lower than 0.1%, as required by ASTM C 1567 for innocuous reaction.

The ASR expansion was quite small up to 28 days. The most significant effect of fly ash is the dilution of active alkali content in cement since only active alkali involves in ASR [Alexander and Mindess, 2005]. Also, the microstructure of mortar, especially near the surface, was improved by pozzolanic reaction of fly ash, thus the porosity and permeability was reduced. Although the amount of alkali in the 1 N NaOH solution would have been sufficient for ASR, the pathway for alkali and water to penetrate into the interior of mortar specimens was clogged and thus the ASR was suppressed.

After 28 days of curing, the surface of all mortar bars remained quite smooth and no crack was observed. The surface of mortar bar, around 1 mm deep, appeared to be more densified than the interior structure, preventing alkali from penetrating inward. Xu et al. [1995] observed the same test results in accelerated mortar bar tests, in which the reaction was confined merely to a few small particles close to the exterior surface of the specimens with no signs of reaction in the center portion of mortar bar specimens [Xu et al., 1995].

The test results showed that 30% fly ash is more than sufficient to suppress ASR expansion caused by recycled glass sand.

b. GGBS

The effect of replacing 60% of cement by GGBS on ASR expansion of green, brown and clear glass sand mortar at different contents are shown in **Tables 3.7-9**. At 14 days, the reference mortar (60% GGBS with no glass sand) showed expansion of 0.018%. The ASR expansions for green, brown and clear glass sand mortar were 0.016, 0.007, 0.006 and 0.006%; 0.002, -0.002, -0.001 and -0.001%; 0.007, 0.008, 0.004 and 0.006%, for 25, 50, 75 and 100% content, respectively. The suppressing mechanism for GGBS on ASR expansion was similar as for fly ash; pozzolanic reaction of GGBS would reduce porosity of paste and Interfacial Transit Zone (ITZ). Also, according to the double-layer theory [Prezzi et al., 1997], the mineral admixtures

could not only reduce the aggressiveness of the pore solution to the acidic aggregates but also reduce the negative surface charge of the glass particles by lowering the pH value of the pore solution in cement paste. The lower the ionic concentration and the surface charge of the particle, the smaller the expansive pressure that can develop for the ASR product gels.

c. Silica fume

The effect of replacing 10% of cement by silica fume on ASR expansion of green, brown and clear glass sand mortar at different contents are shown in **Tables 3.7-9**. At 14 days, the reference mortar (10% silica fume with no glass sand) showed expansion of 0.020%. The ASR expansions for green, brown and clear glass sand mortar were 0.033, 0.018, 0.013 and 0.018%; 0.021, 0.018, 0.015 and 0.013; and 0.021, 0.025, 0.021 and 0.017%, at glass content of 25, 50, 75 and 100%. All the mortars showed expansion much less than 0.1%.

The suppressing effect of silica fume on ASR could be primarily attributed to its ultra fine particle size, which is good for improving the porous microstructure at ITZ and thus reduces porosity and increases strength. The size, distribution and continuity of pores inside the paste could significantly affect ASR, by the ingress of water and the ions diffusion [Prezzi et al., 1997]. If free water loses the pathway to ingress to the particle surface where active silica is dissolved, the ASR gel formed would not cause any damage since it cannot absorb free water. After 28 days, the specimen surface remained un-cracked and was densified due to pozzolanic reaction, same as observed in fly ash mortar. Nevertheless, the pozzolanic behavior of silica fume would also contribute to the reduction in pH of cement paste, densification of microstructure, and formation of a CSH with a low CaO/SiO_2 ratio [Hasparky et al., 2000].

d. Steel fibers

The effect of adding 1.5%, by volume, of steel fibers on ASR expansions of green and brown glass sand mortar at various glass contents are shown in **Tables 3.7** and **8**. At 14 days, the

expansion of reference mortar (1.5% steel fibers with no glass) was 0.025%. The expansions for green and brown glass sand mortars were 0.019, 0.016, 0.005 and -0.008%; 0.021, 0.008, 0.004 and 0.005%. The performance of green and brown glass sand mortars, with the addition of steel fiber, was identical at the same glass content. All mortars showed expansion less than 0.1%, indicative of the efficiency of the steel fibers. At 21 and 28 days, all mortars did not show expansion higher than 0.1%. The function of steel fibers in restraining ASR in glass sand mortar is the same as in normal sand mortar. The internal pressure created by ASR gel causes ASR expansion and cracking and thus could be suppressed by randomly distributing discontinuous single fibers [Park and Lee, 2004]. Crack fiber interactions resist crack propagation and opening due to the chemo-mechanical confinement on the ASR gel. According to Ostertage et al. [2007], fibers could not only impose compressive stress on the expanding ASR gel but also prevent the ASR gel from leaving the reaction site. However, it should be noted that the addition of steel fibers would reduce the flowability of fresh mortar mixture.

e. Glass Powder

The effect of replacing 20% cement by glass powder on ASR expansion of green and brown glass sand at different glass sand contents are shown in **Tables 3.7** and **8**. The suppressing effect of green glass powder was relatively more prominent than brown glass. At 14 days, the green and brown glass powder mortar showed expansion of 0.031, 0.016, 0.012, 0.010, and 0.004%; and 0.040, 0.025, 0.014, 0.012 and 0.006% for 0, 25, 50, 75 and 100% replacement ratio of glass sand. The constraining effect on ASR expansion for green and brown glass powder may be firstly due to the content of Cr_2O_3 and Fe_2O_3, which could effectively reduce the ASR expansion, as mentioned previously regarding color effect. The suppressing effect of glass powder was more obvious at lower glass sand content less than 50%, especially in the reference mortar mix without glass. Moreover, as discussed earlier on the influence of glass particle size, the finer the glass sand, the less ASR expansion. If the glass sand particle is fine enough, such as less than 0.075

mm, the ASR would be totally eliminated while pozzolanic reaction would occur instead. That was why fine glass powder could replace cement and suppress ASR. Taha and Nounu [2009] attributed the ASR suppressing effect of glass powder to the non-availability of both alkali in concrete and reactive silica in glass particles. Dyer and Dhir [2001] explained the chemical reactions of glass powder used as cement component in detail. In the chemical terms, the ASR of glass powder is identical to pozzolanic reaction, except for the time at which each reaction occurs. The fine glass powder has a high surface area and hence favors the rapid pozzolanic reaction over the deleterious ASR. The ASR mitigating use of glass powder as cement replacement could thus widen the application of waste glasses [Shayan and Xu, 2004], resulting in value-added utilization.

f. Lithium Chloride and Lithium Carbonate

The effect of adding 1% LiCl and Li_2CO_3 by weight of cement on ASR expansion of green and brown glass sand mortar at 0, 25, 50, 75 and 100% glass content are shown in **Tables 3.7** and **8**. Green glass sand showed reduced ASR expansion at all glass content, and the effectiveness is more obvious at low glass content. The suppressing effect of Li_2CO_3 is more prominent than LiCl, because of the higher ratio of [Li]/[Na]. The ratio of [Li]/[Na] for 1% LiCl and Li_2CO_3 is 0.74 and 0.84, respectively. For brown glass, the effect of Li_2CO_3 in ASR was similar as for green glass. However, the LiCl did not show any suppression effect in ASR, especially for normal sand mortar. There is a minimum content of lithium compounds required to effectively suppress ASR, below which the expansion would not be reduced but would be higher instead [Collins et al., 2004]. From the test results, the content of lithium compounds used in this study, that is, 1% of cement by mass, is high enough to suppress ASR for green glass but not for brown glass.

So far, the ASR suppressing mechanism of lithium is not well known [Taha and Nounu, 2009]. It was expected that lithium compounds could change the nature and chemical composition of the

ASR gel; reduce the solubility of the reactive silica; and reduce the ability of dissolved silica to be repolymerised and increase the repulsive force between the particles of the ASR gel and thus the expansive ability of the ASR gel will be reduced. Until now, there is no standard to specify the ASR of aggregates with lithium compounds as suppressant.

g. Comparison of different methods

Different ASR suppressing methods are compared, as shown in **Fig. 3.18**, for green, brown and clear glass sand mortars with different glass contents at 14, 21 and 28 days. Fly ash apparently showed the highest reducing effect, followed by GGBS. The restraining effect of silica fume in clear glass sand is much more obvious than in green and brown glass. Both green and brown glass powder showed ASR suppressing effect in glass sand mortar, although the effect was less than fly ash and GGBS. Compared with the substitution of cement, addition of steel fiber or lithium compounds was less effective in reducing ASR expansion. It is suggested that concrete with recycled glass sand should incorporate mineral materials, such as fly ash and GGBS, in preventing potential deleterious ASR expansion, particularly in the case of clear glass. However, the negative effect of such ASR mitigation methods must also be noted. The addition of lithium compound would add to production costs of concrete, although the amount used in this study is low enough to avoid a substantial difference. In addition, the use of fly ash and GGBS could reduce concrete strength at the early age. Moreover, the utilization of steel fibers or silica fume could result in significant decrease in workability, for which superplasticizer would become necessary to maintain the same workability.

3.3.4 Summary

1. Use of waste glass in mortar resulted in higher air content and lower density and flow. It also resulted in lower compressive, flexural and splitting tensile strength, elastic modulus but better dimensional stability. However, the effect was minimal if glass content was

less than 50%. Also, due to a higher degree of contaminations clear glass mortar showed the poorest mechanical performance.

2. Replacement of natural sand by waste glass particles led to higher resistance to chloride ion penetration. With respect to resistance to sulfate attack, glass sand mortar showed results comparable to normal sand mortar.

3. Mortar with clear glass sand exhibited higher ASR expansion and was potentially deleterious if the glass content was higher than 50%; while green and brown glass mortars proved to be innocuous at any glass content. Also, ASR expansion decreased with smaller glass sand size, due to pozzolanic reaction of fine glass particles. Brown glass exhibited the least alkali reactivity, especially in long term, although the reason is not well known.

4. Fly ash and GGBS were the most effective ASR suppressing methods. Addition of steel fibers or lithium compounds was less effective. The effectiveness of different methods, in decreasing order was

   (i) Fly ash, GGBS, Li_2CO_3, Silica Fume, Fiber, Powder, and LiCl for green sand mortar,

   (ii) Fly ash, GGBS, Silica Fume, Fiber, Powder, Li_2CO_3, and LiCl for brown sand mortar, and

   (iii) Fly ash, GGBS, and Silica Fume for clear sand mortar.

5. Green and brown glasses can be used in mortar as fine aggregates without compromising durability properties, regardless of content. For clear glass, ASR could be effectively reduced to acceptable limit using the mitigation methods mentioned above provided that the glass content is more than 25%.

3.4 Recycled Glass in Concrete

3.4.1 Test Program

As shown in **Fig. 3.3b**, properties of concrete containing glass sand as fine aggregates in fresh and hardened states were investigated. They included fresh density, air content and slump; compressive strength, splitting tensile strength and flexural strength, dynamic and static modulus of elasticity and drying shrinkage. In addition, durability in terms of resistance to chloride ion penetration was studied. ASR expansion was also investigated based on accelerated mortar bar test. Moreover, the use of 30% fly ash or 60% GGBS as cement replacement was also studied as ASR mitigation methods for which the compressive strength was also investigated.

3.4.1.1 Mix Proportions of Concrete

Three concrete mixes were designated, according to ACI 211.1, namely C30, C45 and C60, for compressive strength of 30, 45 and 60 MPa at 28 days. The water-cement (*w/c*) ratio was 0.45, 0.38 and 0.32 respectively. The concrete mixes were designed for 100 mm nominal slump, with the use of superplasticizer. For each mix proportion, the natural sand was replaced by glass sand at 0, 25, 50, 75 and 100% by mass. For concrete mixes of different grade, the water and coarse aggregates content were kept constant and the cement content was increased while the sand content decreased with lower *w/c* ratio. In the determination of the properties of glass concrete with mineral admixtures, 30% fly ash and 60% GGBS was used to separately substitute cement by mass in C45 concrete, at each glass sand replacement ratio. There were thus 25 mix proportions in total, as shown in **Table 3.10**.

3.4.1.2 Materials and Test Methods

Compared with the materials used in glass mortar, the only difference for glass concrete is the incorporation of coarse aggregates with maximum size of 19 mm, whose grading is plotted in **Fig. 3.2**. The oven-dry unit weight, specific gravity and water absorption capacity of coarse

aggregate are 1650 kg/m^3, 2.65, and 0.8%, respectively. Apart from compressive strength which was tested following BS EN 12390-3, all the tests were conducted as per ASTM standards as shown in **Table 3.4**. For mixes with fly ash or GGBS, only compressive strength and ASR tests were carried out. It should be noted that the ASR was carried out on mortars screened from fresh concrete mixture. The accelerated mortar-bar tests followed ASTM C 1567 for concrete containing fly ash and GGBS.

3.4.1.3 Preparation of Concrete Specimens

All the concrete specimens were consolidated on a vibration table. For the ASR tests, mortar was collected by sieving the fresh concrete mixture through a 4.75-mm sieve and was then cast into bars. Therefore, the ASR test specimen contained no aggregate particle larger than 4.75-mm. All the specimens stayed in molds with moisture for 24 hours. After demolding, the specimens were thus transferred into a fog room (30 ˚C, 100% RH) until the test age. Regarding drying shrinkage, two prisms were cured in water for 27 days after demolding and then put in controlled room (30 ˚C, 65% RH) for length measurements after 4, 7, 14, 28 and 56 days of drying. For ASR test, the mortar bars were put in 80 ˚C water for 24 hours after demolding, and initial lengths were measured thereafter. They were then transferred into 80 ˚C 1 N NaOH solution and their lengths were measured at the following 4, 7, 10 and 14 days. For long term investigations, the mortar bars were measured weekly till 49 days. The dimensions and numbers of test concrete specimens are summarized in **Table 3.4**.

3.4.2 Test Results and Discussion

3.4.2.1 Fresh Properties

a. Fresh density

The fresh density of glass concrete is shown in **Fig. 3.19**. Fresh density obviously decreased with increasing glass sand replacement ratio and increasing *w/c* ratio. Compared with the specific

gravity of natural sand of 2.65, glass sand had a lower value of 2.53, leading to reduction in density at the same grade. Higher grade concrete mix had a higher proportion of cement which was of a higher specific gravity than sand, contributing to the increase in density. The test results in this study are consistent with other results reported in the literature [Park et al., 2004; Topcu and Canbaz, 2004; Taha and Nounu, 2008].

b. Air content

As shown in **Fig. 3.20**, all concrete mixes had air content between 0.5 and 1.5%. There seemed to be no clear trend in the relation between the air content and concrete grade. The air content did not increase unless the glass sand was higher than 25%. The irregular shape of glass sand gave a larger surface area and thus the concrete was able to retain more air voids. However, on the other hand, the smooth surface area of glass particles would retain less air voids. These two conflicting effects resulted in the minimum air content occurring at a glass content of 25%. The opposite conclusions on air content of glass concrete, by Park et al. [2004] and Topcu and Canbaz [2004], could be explained by these two effects.

c. Slump

In this study, all concrete mixes showed no bleeding or segregation during mixing and casting. All concrete mixes showed slump values of 100±20 mm, meeting the target workability (as shown in **Fig. 3.21**). The dosage of added superplasticizer was constant for each concrete grade, that is, 1.3, 2.6 and 3.6 L/m^3 for C30, C45 and C60 mixes, respectively. There was no clear change in the slump values due to glass sand. Although the sharper edge and more angular shape of crushed glass sand would reduce the slump of concrete [Park et al., 2004; Limbachiya, 2009; Taha and Nounu, 2009], its impermeable smooth surface may also cause poorer cohesion with cement paste [Terro, 2006]. These two opposing actions simultaneously result in non-prominent change on slump values.

Compared to manufactured aggregates and recycled aggregates, one apparent advantage of glass sand is its negligible water absorption. As a result, the glass particles would not absorb water from cement paste, leading to no reduction in workability.

3.4.2.2 Mechanical Properties

a. Compressive strength

The compressive strengths of glass concrete at 7, 28 and 90 days are shown in **Fig. 3.22**. The strength of all concrete mixes increased with time and satisfied the design value at 28 days. At 7 days, compared to the normal concrete, the strength of 25, 50, 75 and 100% glass sand concrete for C30, C45 and C60 were 101(±3), 92(±6), 87(±2) and 93(±6) %; 105(±3), 107(±1), 102(±3) and 108(±4) %; and 98(±3), 101(±2), 102(±6) and 102(±10)%, respectively. At 28 days, the relative strength would become 96(±4), 100(±4), 99(±4) and 97(±3) %; 101(±7), 104(±6), 106(±1), 106(±6); and 96(±2), 96(±9), 96(±6) and 94(±9) %. For C30 concrete mixes, replacement of natural sand by glass sand would reduce the strength slightly. It is also noted that this reduction would be lesser with time, maybe as a result of pozzolanic reaction of glass sand. For C45 concrete mixes, the strength consistently increased with more glass sand, at both 7 and 28 days, while for C60 the glass sand would slightly decrease the compressive strength at 28 days although it increased the strength at 7 days.

At the age of 90 days, all the concrete mixes manifested increasing strength with more glass sand. The relative strength was 102(±2), 113(±3), 111(±7), 121(±3) %; 100(±5), 107(±7), 116(±4), 116(±5) %; and 99(±1), 102(±5), 102(±1), 111(±2) %. It can be attributed to the pozzolanic reaction of fine glass particles at long term. Some researchers reported that the inherent cracks of glass sand would compromise the compressive strength of concrete [Taha and Nounu, 2009]. However, in this study, this was not observed since the glass concrete continued to increase strength with more glass sand, especially in the long term.

From the test results, glass sand would have no obvious trend on compressive strength of concrete, up to 100% replacement. Compared with natural sand, the crushed sand had more angular shape, sharper edge and poorer geometry. Also, usually, the bond strength between glass particles and cement paste would be weakened due to the chemical contamination, which always exists for recycled waste glass. It might be the main reason for the decrease in compressive strength. However, the higher fraction of smaller sized particles would make better distribution or packing of concrete and hence mechanical performances. Moreover, angular particles might be able to improve concrete strength over rounded particles (natural sand in this study). Also, the crushed glass sand had an elongated aspect ratio, compared to natural sand, which may also contribute to the strength increase. The negative factors should be more prominent at early age, when the pozzolanic reaction was not greatly activated.

As an extension of the study on glass concrete, use of mineral admixtures in concrete grade C45 containing glass sand was examined. Fly ash and GGBS were used to replace 30% and 60% of cement, respectively, in C45 concrete. The compressive strengths of glass concrete containing 30% fly ash or 60% GGBS at 7, 28 and 90 days are shown in **Fig. 3.23**. The incorporation of mineral admixtures would not change the glass sand effect on compressive strength. At 7 days, both mineral admixtures resulted in lower strength due to the reduction of cement content and relatively slower pozzolanic reaction of the admixtures compared to cement. However, at 28 days, the differences between mixes with and without fly ash or GGBS were significantly reduced. At 90 days, glass concrete with fly ash showed higher compressive strength than glass concrete without fly ash, while glass concrete with GGBS still showed lower strengths.

b. Flexural strength

As shown in **Fig. 3.24**, the flexural strength at 28 days increased with lower *w/c* ratio or higher grade of concrete. For each concrete grade, the flexural strength continuously increased with higher glass sand content up to 100%. Mix C60-100 exhibited the highest flexural strength of

8.14 MPa. The higher aspect ratio of crushed glass sand might have contributed to the higher flexural strength of concrete, in the same way as fibers in enhancing the resistance of concrete to tension. Kaplan [1959] found that flexural strength was increased more significantly by angular aggregates compared to compressive strength. These improvements can be explained by the greater degree of mechanical interlock, internal friction, and increased surface area associated with angular aggregates [Alexander and Mindess, 2005].

c. Splitting tensile strength

The test results of splitting tensile strength of glass concrete at 28 days are shown in **Fig. 3.25**. The splitting tensile strength increased with higher concrete grade, due to lower *w/c* ratio and thus less porous micro-structure of cement paste. The splitting tensile strength was not reduced by the use of glass sand for all concrete grades. In fact, mixes with 100% glass sand showed the highest splitting tensile strength, for each concrete grade. In contrast to compressive strength, the splitting tensile strength was less vulnerable to the reduced cohesion between particles and paste.

d. Modulus of elasticity

Fig. 3.26 shows the modulus of elasticity of glass concrete at 28 days. The dynamic modulus appeared to be insensitive to both glass sand content and *w/c* ratio, with all mixes showing values between 42.1 and 44.0 GPa. The static modulus of glass concrete varied from 30.0 to 33.0 GPa. It increased slightly with higher concrete grade and glass sand content, especially for C30 concrete. As mentioned earlier, better packing of aggregates can be achieved by crushed glass sand due to its finer size distribution. Uniformly distributed aggregate particles might increase the modulus of concrete because of higher degree of interlocking and particle interference. The higher modulus of elasticity of glass compared with natural sand may lead to higher elastic modulus for concrete containing glass sand [Yang et al., 1995].

e. Drying shrinkage

Drying shrinkages of glass concrete are shown in **Fig. 3.27**. According to ACI 224R-01, a typical value for drying shrinkage strain of concrete in structures is 600×10^{-6} mm/mm. Up to 90 days, all the concrete mixes showed stable shrinkage values less than 600×10^{-6}. At lower *w/c* ratio, the drying shrinkage could be more affected by the glass sand surface characteristics, surface texture and ITZ microstructure. For the C45 and C60 concrete mixes, particularly the latter, use of glass sand could reduce drying shrinkage due to the negligible water absorption of glass sand [Edward, 1966, Alexander and Mindess, 2005; Kou and Poon, 2009; Wang and Huang, 2010; Ling et al., 2011], although the reduction was not always consistent because of the reduced fineness of glass sand. Compared with natural sand, the glass sand may not absorb water from cement paste due to its negligible water absorption, which could lower the moisture loss from cement paste, leading to reduce the drying shrinkage. However, for C30 concrete, no obvious effect of glass sand on drying shrinkage was observed. It is postulated that the porous microstructure at higher *w/c* ratio would dominate the drying shrinkage rather than the aggregate particle properties. As a result, the moisture movement or evaporation was less hindered.

3.4.2.3 Durability

a. Rapid chloride permeability test (RCPT)

The RCPT results at 28 and 90 days are shown in **Figs. 3.28**, together with the migration coefficient calculated by **Eq. (3.1)**. At 28 days, for the same *w/c* ratio, the total charge passed was substantially reduced by increasing glass sand content, except 25% for C30 and C45. For C30 and C45 concretes, plain or 25% glass concrete exhibited test results higher than 2000 Coulombs, indicative of moderate permeability according to ASTM C 1202. With 50 and 75% glass sand, the RCPT result might be reduced to between 1000 and 2000 Coulombs, classified as low permeability concrete. If natural sand was totally replaced, the charge passed of less than 1000 Coulombs could be achieved. For C60 concrete, plain, 25 and 50%, 75 and 100% glass

sand concrete showed moderate, low and very low permeability, respectively. In addition, the total charge passed also decreased with decreasing *w/c* ratio, due to the improved CSH microstructure and reduced porosity. However, this trend could not be clearly seen at 75 or 100% glass sand replacement ratio, indicating that *w/c* ratio was not critical at such high glass sand content. At 90 days, each concrete mix showed reduced permeability because of more hydration of cement and denser microstructure of cement paste. Also, the effect of glass sand on permeability remained unchanged.

The migration coefficient of chloride ions exhibited almost the same trend as RCPT results; it decreased with time from 28 to 90 days, and with lower *w/c* ratio and higher glass sand content. The test results indicated that the resistance of concrete to chloride ion penetration was enhanced in terms of both total charge passed and depth of chloride penetration. The main reason for the higher resistance of glass sand concrete was the improvement in the microstructure of ITZ and cement paste matrix due to the pozzolanic reaction of fine glass particles. The reduced *w/c* ratio also improved the microstructure of cement paste.

b. Alkali-silica reaction (ASR) expansion

The ASR expansion results of C30, C45 and C60 glass concrete are shown in **Fig. 3.29**. All concrete mixes showed expansion less than 0.1% at 14 days, indicative of innocuous sand. Also, at 28 days, all mixes showed expansion below 0.2% except mix C60-0, suggesting that no potential deleterious ASR would occur in glass concrete. At 49 days, all reference concrete mixes without glass sand exhibited expansions greater than 0.2% while mixes with 75 and 100% glass sand consistently showed values less than this limit. ASR expansion decreased with glass sand content, regardless of concrete grade. The reduced ASR expansion indicated that glass sand, at least that of brown color, would not react with alkali in cement to cause ASR expansion.

One rational explanation is that calcium ions dissolved from soda-lime glass led to non-swelling ASR gel, which was confirmed by Rajabipour et al. [2010] via SEM observation and EDS analysis. It was found that the expansive ASR only occurs inside micro-cracks (< 2 μm) of glass particles, with pozzolanic reaction occurring at the glass particle surface. In this study, no large micro-crack was found in the brown glass particles, resulting in non-expansive pozzolanic reaction at the glass surface. This was verified by SEM results, as shown in **Fig. 3.30**. Brown glass particles of various sizes were not subjected to ASR deterioration, as no crack was observed at the surface or inside the particles (**Fig. 3.30a**). From **Figs. 3.30b~d**, the reaction product at glass surface was found to be non-swelling and did not cause cracks, supporting the hypothesis that pozzolanic reaction more readily occurs rather than ASR [Rajabipour et al., 2010]. The pozzolanic reaction product, secondary CSH gel, seemed to produce a densified ITZ microstructure, with lesser porosity. This thin layer of coating (about 2 μm) could hinder the further ingress of hydroxide ions which could corrode the glass structure.

In addition, the ASR expansion was generally lower for concrete mixes with lower compressive strengths (higher *w/c* ratio), as shown in **Fig. 3.31**. Therefore, higher strength would not equate with better durability, in terms of ASR. Also, for concretes containing 25, 50, 75 and 100% glass sand, the maximum ASR expansion occurs at a *w/c* ratio of 0.38, that is, grade C45 concrete.

The mix proportions are shown in the **Table 3.11**. Grade C60 concrete with the lowest *w/c* ratio of 0.32, and lowest sand content, showed the highest expansion at 28 days. The reason may be due to the higher cement content. It is well known that alkalis from cement hydration are the necessary conditions for ASR to occur. In the accelerated mortar bar tests, NaOH solution is thought to provide sufficient amount of alkali for sand to react with. However, the fact that the alkali penetrated only up to the surface layer of mortar would result in no reaction for the sand inside the mortar, due to the absence of alkali. Therefore, mixes containing more cement will facilitate ASR to occur by providing alkalis resulting in swelling of reaction products. On the

other hand, with lower *w/c* ratio, the stiffness and tensile strength of cement paste will increase and thus restrain the development of ASR expansion. In summary, *w/c* ratio could either increase or decrease the ASR expansion. As a result, the largest expansion occurred with C45 concrete containing glass sand.

From the test results shown in **Figs. 3.32** and **3.33**, the ASR expansions of C45concrete mixes were effectively decreased, by cement replacement with fly ash or GGBS, regardless of glass sand content or test age. According to ASTM C 1567, expansion less than 0.1% at 14 days for combinations of cement, fly ash or GGBS and aggregate indicates a low risk of deleterious expansion. All the mixes showed expansion smaller than 0.02% at 14 days, 0.04% at 28 days and 0.1% at 49 days. It is noted that the expansion rate was also reduced compared to concrete with pure cement. The effect of fly ash and GGBS on ASR can be attributed to: (1) the reduced alkalinity of the pore solutions by depletion of cement and thus alkalis content; (2) the restricted transport properties of the cementitious system via reduced porosity and changed nature of the ITZ; and (3) formation of extra CSH phases via pozzolanic reactions and less CH available for ASR [Helmuth, 1993]. The excellent ASR mitigating efficiency of fly ash and GGBS can substantially prolong the life-time of structure, if cracking due to ASR is considered as vital.

3.4.3 Summary

In this study, various contents of glass particles were used as sand substitution in concrete of three grades from 30 to 60 MPa. The following conclusions can be drawn from the test results:

1. Glass sand caused no obvious influence on fresh properties of concrete, that is, only slight reduction in fresh density, marginal increase in air content and negligible change in slump were observed.
2. Up to 100% replacement ratio, glass sand would not reduce mechanical properties. In contrast, it could even increase the compressive strength, splitting tensile strength,

flexural strength, and static modulus. The drying shrinkage would be inconsistently reduced with the use of glass sand at lower *w/c* ratios.

3. Resistance to chloride ion penetration of concrete was significantly improved by using glass sand. Glass concrete at various glass sand contents (with or without mineral admixtures) showed innocuous ASR expansion at 14 and 28 days.
4. Recycled waste glass can be incorporated into concrete as fine aggregates, up to 100% replacement ratio, without deleterious effect on concrete. Mineral admixtures can also be introduced in glass concrete to further improve its durability.

3.5 Comparison of Effect of Glass Sand in Mortar and Concrete

From the experiments on glass sand mortar and concrete, it is found that the effect of replacing natural sand with glass particles was not consistent between mortar and concrete. In the case of mortar, the addition of glass sand resulted in a reduction in flowability and mechanical properties. However, in case of concrete, use of glass sand resulted in similar or improved workability and mechanical properties.

The 4-level micro-structure of concrete and its ITZ are shown in **Figs 3.34** and **3.35**, respectively. Concrete is a three phase material, at the scale of 10^{-1}-10 m, composed of aggregates embedded in a mortar matrix and an ITZ. At the scale of 10^{-3}-10^{-1} m, mortar is also a three phase composite material composed of cement paste matrix, sand particles and ITZ. From the point of view of composites, the properties of mortar depend on the individual properties of each phase while they affect those of concrete. Therefore, the effect of replacing natural sand by glass particles in concrete can be attributed to the change in mortar properties.

As discussed earlier, the effect of glass particles could be negative or positive. For instance, in terms of flowability or workability, the more angular shape, sharper edge and higher aspect ratio

of glass particles are detrimental while the smooth surface texture and negligible water absorption are beneficial. The net effect could be negative or beneficial, depending on which factors are more dominant. It is expected that the net effect is related to the sand/cement (*s/c*) ratio, by mass. The ratio of *s/c* is 2.75 for mortar, and 1.96, 1.33 and 0.93 for C30, C45 and C60 concrete, respectively. A higher *s/c* ratio means less cement paste to coat the surface of sand, which increases the friction between aggregate particles as well as hinders the movement of cement paste. Therefore, the flowability of mortar was greatly reduced while the workability of concrete was not much changed.

Also, the different effect of glass sand on mechanical properties of mortar and concrete could also be explained by the *s/c* ratio. In concrete, a lower *s/c* ratio results in an increased thickness of cement paste between sand particles, which provides a better binding effect for sand particles. It means that the mortar in concrete has better mechanical properties, than on its own.

3.6 Expanded Study on ASR in Mortars with Glass Sand

As ASR remains a major concern in the use of glass sand, an expanded investigation on ASR expansion of mortar with glass sand was carried out, for the better understanding and control of ASR in glass mortar and concrete. The long term performance of green and brown glass sand mortar is first reported herein. Next, ASR was studied using single-size glass sand at 100% replacement of natural sand, and this was aimed at examining the contribution of each single sand size to ASR. Finally, the optimal content was explored for each mitigation method, such as mineral and chemical admixture, and fiber reinforcement, for 1.18-mm green glass sand.

3.6.1 Comparison of ASR in Green and Brown Glass Mortars

An extensive study was carried out to explore the ASR in green and brown glass sand mortars in the long term. The mix proportions were the same as mortar (that is, water, cement and sand)

portion of C30, C45 and C60 concrete mixes, as listed in **Table 3.11**. However, the mortar was not screened from fresh concrete mixture but mixed according to the mix ratio. In the study, the size distributions of both green and brown glass sands were strictly according to ASTM C 1260 requirement (**Table 3.5**).

The ASR expansions of brown glass sand mortars of C30, C45 and C60 mixes are plotted in **Fig. 3.36**. All the mixes showed ASR expansion less than 0.2% at 28 days, suggesting alkali non-reactivity. The test results indicated that ASR expansion consistently decreased with higher brown glass sand content at each mix. At 100% of sand replacement, the ASR expansion and development rate were extremely low; at the end of the test period of 140 days, the expansion was less than 0.05%, regardless of mortar mix. Also, no crack was observed on surface of specimens with 100% brown glass sand. This finding confirmed some previous conclusions that soda-lime glass sand might not exhibit alkali reactivity [Scanni and Bignozzi, 2009; Zhu et al., 2009]. It can be attributed to the pozzolanic reaction of fine glass sand, which has been confirmed by previous literature [Dyer and Dhir, 2001; Xie and Xi, 2002; Shi et al., 2005] and the calcium ions from the soda-lime glass, which could lead to non-expansive ASR gel.

The ASR expansions of green glass sand mortar of C30, C45 and C60 mixes are also shown in **Fig. 3.36**. The ASR behavior of green glass sand mortar was quite different from brown glass sand mortar, especially after 28 days. Within the first 28 days (or 21 days for C45), the green glass sand mortar showed similar trend as brown glass sand mortar, that is, reduced expansion with increasing glass sand content. However, thereafter, the ASR expansion showed a reversed trend, with higher ASR expansion at higher glass sand content. The ASR expansion rate of 75% green glass sand mortar increased noticeably faster than 25 and 50% green glass sand mortar. At 49 days, mortar with 75% green sand showed the highest expansion, followed by 50 and 25%, for both C45 and C60 mixes. Mortar with 100% green sand did not expand faster before 35 days. Although at 49 days, the 100% glass mortar of all mixes did not show the highest ASR

expansion, they exhibited the highest expansion rate which suggested that they might have the greatest expansion at a later age, e.g., that of C60 after 112 days. The visual observation also confirmed this result (**Fig.3.37a**), with a more map-pattern cracks were detected in 100% mortar specimens. In addition, for C30/45/60, mixes with 0, 25, 50 and 75% green glass sand registered 0.2% expansion almost at the same time, indicating comparable durability with respect to ASR. With 100% of green glass sand, mortar would not expand more than 0.2% before 49 to 56 days.

For the effect of *w/c* ratio on ASR, it can be seen from **Fig. 3.38** that C45 mix (*w/c*=0.38) would exhibit the highest expansion while C30 mix (*w/c*=0.49) showed the lowest for both brown and green glass sand regardless of glass sand content (except green C60-100). Higher *w/c* ratio would have two effects on ASR: (1) increased expansion due to reduced tension strength and high susceptibility to tensile cracking; and (2) decreased expansion because of a more porous microstructure, which enables the formed ASR gel to escape from reaction site, releasing the tensile stress which is built up in glass due to the constraint. Therefore, a pessimum effect of *w/c* ratio on ASR expansion may result from these two factors.

3.6.2 Effect of Glass Particle Size on ASR Expansion

The effect of glass particle size on ASR expansion was investigated at two different mixes, that is using ASTM standard mix and a slightly modified mix (see **Table 3.11**). In this study, all mortar mixes contained 100% single-sized glass particles. It is well known that single-size particles will result in larger void content than well-graded particles. Therefore, more paste will be required to fill the increased voids. To produce a good quality mortar, the *s/c* ratio was decreased from 2.25 in ASTM standard mix to 1.6 in modified mix, while the *w/c* ratio remained at 0.47.

The effect of green and brown glass particle size on ASR expansion is shown in **Fig. 3.39**. For green glass sand mortar, the ASR expansion increased with the glass sand size, and peaked at a

particle size of 1.18 mm, regardless of mix ratio. With a larger size of 2.36 mm, the ASR expansion reduced slightly.

Similar results have been reported by Idir et al. [2010]. Smaller glass sand should have larger surface area, which allows ASR to readily occur, causing more expansion. However, with a size lower than the critical value, pozzolanic reaction would occur instead, which may form non-swelling CSH gel. Some models based on the assumption that ASR is a surface reaction have been proposed to explain this pessimum effect [Bazant and Steffens, 2000; Bazant et al., 2000]. However, based on previous discussion, swelling ASR would occur inside inherent micro-cracks of glass particles, rather than at surfaces. Therefore, more inherent micro-cracks would render more reaction and higher expansion.

It is interesting to note that such pessimum was not observed for brown glass sand; as particles of all sizes 2.36 mm showed low expansions except after 49 days regardless of mix ratio (**Figs. 3.39c** and **d**). Therefore, the study on effect of particle size provides a plausible explanation on the different ASR expansion of green and brown glass in the long term. The extremely high alkali reactivity of 1.18 mm and 2.36 mm green sand particles might cause increased expansion and rapid expansion rate. Thus, the following section will discuss the versatile ASR mitigation methods based on the modified mix with 1.18 mm green sand particles.

For natural sand, ASR expansion was largest with 0.3 and 0.6 mm size sand (**Fig. 3.39e**). The results confirm that traditional ASR is a surface reaction, increasing with larger surface area. When a large amount of reactive material is present in a finely divided form (i.e., under 75 μm), there might be considerable petrographic evidence of the ASR and yet no significant expansion [Mehta and Monteiro, 2006].

Fig. 3.40 displays the microstructure of mortar with 1.18-mm green glass sand and shows some representative cracks caused by ASR. There were two types of cracks in glass sand mortar:

cracks inside of the glass particles (**Figs. 3.40a** and **g**); and cracks in the matrix which initiated from inside the glass particles (**Figs. 3.40b** and **c**). No crack was found along the surface of glass particle (**Fig. 3.40d**). **Fig. 3.40g** presents that a typical crack, about 10 μm wide, formed within a glass particle due to the expansive stress of ASR gel after imbibing water. **Fig. 3.40b** shows that the crack extended from the glass sand particle to cement paste and **Fig. 3.40c** clearly displays that the crack, around 15 μm wide, was filled with the ASR gel, which was obviously different from cement paste in morphology and microstructure. It is postulated that the ions, such as OH^-, Na^+, Ca^{2+} penetrate into the glass structure (inherent micro-cracks inside the glass particles could render this penetration) and form ASR gel which causes expansion. This expansion results in tensile stress inside glass particles. Moreover, this expansion would be restrained by the surrounding cement paste matrix, thus causing tensile stress to develop in the matrix. Once the tensile stress exceeds the tensile strength of glass, cracks would initiate and propagate in the glass particles (**Figs. 3.40e, f** and **g**). Subsequently, such cracks may extend to cement paste matrix if the tensile stress is more than the tensile strength of cement paste (**Figs. 3.40b** and **c**). It is noted that there were also some micro-cracks in cement paste matrix, far away from the glass surface (**Fig. 3.40i**), which seemed to be caused by drying shrinkage during the SEM sample preparation. The ASR mechanism for glass particle is represented in **Fig. 3.41**.

3.6.3 Optimal Content of ASR Mitigation Methods

From earlier test results (section 3.3.3.2), the content of each ASR mitigation method was fixed corresponding to common usage. The effect of content (or the optimal content) was determined in this extensive study. The various amounts investigated for different methods are summarized in **Table 3.12**. Three types of ASR mitigation methods were considered: (a) replacement of cement by supplementary cementitious material (SCM); (b) addition of fiber reinforcement; and (c) addition of lithium compounds. The results (with average and variation) of each method at different days are shown in **Fig. 3.42**. The ASR reduction efficiency (defined as the ratio of

reduced ASR expansion over the value for 1.18 mm green glass sand mortar) for each method is listed in **Table 3.13**, for 14, 21, 28 and 56 days.

3.6.3.1 Supplementary Cementitious Materials (SCM)

As expected, the replacement of cement by SCM, e.g. fly ash, GGBS and silica fume in this study, can prevent or minimize ASR, because of their pozzolanic reaction. A number of studies have established the ASR suppressing mechanism of pozzolanic reaction [Diamond, 1981; Hasparyk et al., 2000; Helmuth, 1993; Monteiro, et al., 1997; Turanli et al., 2003; Xu et al., 1995], which results in: (a) enhanced impermeability of cement paste and hence reduced mobility of ions (particularly OH^- in AMBT in this study); (b) reduced alkalinity of pore solutions as a result of depletion of cement; (c) reduced amount of $Ca(OH)_2$, which formed into secondary CSH gel; and (d) increased strength of cement paste provided by mineral admixtures, leading to higher resistance to the expansive stress developed by ASR.

In the case of fly ash, the ASR restraining effect was clearly significant, both in terms of absolute expansion and expansion rate (**Figs. 3.37c** and **3.42a**). All mortar specimens with fly ash showed significantly low expansion values, less than 0.02% at all the ages up to 56 days. This effect was prominent even with 10% of fly ash, and higher fly ash content did not change the results. It is also noted that some early-age values were negative, indicative of autogenous shrinkage instead of expansion. Although ASR expansion generally increased with time, a decrease in expansion was also observed from 14 to 21 days and from 49 to 56 days. Some researchers have reported the self-healing of micro-cracks in cement systems due to fly ash [Termkhajornkit et al., 2009]. It has been specifically reported that cracks with widths below 0.1 mm can be closed by a self-healing process [Reinhardt and Jooss, 2003; Sahmaran et al., 2008]. The self-healing capacity due to fly ash may origin from its pozzolanic characteristics, which can occur at later age, thus filling the pores and micro-cracks. As a result, the resistance of paste to alkali diffusion from external NaOH solution would increase.

With cement partially replaced by GGBS, the ASR expansion of glass mortar decreased with higher content of GGBS (see **Figs. 3.37d** and **3.42b**). Up to 28 days, mixes with 30% or more GGBS exhibited less than 0.2% ASR expansion. Also, at 56 days, the ASR expansion was less than 0.2% with 45% GGBS, while with 60% GGBS it was only 0.02%. Based on the test results, GGBS was effective in reducing ASR expansion if at least 30% of cement content was replaced by it.

With silica fume, ASR expansion was effectively suppressed when it replaced 12.5% of cement. The expansion was higher than 0.20% at 14 days, with 5%, 7.5% and 10% silica fume, although they all exhibited less expansion than the reference mortar specimen. Compared with the first 14 days, the ASR expansion increased very slowly thereafter. **Fig. 3.37e** shows the cracks on the surface of mortar bars with silica fume at low silica fume contents. There were only few major cracks which increased in width with time, while the remaining surface area remained uncracked.

In addition, mortar with 10% silica fume showed the highest expansion, indicating a pessimum content. Chen et al. [1993] reported that the pessimum replacement for densified silica fume in suppressing ASR expansion was 15%. Hasparyk et al. [2000] also observed a pessimum for silica fume at 4% replacement when dealing with the ASR of quartzite aggregate, while 12% replacement would produce innocuous behavior. This critical content agrees well with the result in this study. However, no plausible reason has been provided to explain this pessimum effect.

The addition of silica fume can significantly reduce the porosity of cement paste, especially at ITZ, because of its ultra-fine particle size (average 0.1 μm compared with 10 μm of cement particle). Compared to this filling effect, the pozzolanic reaction might play a secondary role in restraining ASR expansion. The less produced gel, due to the reduced alkaline and higher restraining, will increase the volume and stress in the vicinity of reaction site and crack will occur once the expansive stress exceeds the tensile strength of cement paste. Thus, it can result in

higher expansion due to higher degree of restraining if more silica fume is used. However, if enough cement is substituted by silica fume (12.5% in this study) the alkali will be quite low and less likely to react with glass particles. Furthermore, Diamond [1997] stated that silica fume in concrete does not always prevent ASR distress; instead, sometimes it can induce ASR distress particularly when oversized or un-dispersed grains can react to generate expansive ASR gel if the alkali hydroxide concentration is high enough.

In summary, it should be noted that not all the SCMs were able to adequately reduce ASR. It depends on the ASR refraining mechanisms of each SCM and the amount used.

3.6.3.2 Fiber Reinforcement

The ASR expansion of mortar bars with varying amount of steel fibers (smooth fiber with length of 5 mm and diameter of 0.16 mm) is shown in **Fig. 3.42d**. The overall ASR restraining efficiency of steel fiber was less than SCMs. Adding more than 1% of steel fiber could effectively reduce the expansion below 0.1% at 14 days. However, all mortars with steel fibers had expansion exceeding 0.2% at 28 days and 0.7% at 56 days. Also, a pessimum content of 1% was observed at 28 days. At less than this content, more fibers may cause greater expansion. Turanli et al. [2001] reported that 1% of steel microfiber would instead increase the ASR expansion than the reference plain specimen, but no reason was provided. The possible reason could be the relatively weak bond at fiber-matrix interface (as shown in **Fig. 3.40i**), through which the alkali ions can penetrate to reach the glass particles more easily. Exceeding this pessimum content, more fibers may effectively restrain crack growth via fiber bridging function. Based on the chemo-mechanical confinement model [Ostertag et al., 2007], if the ASR gel is prevented from leaving the reaction site through the cracks, the Si^{4+} ion concentration would increase, retarding further dissolution of glass sand. However, this pessimum effect disappeared after 28 days. At 56 days, cracks were clearly observed on the surface of mortar bars although the expansion decreased consistently with higher steel fiber content (**Fig. 3.37f**).

3.6.3.3 Lithium Compounds

The appearance of mortar bars with of LiCl and Li_2CO_3 are shown in **Figs 3.37g** and **h**, and test results are shown in **Figs. 3.42e** and **f**. Both lithium salts can reduce the ASR expansion remarkably, to far below 0.1%. The difference between 0.5 and 2% of lithium compound was quite small. The efficiency of LiCl and Li_2CO_3 was comparable. Some literature reported the minimum value of molar ratio of [Li]/[Na] to effectively reduce ASR expansion, such as 0.9 for LiCl [Collins et al., 2004], which was not observed in this study, suggesting that 0.5% by mass of cement should be enough for LiCl and Li_2CO_3 to control ASR.

3.6.3.4 Comparison of Different Methods

From **Table 3.13**, the optimum content for each method is determined as follows: 10-50% for fly ash; 45-60% for GGBS; 12.5% for silica fume; 1.5-2.0% for steel fiber; and 0.5-2.0% for lithium chloride or lithium carbonate. Moreover, the effectiveness of different methods, at corresponding optimum content, generally decreases in the order of: fly ash, lithium compounds, GGBS, silica fume, and steel fibers.

The type and amount of ASR suppressor to be used should be selected according to user's requirement, such as compressive strength. The compressive strengths of mortar with different amounts of each method at 28 days are shown in **Table 3.14**. From the test results, more than 20% strength will be lost if fly ash content exceeds 40%. Although this strength loss can be offset by pozzolanic reaction at a later age, caution should be exercised if early strength of concrete is of main concern. In contrast, even at 60% replacement ratio of cement by GGBS, compressive strength would not be affected. This is due to the high CaO content of 40%, which could be converted to $Ca(OH)_2$ and result in pozzolanic reaction at an early age. This is also the reason for the usage of high GGBS content as cement replacement.

However, silica fume appeared to actually reduce the compressive strength rather than increase it. Silica fume may be more pronounced in pore structure refinement with *w/c* ratio lower than 0.47,

which is used in this study. The other reason may be the un-dispersed grains of silica fume, as discussed by Diamond [1997]. It should be mentioned that in this study no superplasticizer was used for the dispersion of silica fume to avoid complexity in analyzing the results. All mortars containing silica fume exhibited sufficient flowability for casting.

The deformability (or strain at peak stress) of mortar with steel fibers under compression was significant increased, although the compressive strength was actually reduced. The benefit of fiber reinforcement for cement-based composites is in toughness, ductility, impact resistance, fatigue endurance and impermeability, rather than on compressive strength.

With regard to the addition of lithium compounds, particularly Li_2CO_3, the compressive strength of mortar would also be reduced. It is postulated that the carbonate retards the hydration of Portland cement and thus delay the alkali-silica reaction. Since lithium treatment is expensive, it would presumably be applied only to those concretes at high risk of ASR [McCoy and Caldwell, 1951; Diamond, 1997].

3.6.3.5 Practical Use of Fly Ash and GGBS as ASR Suppressor

For practical ASR mitigation, fly ash and GGBS are recommended, especially if sustainability and economy concerns are taken into account. It is well known that fly ash and slag, as industry by-products, are disposed in landfills in massive quantities all over the world since they are not yet re-utilized in sufficiently large amount. If they can be used as cement replacement, not only negative environmental impacts are reduced but also better concrete durability (i.e. the reduced ASR expansion for glass mortar in this study) can be achieved.

With respect to ASR restraining, steel fiber, silica fume and lithium compound may lose competition due to their higher prices, since concrete is a cost-sensitive industry.

As a final stage of study, 30% fly ash and 60% GGBS were selected as ASR reducing methods to examine the expansion of C45 green glass sand mortar (with sand grading following ASTM C

1260). The results are shown in **Fig. 3.43**. The ASR reductions at different ages are also listed in **Table 3.15**. Compared with the reference green glass sand mortar, all mortars with 30% fly ash or 60% GGBS exhibited substantially smaller expansions, less than 0.1% up to 49 days regardless of glass sand content. With the use of fly ash or GGBS, the alkali reactivity of green glass sand was found to diminish since mortar with higher content of green glass showed less expansion. In addition, the suppressing effect of fly ash and GGBS was more pronounced at later age, from less than 70% (mostly) at 7 days to more than 90% (except the reference mortar) at 49 days. It is noted that at early age, some mortar mixes with green glass sand such as C45-100 exhibited higher expansion instead (**Table 3.15**). It might be due to the extremely small expansion of reference mortar at early age (**Fig. 3.36e**). After 21 days, all mortar mixes containing fly ash or GGBS exhibited less expansion compared with the reference mortar with the same glass content. Therefore, fly ash and GGBS were proved to be effective at restraining ASR expansion for glass sand mortar.

3.6.4 Summary

From the experimental investigations on ASR expansions of green and brown glass sand mortars, the following conclusions can be drawn:

1. Brown glass sand showed better ASR resistance than green glass sand in the long term. The reason is attributed to the extreme alkali reactivity of 1.18 mm glass particles in green glass sand.
2. Higher strength (or lower *w/c* ratio) does not necessarily mean better durability of concrete with respect to ASR, due to the reduced porosity which caused slower release of formed expansive ASR gel.
3. Not all the mitigation methods showed increasing efficiency with higher utilization amount. The optimal content for each mitigation method is determined as 10-50% for fly

ash, 45-60% for GGBS, 12.5% for silica fume, 1.5-2.0% for steel fibers and 0.5-2.0% for lithium compounds.

4. Fly ash and GGBS could be used for practical application on the basis that they both remarkably suppressed ASR expansion.

3.7 Summary

Recycled waste glass was used as alternative to natural sand, up to 100 percent, in cement mortar and concrete. The influences of glass sand on major properties of mortar and concrete have been reported in this Chapter. The conclusions can be drawn:

1. Mechanical performance of mortar would be reduced by the use of glass sand while that of concrete was enhanced instead. The durability properties of both mortar and concrete were improved due to the pozzolanic reaction of fine glass particles.

2. Clear glass showed much higher alkali reactivity compared to brown and green glass. At the same time, green glass exhibited larger ASR expansion in the long term, attributed to the extremely low alkali resistance of green glass particles with size of 1.18 mm.

3. It was observed that ASR for glass particle was not a surface reaction but initiated from pre-existed internal cracks of glass particle. Cracks form initially inside glass particles and grow in width and finally expand to surrounding cement paste.

4. Among various ASR mitigation methods, fly ash and GGBS proved to be the most efficient at optimum cement replacement of 10-50% and 45-60%, respectively.

Table 3-1: Chemical compositions of green, brown and clear glass, and natural sand

Composition, %	Green	Brown	Clear	Natural Sand
SiO_2	71.22	72.08	72.14	88.54
Al_2O_3	1.63	2.19	1.56	1.21
Fe_2O_3	0.32	0.22	0.06	0.76
CaO	10.79	10.45	10.93	5.33
MgO	1.57	0.72	1.48	0.42
Na_2O	13.12	13.71	13.04	0.33
K_2O	0.64	0.16	0.62	0.31
TiO_2	0.07	0.1	0.05	0.05
Cr_2O_3	0.22	0.01	—	—

Table 3-2: Chemical compositions of cement, fly ash, GGBS and silica fume

Composition, %	Cement	Fly ash	GGBS	Silica fume
SiO_2	20.8	38.9	32.15	95.95
Al_2O_3	4.6	29.15	12.87	0.28
Fe_2O_3	2.8	19.64	0.36	0.32
CaO	65.4	2.5	40.67	0.16
MgO	1.3	2.1	6.05	0.37
SO_3	2.2	0.19	4.95	0.18
Na_2O	0.31	0.26	0.28	0.05
K_2O	0.44	0.48	0.51	0.57

Table 3-3: Physical properties of cement, fly ash, GGBS and silica fume

Physical test	Cement	Fly ash	GGBS	Silica fume
Fineness	Blaine specific surface area of 393 m^2/kg	85% passing 45 μm	Average primary particle of 16.7 μm	BET surface area of 21.33 m^2/g
Specific gravity	3.15	2.20	2.93	2.20

Table 3-4: Test properties, specimen numbers, test age and dimensions, and standard methods for glass mortar and concrete

Test	No. of specimens	Test age, days	Dimensions, mm	ASTM standards
Mortar				
Fresh density				C 185
Air content				C 185
Flow				C 1437
Compressive strength	6	7, 28	50×50×50	C 109
Flexural strength	6	7, 28	40×40×160	C 348
Elastic modulus	3	28	Ø100×200	C 469 & 215
Splitting tensile strength	3	28	Ø100×200	C 496
Drying shrinkage	3	56	25×25×285	C 596
RCPT	3	28	Ø100×50	C 1202
ASR	3	7-28	25×25×285	C 1260 & 1567
Sulfate attack	3	28	40×40×160	C 267
Concrete				
Fresh density				C 138
Air content				C 138
Slump				C 143
Compressive strength	9	7, 28, 90	100×100×100	BS EN 12390-3
Flexural strength	3	28	100×100×400	C 78
Elastic modulus	3	28	Ø100×200	C 469 & 215
Splitting tensile strength	3	28	Ø100×200	C 496
Drying shrinkage	2	90	75×75×285	C 157
ASR	3	7-49	25×25×285	C 1260 & 1567
RCPT	6	28, 90	Ø100×50	C 1202

Table 3-5: Grading requirement of sand by ASTM C 1260

Sieve size		Mass, %
Passing	**Retained on**	
4.75 mm	2.36 mm	10
2.36 mm	1.18 mm	25
1.18 mm	600 μm	25
600 μm	300 μm	25
300 μm	150 μm	15

Table 3-6: Mix proportions of glass mortar for ASR study

Mix No.	Water, g	Cement, g	Pozzolan, g	Sand, g	Glass sand, g	Addition, g
Ref-0	207	440	—	990	0	—
Ref-25	207	440	—	743	248	—
Ref-50	207	440	—	495	495	—
Ref-75	207	440	—	248	743	—
Ref-100	207	440	—	0	990	—
FA-0	207	308	132	990	0	—
FA-25	207	308	132	743	248	—
FA-50	207	308	132	495	495	—
FA-75	207	308	132	248	743	—
FA-100	207	308	132	0	990	—
GGBS-0	207	176	264	990	0	—
GGBS-25	207	176	264	743	248	—
GGBS-50	207	176	264	495	495	—
GGBS-75	207	176	264	248	743	—
GGBS-100	207	176	264	0	990	—
SF-0	207	396	44	990	0	—
SF-25	207	396	44	743	248	—
SF-50	207	396	44	495	495	—
SF-75	207	396	44	248	743	—
SF-100	207	396	44	0	990	—
GP-0	207	352	88	990	0	—
GP-25	207	352	88	743	248	—
GP-50	207	352	88	495	495	—
GP-75	207	352	88	248	743	—
GP-100	207	352	88	0	990	—
Fiber-0	207	440	—	990	0	85
Fiber-25	207	440	—	743	248	85
Fiber-50	207	440	—	495	495	85
Fiber-75	207	440	—	248	743	85
Fiber-100	207	440	—	0	990	85
LiCl-0	207	440	—	990	0	4.4
LiCl-25	207	440	—	743	248	4.4
LiCl-50	207	440	—	495	495	4.4
LiCl-75	207	440	—	248	743	4.4
LiCl-100	207	440	—	0	990	4.4
LiCO-0	207	440	—	990	0	4.4
LiCO-25	207	440	—	743	248	4.4
LiCO-50	207	440	—	495	495	4.4
LiCO-75	207	440	—	248	743	4.4
LiCO-100	207	440	—	0	990	4.4

FA: Fly ash, GGBS: Ground granulated blast-furnace slag; SF: Silica fume; GP: Glass powder; Fiber: Steel fiber; LiCl: Lithium chloride; LiCO: Lithium carbonate.

Table 3-7: ASR expansion (%) of mortar with green glass sand

Time, day	Glass content, %	Reference	Fly Ash	GGBS	Silica Fume	Steel Fiber	Powder	LiCl	Li_2CO_3
7	0	0.0165	0.0026	0.0062	0.0076	0.0086	0.0050	0.0212	0.0117
	25	0.0121	-0.0004	0.0029	0.0203	0.0012	0.0034	0.0058	0.0074
	50	0.0059	0.0016	-0.0025	0.0094	0.0006	0.0005	0.0029	0.0054
	75	0.0067	0.0018	-0.0002	0.0079	-0.0041	-0.0027	0.0036	0.0050
	100	0.0028	0.0011	-0.0019	0.0126	-0.0062	-0.0018	0.0001	0.0040
14	0	0.0533	0.0100	0.0186	0.0202	0.0253	0.0311	0.0594	0.0188
	25	0.0361	0.0044	0.0164	0.0333	0.0194	0.0136	0.0248	0.0122
	50	0.0222	0.0070	0.0072	0.0179	0.0155	0.0100	0.0158	0.0080
	75	0.0121	0.0075	0.0056	0.0126	0.0054	0.0056	0.0102	0.0063
	100	0.0051	0.0061	0.0061	0.0177	-0.0008	0.0037	0.0058	0.0045
21	0	0.1040	0.0135	0.0293	0.0348	0.0493	0.0582	0.1006	0.0283
	25	0.0825	0.0091	0.0248	0.0423	0.0276	0.0300	0.0437	0.0176
	50	0.0354	0.0094	0.0120	0.0245	0.0172	0.0203	0.0228	0.0114
	75	0.0282	0.0112	0.0089	0.0192	0.0058	0.0083	0.0095	0.0071
	100	0.0150	0.0079	0.0100	0.0195	0.0016	0.0055	0.0044	0.0053
28	0	0.1490	0.0230	0.0411	0.0542	0.0844	0.0911	0.1388	0.0608
	25	0.1357	0.0169	0.0335	0.0530	0.0606	0.0533	0.0734	0.0417
	50	0.0742	0.0140	0.0171	0.0350	0.0400	0.0365	0.0427	0.0290
	75	0.0704	0.0144	0.0127	0.0229	0.0230	0.0189	0.0185	0.0220
	100	0.0304	0.0130	0.0087	0.0247	0.0055	0.0126	0.0076	0.0166

Table 3-8: ASR expansion (%) of mortar with brown glass sand

Time, day	Glass content, %	Reference	Fly Ash	GGBS	Silica Fume	Steel Fiber	Powder	LiCl	Li_2CO_3
7	0	0.0165	0.0031	0.00624	0.00758	0.00863	0.0085	0.0212	0.0142
	25	0.0142	0.0030	0.0013	0.0077	0.019	0.0069	0.0237	0.0100
	50	0.0087	0.0062	0.0008	0.0048	0.0048	0.0041	0.0117	0.0022
	75	0.0040	-0.001	0.0004	0.0068	0.0033	0.002	0.009	0.0028
	100	0.0052	0.0054	0.0005	0.0023	0.0035	0.003	0.0086	0.0019
14	0	0.0533	0.0100	0.0186	0.0202	0.0253	0.0402	0.0594	0.0288
	25	0.0320	0.0097	0.002	0.021	0.0213	0.0247	0.0520	0.0257
	50	0.0196	0.0112	-0.0017	0.0175	0.0081	0.0139	0.0225	0.0126
	75	0.0087	0.0014	-0.0008	0.0148	0.0043	0.0115	0.0115	0.0050
	100	0.0090	0.0066	-0.0011	0.0126	0.0049	0.0056	0.0133	0.0029
21	0	0.104	0.0135	0.0293	0.0348	0.0493	0.0802	0.1006	0.0506
	25	0.0916	0.0095	0.0086	0.0326	0.0420	0.0595	0.0919	0.0476
	50	0.0355	0.0086	0.0078	0.0224	0.0190	0.0403	0.0371	0.0235
	75	0.0194	0.0008	0.0034	0.0209	0.0120	0.0267	0.0196	0.0125
	100	0.012	0.0065	0.0005	0.0141	0.0082	0.0142	0.0164	0.0075
28	0	0.1490	0.0230	0.0411	0.0542	0.0844	0.1117	0.1388	0.0839
	25	0.1305	0.0105	0.0225	0.0554	0.064	0.075	0.1278	0.0781
	50	0.0594	0.0109	0.026	0.028	0.043	0.0493	0.059	0.0383
	75	0.0262	0.0007	0.0086	0.0234	0.0373	0.0339	0.0343	0.0212
	100	0.0123	0.0049	0.0094	0.011	0.0184	0.0134	0.0233	0.0111

Table 3-9: ASR expansion (%) of mortar with clear glass sand

Time, days	Glass content, %	Reference	Fly Ash	GGBS	Silica Fume
7	0	0.0165	0.0026	0.0062	0.0076
	25	0.0175	0.0021	-0.0012	0.0092
	50	0.0188	0.0000	-0.0022	0.0131
	75	0.0186	0.0018	-0.0007	0.0111
	100	0.0149	0.0029	-0.0001	0.0069
14	0	0.0533	0.0100	0.0186	0.0202
	25	0.0486	0.0098	0.0071	0.0213
	50	0.0654	0.0057	0.0143	0.0252
	75	0.1284	0.0073	0.0043	0.0206
	100	0.1368	0.0080	0.0057	0.0171
21	0	0.1040	0.0135	0.0293	0.0348
	25	0.0888	0.0127	0.0162	0.0299
	50	0.1334	0.0084	0.0201	0.0304
	75	0.2768	0.0101	0.0124	0.0274
	100	0.3435	0.0093	0.0104	0.0267
28	0	0.1490	0.0230	0.0411	0.0542
	25	0.1198	0.0168	0.0199	0.0425
	50	0.2118	0.0149	0.0224	0.0549
	75	0.4710	0.0121	0.0134	0.0384
	100	0.7046	0.0108	0.0120	0.0389

Table 3-10: Mix proportions of glass concrete

Mix No.	Content, kg/m^3						
	Water	**Cement**	**Pozzolan**	**CA**	**sand**	**glass**	***w/c***
C30-0	187	382	—	1058	748	0	0.49
C30-25	186	381	—	1056	560	187	0.49
C30-50	186	379	—	1052	372	372	0.49
C30-75	185	378	—	1047	185	555	0.49
C30-100	184	376	—	1043	0	737	0.49
C45-0	187	492	—	1060	656	0	0.38
C45-25	187	491	—	1057	491	164	0.38
C45-50	185	488	—	1051	325	325	0.38
C45-75	185	487	—	1048	162	487	0.38
C45-100	184	485	—	1044	0	647	0.38
C60-0	187	585	—	1060	578	0	0.32
C60-25	187	585	—	1060	434	145	0.32
C60-50	186	582	—	1055	288	288	0.32
C60-75	186	580	—	1051	143	430	0.32
C60-100	185	577	—	1047	0	571	0.32
C45-0-FA	181	334	143	1027	636	0	0.38
C45-25-FA	181	333	143	1024	476	158	0.38
C45-50-FA	180	332	142	1021	317	317	0.38
C45-75-FA	180	331	142	1018	157	473	0.38
C45-100-FA	179	330	141	1015	0	629	0.38
C45-0-GGBS	184	194	290	1041	645	0	0.38
C45-25-GGBS	183	193	289	1038	482	160	0.38
C45-50-GGBS	183	192	288	1034	321	321	0.38
C45-75-GGBS	182	192	288	1032	160	480	0.38
C45-100-GGBS	182	191	287	1029	0	637	0.38

CA: coarse aggregates; FA: Fly ash, GGBS: Ground granulated blast-furnace slag.

Table 3-11: Mix proportions of ASTM standard mortar and screened mortar from concrete (by mass)

Mix	Water	Cement	Sand	CA
ASTM C1260	0.475	1	2.25	—
C30	0.49	1	1.96	2.77
C45	0.38	1	1.33	2.15
C60	0.32	1	0.93	1.81
Modified mix	0.475	1	1.6	—

CA: coarse aggregates.

Table 3-12: Amounts of each ASR mitigation method

ASR mitigation method and amounts, %					
Fly ash*	GGBS*	Silica fume*	Steel fiber#	LiCl*	Li_2CO_3*
10	15	5	0.5	0.5	0.5
20	30	7.5	1	1	1
30	45	10	1.5	1.5	1.5
40 50	60	12.5	2	2	2

*content of cement by mass; #content of total mixture by volume

Table 3-13: Effect of different methods on expansion of mortar with 100% green 1.18-mm glass sand

Method	Amount, %	Expansion, %				Reduction in expansion$^{\Psi}$, %			
		14 d.	21 d.	28 d.	56 d.	14 d.	21 d.	28 d.	56 d.
Reference	—	0.5667	1.0705	1.3146	1.7412	—	—	—	—
*Fly ash**	10	.0043	-.0004	.0055	.0121	99	100	100	99
	20	-.0008	-.0069	-.0029	.0032	100	100	100	100
	30	.0078	.0001	.0114	.0121	99	100	99	99
	40	.0038	.0004	.0086	.0126	99	100	99	99
	50	.0084	.0038	.0076	.0114	99	100	99	99
*GGBS**	15	.0216	.2097	.5001	1.0532	96	80	62	40
	30	.0114	.0205	.1707	.7961	98	98	87	54
	45	.0118	.0150	.0199	.1807	98	99	98	90
	60	.0088	.0098	.0100	.0202	98	99	99	99
*Silica fume**	5.0	.2622	.3123	.3137	.3661	54	71	76	79
	7.5	.3632	.3820	.3853	.4144	36	64	71	76
	10.0	.4634	.5378	.5417	.5696	18	50	59	67
	12.5	.0139	.0314	.0353	.0456	98	97	97	97
Steel fiber#	0.5	.1314	.3501	.6399	1.0902	77	67	51	37
	1.0	.2376	.4396	.6930	1.1017	58	59	47	37
	1.5	.0420	.1177	.3763	.8504	93	89	71	51
	2.0	.0288	.0569	.2268	.7185	95	95	83	59
*LiCl**	0.5	.0095	.0156	.0125	.0152	98	99	99	99
	1.0	.0094	.0142	.0098	.0155	98	99	99	99
	1.5	.0083	.0105	.0093	.0117	99	99	99	99
	2.0	.0113	.0148	.0079	.0140	98	99	99	99
*Li_2CO_3**	0.5	.0084	.0131	.0170	.0203	99	99	99	99
	1.0	.0096	.0157	.0157	.0194	98	99	99	99
	1.5	.0084	.0123	.0154	.0177	99	99	99	99
	2.0	.0093	.0136	.0175	.0209	98	99	99	99

*content of cement by mass; #content of total mixture by volume,
$^{\Psi}$reduction compared to reference mortar at the same age.

Table 3-14: Mortar compressive strength and relative strength of each method at 28 days

Method	**Amount, %**	**Compressive strength, MPa**	**Relative strength, %**
Reference	—	50.8	100
*fly ash**	10	47.6	94
	20	42.8	84
	30	43.5	86
	40	37.9	75
	50	29.2	58
*GGBS**	15	53.3	105
	30	52.5	103
	45	48.7	96
	60	49.3	97
*Silica fume**	5.0	48.3	95
	7.5	47.0	93
	10.0	45.8	90
	12.5	43.6	86
Steel fiber[#]	0.5	52.3	103
	1.0	49.2	97
	1.5	44.6	88
	2.0	43.3	85
*LiCl**	0.5	48.8	96
	1.0	42.3	83
	1.5	41.4	82
	2.0	39.3	77
*Li_2CO_3**	0.5	36.7	72
	1.0	31.3	62
	1.5	28.2	56
	2.0	27.8	55

*content of cement by mass; [#]content of total mixture by volume

Table 3-15: Effect of 30% fly ash or 60% GGBS on ASR expansion of C45 green glass sand mortar

Method	Amount, %	Expansion, %				Reduction in expansion*, %			
		14 d.	21 d.	28 d.	49 d.	14 d.	21 d.	28 d.	49 d.
Reference	0	.0680	.1617	.1778	.3121				
	25	.0705	.1698	.2649	.4971				
	50	.0489	.1691	.3003	.5978		—		
	75	.0235	.1042	.2867	.6749				
	100	.0068	.0145	.0210	.3435				
Fly ash	0	.0121	.0190	.0245	.0505	82	88	86	84
	25	.0081	.0121	.0150	.0337	89	93	94	93
	50	.0058	.0099	.0125	.0343	88	94	96	94
	75	.0088	.0119	.0128	.0292	63	89	96	96
	100	.0092	.0124	.0107	.0233	-36	14	49	93
GGBS	0	.0198	.0274	.0342	.0746	71	83	81	76
	25	.0092	.0212	.0283	.0460	87	88	89	91
	50	.0071	.0185	.0243	.0365	86	89	92	94
	75	.0094	.0190	.0249	.0323	60	82	91	95
	100	.0077	.0169	.0195	.0224	-14	-17	7	93

Note: -means expansion increase,
*reduction compared to reference mortar at the same age and glass content.

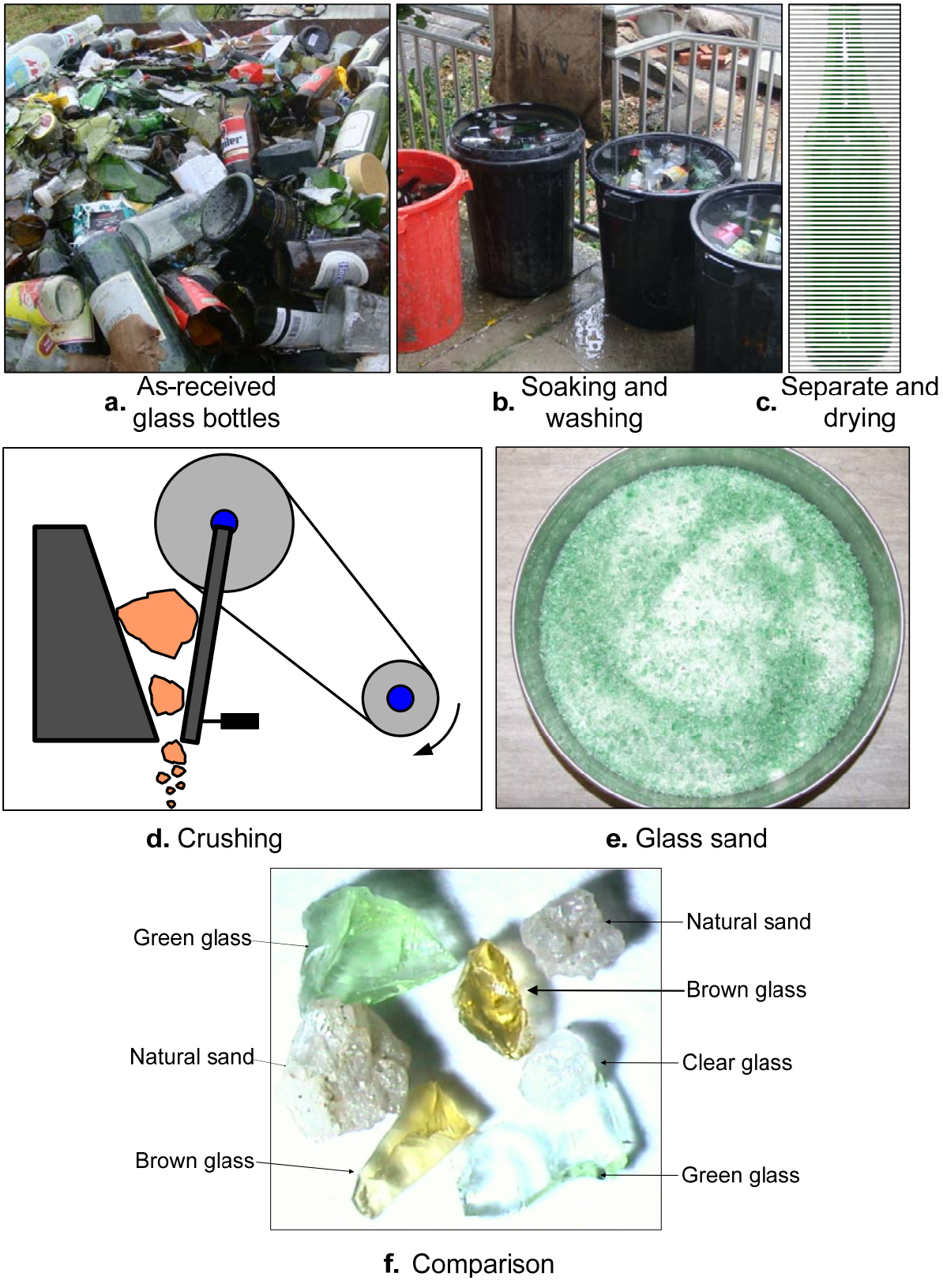

Figure 3-1: Processing of recycled waste glass sand.

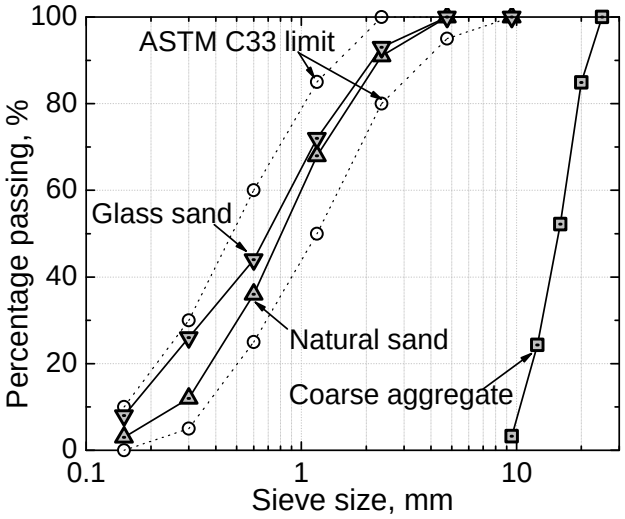

Figure 3-2: Grading curve of crushed glass sand and natural aggregates.

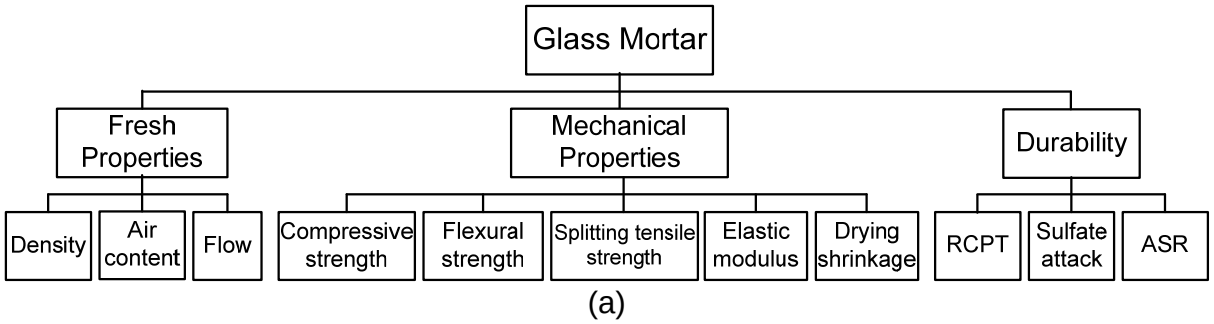

Figure 3-3: Test program for recycled glass sand in (a) mortar, and (b) concrete.

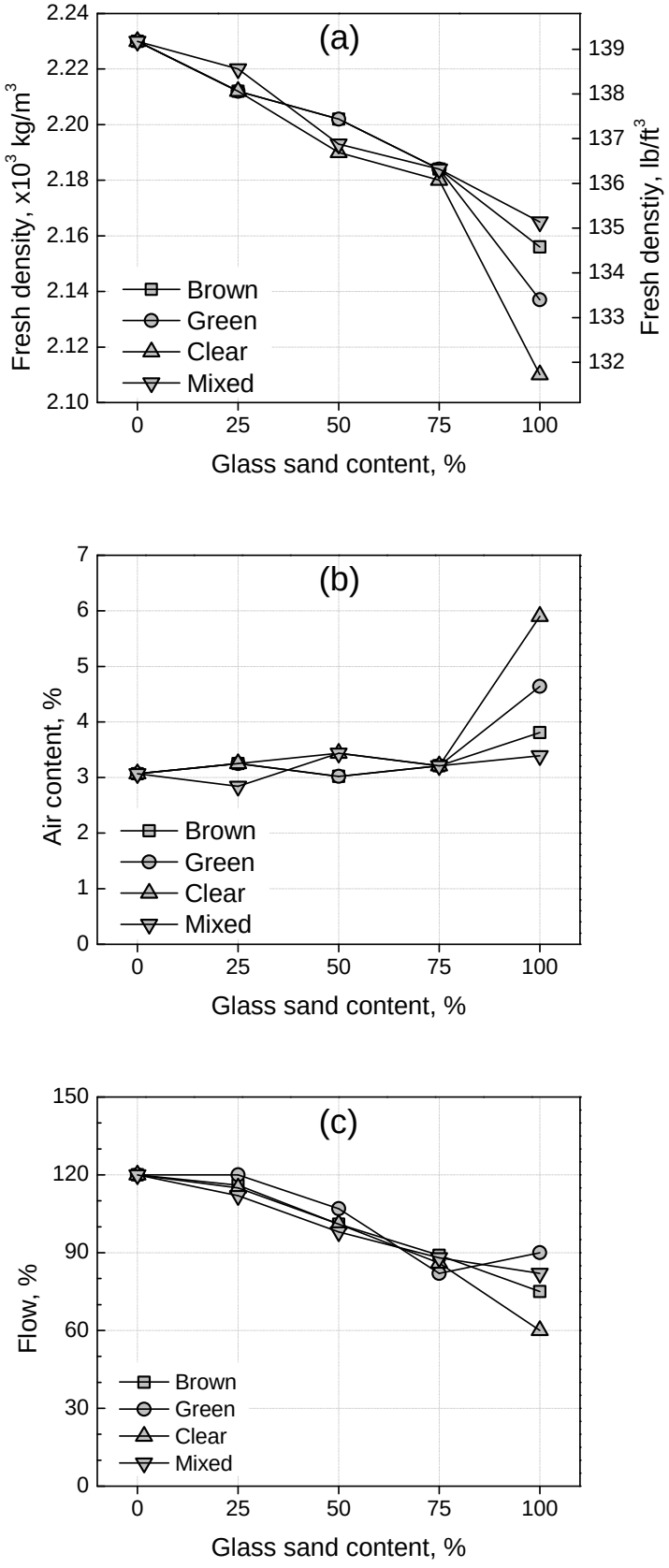

Figure 3-4: Fresh properties of glass mortar: (a) density, (b) air content, and (c) flowability.

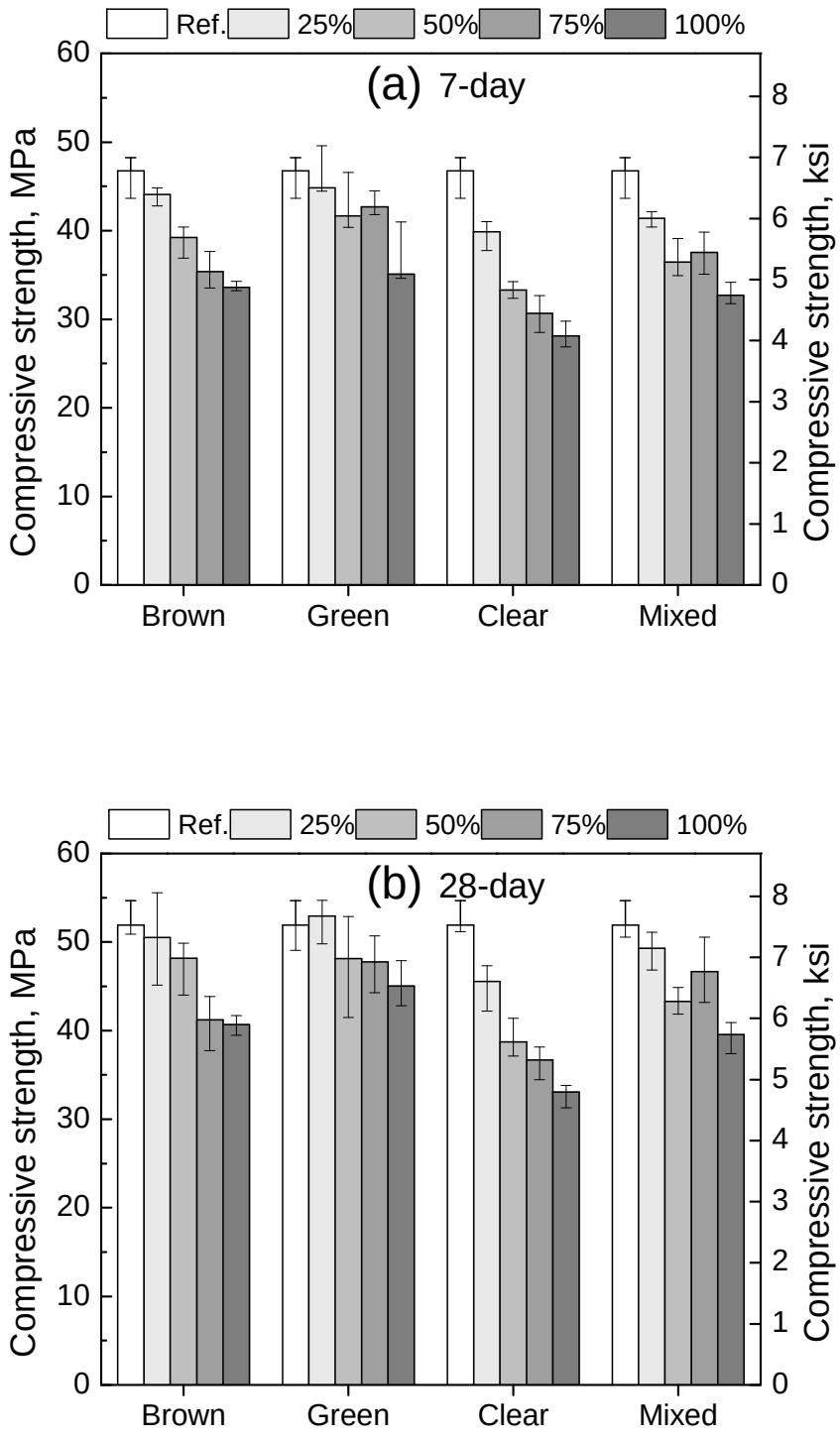

Figure 3-5: Compressive strength of glass mortar.

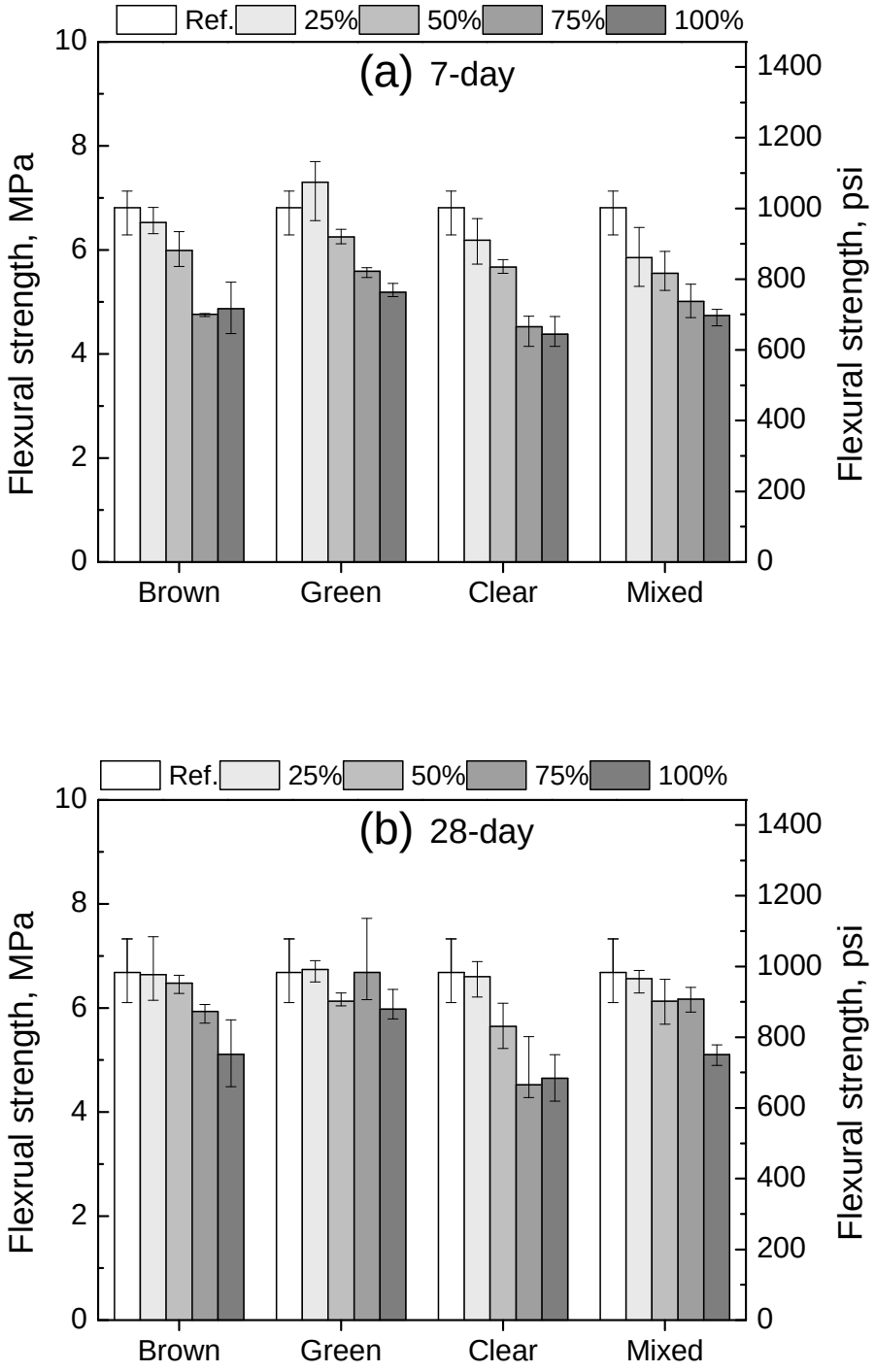

Figure 3-6: Flexural strength of glass mortar.

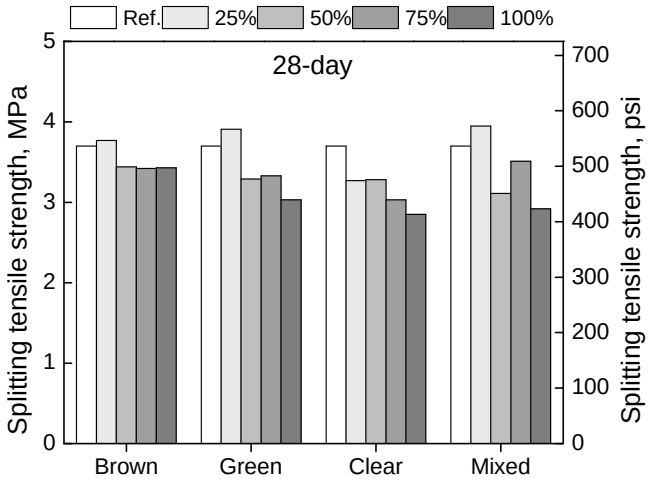

Figure 3-7: Splitting tensile strength of glass mortar.

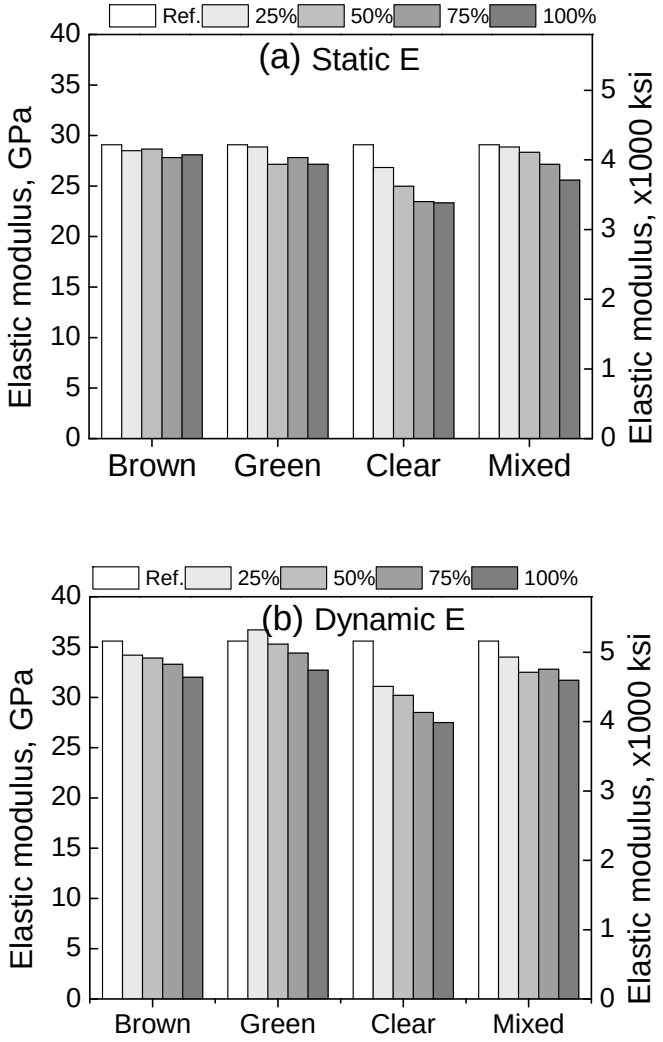

Figure 3-8: Static and dynamic modulus of elasticity of glass mortar.

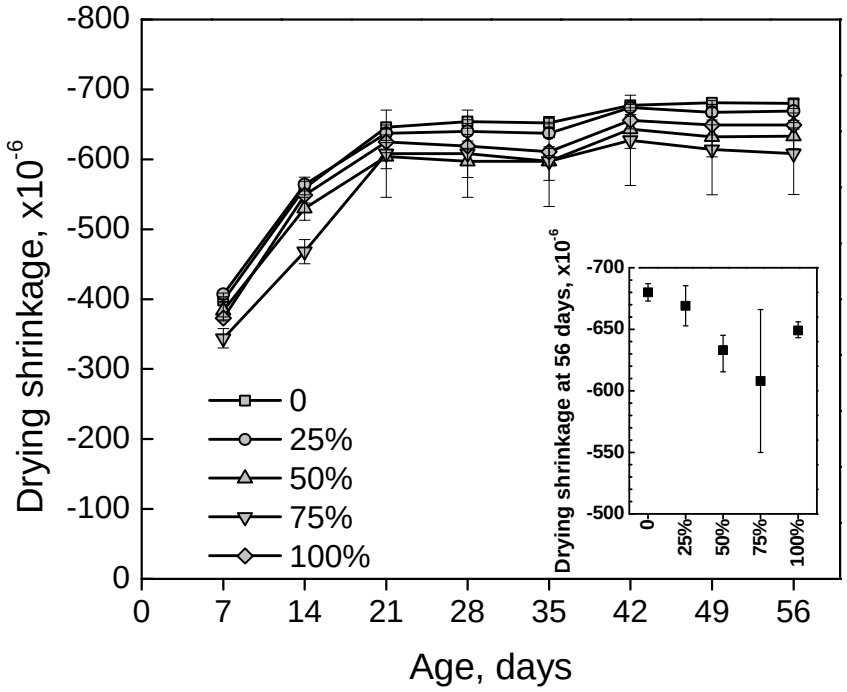

Figure 3-9: Drying shrinkage of mixed color glass mortar.

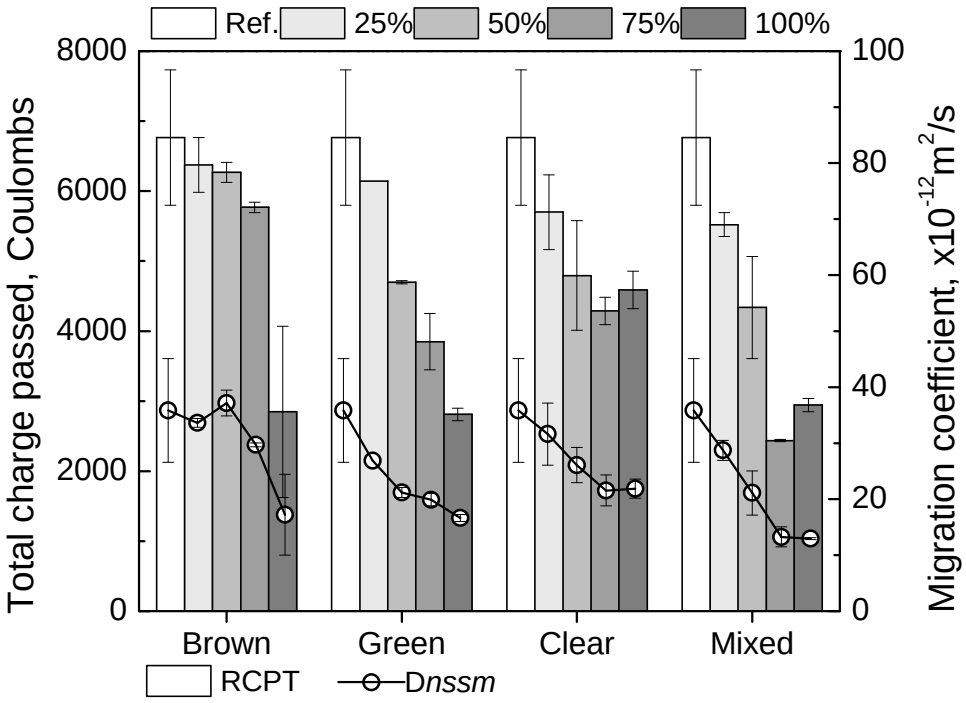

Figure 3-10: RCPT results of glass mortar at 28-day.

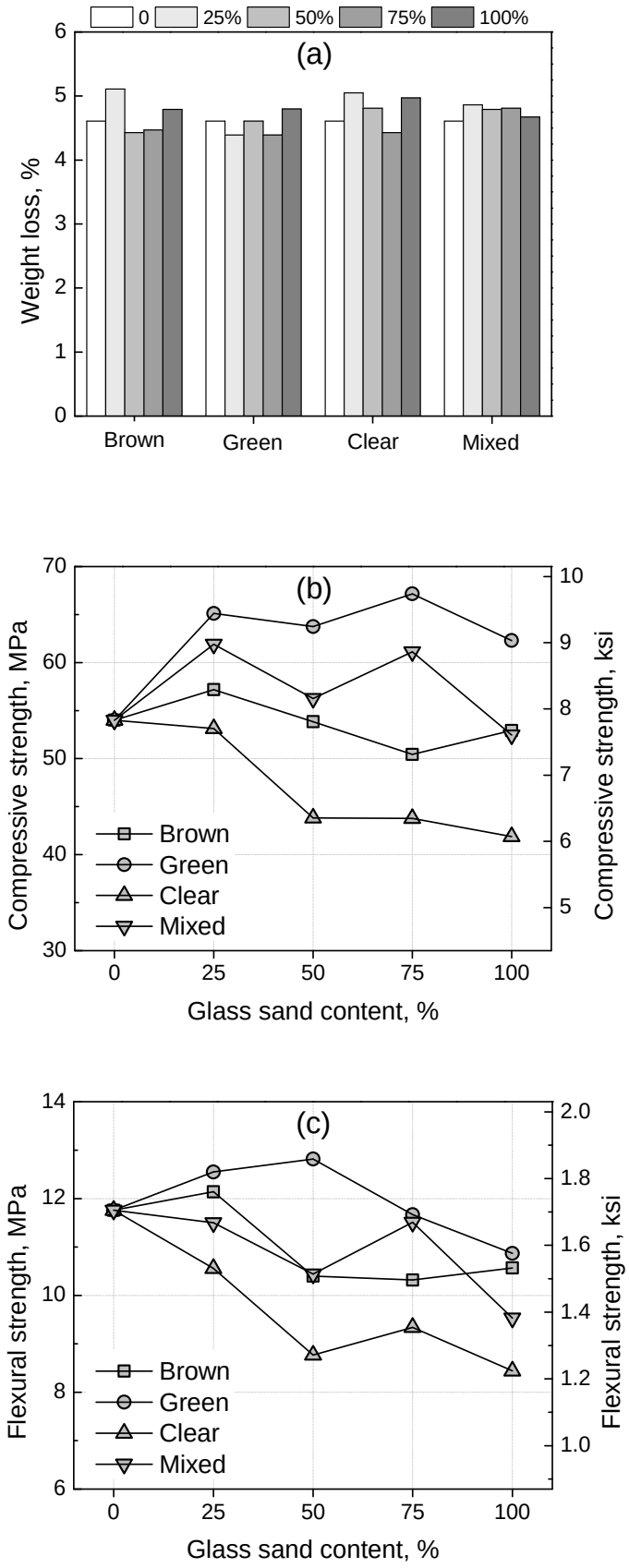

Figure 3-11: Sulfate attack test results of glass mortar: (a) weight loss, (b) compressive strength, and (c) flexural strength.

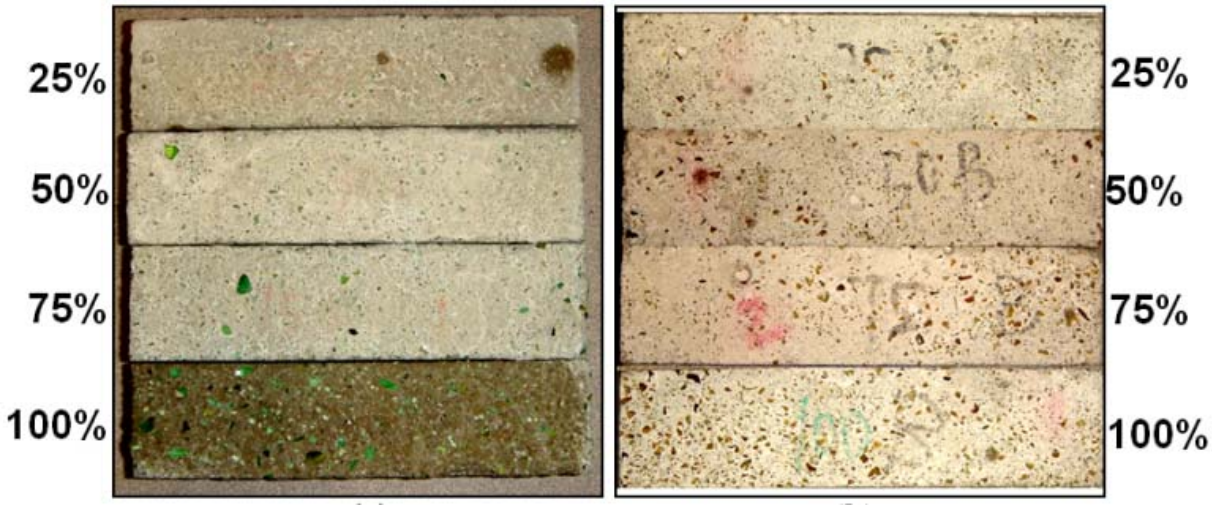

(a) Green glass sand (b) Brown glass sand

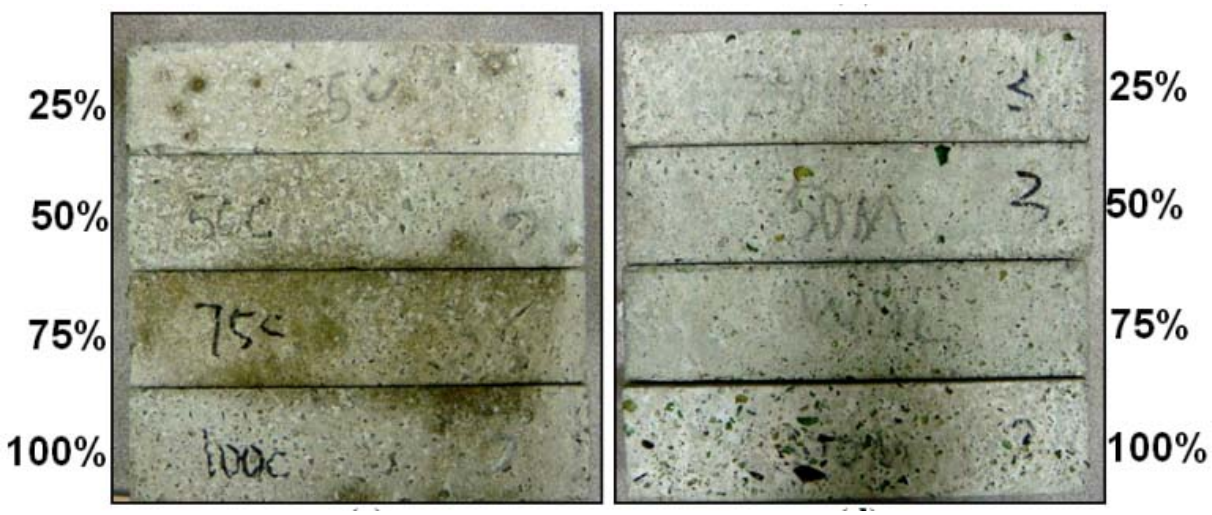

(b) Clear glass sand (d) Mixed glass sand

Figure 3-12: Picture of mortar specimens with (a) green, (b) brown, (c) clear, and (d) mixed color glass sand after sulfate attack tests.

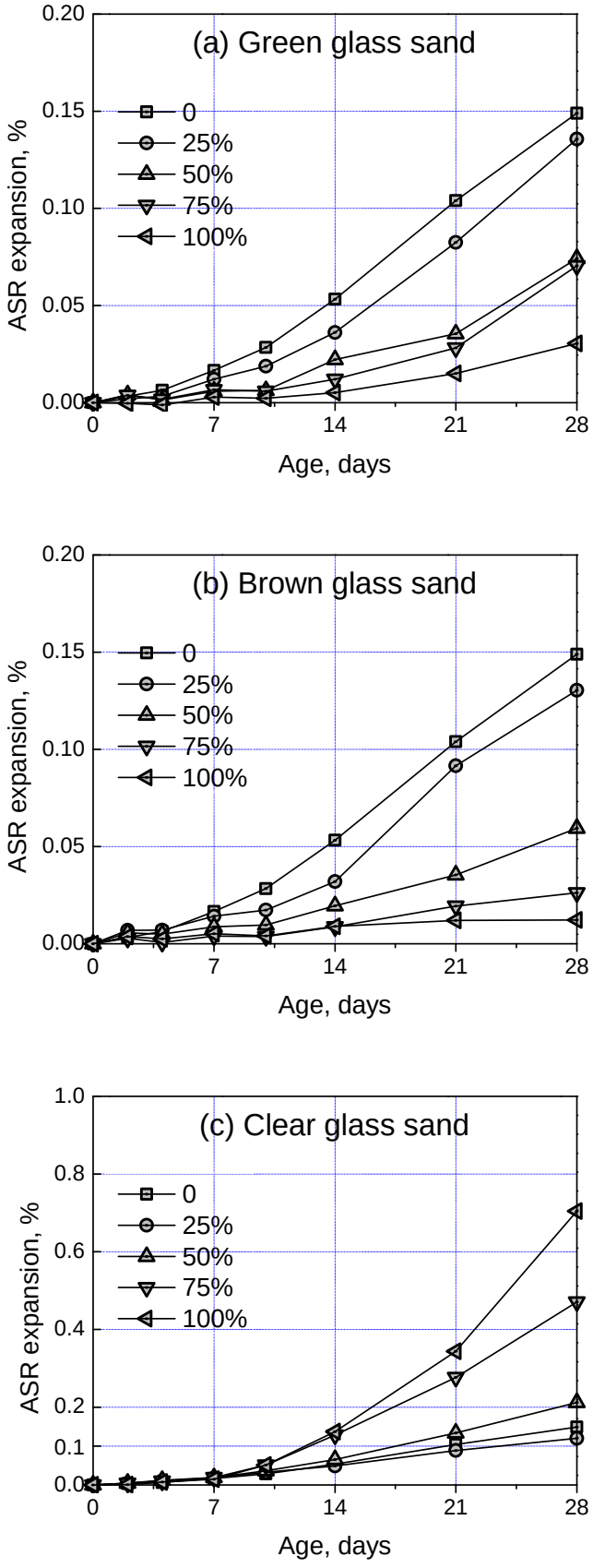

Figure 3-13: ASR expansion of mortar with different colored glass sands.

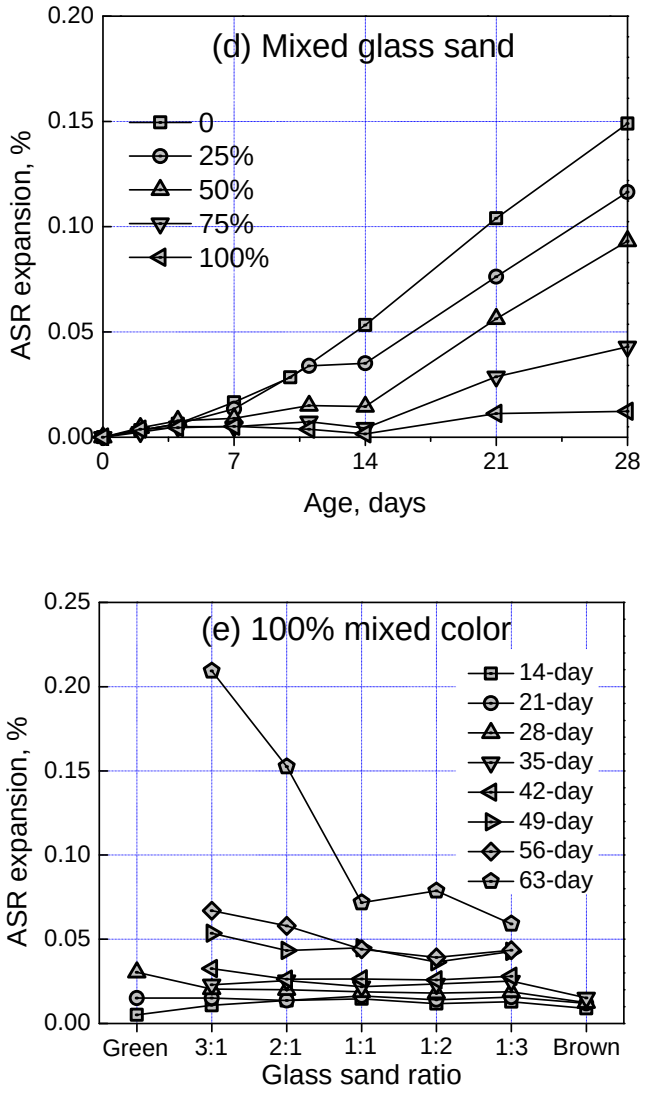

Figure 3-13 (continued): ASR expansion of mortar with different colored glass sands.

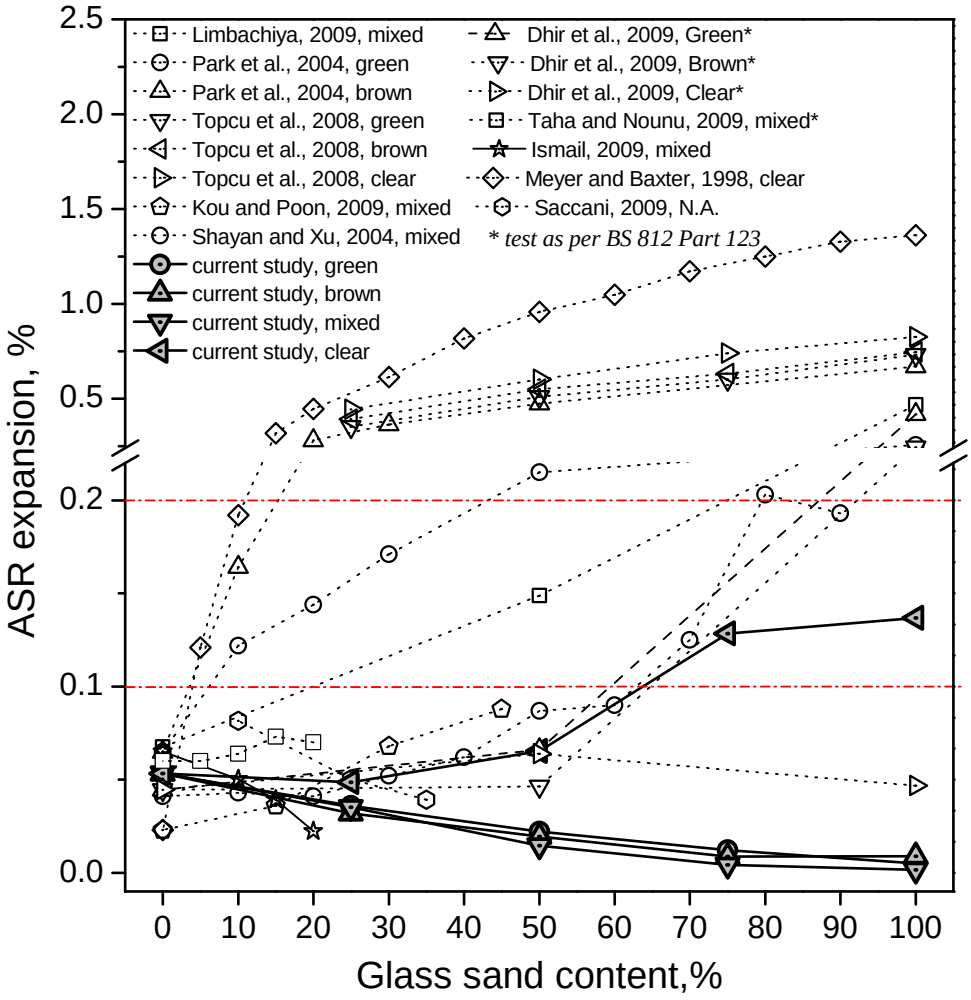

Figure 3-14: Effect of glass sand content on ASR expansion at 14 days.

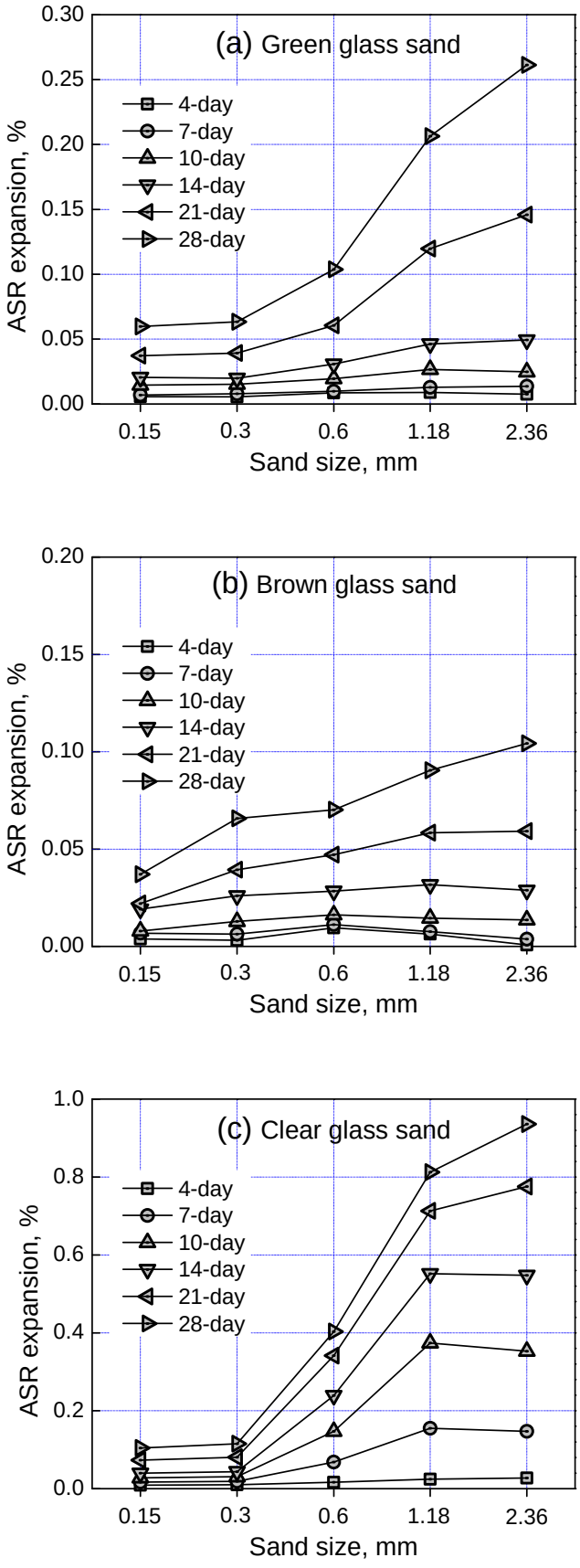

Figure 3-15: Effect of glass particle size on ASR expansion (glass content of 25%).

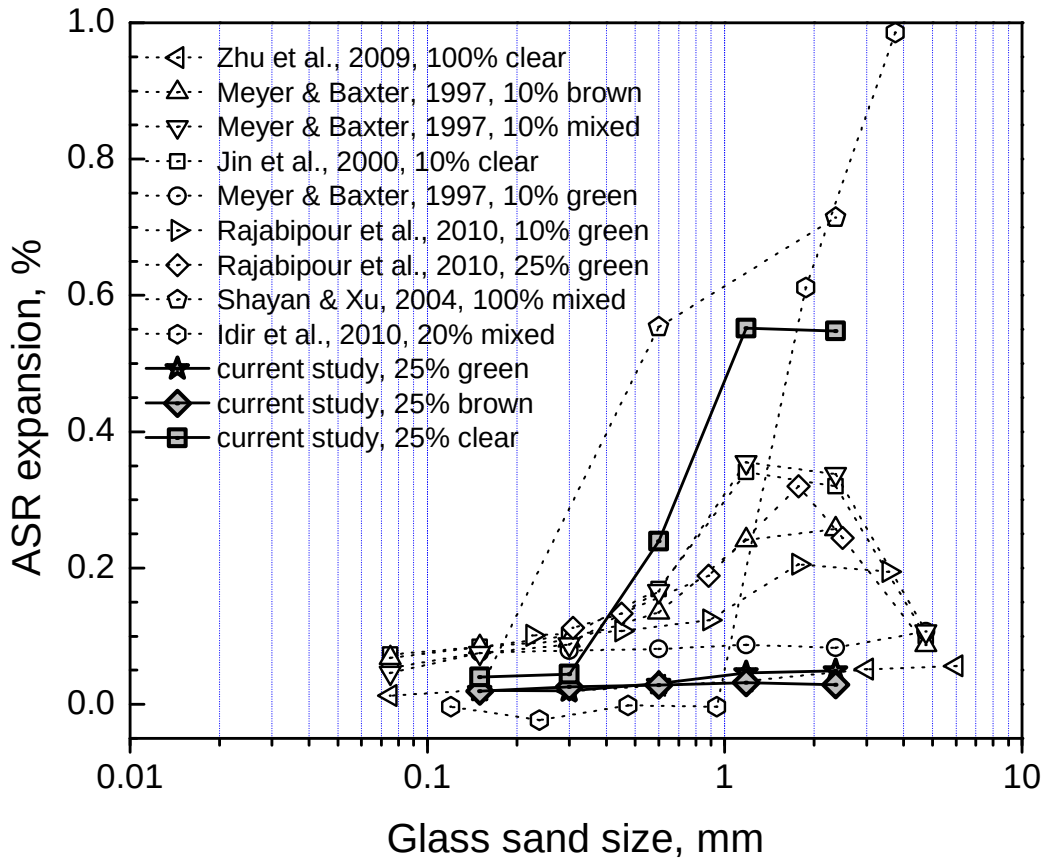

Figure 3-16: Comparison of effect of glass particle size on ASR expansion.

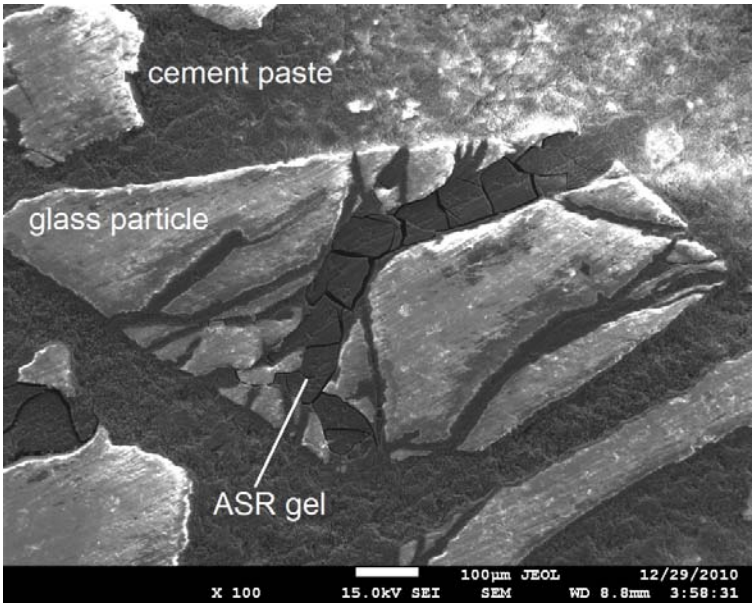

(a) cracks initiated from internal cracks in mortar with 100% clear glass sand.

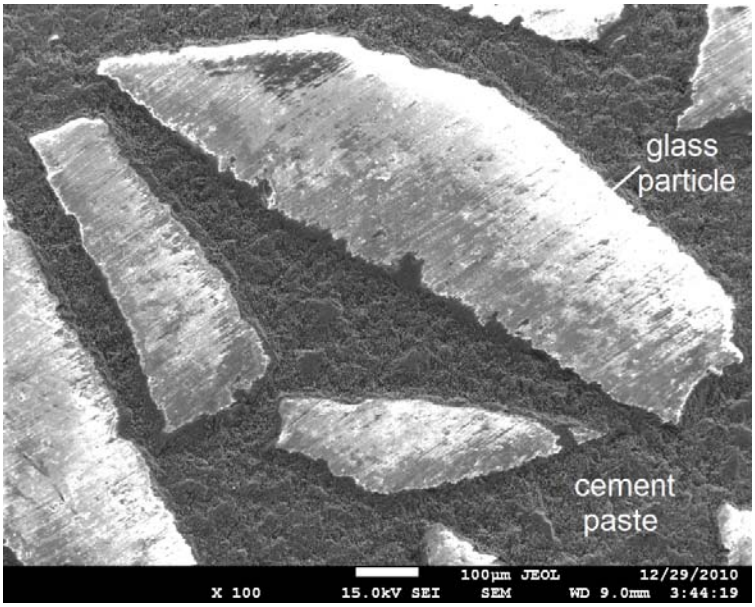

(b) no crack in mortar with 100% green glass sand.

Figure 3-17: SEM micrographs of glass mortar.

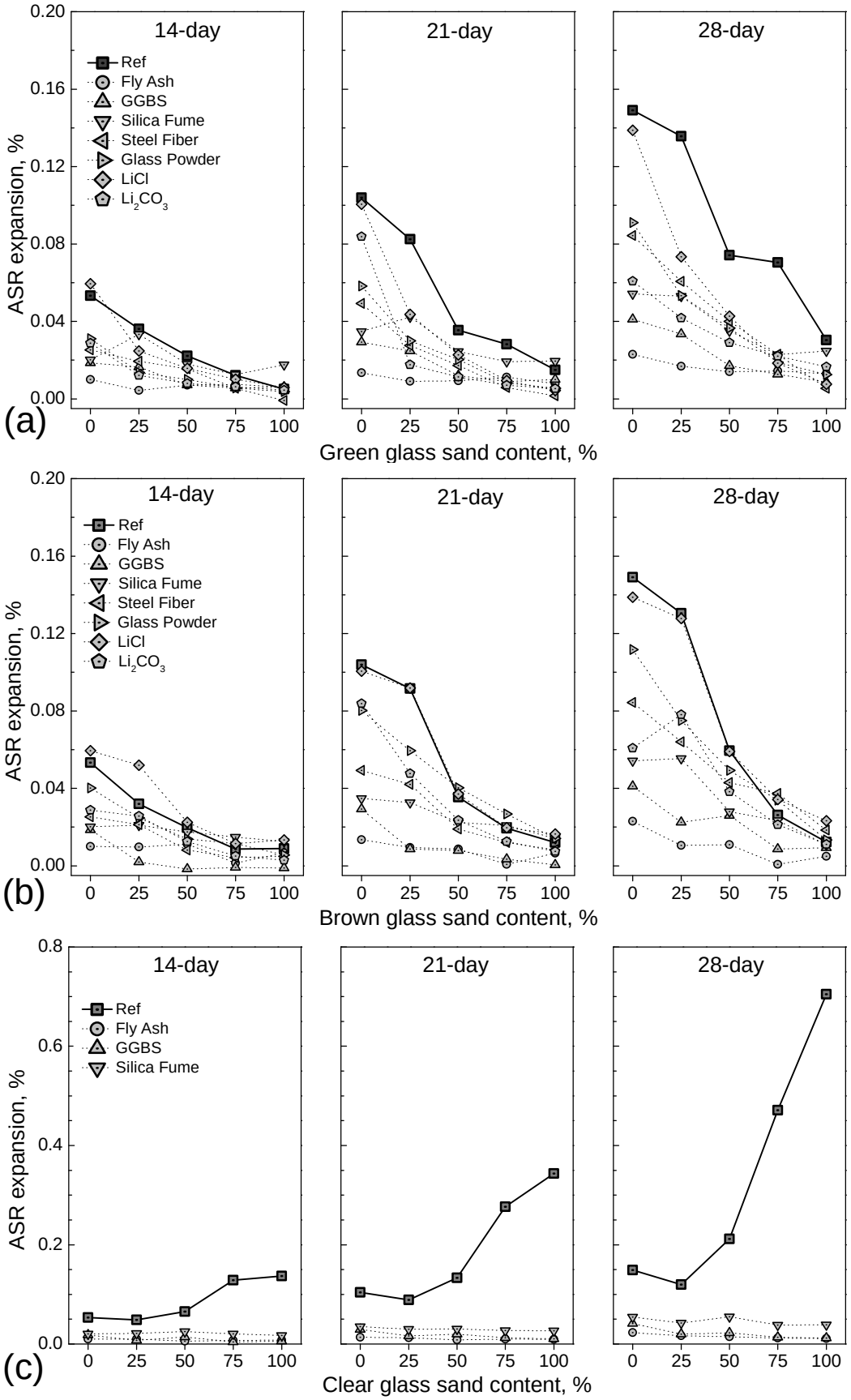

Figure 3-18: Comparison of different mitigation methods on ASR expansion of mortar with (a) green, (b) brown, and (c) clear glass sand.

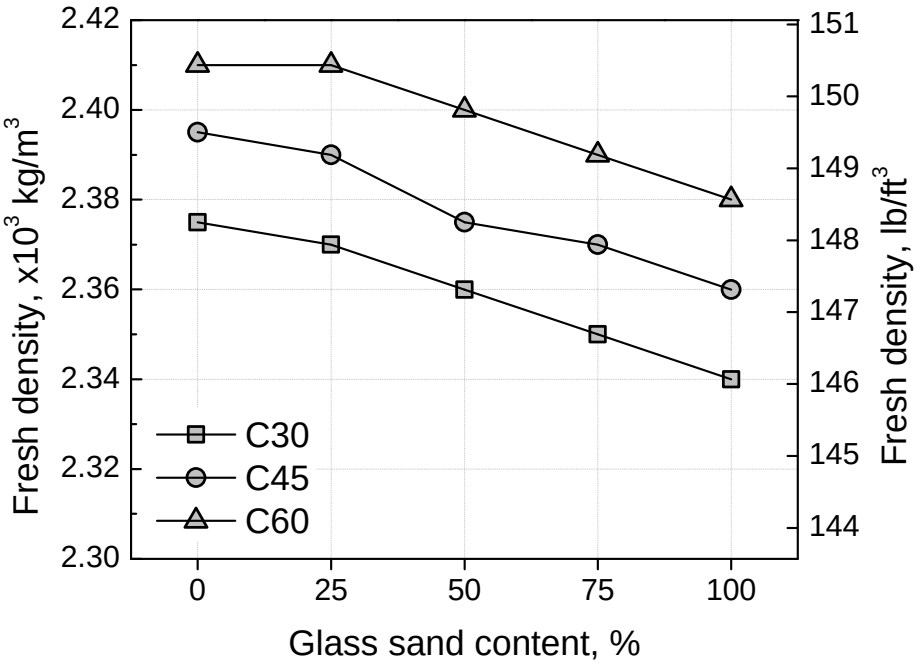

Figure 3-19: Fresh density of glass concrete.

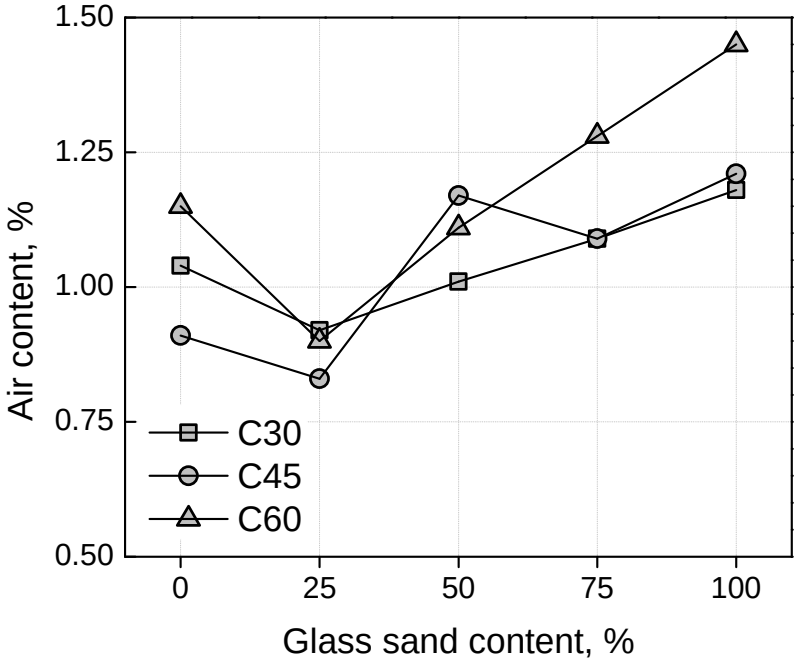

Figure 3-20: Air content of fresh glass concrete.

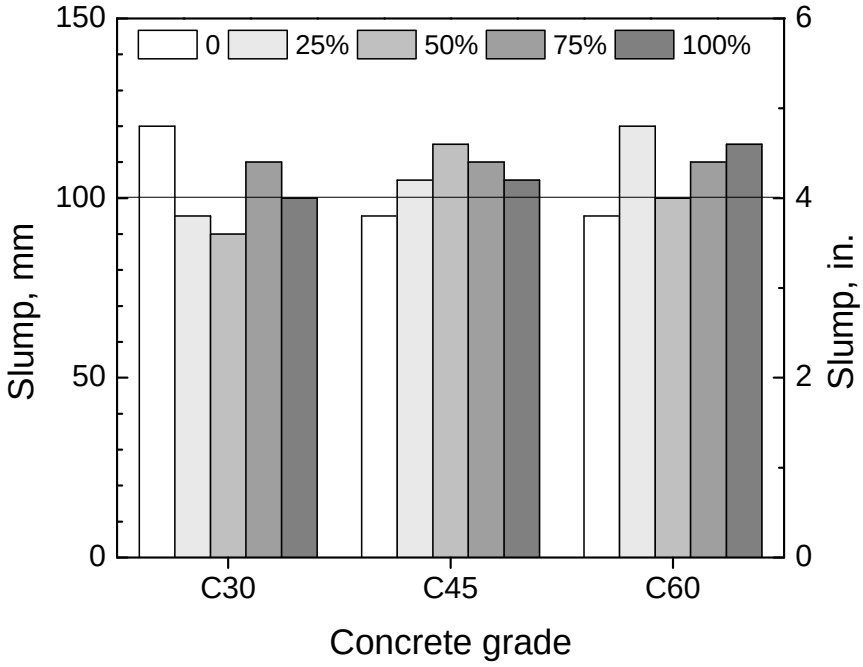

Figure 3-21: Slump of glass concrete.

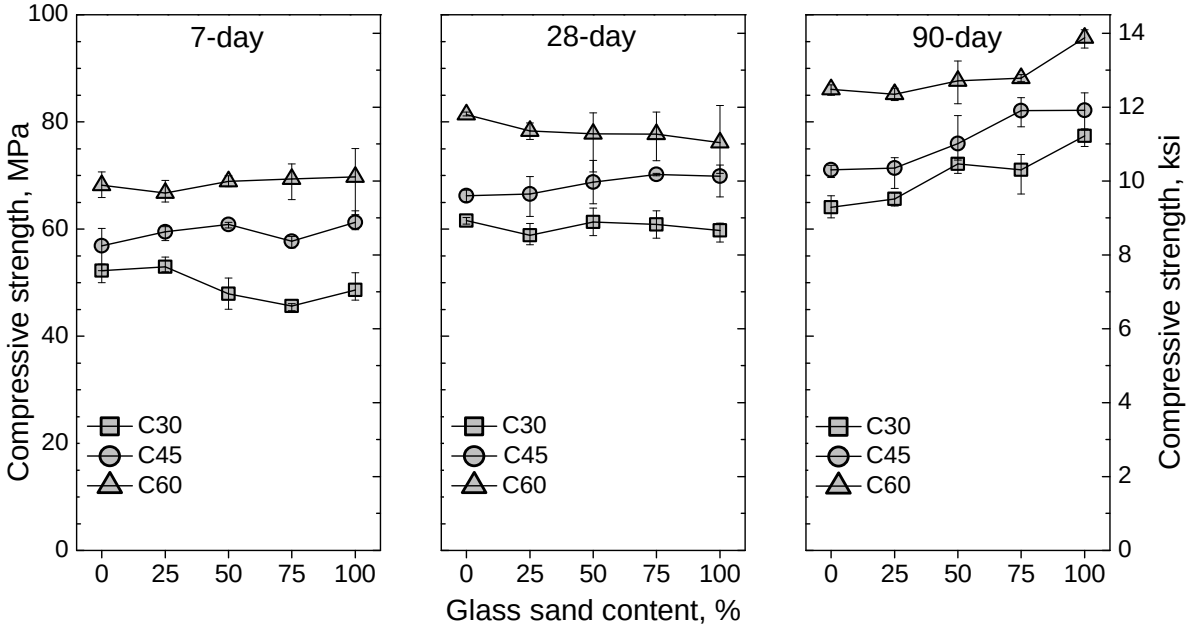

Figure 3-22: Compressive strength of glass concrete.

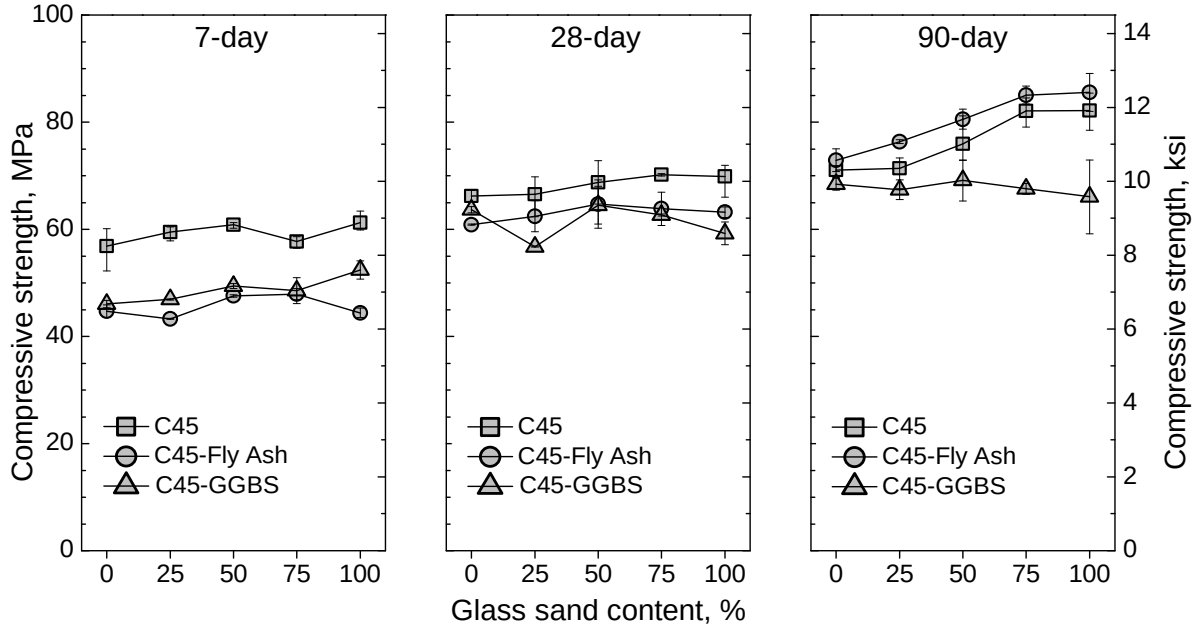

Figure 3-23: Compressive strength of glass concrete with 30% fly ash or 60% GGBS.

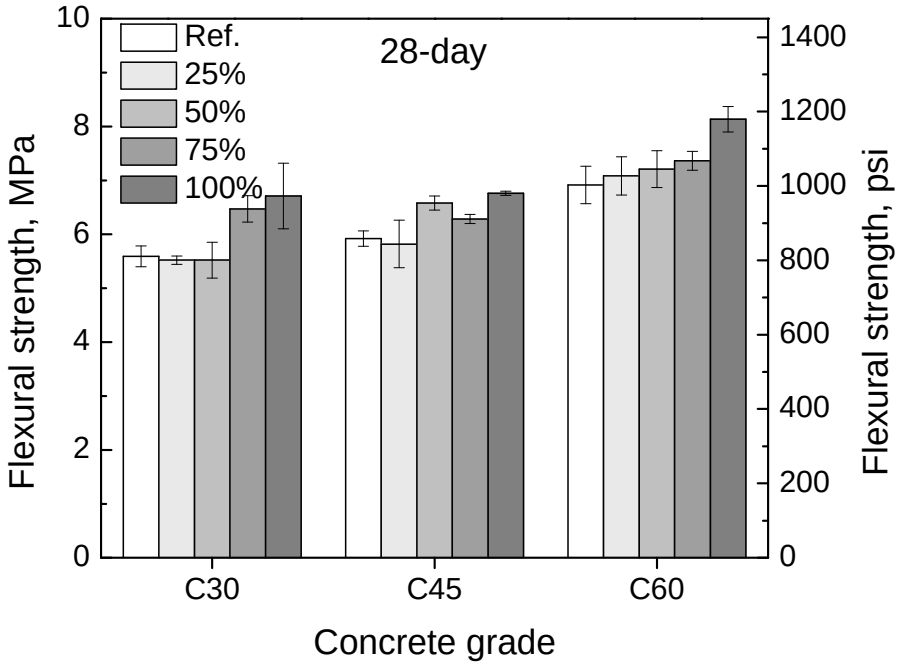

Figure 3-24: Flexural strength of glass concrete.

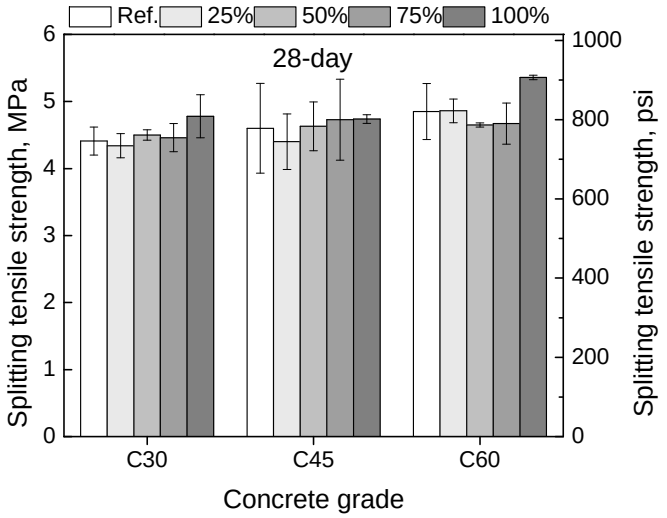

Figure 3-25: Splitting tensile strength of glass concrete.

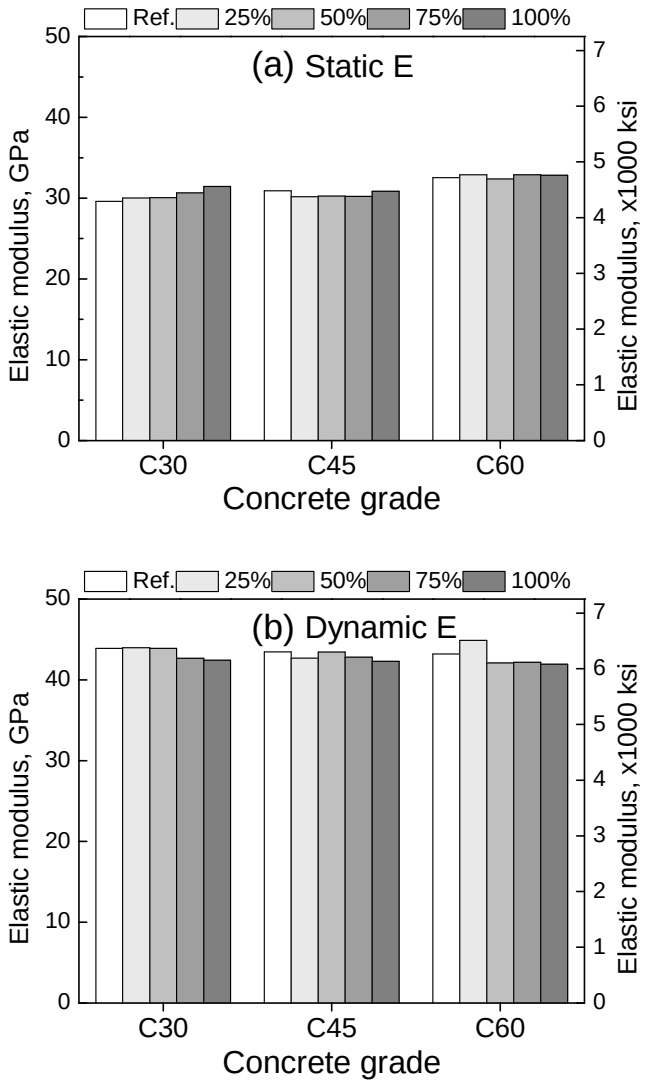

Figure 3-26: Static and dynamic modulus of elasticity of glass concrete.

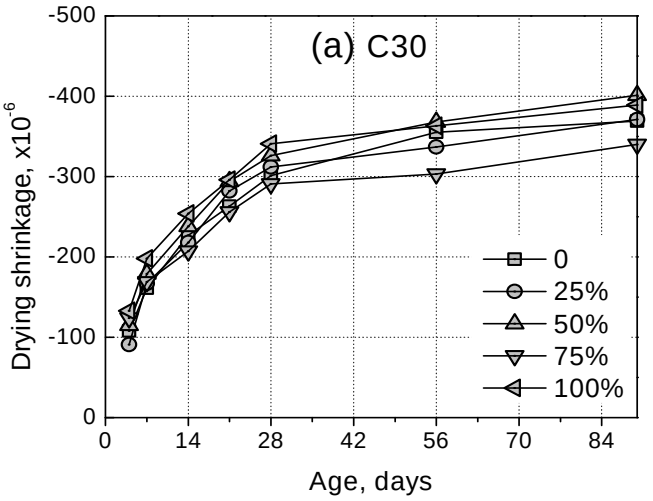

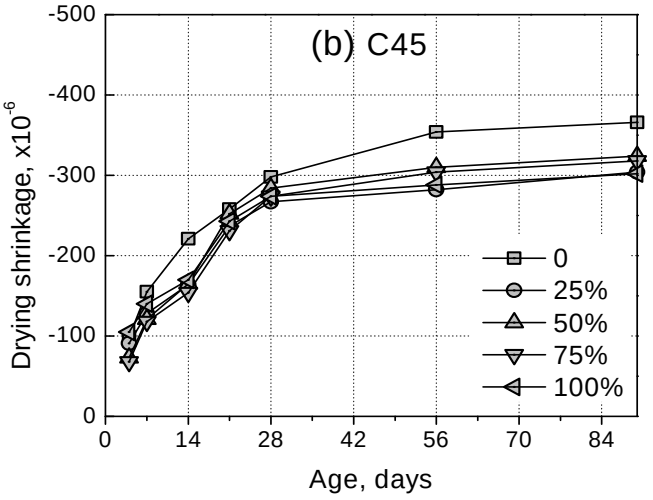

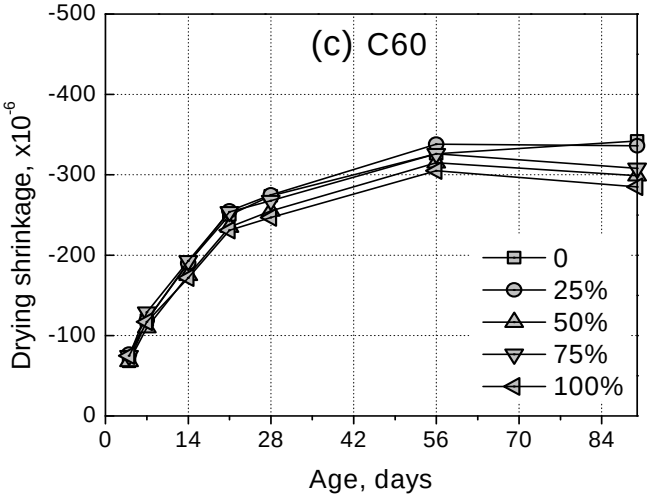

Figure 3-27: Drying shrinkage of glass concrete.

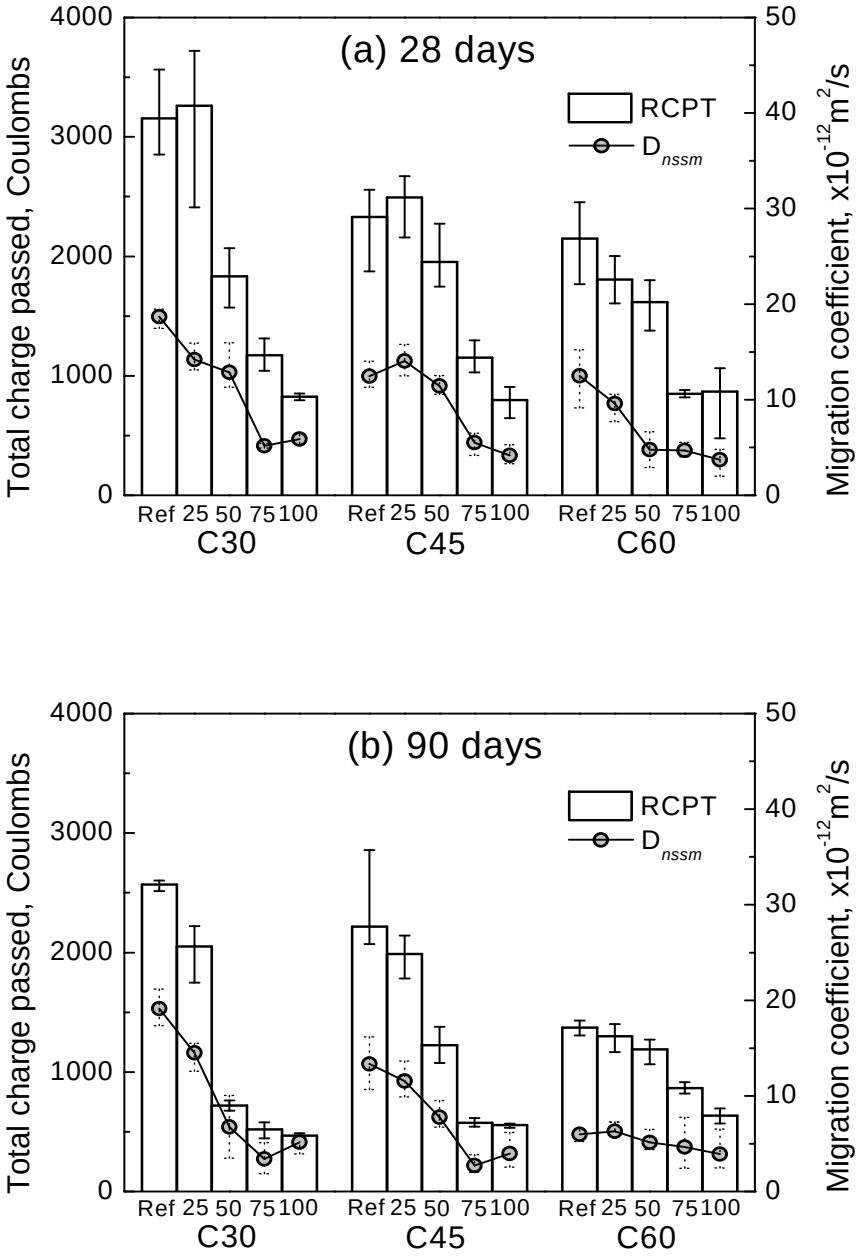

Figure 3-28: RCPT results of glass concrete.

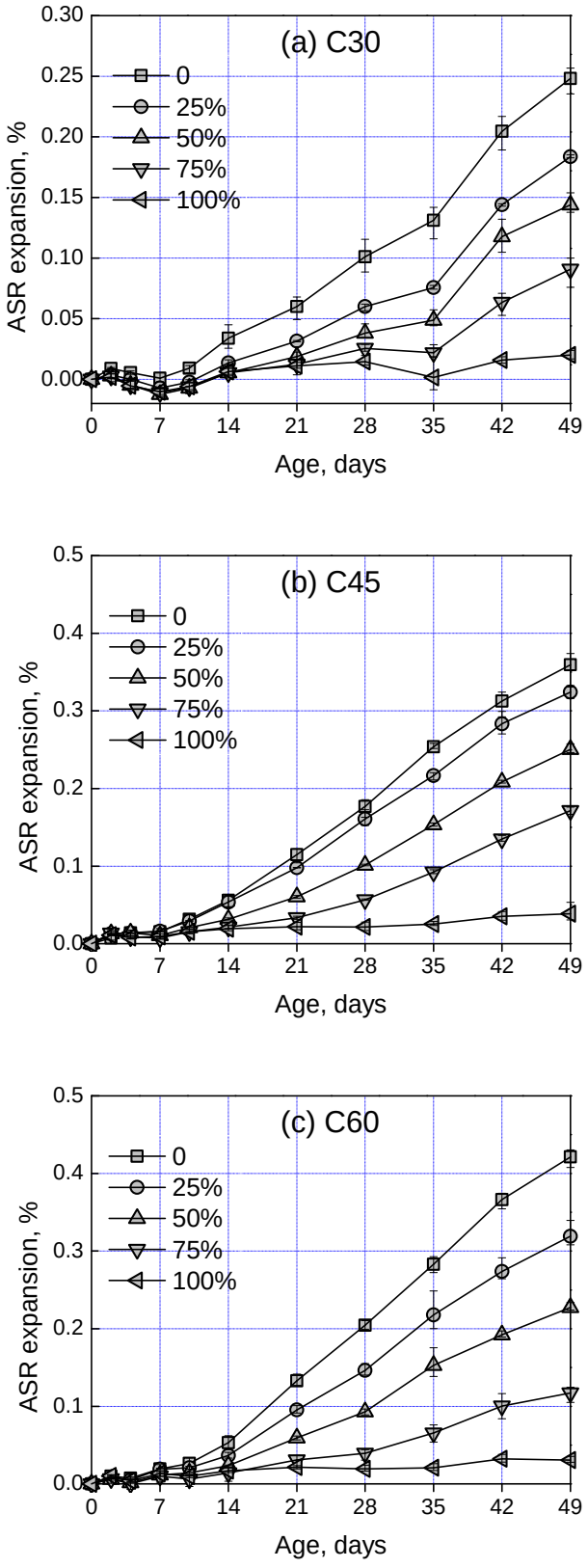

Figure 3-29: ASR expansion of concrete with brown glass sand.

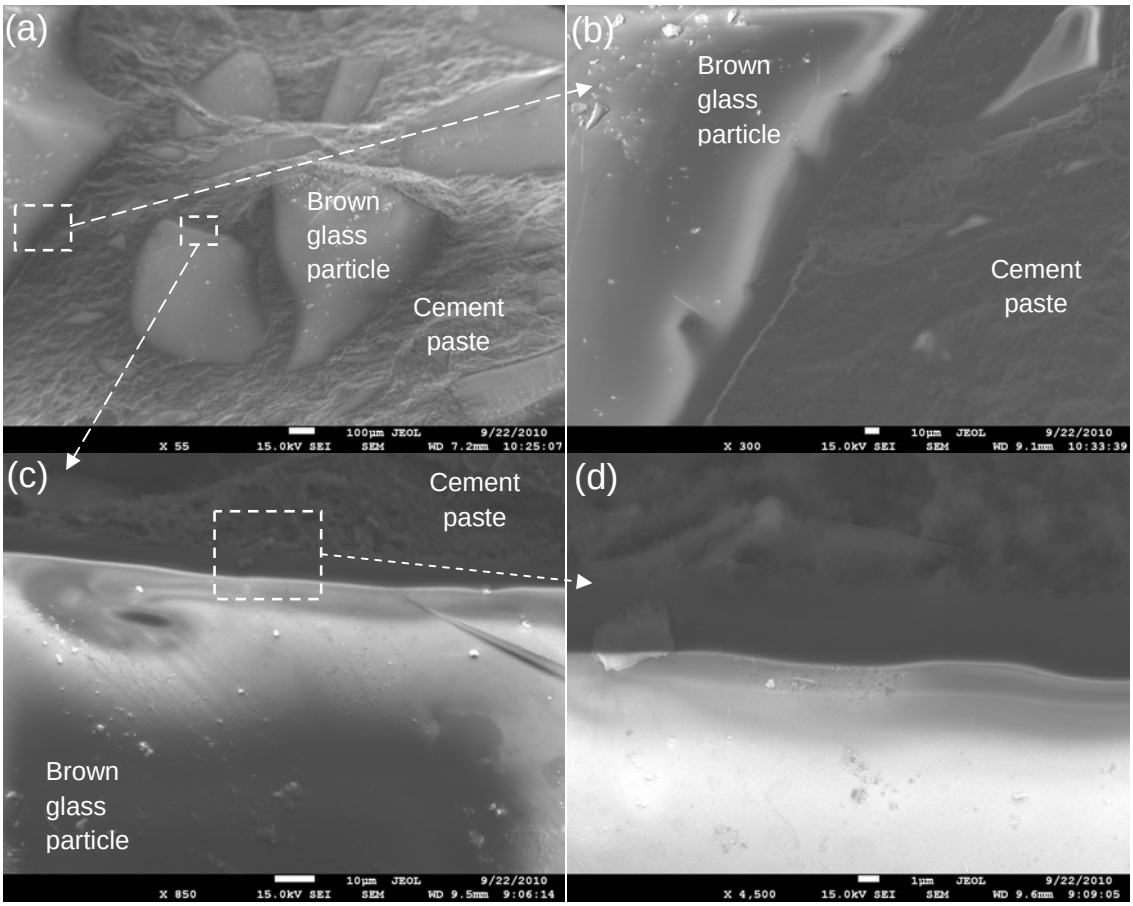

Figure 3-30: SEM micrographs of brown C45-100 glass mortar after 49 days of ASR testing.

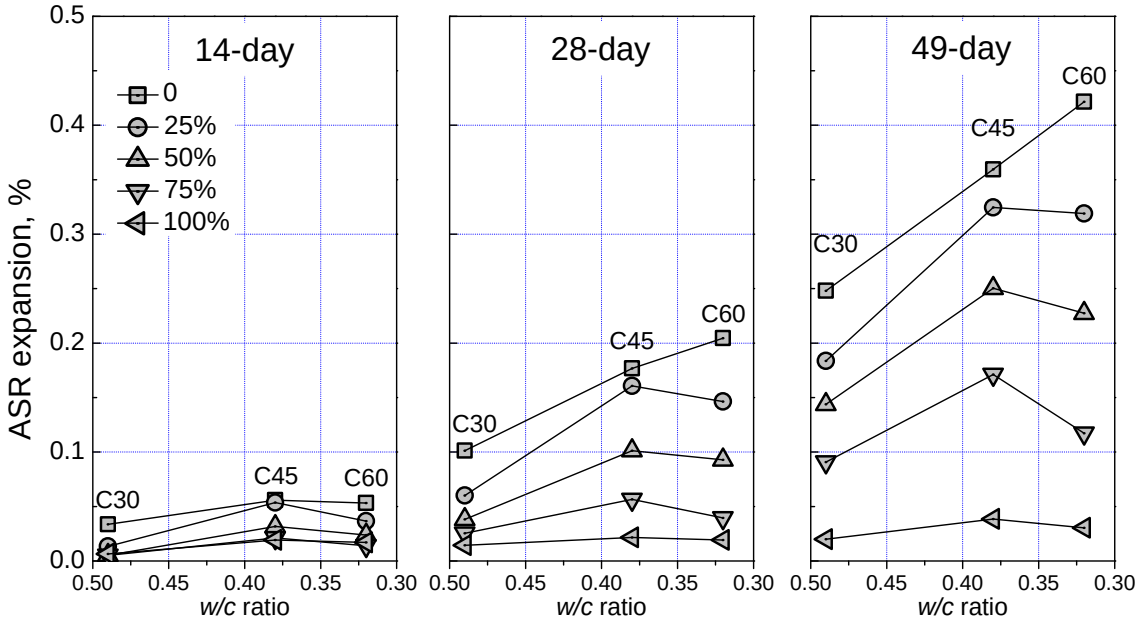

Figure 3-31: Effect of *w/c* ratio on ASR expansion.

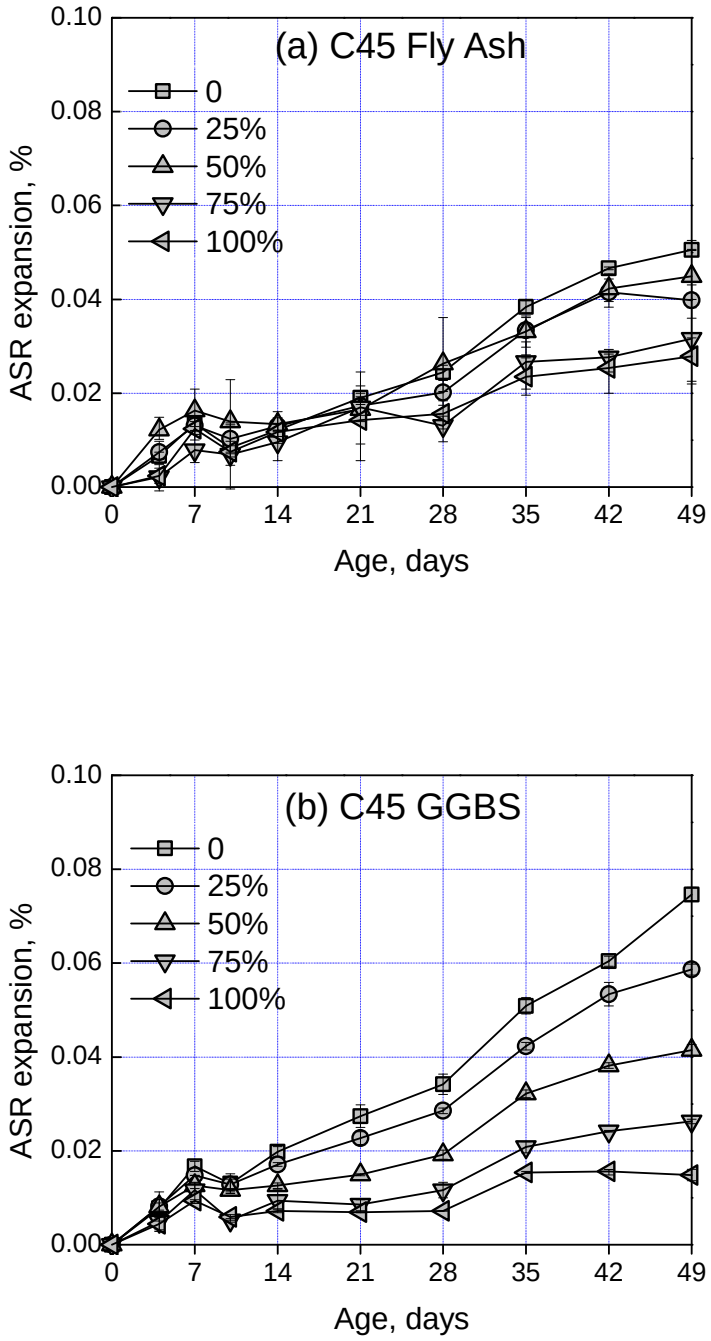

Figure 3-32: ASR expansions of brown glass concrete C45 with (a) 30% fly ash, and (b) 60% GGBS.

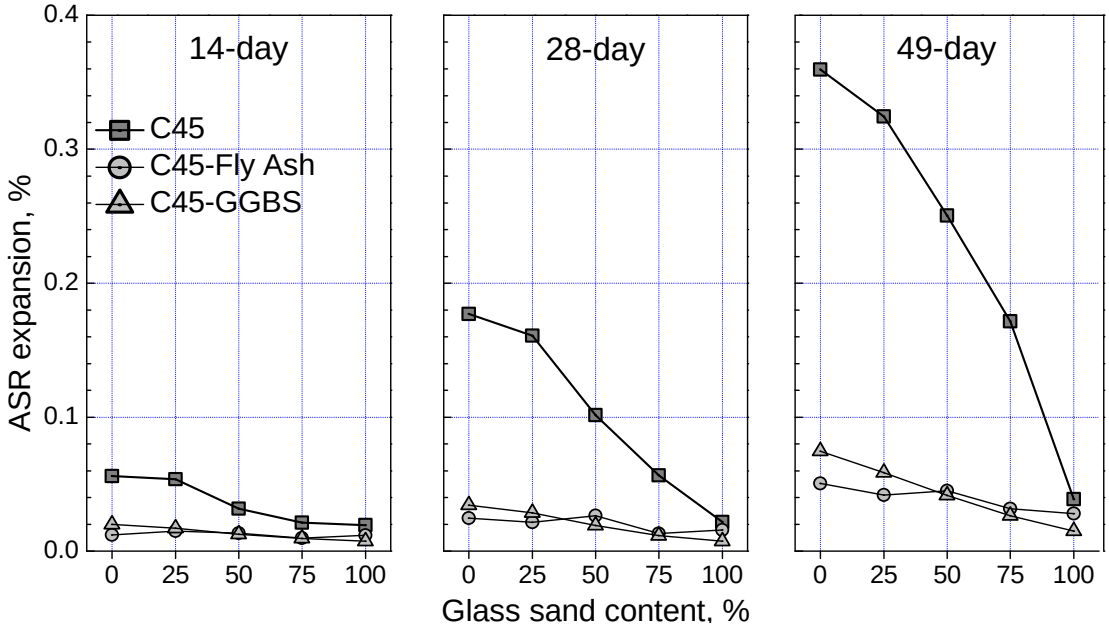

Figure 3-33: ASR expansion comparison.

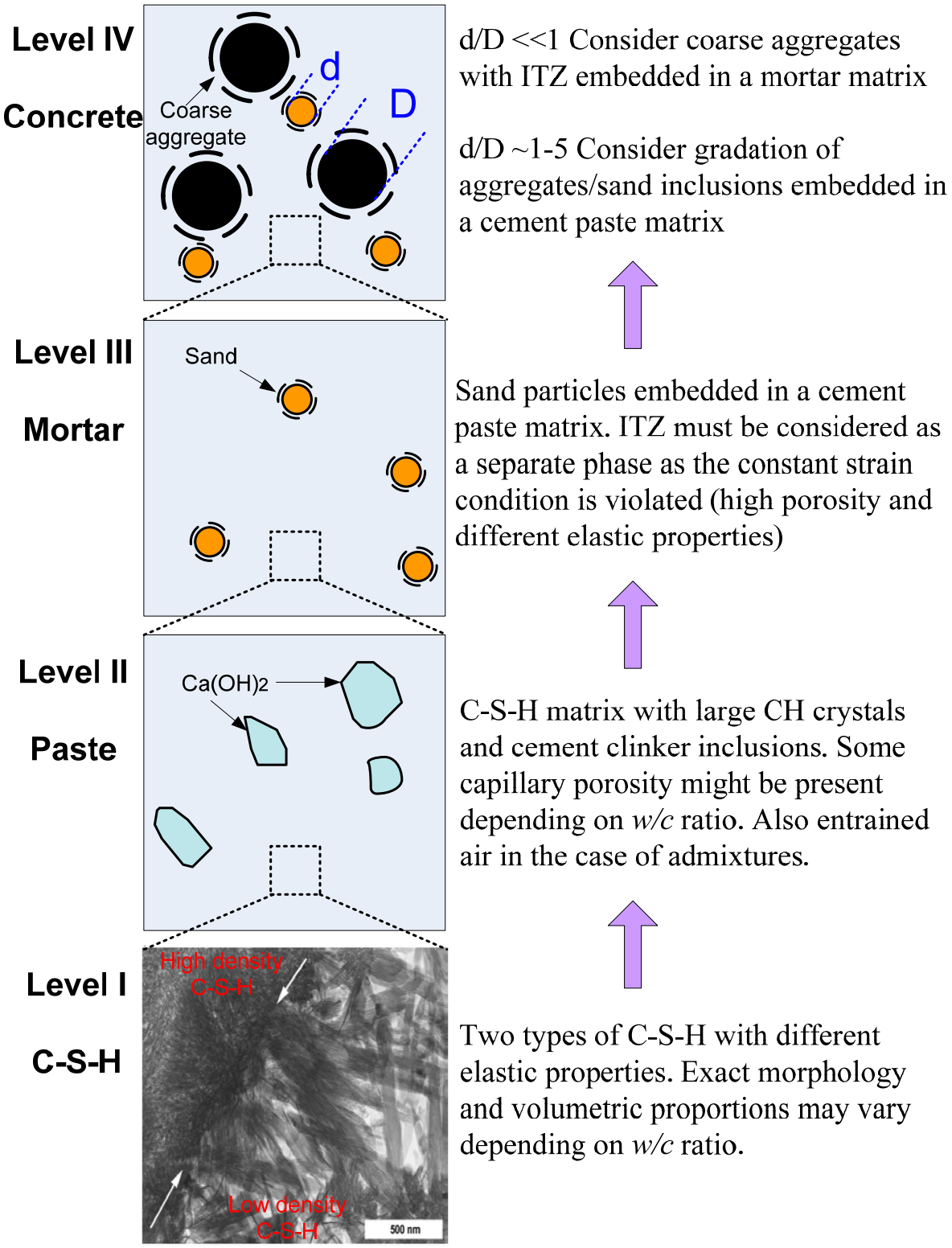

Figure 3-34: Four level microstructure of cement-based composite materials [Constantinides and Ulm, 2004; Richardson, 2004].

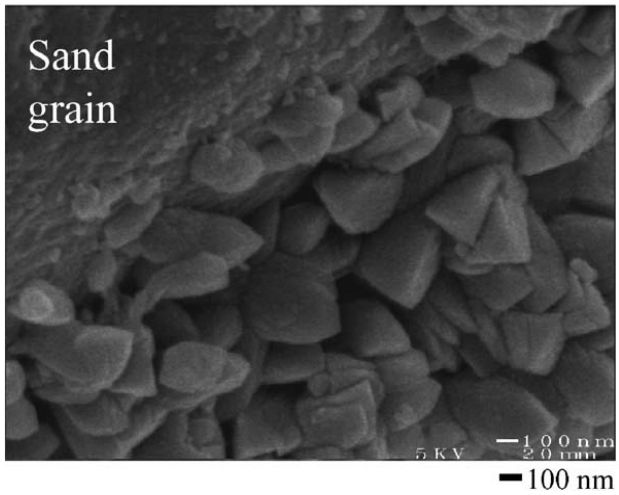

(a) SEM micrograph

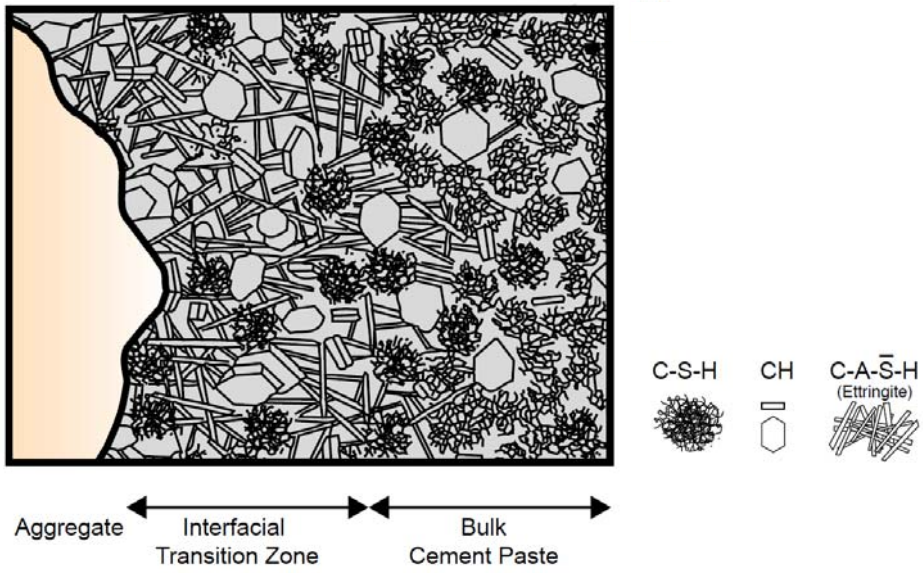

(b) Diagrammatic representation

Figure 3-35: (a) SEM micrograph of higher Portlandite (CH) concentration in the ITZ (wall effect) of mortar [Heukamp et al., 2003]; (b) Diagrammatic representation of the ITZ and bulk cement paste in concrete [Mehta and Monteiro, 2006].

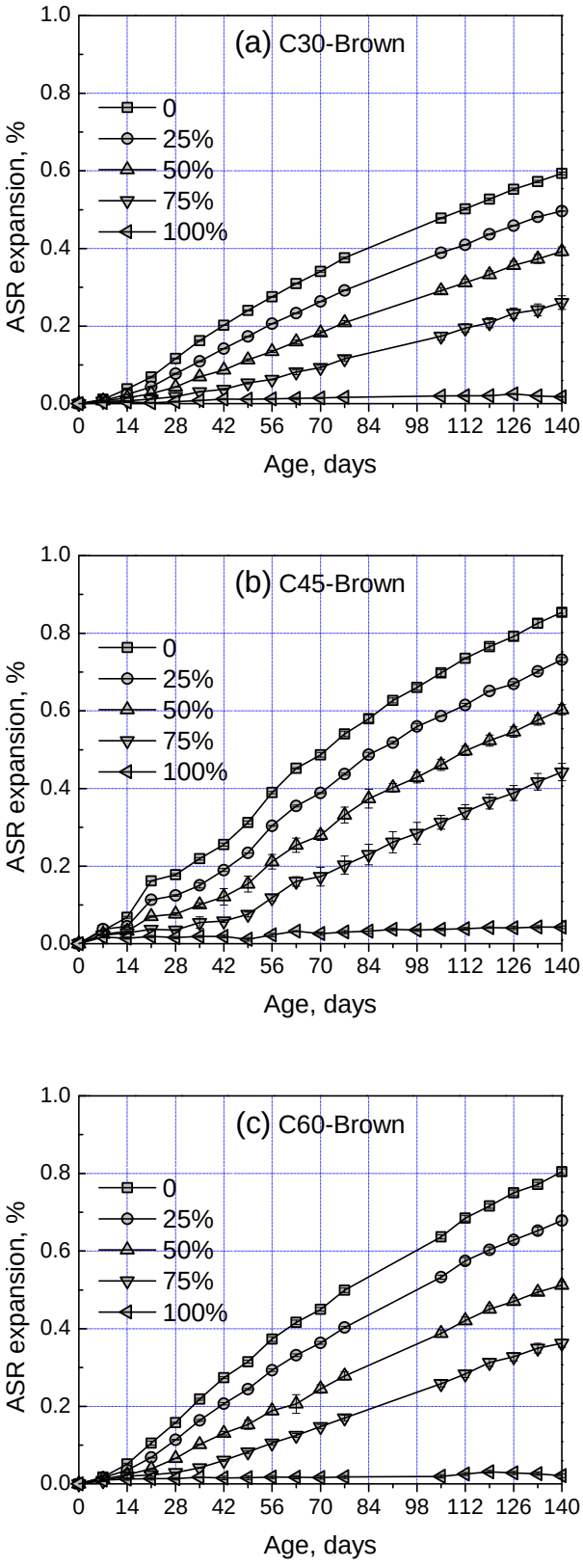

Figure 3-36: ASR expansion of mortar containing brown and green glass sand.

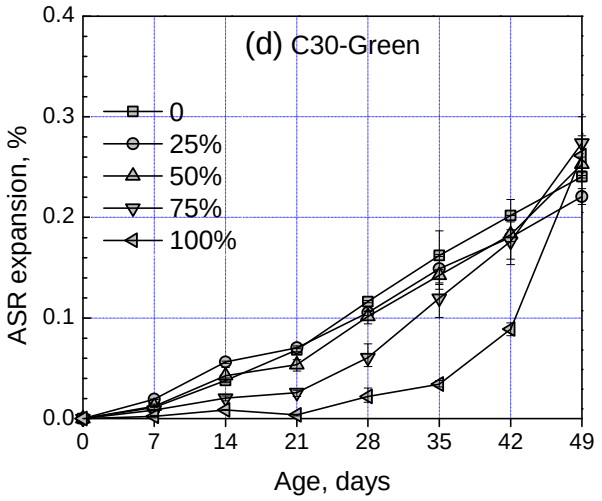

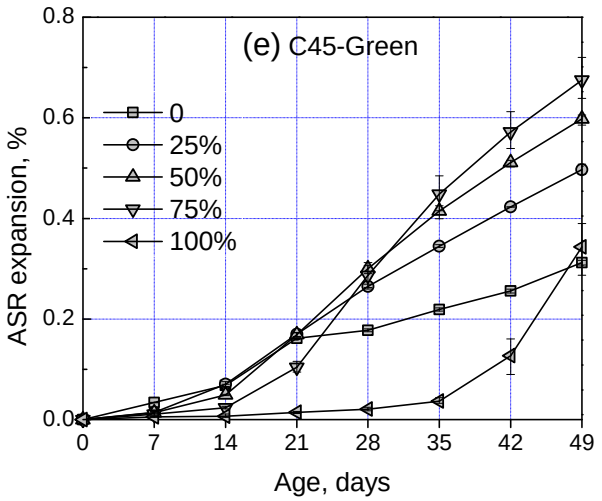

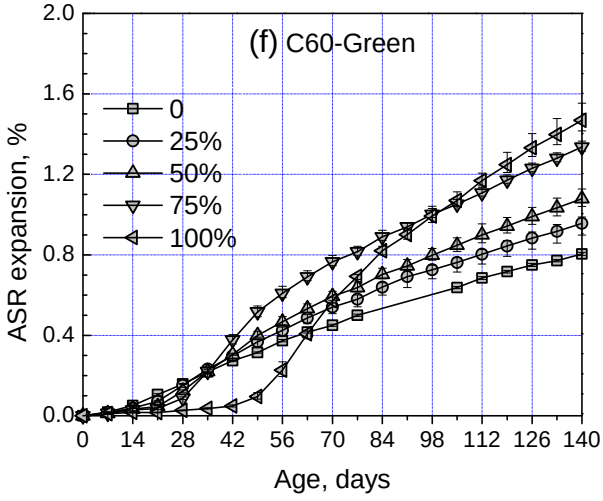

Figure 3-36 (continued): ASR expansion of mortar containing brown and green glass sand.

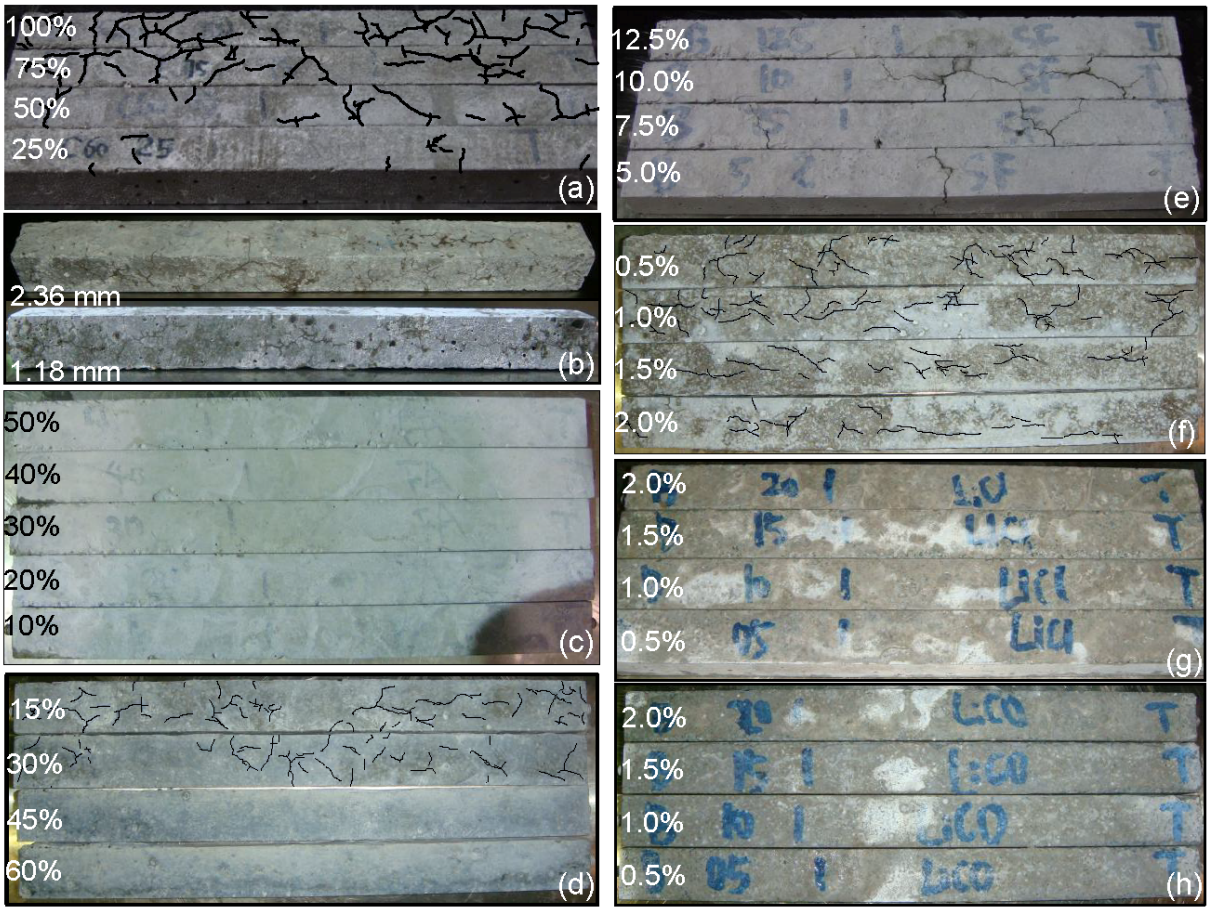

Figure 3-37: Pictures of (a) C60 mortars with different green glass sand contents, (b) mortars with 100% 2.36- and 1.18-mm green glass sand, and mortar with 1.18-mm green glass sand mitigated by (c) fly ash, (d) GGBS, (e) silica fume, (f) steel fiber, (g) LiCl, and (h) Li_2CO_3.

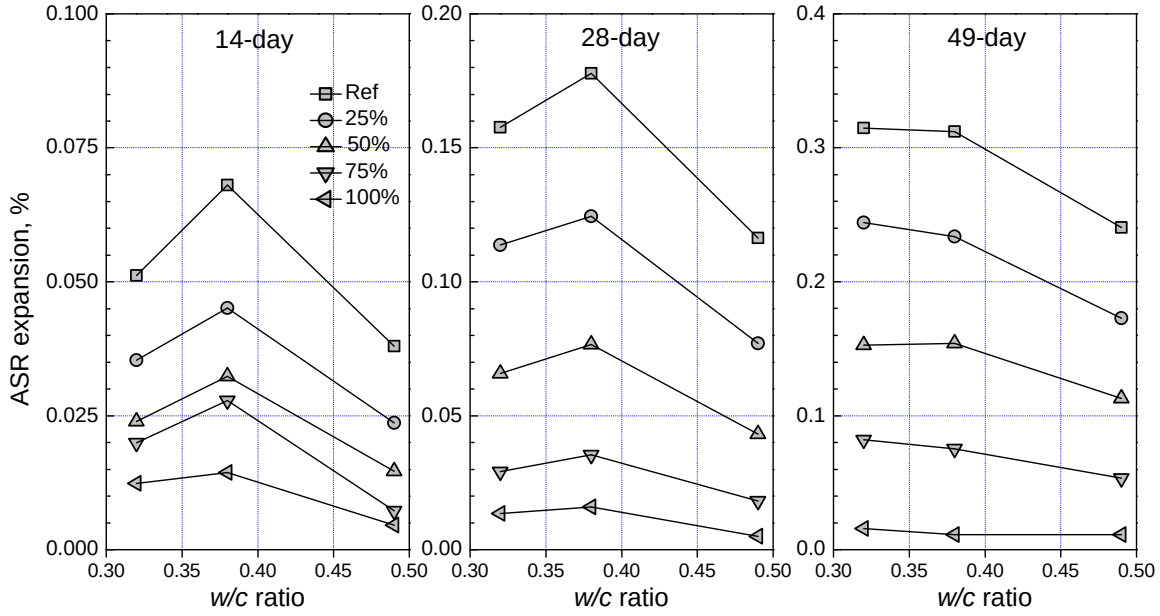

(a) Brown glass sand mortar

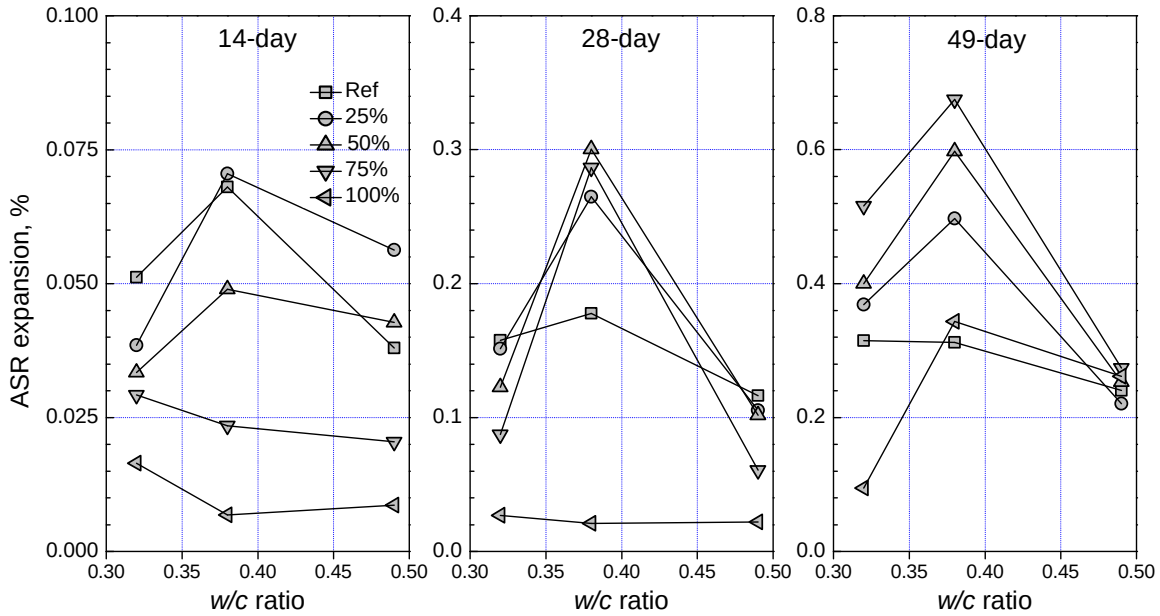

(b) Green glass sand mortar

Figure 3-38: Effect *w/c* ratio on glass sand mortar ASR expansion.

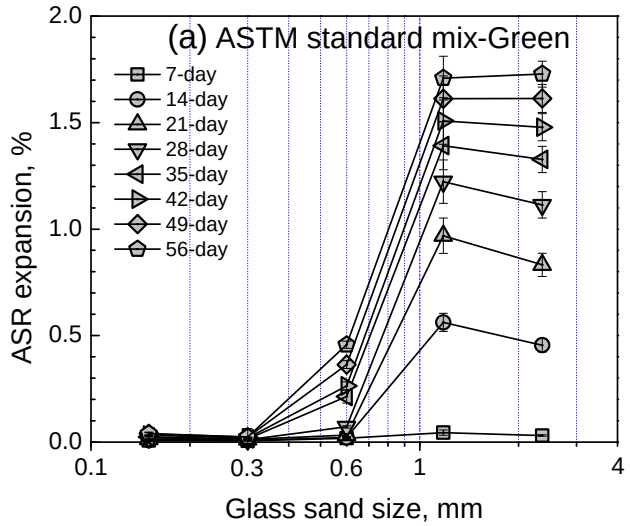

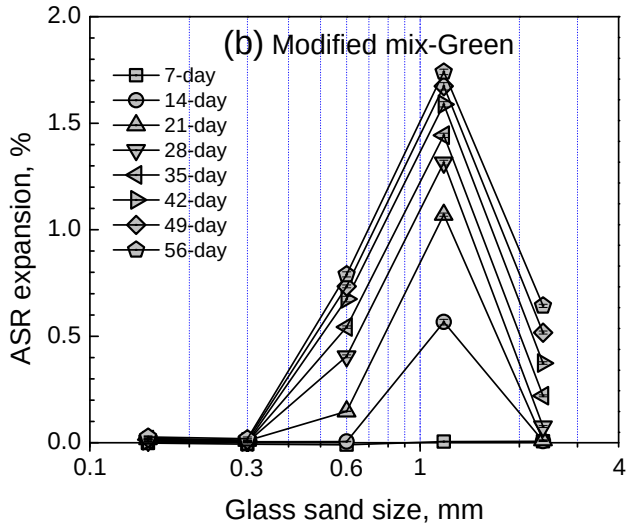

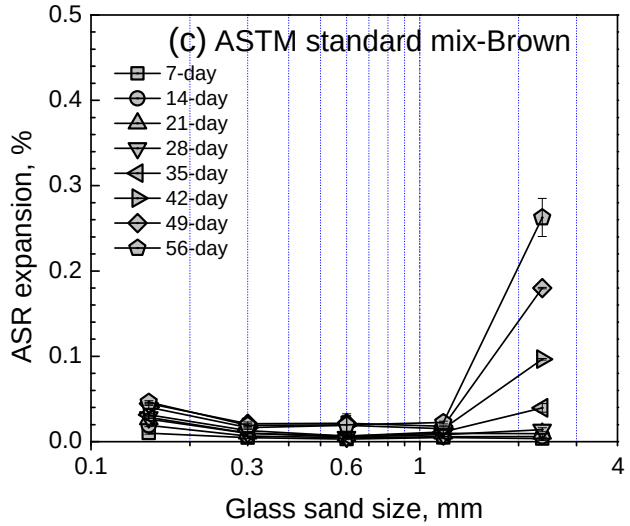

Figure 3-39: Effect of glass particle size on ASR expansion.

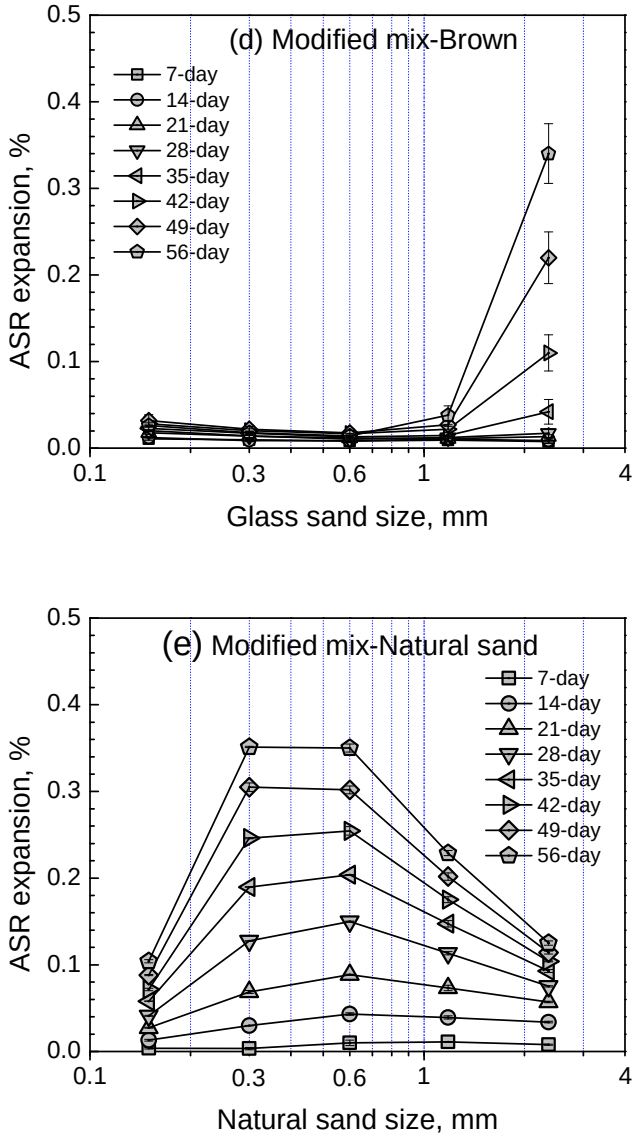

Figure 3-39 (continued): Effect of glass particle size on ASR expansion.

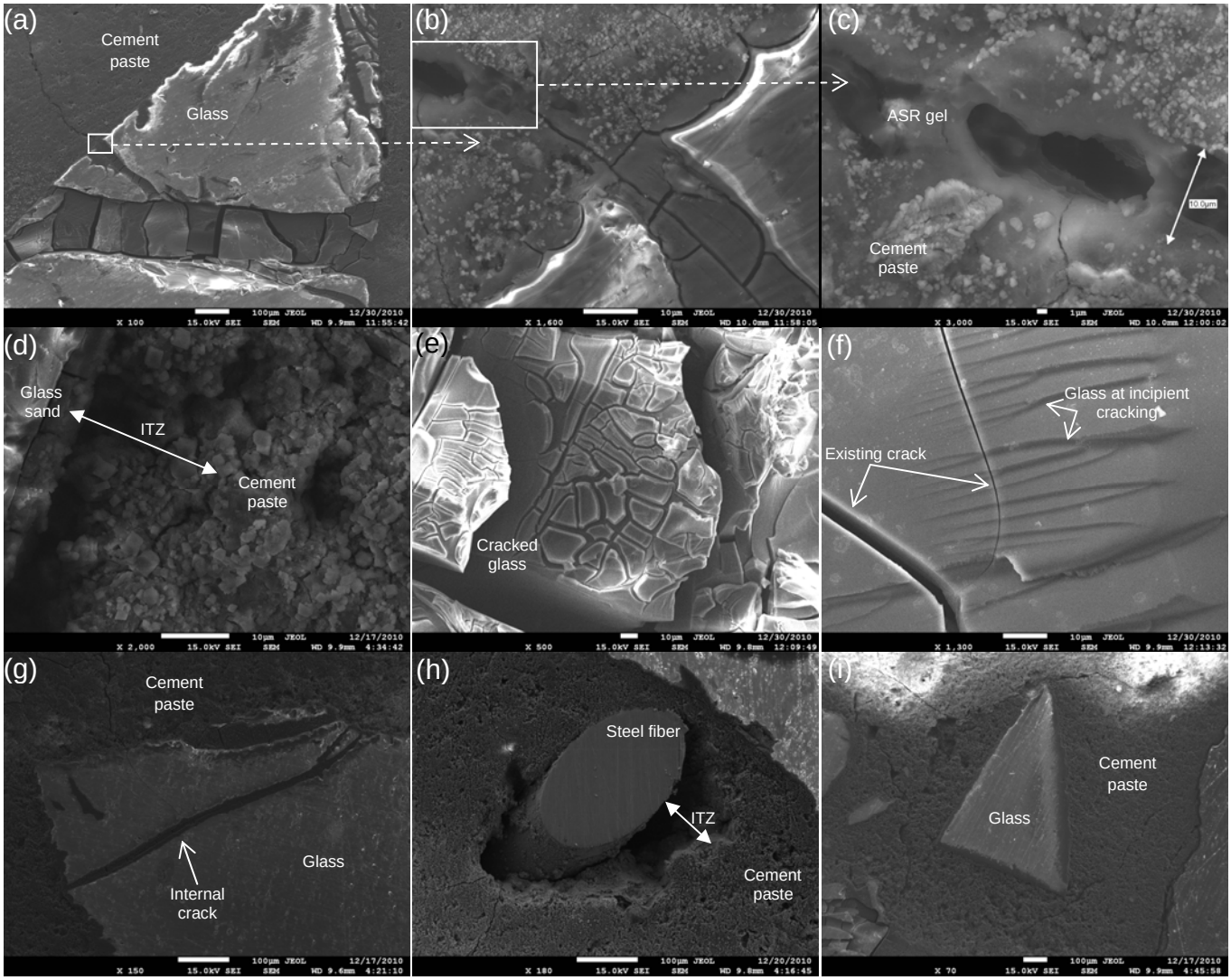

Figure 3-40: SEM pictures of mortar with 1.18-mm green glass sand.

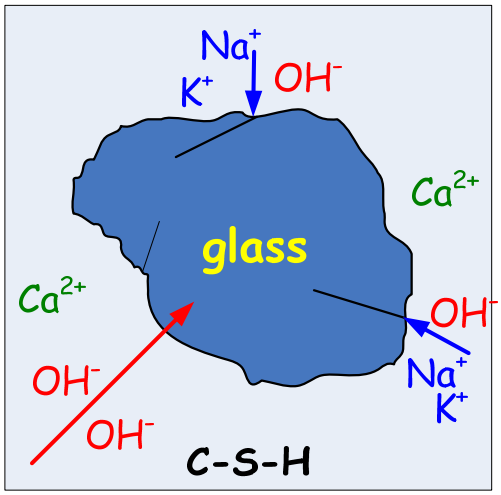

(a)

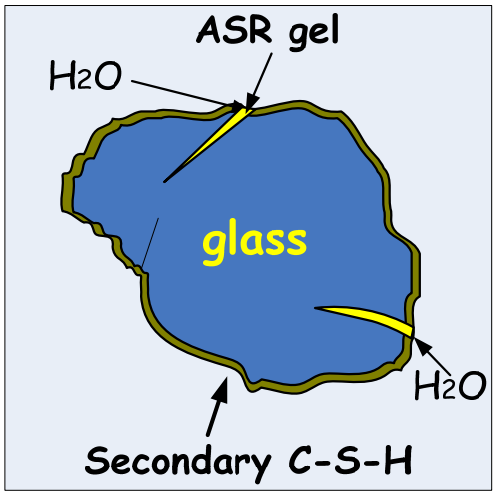

(b)

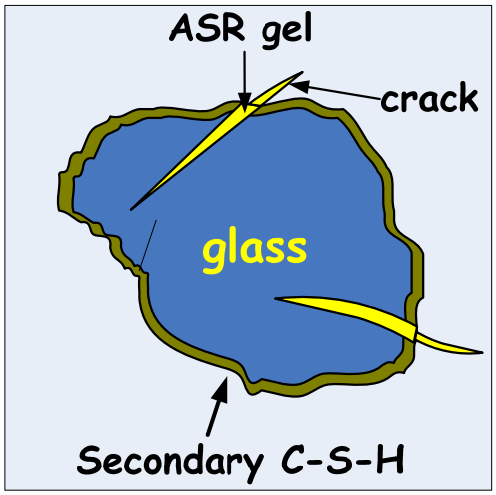

(c)

Figure3-41: Mechanism for ASR of glass particle.

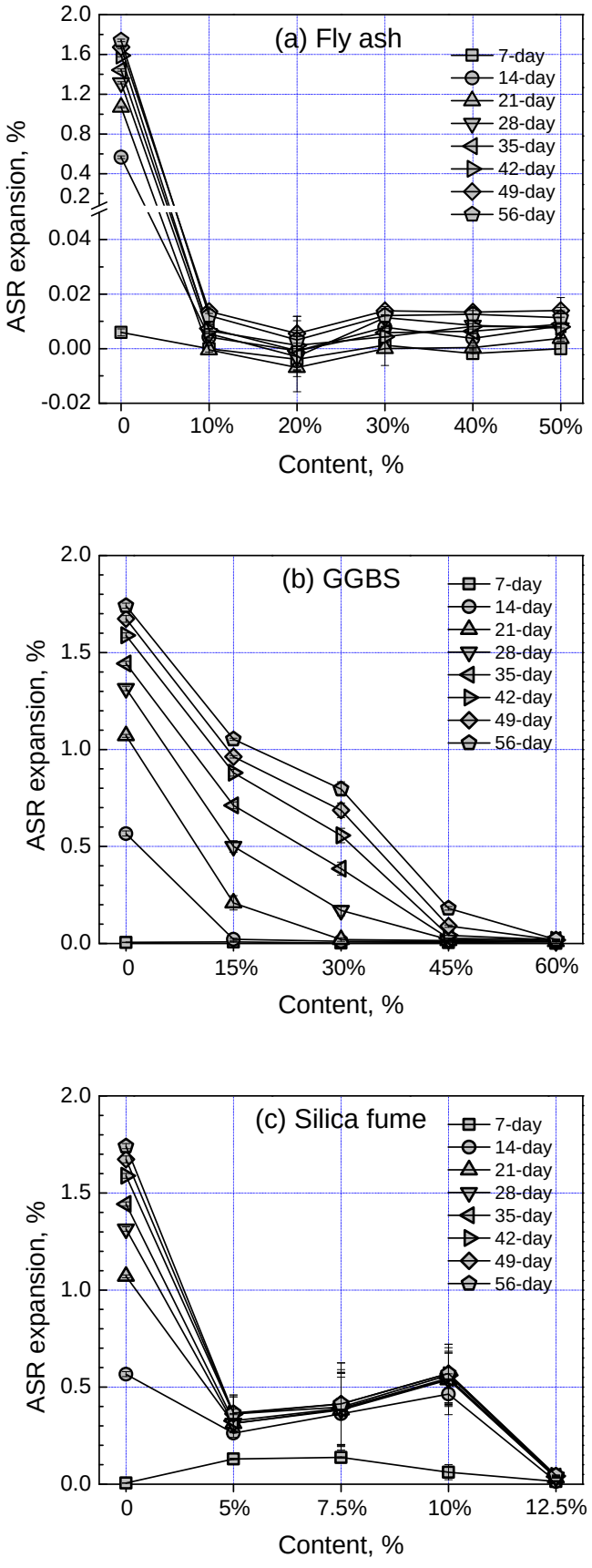

Figure 3-42: ASR expansion of mortar with different mitigation methods.

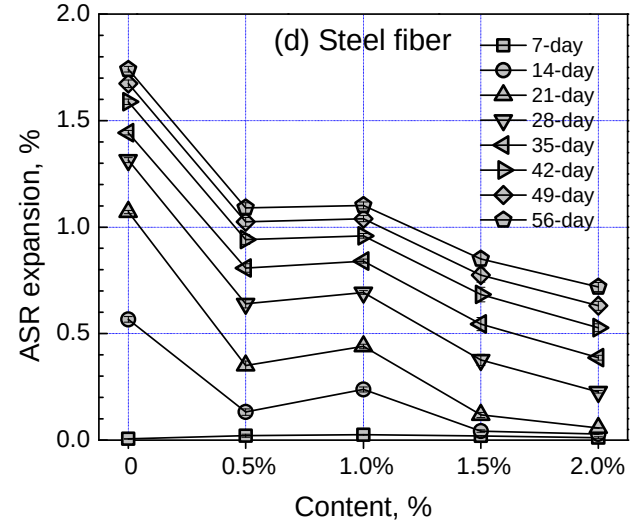

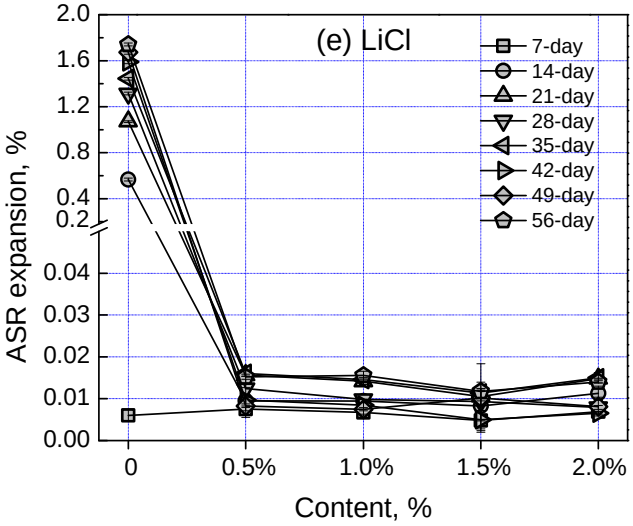

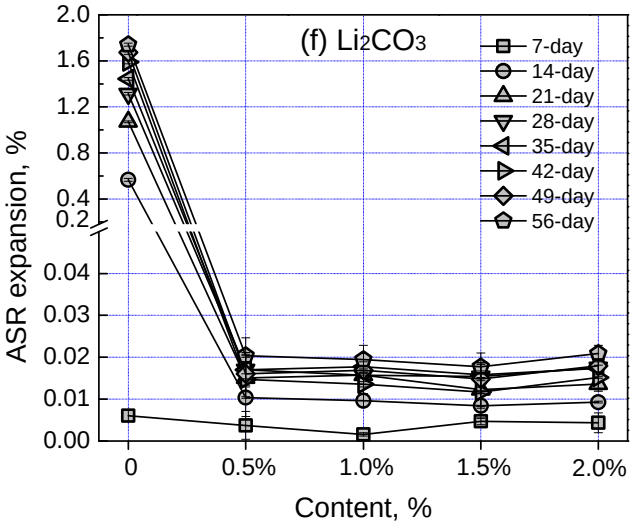

Figure 3-42 (continued): ASR expansion of mortar with different mitigation methods.

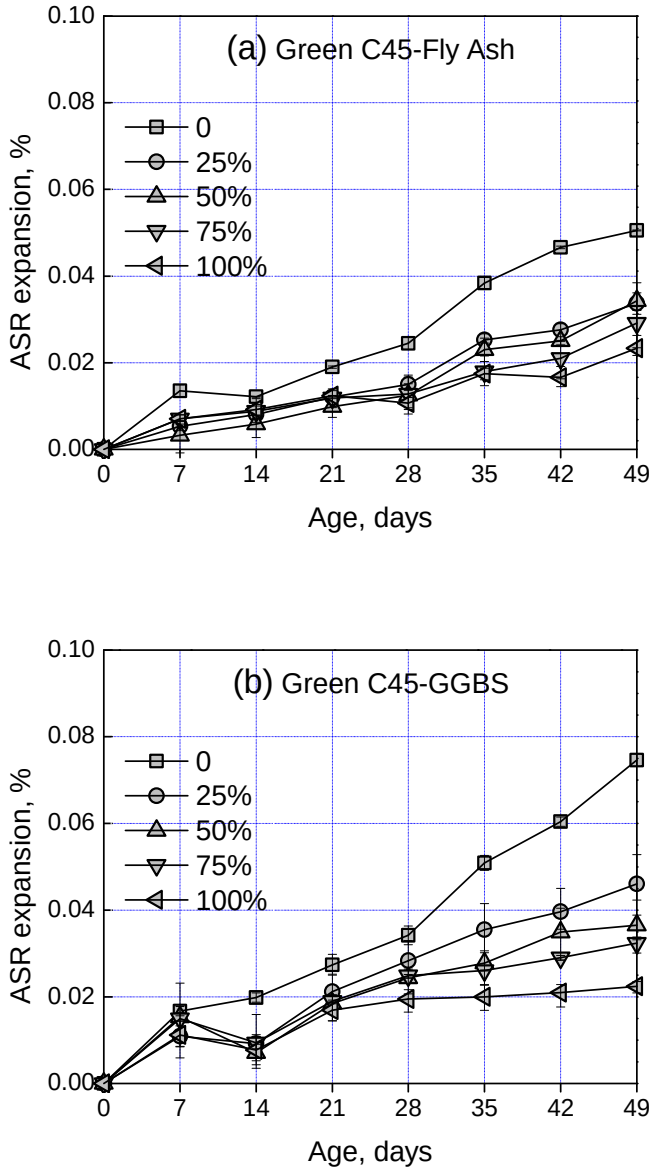

Figure 3-43: ASR expansions of green glass mortar C45 with (a) 30% fly ash and (b) 60% GGBS.

Chapter 4. Sandless Concrete

4.1 General

In this chapter, the concept of "sandless concrete", that is concrete containing no sand, either natural or manufactured, is proposed. The designation of mix proportions for "sandless concrete" is first elaborated, followed by a study into "sandless concrete" properties. The fresh, mechanical and durability characteristics of "sandless concrete" were investigated and discussed.

4.2 Methodology

As mentioned previously, there is no sound alternative material to totally replace natural sand. In this study, "sandless concrete" was proposed and examined to meet the challenge of depleting raw materials without negatively affecting concrete characteristics. The volume fraction of sand in normal concrete is between 20 and 27%. If totally eliminated from the concrete mixture, this volume should be filled by other ingredients, that is, coarse aggregates, cement and water. The mix design of "sandless concrete" is therefore to seek a suitable mix ratio among coarse aggregates, cement and water. The mix design of "sandless concrete" was studied using two different approaches. The first method can be considered as an extension of no-fines concrete, while the other one is based on coarse aggregates packing and excess paste theory.

In no-fines concrete, there are two key parameters in governing the mix proportions: aggregate/cement (*A/C*) ratio and water-cement (*w/c*) ratio. To ensure a high air void content and water permeability, the *A/C* ratio in no-fines concrete is higher than 4:1, and normally ranges

from 6 to 10. The *w/c* ratio ranges from 0.26 to 0.45, which provides good aggregate coating and paste stability. It is logical to increase the cement paste content and replace the single-sized aggregates in no-fines concrete with multi-sized aggregates to make a dense and non-pervious concrete mixture. Therefore, in this study, the effect of *A/C* ratio and the gradation of coarse aggregates on compressive strength are first studied with various *w/c* ratios, to obtain suitable mix proportions (that is, *A/C* and *w/c* ratios) for further study of various properties of "sandless concrete".

The second approach is based on the least void content of coarse aggregates (or maximum aggregates packing) and excess paste theory [Powers, 1968]. Mix design requires the engineer to produce concrete of the appropriate workability, strength and durability, as economically as possible [Mindess et al., 2003; Alexander and Mindess, 2005]. The packing of coarse aggregates is important in the mix design since it determines the voids content. Better packing will provide a perfect option to fill the voids between coarse aggregates, thus reducing the required amount of cement paste. According to excess paste theory, excess cement paste is necessary to form a thin layer of coating on the surface of aggregates to overcome frictions between aggregate particles and provide lubrication for the movement of aggregates. The volume of cement paste in excess of the amount required to fill the voids of the compacted aggregate is vital in the consistency of concrete [Kennedy, 1940]. Therefore, in this study, the dense packing of coarse aggregates is first obtained by a binary mixture of 10- and 20-mm aggregates. The cement content was determined by the above approaches and the water content would be controlled by the desired *w/c* ratios.

The details of each method are illustrated in the following two distinct test programs.

4.3 Approach 1: Extension of No-Fines Concrete

4.3.1 Test Program

In this test program, the mix design was a modification of that for no-fines concrete, but with lower *A/C* ratio and the use of multi-sized aggregates. The test program consisted of two parts. The first part was aimed at arriving at suitable mix proportions for the production of "sandless concrete". Focus was placed on the compressive strength since it is the most important parameter for concrete mix design from the structural point of view. The compressive strength depends on water-cement (*w/c*) ratio, aggregate-cement (*A/C*) ratio [Gilkey, 1961; Mindess et al., 2003], presence of chemical and mineral admixtures and type and maximum size of aggregates. At the same time, aggregate gradation is also important. The second part dealt with the effect of cement replacement by Class F fly ash in "sandless concrete". From the first part of the study, it was noted that the cement content was quite high for mixes with an *A/C* ratio less than 3. Instead of increasing the volume of aggregates which could reduce the workability of concrete, it would be more practical and economical to reduce the cement content by replacing it with other cementitious materials, keeping the total amount of cementitious materials unchanged. Thus, Class F fly ash was used to partially replace cement by up to 50%, by mass, to investigate its effect on the properties of "sandless concrete" in its fresh and hardened states.

4.3.1.1 Materials

Ordinary Portland cement (OPC) conforming to ASTM C 150 Type I cement was used for all mixtures in this study. The crushed granite aggregates had a nominal size ranging from 1.18 to 9.5 mm, and the gradation is shown as GI in **Fig. 4.1**. It complied with the grading requirement for aggregate size No. 89 in ASTM C 33, bounded by GU (upper bound) and GL (lower bound). The aggregates had an oven-dry (OD) specific gravity of 2.65, effective water absorption

capacity of 0.5%, and dry bulk density of 1650 kg/m^3. The chemical compositions of the fly ash complied with ASTM C 618. Natural sand with a maximum size of 4.75 mm was used as fine aggregates in a normal concrete mix that was included in the test program for comparison purpose. The sieve analysis result of the natural sand is also shown in **Fig. 4.1**.

4.3.1.2 Aggregate Grading and Mix Proportions

In the first part of the study, three aggregate gradations, GU, GI and GL, as shown in **Fig. 4.1**, were investigated. Gradations GU and GL were obtained by sieving the coarse aggregates into different sizes and then recombining them manually. For aggregate grading GI, four different *A/C* ratios, namely 2.0, 2.5, 3.0, and 3.5 were included; while for aggregate gradings GU and GL, only mixes with an *A/C* ratio of 2.5 were cast. Also, for each aggregate grading and *A/C* ratio, the *w/c* ratio was varied from 0.30 to 0.55 in steps of 0.05. In all, 36 batches were prepared.

In the second part of this test program, eight mix proportions using aggregates of grading GI (**Fig. 4.1**), as shown in **Table 4.1**, were investigated. The mix M-0 was a "sandless concrete" without fly ash, and was proportioned with *A/C*=2.5 and *w/c*=0.45, according to the first part of the study, to obtain a 28-day cube compressive strength of 40 MPa. There were six other "sandless concrete" mixes, M-10 to M-50, containing Class F fly ash which replaced the cement content by 10%, 20%, 25%, 30%, 40% and 50% by mass, respectively. The reference mix M-N was a normal concrete with the same cement content as mix M-0, and was included in the program for the purpose of comparison. It was designated such that 40% of the total aggregates content was natural sand by mass while other proportions remained unchanged. It should be mentioned that mix M-N in this study seems to be not representative of normal concrete due to its high water and cement content. The purpose of selecting M-N as reference is primarily to determine the possible influences of total elimination of sand in concrete.

4.3.1.3 Test Specimens

In the first part of the test program, three 100 mm cubes each were cast to determine the 7- and 28-day compressive strength. For each batch of concrete mixes in the second part, three 100 mm concrete cubes each were cast for the determination of compressive strengths at 1, 3, 7, 28 and 90 days, three 100×200 mm cylinders each for splitting tensile strengths at 7 and 28 days, three 100×100×400 mm beams each for flexural strengths at 7 and 28 days, and two 75×75×285 mm prisms for drying shrinkage measurement. Also, six 100×200 mm cylinders were prepared for compressive strength at 7 and 28 days. In addition, a 100×200 mm cylinder was prepared for the purpose of Rapid Chloride Permeability Test (RCPT) at 28 days and another three cylinders each to determine the cylinder compressive strengths at 7 and 28 days.

The component materials were mixed in a power-driven pan mixer. All the specimens were compacted on a vibration table. After casting, the test specimens were finished with a steel trowel and covered with a plastic sheet, to prevent water loss, for a period of 24±1 hours. They were then demolded and stored in a fog room (30 ˚C and 100% RH) until the age of testing.

4.3.1.4 Test Methods

Fresh concrete properties, including slump, unit weight and air content, were determined according to ASTM C 143, C 138 and C 231, respectively. Setting times were measured from penetration resistance in accordance with ASTM C 403. Cube compressive strength was obtained as per BS EN 12390-3 and cylinder compressive strength as per ASTM C 39. Splitting tensile strength, flexural strength and elastic modulus were determined according to ASTM C 496, C 78 and C 469, respectively. Resistance to chloride ion penetration was investigated based on ASTM C 1202.

For drying shrinkage, two concrete prisms were placed in a conditioned room (30 °C and 65% RH) immediately after demolding. Specifications [ACI 224R] often require moist curing of at least 7 days for higher degree of cement hydration. Moist curing of 1 day for concrete overestimates the drying shrinkage, which can simulate a more severe environment. However, regarding the use of fly ash, the drying shrinkage may be underestimated because of the reduced amount of hydrated cement paste. Therefore, the drying shrinkage of "sandless concrete" with fly ash under longer moist curing condition should be compared in future. However, the comparison between normal and "sandless" concrete can still be obtained from this curing scheme. A pair of metal pins was attached using epoxy glue to the two side surfaces of each prism, at a distance of 200 mm apart. Measurements of the distance between the pins were recorded for more than 120 days after the specimens had been placed in the conditioned room.

4.3.2 Test Results and Discussion

4.3.2.1 Mix Design

A dense concrete was obtained for each batch of "sandless concrete" for all mixes, except for the mix with aggregate grading GI and *A/C* ratio of 3.5, in which the amount of cement paste was insufficient to fill the voids, resulting in large voids (see **Figs. 4.2a** and **b**). For such a concrete mix, only the bottom of the cube was filled with cement paste while the aggregates near the top face were merely coated and cemented together by a thin binder layer. The structure was similar to that of no-fines or pervious concrete. However, for the other mixes with sufficient cement paste, the behavior of the concrete cubes under compression was similar to normal concrete (**Figs. 4.2c** and **d**). For "sandless concrete" with low compressive strength (that is, those having *w/c* ratio higher than 0.4 or with *A/C* ratio more than 3.5), the hardened concrete failed along the

interfacial area between the aggregates and the cement paste, with the aggregates remaining unbroken.

4.3.2.2 Effect of Aggregate Gradation

Fig. 4.3 shows the average 7- and 28-day compressive strength of "sandless concrete" for mixes with aggregate gradations GU, GI and GL, and *A/C* ratio equaled to 2.5. Mixes with gradation GU exhibited a slightly lower strength than the mixes with other gradings, particularly when *w/c* ratio exceeded 0.4. One possible reason is that there was a larger percentage of smaller size particles, resulting in a weaker interlock action among the coarse aggregates. Also, at higher *w/c* ratios, the bond at the interfacial zone becomes weaker due to bleeding. The difference in compressive strength due to the different aggregate gradations was however generally small, especially at lower *w/c* ratios.

4.3.2.3 Effect of A/C and w/c Ratios

Fig. 4.4 shows the average 7- and 28-day compressive strength of "sandless concrete" for mix GI with various *A/C* and *w/c* ratios. In general, the compressive strength decreased linearly with *w/c* ratio for a given *A/C* ratio. Mixes with *A/C* ratio of 3.5 exhibited much lower strengths, compared with other mixes with *A/C* ratios of 2.0, 2.5 and 3.0. There was no significant difference in compressive strengths among mixes with *A/C* ratios between 2.0 and 3.0. A compressive strength of higher than 30 MPa could be readily obtained at 28 days. Moreover, all mixes other than those with *A/C* ratio of 3.5, gained higher strength than 40 MPa at 28 days, if the *w/c* ratio was less than 0.5. As shown in **Fig. 4.4**, a reduction in *w/c* ratio led to an increase in the compressive strength. This is the same as in normal concrete, for which the strength largely depends on the capillary/space ratio of the paste, which is governed by the *w/c* ratio [Mindess et al., 2003].

Based on the preliminary study on the mix design with respect to compressive strength, the mix proportion was determined as *A/C*=2.5 and *w/c*=0.45 with aggregate gradation GI in order to obtain 40 MPa strength at 28 days. Thus mix proportion, as shown in **Table 4.1**, was used for the second part of the study.

4.3.2.4 Properties in the Fresh State

During the mixing and vibration processes, no obvious bleeding or segregation was observed. The fresh properties of "sandless concrete", including air content, slump and unit weight are listed in **Table 4.2**. All mixes gave a slump of at least 100 mm, without the need for superplasticizer. Normal concrete had a more uniform aggregate gradation and thus better workability than "sandless concrete", regardless of fly ash content. Compared with mix M-0, the slump of each mix increased with the percentage of cement replaced by fly ash. The spherical shape and smoother surface coupled with the smaller specific gravity of fly ash make it more efficient in filling voids than cement, thereby improving the workability.

The finish-ability of the concrete improved with partial cement replacement by fly ash. The total air content in "sandless concrete" ranged from 1.3% to 1.9%, compared to 1.6% in the normal concrete mix M-N. The unit weight varied from 2230 to 2305 kg/m^3, which was similar to that of normal concrete mix M-N with a unit weight of 2285 kg/m^3, and decreased with fly ash replacement ratios higher than 25%.

The setting times of the mixes are shown in Table 4.2. The times of initial and final setting are defined as when the penetration resistance reached 3.5 and 27.6 MPa, respectively. Mix M-N and M-0 showed similar initial and final setting times because of the same cement and water content while all other mixes except M-10 showed extended setting times due to the replacement of

cement with fly ash. The maximum delay was 58 min and 55 min for the initial and final setting times, respectively, both occurring at 50% fly ash replacement level. This was due to the relatively low cement content and slow reaction process of fly ash with cement hydration product, which contributed to the retardation in concrete setting. The time interval between initial and final setting however seemed unaffected.

4.3.2.5 Mechanical Properties

a. Compressive Strength

The variation of cube compressive strength with fly ash replacement ratio at various ages of concrete is shown in **Fig. 4.5a**. It is well known that the addition of fly ash would reduce the early-age strength but increase the long term strength of concrete. The same was observed in "sandless concrete" mixes with fly ash, which showed lower strength than M-0 at 1, 3 and 7 days. With higher fly ash replacement ratio, this trend was more obvious. For example, the early strength of M-50 (50% fly ash) was significantly reduced to only 30% and 50% of that of M-0 at 1 and 3 days, respectively. For all tested mixtures, the proportional increase in compressive strength was measured up to 7 days. However, beyond 7 days, mixes with fly ash replacement ratio of between 20 and 30% showed a much faster rate of increase in compressive strength, and had strengths almost equal to that of the normal concrete at 90 days.

The relation between the cylinder compressive strength f_c' and cube compressive strength f_{cu} at both 7 and 28 days is shown in **Fig. 4.5d**. The relation between f_c' and f_{cu} was found to be

$$f_c^{'} = 0.941 f_{cu} \tag{4.1}$$

with a coefficient of correlation of 0.9168.

b. Splitting Tensile Strength

The splitting tensile strength at 7 and 28 days for all mixes are shown in **Fig. 4.5b**. All the "sandless concrete" mixes showed lower splitting tensile strength than normal concrete mix M-N. This is because the packing of aggregates in "sandless concrete" was not as good as that in normal concrete. At 7 days, the splitting tensile strength of "sandless concrete" was about 75% that of normal concrete unless the fly ash replacement ratio was more than 30%. With a replacement ratio of 50%, the splitting tensile strength of M-50 was 83% of that of M-0 without fly ash. However, at 28 days, the splitting tensile strength continuously increased with the replacement ratio, with the peak occurring at a fly ash replacement ratio of 40%. This is the same as what has been reported for conventional concrete [Siddique, 2004], and could be due to the late pozzolanic reaction of the fly ash. The increase in splitting tensile strength from 7 to 28 days varied from 7 to 52% when the fly ash replacement ratio increased from 0 to 50%.

c. Flexural Strength

The flexural strength, in terms of average modulus of rupture, of "sandless concrete" is shown in **Fig. 4.5c**. All "sandless concrete" mixes exhibited lower flexural strength than normal concrete mix M-N, similar to splitting tensile strength. The flexural strength at 7 days did not show a clear decrease with the increase in fly ash replacement ratio up to 30%. The flexural strength of M-50 with 50% fly ash was 87% that of M-0 without fly ash. The increase in flexural strength from 7 to 28 days ranged from 19% for M-0 to 36% for M-50. Mixes with higher fly ash content exhibited higher strength gain. At 28 days, the flexural strength continued to increase with the increase in the replacement ratio, also up to 30%, and the increase in strength over that of M-0 was significant. Mix M-30, with 30% fly ash, exhibited the highest flexural strength, 118% of

that of M-0. This is attributed to the pozzolanic reaction and enhanced interfacial bond between the paste and coarse aggregates.

Fig. 4.6a shows the relation between the splitting tensile strength f_{st} and the cylinder compressive strength f_c' of "sandless concrete". From regression analysis, the following relation was established:

$$f_{st} = 0.586\sqrt{f_c'} \tag{4.2a}$$

with a coefficient of correlation of 0.631, in which f_{st} and f_c' are both expressed in MPa, or in view of Eq (4.1),

$$f_{st} = 0.568\sqrt{f_{cu}} \tag{4.2b}$$

The ratio of the splitting tensile to compressive strength f_{st}/f_c' on the other hand ranged from 0.071 to 0.113, with an average of 0.094. The ratio was dependent on the compressive strength of "sandless concrete", being higher at lower strength. This was in agreement with that for normal concrete [Mindness et al., 2003]. It was also noted that this ratio generally increased with the increase in the fly ash replacement level, due to the pozzolanic reaction.

The relationship between the flexural strength f_r and the cylinder compressive strength f_c' is shown in **Fig. 4.6b**, and the following expression was established through regression analysis:

$$f_r = 0.758\sqrt{f_c'} \tag{4.3a}$$

with a coefficient of correlation of 0.737, in which f_r and f_c' are both expressed in MPa, or in view of Eq. (4.1),

$$f_r = 0.735\sqrt{f_{cu}} \tag{4.3b}$$

d. Elastic modulus

The elastic modulus of the "sandless concrete" are listed in **Table 4.2**. The "sandless concrete" exhibited lower modulus than normal concrete due to the elimination of sand. Compared with mortar, the lower modulus of pure cement paste in "sandless concrete" resulted in lower elastic modulus of concrete as a composite of coarse aggregates and cement paste. Also, it is noted that the elastic modulus of "sandless concrete" containing fly ash was generally lower than that without fly ash. However, there was no clear relation between the elastic modulus and fly ash replacement ratio.

The elastic modulus of the specimen is plotted against the cylinder compressive strength in **Fig. 4.6c**. The modulus increased with the increase in concrete strength, similar to normal concrete. The relation between E_c and f_c' according to ACI 318 Building Code [2008] for normal concrete is also plotted in **Fig. 4.6c**. The elastic modulus of "sandless concrete" was smaller than that of normal concrete for the same compressive strength. The reduced modulus was probably caused by the weak and soft paste between aggregate particles in "sandless concrete" compared to a stiffer sand mortar in normal concrete. From the regression analysis of the test data, the relation between E_c and f_c' of "sandless concrete" is established as:

$$E_c = 3784\sqrt{f_c'} \tag{4.4a}$$

with a coefficient of corrosion of 0.7078, in which E_c and f_c' are both expressed in MPa, or in view of Eq. (4.1),

$$E_c = 3671\sqrt{f_{cu}} \quad (4.4b)$$

4.3.2.6 Durability

a. Drying Shrinkage

The drying shrinkage of "sandless concrete", taken as the average measurements from two prisms, after 1 day of initial moist curing is shown in **Fig. 4.7**. All the mixes showed stable readings after 90 days and all the measured shrinkages were below 750 $\times 10^{-6}$. Normal concrete mix M-N showed the highest drying shrinkage of 709 $\times 10^{-6}$ at 90 days, while M-50 with 50% fly ash replacement exhibited the lowest drying shrinkage of 553 $\times 10^{-6}$. At 90 days, mixes M-0 to M-40 had drying shrinkage of between 86% and 99% that of normal concrete. "Sandless concrete" showed lesser drying shrinkage due to the increased percentage of large coarse aggregates which could more effectively restrain the length change of paste. Fly ash generally reduced the drying shrinkage, although this effect was inconsistent for M-20 and M-30 which exhibited slightly higher shrinkages than M-0.

b. Rapid Chloride Permeability Test (RCPT)

RCPT is the most widely used method to determine resistance of concrete to chloride ion penetration because of its simplicity and short test duration. Although there has been criticism of this technique, especially for concrete with added pozzolans [Feldman et al., 1994; Shi, 2004; Scanlon and Sherman, 1996], the RCPT can be seen as an indicator of both permeability and resistivity properties of concrete [Smith et al., 2004].

The RCPT results at 28 days are shown in **Fig. 4.8** in terms of the total charge passing the specimen in 6 hours. In this study, the total charge passed was lower in "sandless concrete" than in normal concrete M-N. This is because of a smaller ITZ between aggregate particles and

cement paste in “sandless concrete”. Sand is smaller in size but larger in surface area than coarse aggregate, thus the interfacial surface area, which is dominated by porous and weak cement paste, is higher in normal concrete.

The total charge passed was significantly reduced with fly ash replacement ratio. For mixes M-10 and M-50, the total charge passed was 3589 and 2308 Coulombs respectively and classified as “moderate penetration”, while those for M-20, M-25, M-30 and M-40, with fly ash replacement ratios of 20, 25, 30 and 40%, were lesser than 2000 Coulombs and leveled as “low penetration”. Mix M-30 showed the least total charge passed of 1376 Coulombs. The hydration process of fly ash was accelerated by the high amount of cement. The secondary CSH refined the microstructure and decreased the concrete porosity. Therefore, the total charge would reduce with increasing amount of fly ash. In this study, the 30% fly ash mixture showed the least RCPT values, probably due to the higher chloride binding capability at this fly ash replacement ratio [Dhir and Jones, 1999]. Also, when fly ash was used as cement replacement at high content, the increase in capillary porosity might be due to reduced cement hydration products in the system and delayed pozzolanic reaction.

4.3.3 Summary

Based on the study carried out, the following conclusions may be made:

1. Aggregates complying with ASTM No. 89 grading requirement were found suitable for use in “sandless concrete”. The compressive strength did not vary significantly for different aggregate gradations, especially if the *w/c* ratio was less than 0.4. The compressive strength increased with decreasing *w/c* ratio. A cube compressive strength greater than 40 MPa at 28 days can be readily obtained if the *A/C* ratio is below 3 and the

w/c ratio between 0.3 and 0.5. Similar to normal concrete, "sandless concrete" failed along the interfacial area between aggregate and cement paste under axial compression.

2. "Sandless concrete" with fly ash exhibited good workability and the air content for all mixes was low and comparable to normal concrete. The times of initial and final setting were both extended with cement partially replaced by fly ash.

3. The development of compressive strength was similar in all "sandless concrete" mixes up to 7 days. The strength continuously decreased with higher fly ash replacement ratio. However, after 7 days, mixes with 20% to 30% fly ash replacement ratio exhibited higher rates in strength gain, and exhibited comparable strength to normal concrete at the end of 90 days. Splitting tensile and flexural strengths of "sandless concrete" also decreased with an increase in fly ash replacement ratio at 7 days, but they generally increased at 28 days due to pozzolanic reaction of fly ash, peaking at a replacement ratio of between 30% and 40%. Elastic modulus of "sandless concrete" was smaller than that of normal concrete due to the filled cement paste between coarse aggregates rather than mortar in normal concrete.

4. The "sandless concrete" showed lesser drying shrinkage than normal concrete, and fly ash could further reduce the drying shrinkage despite inconsistency. The resistance to chloride ion penetration of "sandless concrete" was highest with a fly ash replacement ratio of between 20 to 40%.

4.4 Approach 2: Aggregates Packing and Excess Paste Theory

In this test program, the mix design is based on the packing of coarse aggregates and excess paste theory.

4.4.1 Test Program

4.4.1.1 Mix Design

In order to produce a workable "sandless concrete", the cement paste has to bind and lubricate the coarse aggregates adequately. From the economical point of view, the paste should be minimal, which requires the coarse aggregates to be densely packed. The concept of void content is illustrated in **Fig. 4.9**, of which Kosmatka et al. [1995] explained that a smaller void content could be obtained by mixing portions of two aggregate sizes. Thus, it was decided to use two coarse aggregate sizes of 10- and 20-mm in the mix proportion so as to reduce the void content in the concrete. The voids in the aggregates for different combinations of 10- and 20-mm aggregates were determined following ASTM C 29. **Fig. 4.10a** shows that a void content of less than 0.31 (or 31%) could be obtained if the volume fraction of 20-mm aggregates is between 60% and 100%. The ratio of 10- to 20-mm aggregates was thus selected as 40:60 in this study, and the corresponding aggregate size distribution is shown in **Fig. 4.10b**, which satisfies the ASTM C 33 grading requirement for size No.67 aggregates. The paste volume was designed to fill the void and coat the aggregate particles so as to lubricate the movement of aggregate particles (**Fig. 2.10**). The amount of excess paste was selected by experiments. Different volumes of excess paste was examined to determine the suitable or the minimum amount of excess paste for accepted workability. In this study, an amount of about 10% excess paste was found to provide the concrete acceptable workability, which means that the total paste volume is 341 L/m^3. The

cement and water content were then calculated based on the desired *w/c* ratio and total paste volume. **Fig. 4.11** summarizes the steps for mix design approach 2.

As shown in **Table 4.3** and **Fig. 4.12**, four groups of "sandless concrete" with *w/*c ratios of 0.40, 0.45, 0.50 and 0.55 were investigated. For comparison purpose, four corresponding groups of normal concrete containing natural sand were also included. At the same *w/c* ratio, both "sandless concrete" and normal concrete mixes had the same cement and water content. For normal concrete, the content of coarse aggregates was selected according to ACI 211.1, with ratio of 10- to 20-mm coarse aggregates remaining at 40:60 as in "sandless concrete", while natural sand was determined as per volume method. Furthermore, for each "sandless concrete" mixture, Class F fly ash was used to replace cement at 0, 10, 20, 30, 40 and 50%, by mass.

4.4.1.2 Materials

Apart from the coarse aggregates, the other materials used, that is, cement, fly ash and sand, were the same as in previous section (Section **4.3**). The physical properties of the two categories of coarse aggregates were as follows: oven-dry (OD) specific gravity = 2.60; surface-dry (SSD) specific gravity = 2.61; and effective water absorption capacity = 0.56%. A polycarboxylate-based superplasticizer was used in concrete production. Tap water was used as mixing water.

4.4.1.3 Preparation of Test Specimens

For each mixture, 100-mm cubes were cast for the determination of compressive strengths at 1, 7, 28 and 90 days; Ø100×200 mm cylinders for splitting tensile strength and elastic modulus at 28 days; 100×100×400 mm beams for flexural strength at 28 days; and 75×75×285 mm prisms for drying shrinkage. For each of the above properties, three specimens were prepared and the average readings reported herein.

For the resistance to chloride ion penetration and sulfate attack tests, Ø100×200 mm cylinders were prepared. Three specimens were cast for RCPT for each mix, and four specimens for sulfate attack tests. All specimens were covered by plastic sheets for 24 hours after casting, then demolded and transferred into a fog room (30 ˚C and 100% RH) and cured until the testing age.

4.4.1.4 Test Methods

Cube compressive strength of concrete was determined according to BS EN 12390-3, and splitting tensile strength and flexural strength were tested as per ASTM C 496 and C 78, respectively. For drying shrinkage measurements, specimens were demolded one day after casting and then placed in a curing room (30 ˚C and 65% RH) to simulate a real-life environment [Atis, 2003]. Measurements were taken at 7, 14, 28, 56, 90, 120, 180 and 360 days.

The resistance of concrete to chloride ion penetration was investigated at the concrete age of 180 days using RCPT method as per ASTM C 1202. The resistance to sulfate attack was determined according to ASTM C 267. After curing in the fog room for 180 days, two concrete cylindrical specimens were immersed in saturated $MgSO_4$ solution for 24 hours followed by oven drying (at 110 ˚C) for another 24 hours. After 20 such cycles, the specimens were weighed and tested for dynamic modulus and compressive strength to determine the loss in weight, modulus and strength when compared with two other specimens that remained in the fog room.

4.4.2 Test Results and Discussion

4.4.2.1 Fresh Properties

No bleeding or segregation was observed in each concrete mix. The target slump was 50 mm, and a polycarboxylate-based superplasticizer was added for this purpose. The dosage of superplasticizer was limited to 2% of the total weight of cement and fly ash so as not to cause

other problems, such as delayed setting or severe bleeding. The "sandless concrete" exhibited slump values of between 50 and 100 mm, except for the group with *w/c* ratio of 0.40, as shown in **Fig. 4.13**, which had slump values between 25 and 50 mm. According to ACI 211.1 [2002], the minimum slump requirement for structural construction is 25 mm; thus the "sandless concrete" mix satisfied this requirement. It is also noted that the replacement of cement by fly ash did not substantially improve the workability due to the reduced paste volume of "sandless concrete".

Except slump test, no other quantitative measurement was taken for fresh concrete mixtures. However, the flowability of "sandless concrete" was qualitatively reduced compared to normal concrete based on visual observation, due to the increased content of coarse aggregates, which resulted in a higher degree of particle interlocking and absence of lubrication provided by fine particles. Also, the flowability generally decreased with decreasing *w/c* ratio for "sandless concrete" because of the lower water content. However, the effect of fly ash was not obvious.

4.4.2.2 Compressive Strength

The developments of compressive strength for all mixtures are shown in **Fig. 4.14**. The normal concrete exhibited similar compressive strength as "sandless concrete" without fly ash. It is clear that the use of fly ash would result in reduced early age strength. In the first 7 days, the compressive strength of "sandless concrete" decreased continuously with increasing fly ash content. The compressive strength of "sandless concrete" with 50% of cement replaced by fly ash were 50%, 51%, 41% and 36% of those mixes without fly ash, at *w/c* ratios of 0.40, 0.45, 0.50 and 0.55, respectively. However, the strength ratio increased to 80%, 72%, 62% and 54% at 28 days, and 90%, 89%, 77% and 73% at 90 days. The improved long-term compressive strength was due to the pozzolanic reaction between fly ash and cement hydration products, which

densified the microstructure of concrete and improved the ITZ between aggregate and paste matrix. The pozzolanic reaction of fly ash occurred at later stages with higher *w/c* ratios.

Also, the compressive strength of "sandless concrete" decreased as the *w/c* ratio increased, especially above 0.50. At 90 days, all the mixtures with *w/c* ratios of 0.40 and 0.45 showed similar compressive strength. However, at *w/c* ratio of 0.50, replacing 50% of cement by fly ash resulted in obvious reduction in compressive strength. Also, at *w/c* ratio of 0.55, the compressive strength decreased significantly if fly ash content was more than 20%.

4.4.2.3 Splitting Tensile Strength

The splitting tensile strengths at 28 days are shown in **Fig. 4.15a**. At lower fly ash contents, all the concrete mixes showed comparable splitting tensile strength regardless of the *w/c* ratio. The effect of fly ash on splitting tensile strength was not significant if the content was lower than 30%. It is noted that with 20% and 30% fly ash content, "sandless concrete" even showed higher tensile strength compared to normal concrete and "sandless concrete" without fly ash.

The contribution to splitting tensile strength by the inclusion of fly ash was again attributed to pozzolanic reaction which improved the CSH structure of the concrete. Compared to normal concrete, "sandless concrete" with or without fly ash showed comparable splitting tensile strength at *w/c* ratios of 0.40 and 0.45. However, at higher *w/c* ratios of 0.50 and 0.55, the splitting tensile strength reduced with fly ash content higher than 30%.

4.4.2.4 Flexural Strength

The effect of *w/c* ratio on flexural strength (modulus of rupture) at 28 days was not obvious (see **Fig. 4.15b**). All the mixes exhibited flexural strengths between 4.1 and 5.5 MPa, except the mix with a *w/c* ratio of 0.55 and 50% fly ash content. At *w/c* ratios of 0.40 and 0.45, "sandless

concrete" exhibited slightly higher flexural strength than normal concrete and incorporation of fly ash did not reduce the flexural strength if it was less than 20%. At *w/c* ratios of 0.50 and 0.55, the flexural strength of "sandless concrete" was lower than that of normal concrete, probably due to weaker bond between paste and coarse aggregates. For all *w/c* ratios, fly ash higher than 30% would lead to reduction in flexural strength.

4.4.2.5 Elastic Modulus

The elastic modulus at 28 days is shown in **Fig. 4.15c**. Generally, the elastic modulus decreased with *w/c* ratio from 0.40 to 0.55, for the same fly ash content. For a given *w/c* ratio, "sandless concrete" showed lower elastic modulus than normal concrete because of the lack of fine aggregates. As a composite material, the modulus of concrete depends on its constituents and their volumetric fractions. In "sandless concrete", the phase between coarse aggregates is cement paste instead of mortar in concrete, which is of higher modulus. This may explain the reduction in modulus for "sandless concrete" although the volume of aggregates remained the same. The influence of fly ash on modulus did not show a universal trend for various *w/c* ratios. The elastic modulus started to decrease at a critical fly ash content, which was 10%, 20%, 20% and 30%, respectively, for concrete with *w/c* ratios of 0.40, 0.45, 0.50 and 0.55. Thus, the reduction in modulus due to fly ash was more prominent in "sandless concrete" with lower *w/c* ratio. However, the increase in the paste volume, due to the less specific gravity of fly ash especially at high content, may also contribute to the reduced modulus of concrete. This effect should be further studied in future by replacing cement with fly ash by volume instead of by mass.

4.4.2.6 Relations between Compressive Strength and other Mechanical Properties

From regression analysis, the relations between compressive strength f_{cu} and splitting tensile strength f_{st}, flexural strength f_r, and elastic modulus E_c, were obtained as follows and shown in **Fig. 4.16**:

$$f_{st} = 0.573\sqrt{f_{cu}} \quad \text{(current study)} \tag{4.5a}$$

$$f_{st} = 0.56\sqrt{f_c'} = 0.50\sqrt{f_{cu}} \quad \text{(ACI 318)} \tag{4.5b}$$

$$f_r = 0.684\sqrt{f_{cu}} \quad \text{(current study)} \tag{4.6a}$$

$$f_r = 0.62\sqrt{f_c'} = 0.55\sqrt{f_{cu}} \quad \text{(ACI 318)} \tag{4.6b}$$

$$E_c = 4144\sqrt{f_{cu}} \quad \text{(current study)} \tag{4.7a}$$

$$E_c = 4730\sqrt{f_c'} = 3706\sqrt{f_{cu}} \quad \text{(ACI 318)} \tag{4.7b}$$

with coefficient of correlation of 0.6345, 0.5405 and 0.4486 respectively, in which, f_{st}, f_r, E_c and f_{cu} are all expressed in MPa. Approximated relationships by present design code ACI 318 [2008] are also provided below each corresponding equation, where the cylinder strength f_c' is estimated as 80% of cube strength f_{cu} for normal weight concrete [Mehta and Monteiro, 2006].

Compared with Eqs. (4.2b, 4.3b and 4.4b), the relation with compressive strength of splitting tensile strength and flexural strength showed slight lower value, which means the tensile strength of "sandless concrete" by design Approach 2 exhibited lower tensile strength at the same compressive strength. This was thought to be caused by the reduced amount of cement paste

between coarse aggregate particles, resulting in smaller bond to resist tensile stress. However, it is noted that elastic modulus showed higher value by Approach 2 at the same compressive strength. It is due to the higher degree of aggregate particle interlock or contact, leading to composites with higher stiffness.

Compared with ACI 318, "sandless concrete", either by Approach 1 or 2, exhibits higher value of splitting tensile and flexural strength compared to normal concrete, with the equal compressive strength. Moreover, by Approach 2, the "sandless concrete" have higher modulus of elasticity than normal weight concrete of the same compressive strength. This means that designated "sandless concrete" is more conservative in tensile strength if the compressive strength is identical to normal concrete. Approach 2 will also produce conservative "sandless concrete" in terms of elastic modulus while Approach 1 shows lower modulus, which should be taken into consideration during design.

The low values of R^2 for Eqs. (4.5a, 4.6a and 4.7a) indicated that other parameters, such as density apart from compressive strength, may also affect the tensile strength and modulus. This could be further studied in future.

4.4.2.7 Drying shrinkage

The drying shrinkages of all concrete mixes up to 360 days are shown in **Fig. 4.17**. All the drying shrinkage strains were less than 700×10^{-6} at 360 days, regardless of *w/c* ratio or fly ash content. At a *w/c* ratio of 0.40, normal concrete showed the highest drying shrinkage at all ages; and the drying shrinkage consistently decreased with more cement replaced by fly ash. The "sandless concrete" showed less drying shrinkage than normal concrete, due to a higher content of coarse aggregates which could more effectively restrain shrinkage of paste than finer size

aggregates. Also, the densified microstructure due to pozzolanic reaction of fly ash which prevented moisture evaporation further helped in reducing the drying shrinkage. As published in literature [Atis, 2003; Bilodeau and Malhotra, 2000; Kumar et al., 2007], this study shows that fly ash, as cement replacement, could effectively reduce drying shrinkage, even with the same water content (see **Table 4.3**). With incorporation of fly ash, the reduced water loss, from capillary and gel pores, indicated that the pore sizes were reduced or refined. The drying shrinkage strains of "sandless concrete" were close to or slightly less than normal concrete, at *w/c* ratios of 0.45 and 0.50. However, at *w/c* ratio of 0.55, "sandless concrete" mix with less than 20% fly ash showed higher shrinkage than normal concrete.

The drying shrinkage of "sandless concrete" increased with higher *w/c* ratio up to 0.50. At a *w/c* ratio of 0.55, the shrinkage was, however, lower, especially with cement replaced by fly ash by more than 20%. One possible explanation might be due to the better interlock between coarse aggregates in "sandless concrete" at higher *w/c* ratios.

4.4.2.8 Resistance to Chloride Ion Penetration

RCPT was carried out as per ASTM C 1260 for "sandless concrete" at the age of 180 days. Some literature has stated that fly ash could effectively decrease permeability of concrete, based on RCPT results [Bilodeau and Malhotra 2000; Malhotra 2002]. However, RCPT has been criticized for its drawbacks for testing concrete with supplementary cementing materials, such as fly ash, silica fume and ground granulated blast-furnace slag. The current passed during RCPT is related to all ions, especially OH^-, in the pore solution and not only chloride ions. It was pointed out that the significant reduction in total charge passed with mineral materials, was mainly caused by the OH^- consumption by pozzolanic reaction, although this led to improved microstructure [Wee et al., 2000].

All the normal concrete mixes exhibited moderate penetrability except the one with *w/c* ratio of 0.50 which showed high penetrability of chloride ion (**Fig. 4.18a**). Compared with normal concrete, "sandless concrete" showed less total charge passed, probably due to decreased ITZ between cement paste matrix and aggregates. Moreover, the total charge passed decreased with increasing *w/c* ratio from 0.40 to 0.55. However, this difference became quite insignificant when fly ash content was higher than 20%, for which all concrete mixtures had total charge passed less than 1000 Coulombs, indicative of very low permeability of chloride ion.

As a comparison, the RCPT results of concrete with *w/c* ratio of 0.45 at 28 days are also plotted in **Fig. 4.18a**. The total charge passed was significantly reduced from 28 to 180 days, due to continuous cement hydration. It is noted that the reduction effect of fly ash was more obvious at 180 days than at 28 days. At 28 days, the pozzolanic reaction between fly ash and cement hydration product was not completed, but with time passing the microstructure of concrete was enhanced by further pozzolanic reaction, resulting in lower charge passed.

At the end of RCPT tests, the specimens were axially split to measure the depth of chloride ion penetration via spraying 0.1 N $AgNO_3$ solution. Similar to NT build 492, the non-steady-state migration coefficient D_{nssm} of chloride could be calculated by Eq. (3.1) and plotted in **Fig. 4.18c**. The penetration depth and migration coefficient of chloride ion were also reduced by the incorporation of fly ash. It is noted that both RCPT and migration coefficient did not decrease significantly at higher contents of fly ash. This could be because the pozzolanic reaction would not be fully realized due to the limited amount of cement hydration product, $Ca(OH)_2$ at high fly ash content.

If all test results regarding chloride permeability, including those for glass mortar (section 3.3.2.3a), glass concrete (section3.4.2.3a) as well as "sandless concrete" are considered, a good linear relation is found to exist between RCPT results and chloride ion migration coefficient, as shown in **Fig. 4.18c**, and given by.

$$D_{nssm} = 0.0057\,Q \tag{4.8}$$

with an coefficient of correlation of 0.8874, in which D_{nssm} and Q are expressed in 10^{-12} m^2/s and Coulombs, respectively.

4.4.2.9 Sulfate Resistance

The action of sulfates present in groundwater and seawater on concrete is perhaps the most widespread and common form of chemical attack [Mindess et al., 2003]. The damage caused by sulfate attack may involve expansion and cracking of concrete as a whole, as well as softening and disintegration of cement paste. The replacement of cement by Class F fly ash as mineral admixture would increase the resistance to sulfate attack due to: (1) reduction in $Ca(OH)_2$ concentration in cement paste; and (2) reduction in the porosity and permeability in microstructure of cement paste due to pozzolanic reaction by the fly ash.

The reduction in weight, dynamic modulus and compressive strength of "sandless concrete" specimens after sulfate resistance tests, compared to specimens placed in the fog room for the same time period, are shown in **Fig.4.19**. In general, the reductions in properties were more prominent with higher *w/c* ratio and fly ash content. The weight loss of all concrete mixes with a *w/c* ratio of 0.40 was about 4% to 5%, and the effect of fly ash was insignificant. For other concrete mixes, the weight loss increased quickly with fly ash content of more than 20%. The

"sandless concrete" with a *w/c* ratio of 0.55 and fly ash replacement content of 50% suffered the maximum weight loss of 10.9%.

The same concrete mix also showed the highest reduction, 84%, in dynamic modulus. Other concrete mixes with *w/c* ratios equal or exceeding 0.45 and with fly ash replacement ratio more than 20% also suffered more than 60% reduction in dynamic modulus, indicating a loss in structural integrity of composite material. The reduction in dynamic modulus was due to the softening and spalling of concrete, as well as development of internal and external cracks between the aggregates and cement paste.

Also, the reduction in compressive strength varied among the different concrete mixes. For the concrete mixes with low *w/c* ratios of 0.40 and 0.45, the reduction was minimal when the fly ash replacement ratio was less than 40% and 30%, respectively. Otherwise, the maximum reduction in compressive strength was about 10% and 20% respectively. However, for concrete mixes with higher *w/c* ratios of 0.50 and 0.55, the reduction was as high as 77 and 71% respectively. It appeared that the compressive strength was less affected than the dynamic modulus.

The appearance of "sandless concrete" specimens after sulfate attack tests are shown in **Fig. 4.20,** with *w/c* ratios of 0.45 and 0.50. For each *w/c* ratio, normal concrete mix and "sandless concrete" without fly ash showed the least vulnerability to sulfate attack while mix with 50% fly ash exhibited the most vulnerability. For concrete mix with *w/c* ratio of 0.50 and 50% fly ash, its surface layer of cement paste was completely dissolved by the $MgSO_4$ solution, leaving coarse aggregates exposed. Wide cracks could be seen between aggregate particles and paste.

4.4.3 Summary

Based on the experimental studies, the following conclusions can be achieved,

1. “Sandless concrete” showed almost the same mechanical properties as normal concrete at various *w/c* ratios.

2. Up to 50% of cement content, fly ash would compromise early age strengths but show comparable mechanical properties at later stage. Fly ash could effectively reduce drying shrinkage with higher content, due to densified microstructure.

3. Fly ash could significantly improve the resistance to chloride ion penetration. At the same time, RCPT was proved to be reliable for concrete with fly ash. However, the addition of fly ash would reduce the resistance to wet-and-drying sulfate attack.

4.5 Comparison of Mix Design Approaches

Although both mix design approaches could work out suitable mix proportions for “sandless concrete” with almost the same properties as normal concrete, the two approaches are governed by different factors. The first approach uses *A/C* and *w/c* ratio to determine the mix proportion. Cement content is the key link between water and aggregates, which will vary if any ratio changes, resulting in substantial difference. It is difficult to compare the influence of one factor while keeping the other constant, since the ingredient content would be changed.

Compared to the first approach, the latter approach, which is based on the maximum aggregate packing and excess paste theory, is more economical. The necessary information for this method is the optimization of aggregate packing and excess paste amount. After the determination of these two parameters, the amount of coarse aggregates and cement paste remains unchanged

while cement and water content varies responding to different *w/c* ratio. Therefore, for the sake of economy and practice, the second method is recommended.

4.6 Summary

Two mix design approaches have been proposed for "sandless concrete" (concrete without fine aggregates) in this Chapter. The major properties of resulted "sandless concrete" were investigated. Also, fly ash was incorporated as cement substitution up to 50% in sandless concrete. From the experimental study, the following conclusions can be drawn:

1. No distinct properties were found for "sandless concrete", made by either design approach, from conventional concrete, except the reduced workability.

2. The mix design approach based on maximum aggregate packing and excess paste theory is preferable, due to its advantages in economy.

3. For "sandless concrete", substitution of cement by fly ash showed comparable mechanical behaviors at late age although the early age strengths were reduced. Fly ash could significantly reduce drying shrinkage and chloride ion penetration of "sandless concrete", due to the densified microstructure caused by pozzolanic reaction.

Table 4-1: Mix proportions for "sandless concrete" by Approach 1

Mix No.	Content, kg/m^3				
	Cement	CA	Water	Fly Ash	Sand
M-N	588	882	265	—	588
M-0	588	1470	265	—	—
M-10	530	1456	265	59	—
M-20	470	1445	265	118	—
M-25	441	1438	265	147	—
M-30	412	1432	265	176	—
M-40	353	1420	265	235	—
M-50	294	1407	265	294	—

CA: coarse aggregates.

Table 4-2: Properties of "sandless concrete" by Approach 1

Mix No.	Slump, mm	Air Content, %	Density, kg/m^3	Time of initial setting / final setting, h: min	Modulus, GPa
M-N	210	1.6	2285	4: 16 / 5: 35	27.3 ±0.52
M-0	100	1.8	2305	4: 17 / 5: 48	24.5 ±0.94
M-10	110	1.9	2290	4: 11 / 5: 37	23.2 ±0.10
M-20	125	1.4	2295	4: 22 / 5: 45	20.9 ±0.58
M-25	160	1.4	2285	4: 30 / 5: 57	20.5 ±0.26
M-30	130	1.5	2250	4: 40 / 6: 20	25.1 ±0.49
M-40	135	1.3	2235	4: 56 / 6: 11	24.0 ±0.54
M-50	160	1.8	2230	5: 15 / 6: 43	20.9 ±0.80

Table 4-3: Mix proportions for "sandless concrete" by Approach 2

Mix No.	Content, kg/m^3							Paste volume L/m^3
	Cement	Fly Ash	Water	CA-10	CA-20	Sand	*w/c*	
NC40	475	0	190	457	685	571	0.40	341
SLC40-1	475	0	190	685	1027	—	0.40	341
NC45	444	0	200	457	685	571	0.45	341
SLC45-1	444	0	200	685	1027	—	0.45	341
NC50	417	0	209	457	685	571	0.50	341
SLC50-1	417	0	209	685	1027	—	0.50	341
NC55	393	0	216	457	686	571	0.55	341
SLC55-1	393	0	216	685	1027	—	0.55	341

Note: NC: normal concrete; SLC: "sandless concrete";
CA-10: coarse aggregates with maximum size of 10 mm;
CA-20: coarse aggregates with maximum size of 20 mm.

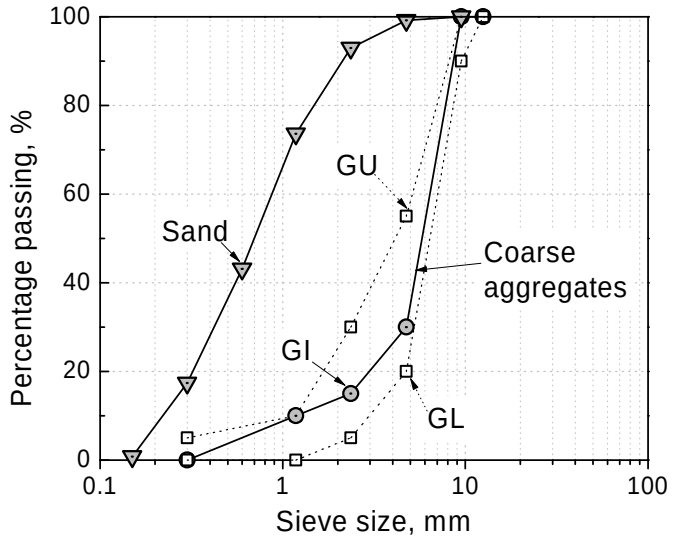

Figure 4-1: Aggregate grading curves.

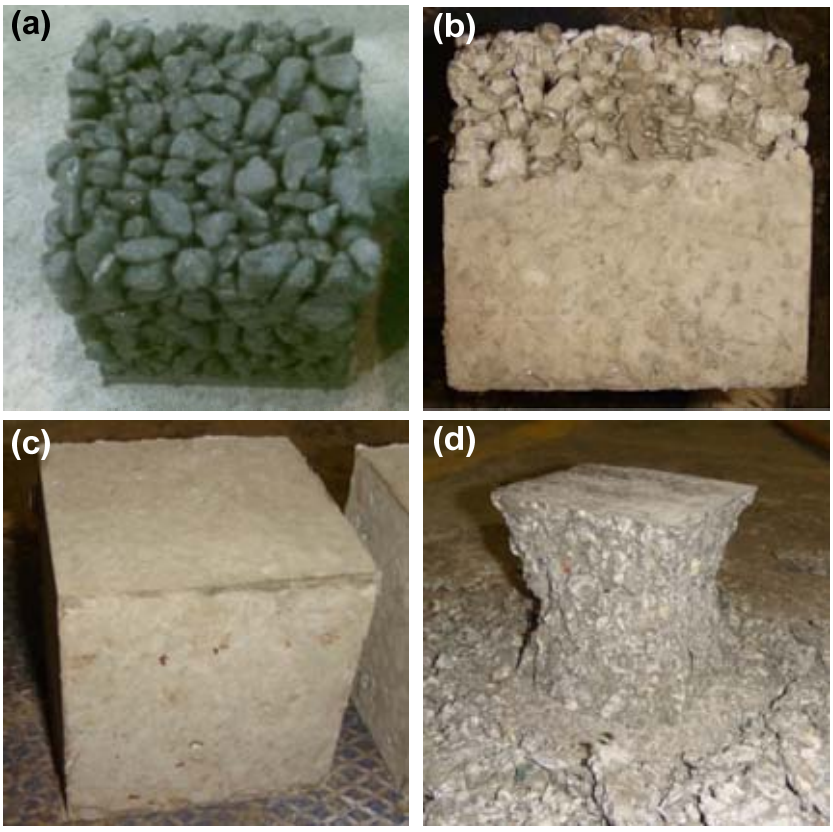

Figure 4-2: Photographs of "sandless concrete" cube specimens:
(a) & (b) - With insufficient cement paste (*A/C*=3.5, *w/c*=0.5),
(c) & (d) - With sufficient cement paste (*A/C*=2.5, *w/c*=0.45).

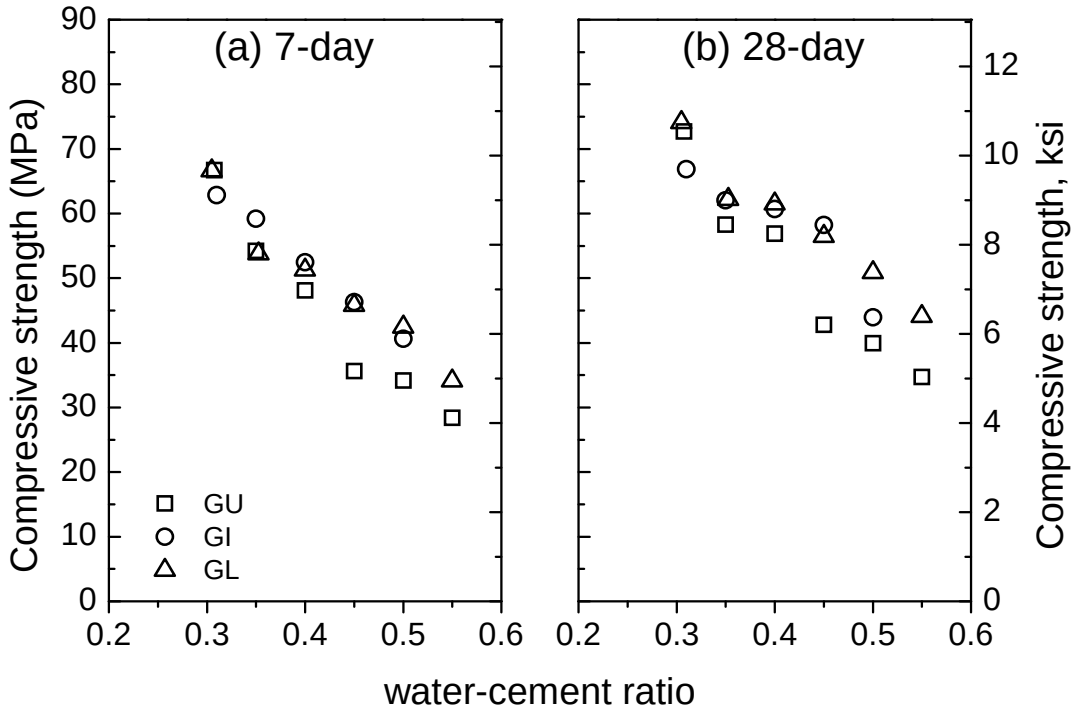

Figure 4-3: Compressive strength with different grading of coarse aggregates.

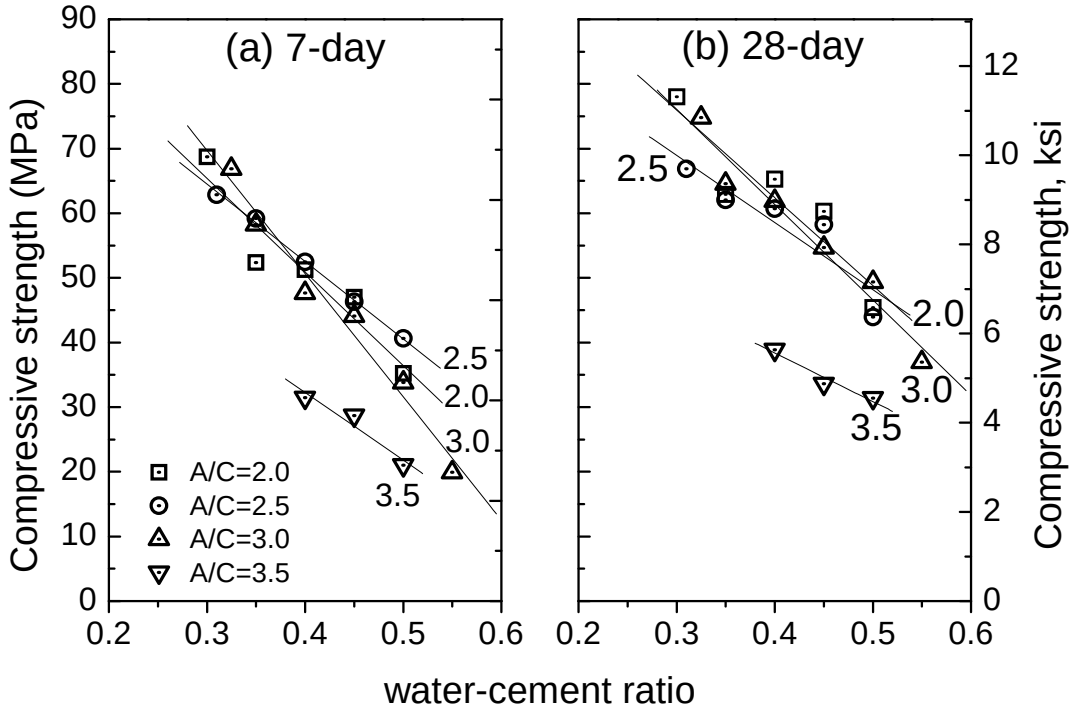

Figure 4-4: Compressive strength with different aggregate-cement (*A/C*) ratios.

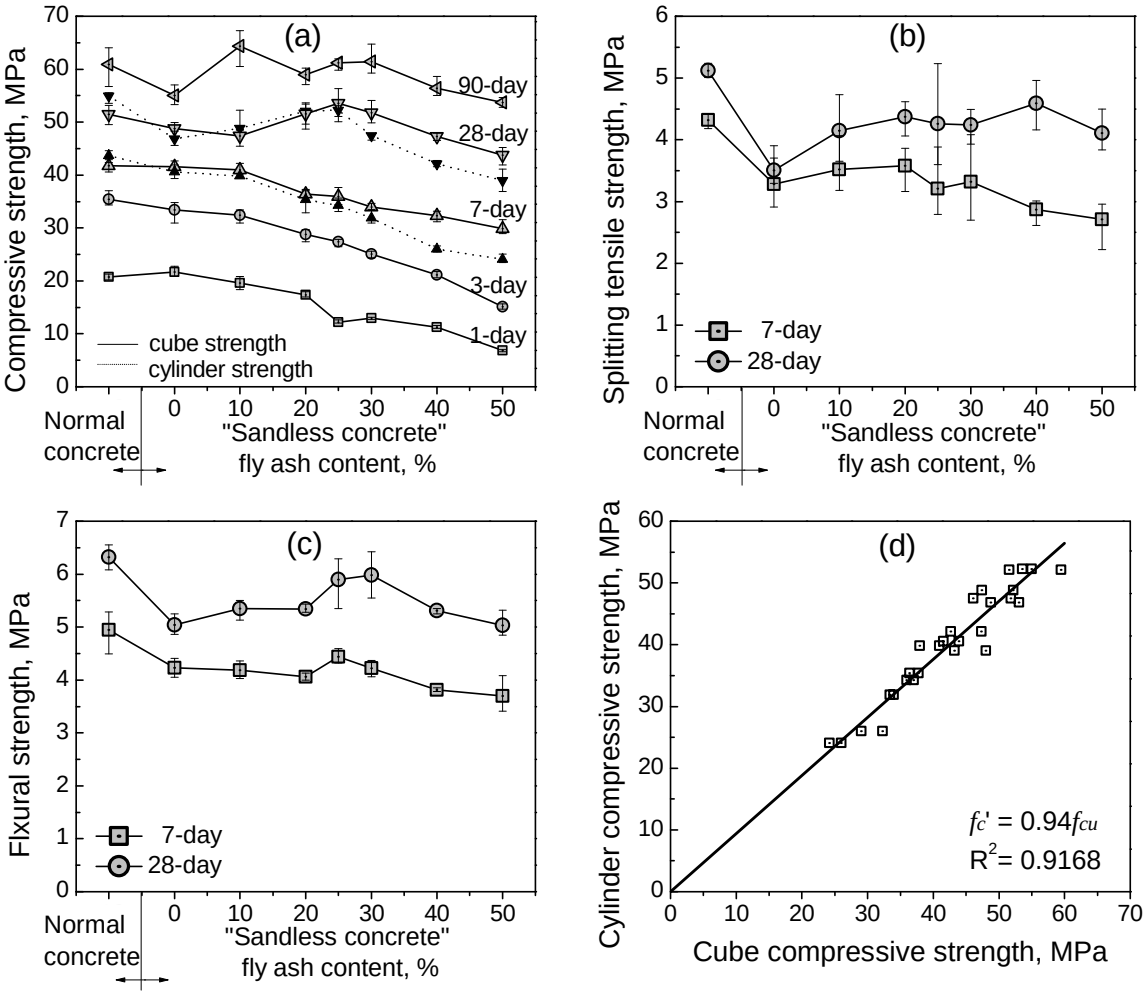

Figure 4-5: Strength development of "sandless concrete": (a) compressive strength, (b) splitting tensile strength, (c) flexural strength, (d) relation between cylinder and cube strength.

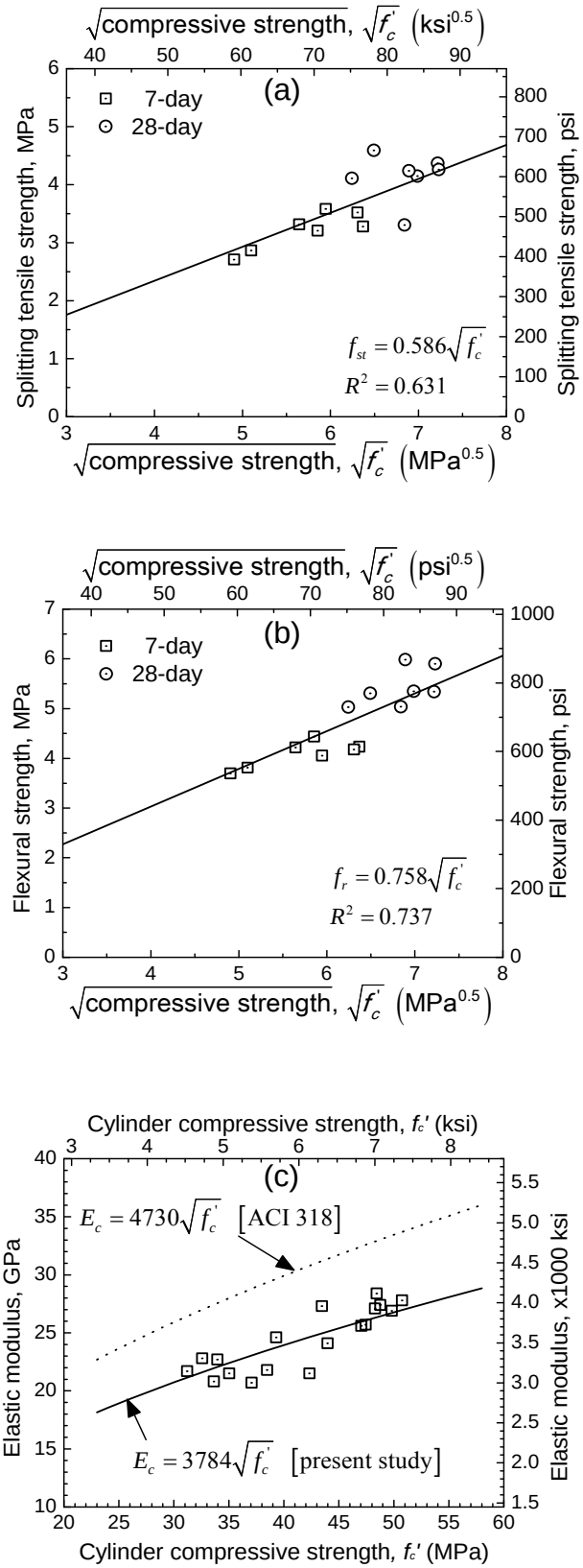

Figure 4-6: Relations between compressive strength and (a) splitting tensile strength, (b) flexural strength, and (c) elastic modulus.

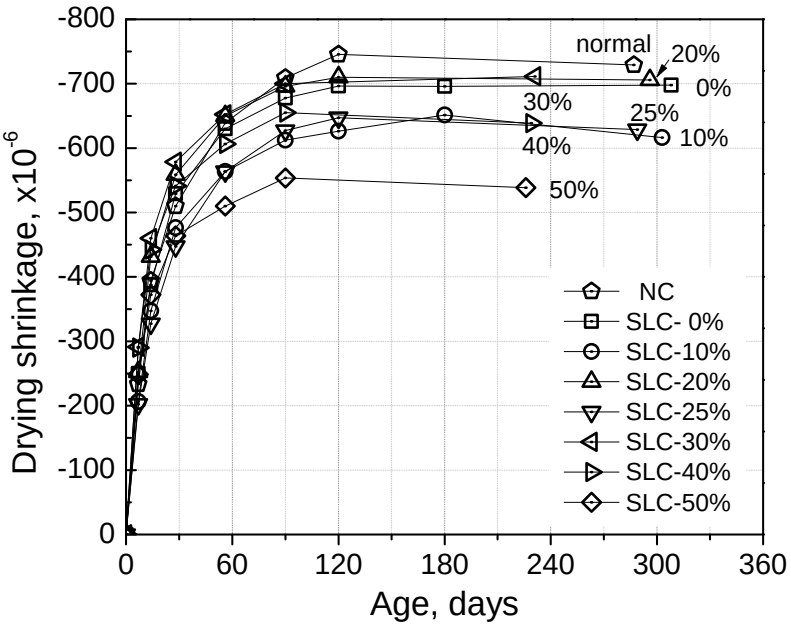

Figure 4-7: Drying shrinkage of "sandless concrete".

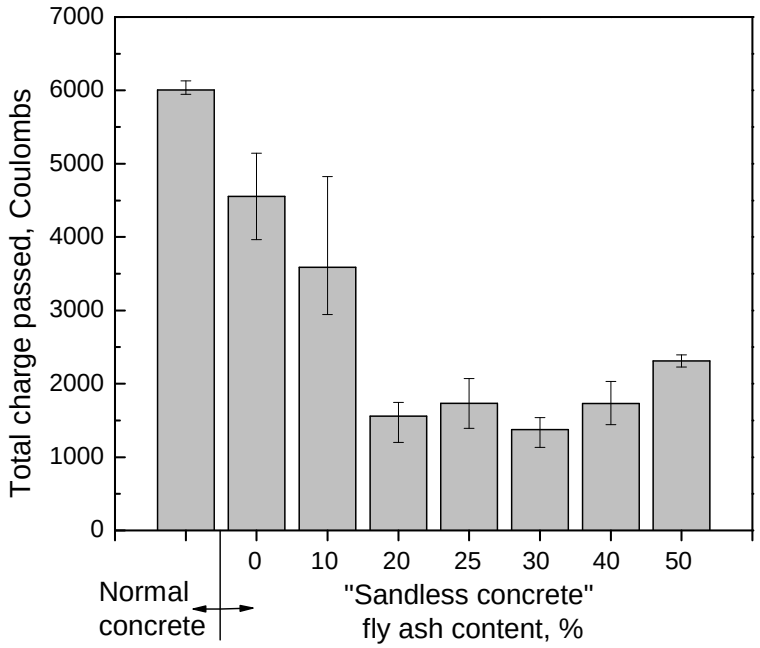

Figure 4-8: RCPT results at 28 days.

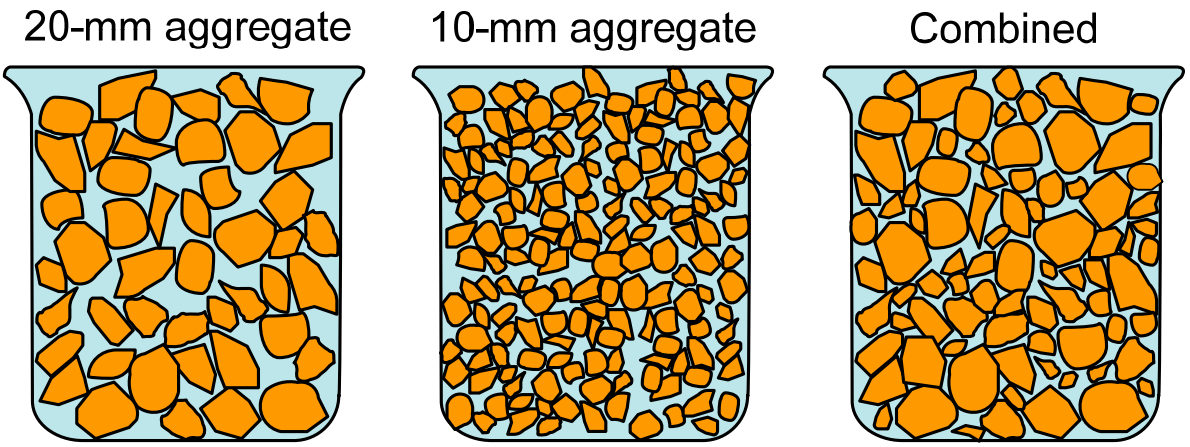

Figure 4-9: Illustration of void content of aggregate particles [Kosmatka et al., 1995].

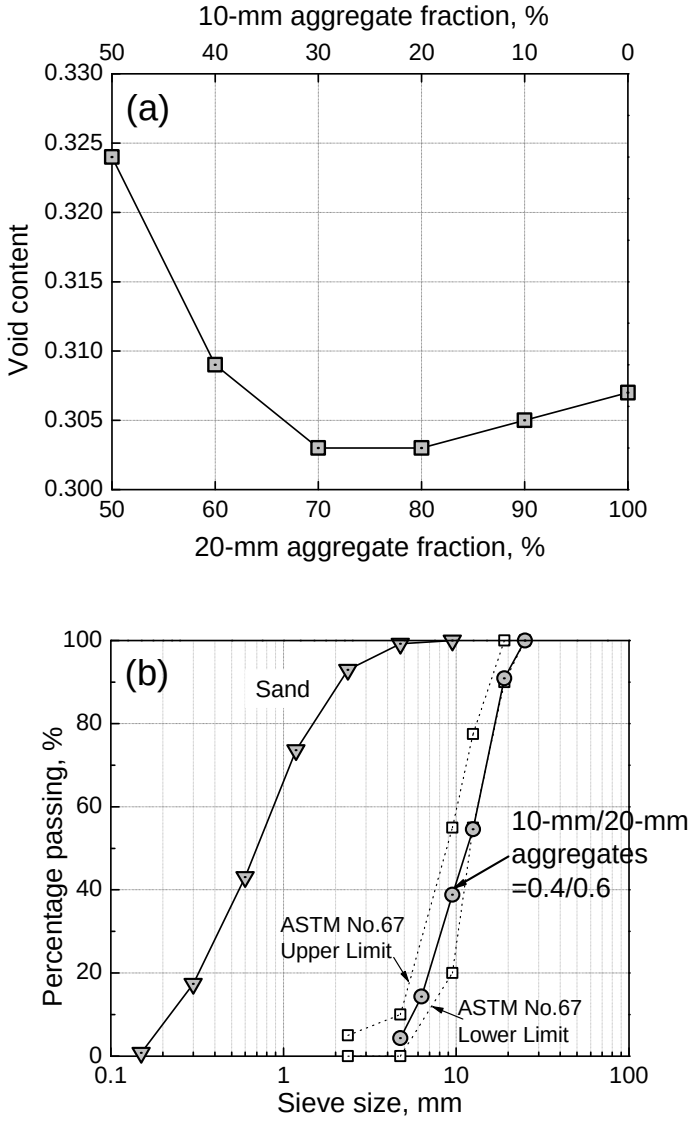

Figure 4-10: (a) Void content, and (b) grading curve of combined aggregates.

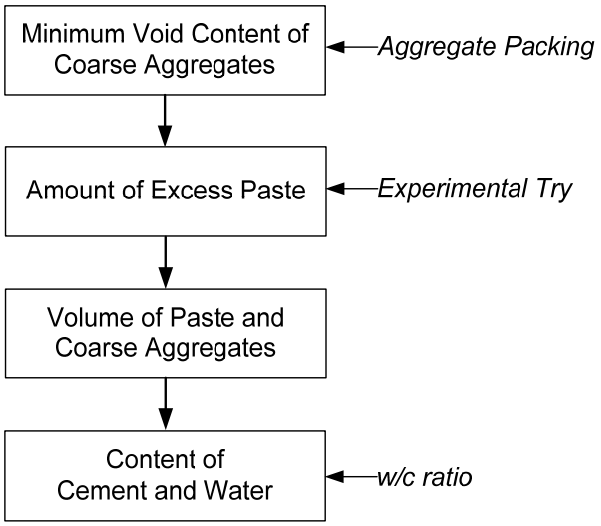

Figure 4-11: Steps for mix design Approach 2.

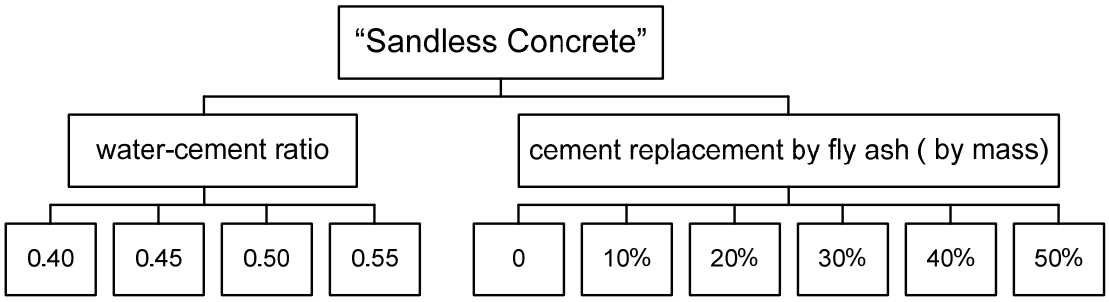

Figure 4-12: Test program of the second mix design method.

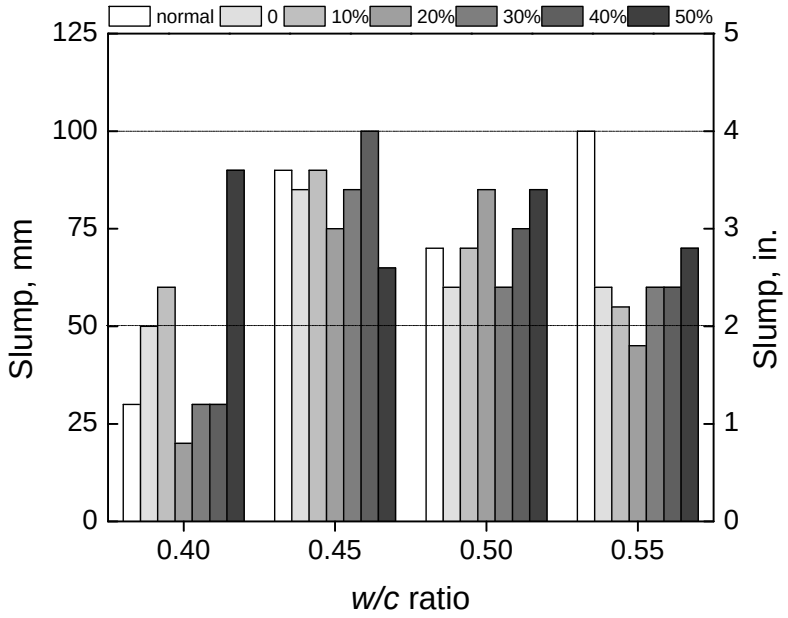

Figure 4-13: Slump of "sandless concrete".

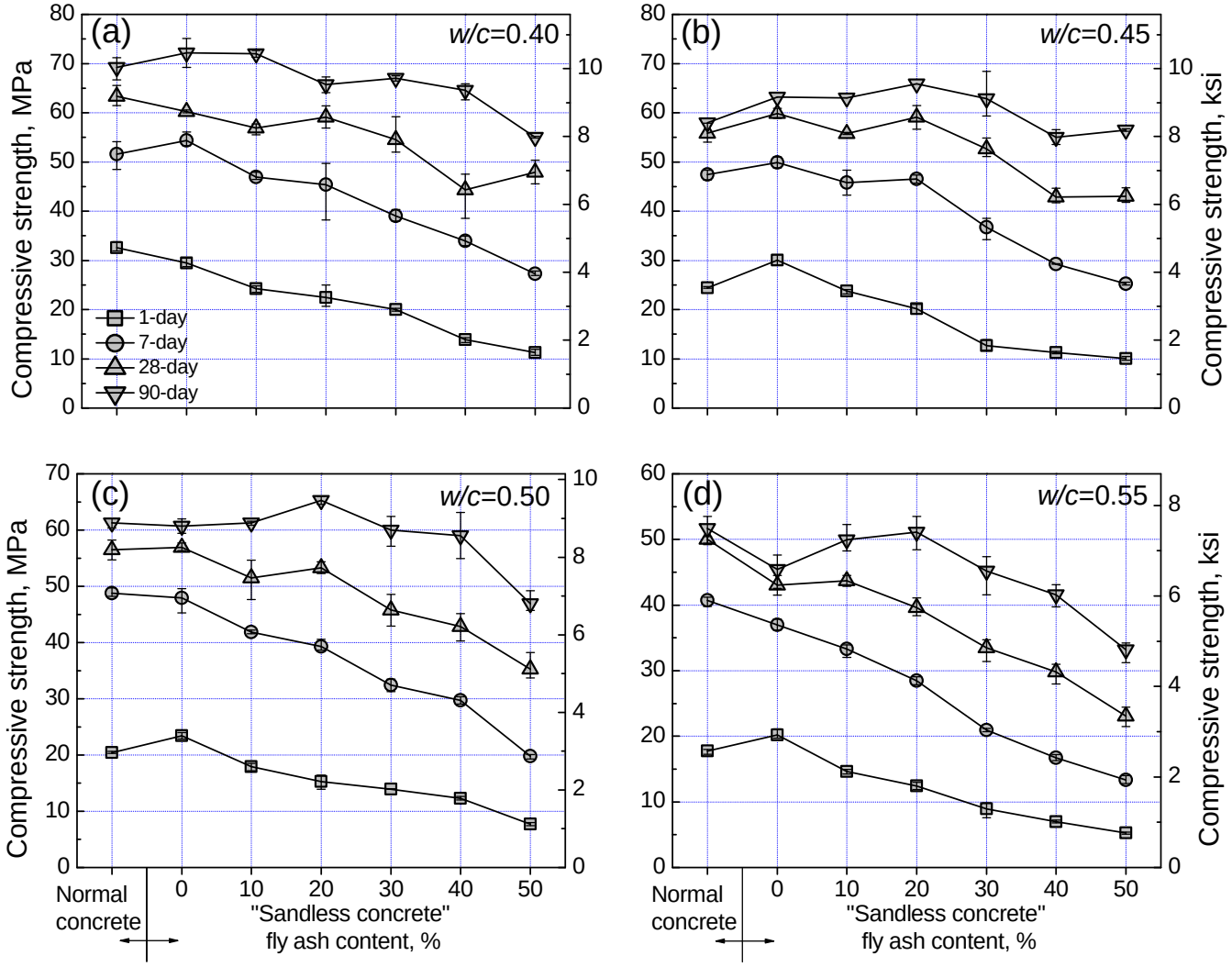

Figure 4-14: Compressive strength of "sandless concrete".

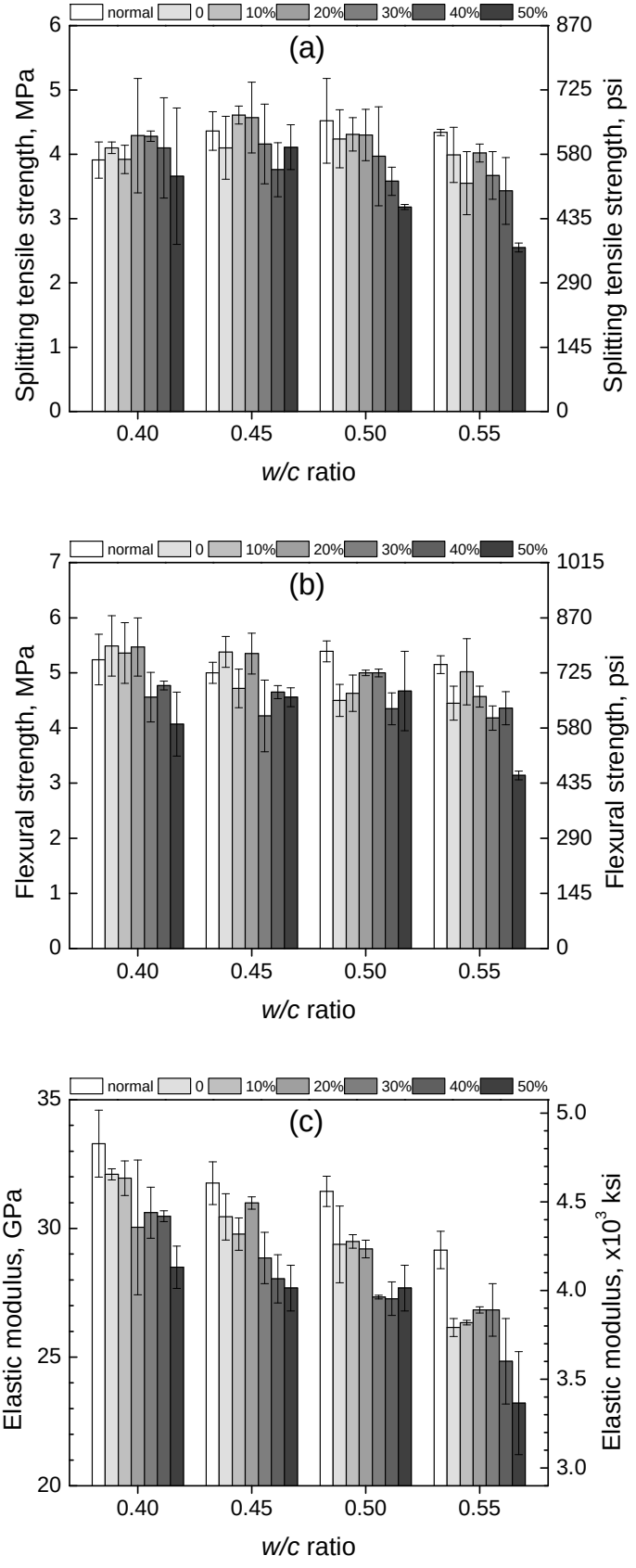

Figure 4-15: (a) Splitting tensile strength, (b) flexural strength and (c) elastic modulus of "sandless concrete".

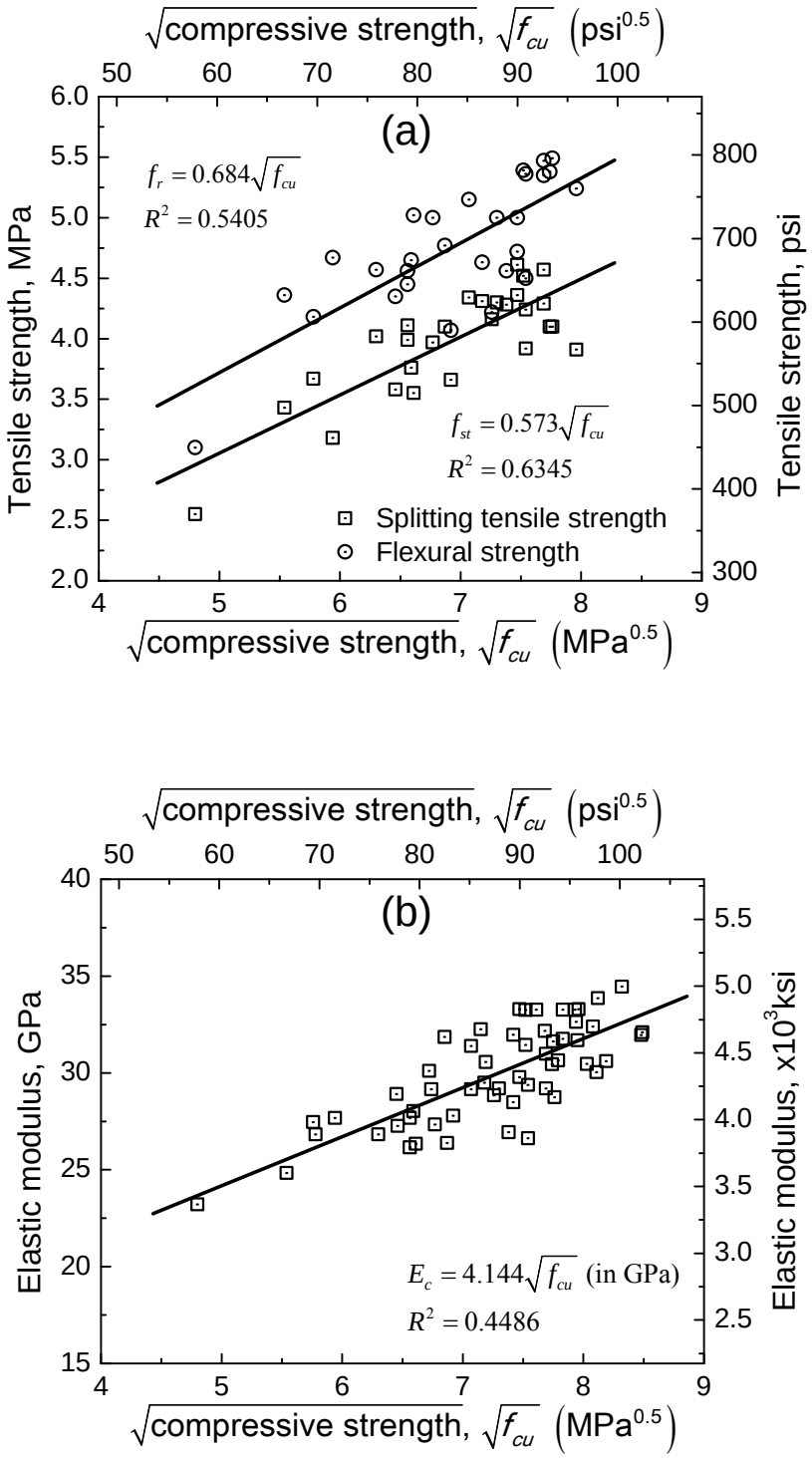

Figure 4-16: Relation between compressive strength and (a) flexural and splitting tensile strength, and (b) elastic modulus.

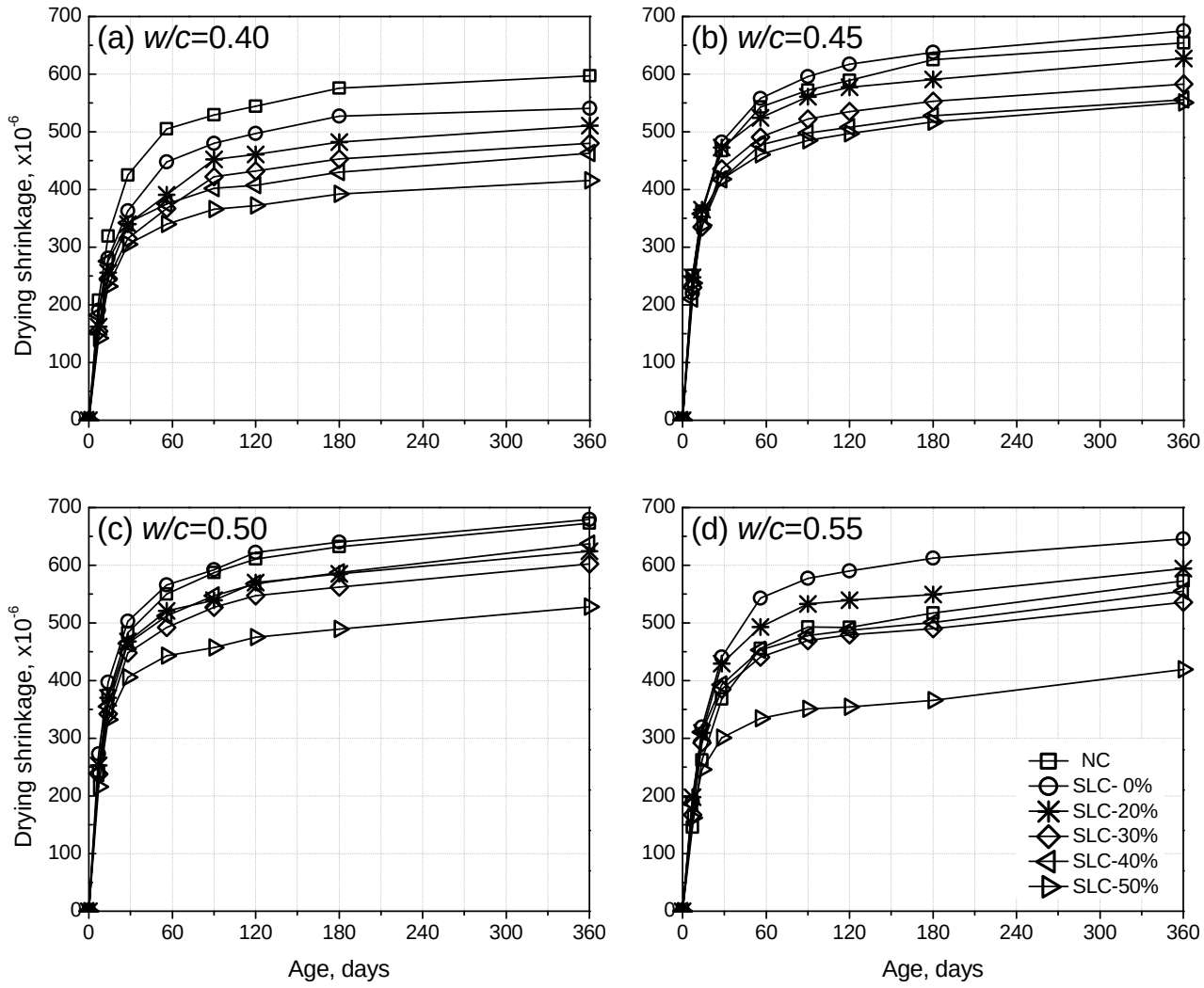

Figure 4-17: Drying shrinkage of "sandless concrete".

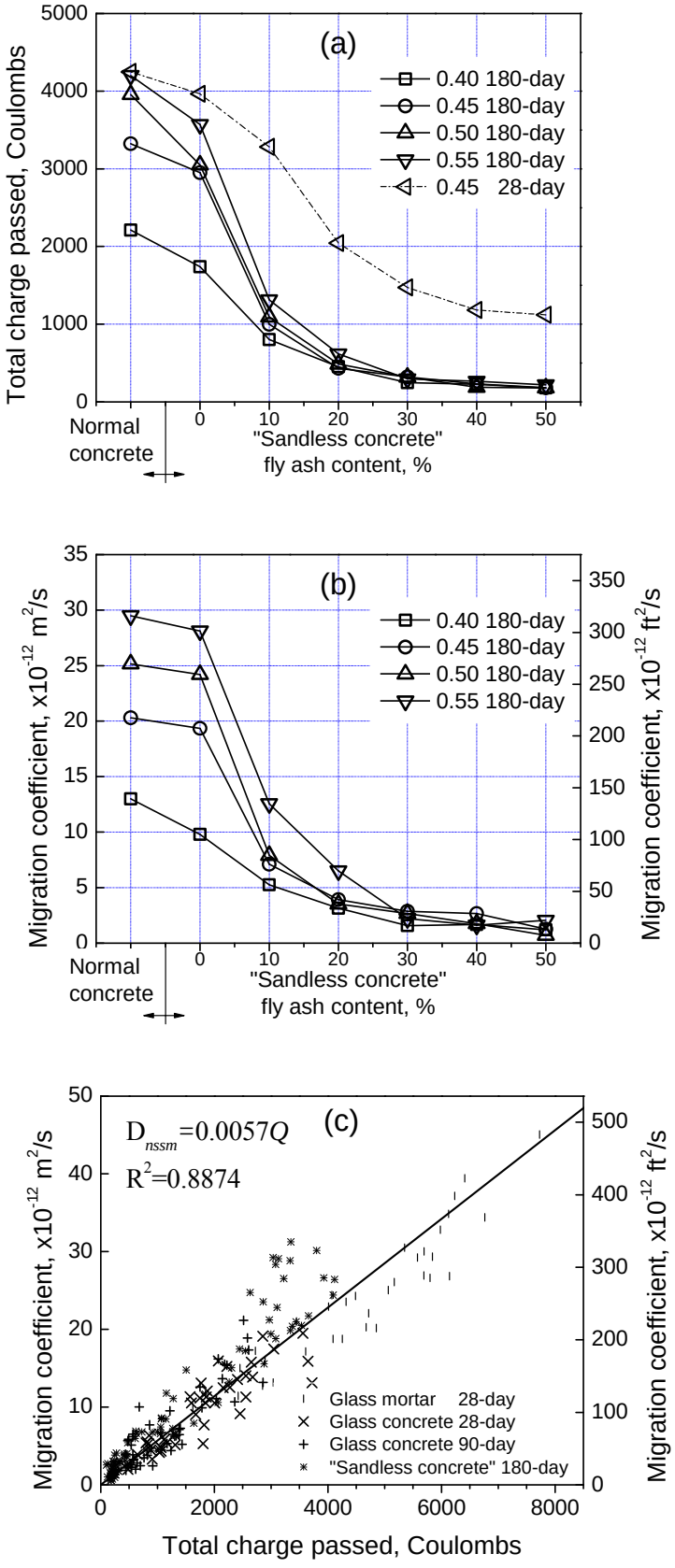

Figure 4-18: (a) RCPT result, (b) D_{nssm} of "sandless concrete", and (c) Relation between RCPT and D_{nssm}.

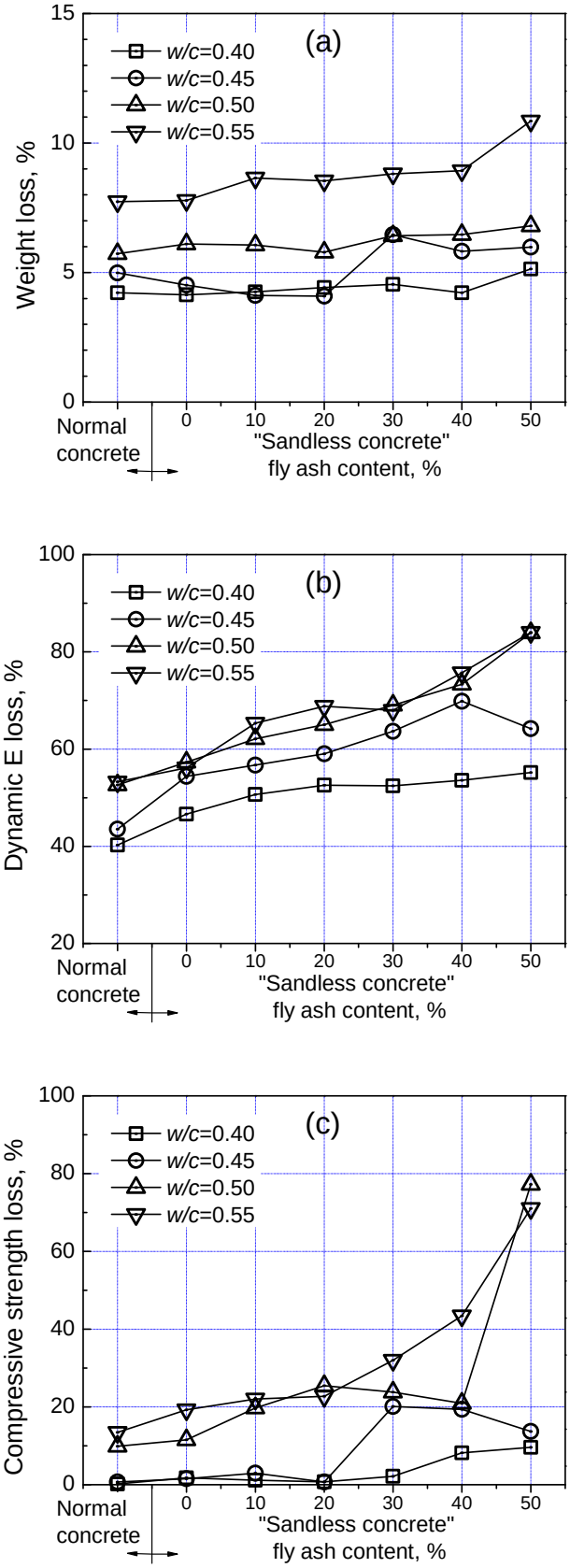

Figure 4-19: (a) Weight, (b) Dynamic modulus, and (c) Compressive strength loss of "sandless concrete" after sulfate attack.

Figure 4-20: Pictures of "sandless concrete" after sulfate attacks with *w/c* ratio of (a) 0.45, and (b) 0.50.

Chapter 5. Conclusions and Recommendations

5.1 Review of Work

This study was carried out to ensure the sustainability of concrete from the perspective of replacing or eliminating natural sand as an ingredient in making concrete. In the first part, the effects of waste glass particles on mortar and concrete properties were experimentally determined, at both fresh and hardened states, by replacing natural sand with different colored glass particles by up to 100%. The different effects of glass particles on mortar and concrete, especially for fresh and mechanical properties, were compared and discussed. Durability properties, in terms of resistance to chloride ion penetration as well as sulfate attack, were also examined.

Of primary concern for mortar and concrete containing waste glass particles, alkali-silica reaction (ASR) was thoroughly studied. The effects of glass color, content and particle size on ASR were investigated based on accelerated mortar-bar tests. Moreover, microstructure of ASR gel was observed to study the ASR mechanism for glass particles in cementitious composites. Also, different mitigation methods were carried out to suppress ASR expansion in mortar with glass particles. Finally, the optimal content for each mitigation method was determined.

In the second part, this study proposes the concept of "sandless concrete" which means that no sand (or fine aggregates) is contained in concrete mixture. Its viability was examined based on two different mix design approaches. The first approach extends the idea of no-fines concrete, for which two parameters are dominating, namely, aggregate/cement ratio and water/cement

ratio. The second approach is based on the maximum aggregates packing and excess paste theory. For each mix design approach, "sandless concrete" was investigated for its fresh, mechanical and durability properties, and compared with normal concrete. In addition, class F fly ash was used to substitute cement in "sandless concrete" by up to 50%, in order to decrease its high content of cement. Finally, the two mix design approaches were compared and discussed.

5.2 Summary of Main Findings

From the studies carried out on waste glass mortar and concrete, as well as "sandless concrete", the following conclusions, as summarized in **Table 5.1**, can be drawn:

1. Mortar and concrete containing waste glass particles as sand replacement
    a. The fresh density and air content of mortar and concrete were not significantly affected by the incorporation of glass sand particles. Slump tests suggested that the use of glass sand would not compromise the workability of concrete, although it decreased the flowability of glass mortar.

    b. Use of glass sand particles, regardless of color, resulted in a reduction in compressive, flexural and splitting tensile strength, and elastic modulus for mortar. This was due to a weakened ITZ. However, in the case of concrete, the mechanical properties might benefit from the pozzolanic reaction of fine glass particles, which refined the pore size and reduced the porosity of cement paste. Also, the higher aspect ratio of waste glass particles compared to natural sand contributed to the improvement in mechanical properties by a bridging effect. For both mortar and concrete, drying shrinkage was reduced, which implied a better

dimension stability, and this was primarily attributed to the negligible water absorption. The different effects of waste glass particles on the mechanical properties, of mortar and concrete, were first illustrated by this study. The differences were caused by the relative fraction of sand and cement in the two composites. The higher ratio of sand/cement ratio in mortar indicated less cement paste to coat the surface of sand and higher friction between sand particles, which hindered the movement of cement and reduce bond strength at ITZ between sand particles.

c. The resistance to chloride ion penetration could be substantially improved by incorporating glass particles in both mortar and concrete, due to pozzolanic reaction of the glass particles. With respect to sulfate resistance, glass mortar showed comparable physical and mechanical performance as mortar with natural sand. Such findings on durability properties were in agreement with previous literature [Kou and Poon, 2009; Ling et al., 2011].

d. ASR was potentially deleterious for glass mortar with clear color glass but not for green or brown glasses, judging by their small expansions (less than 0.1% at 14 days) from accelerated mortar-bar tests. ASR expansion increased with larger glass particle size, regardless of glass color, which is in agreement with previous results (**Fig. 3.16**). In the long term, green glass sand mortar showed significantly higher expansion than brown glass sand. This is the first sophisticated study to find the high reactivity of green glass particles larger than 0.6 mm.

e. Furthermore, from the microstructure study, ASR cracks first occurred within the glass particles and then extended to the surrounding cement paste. It is in agreement with a recent publication [Maraghechi et al., 2012].

f. This study first evaluated the efficiency of different ASR mitigating methods. Based on the performance, 30% fly ash or 60% GGBS was recommended to suppress the ASR expansion for mortar and concrete containing glass particles, compared with other mitigation methods.

2. "Sandless concrete"

a. The concept and viability of "sandless concrete" for structural application were first investigated. Two different mix design methods were investigated to produce a satisfactory "sandless concrete". It was found that the principle of "excess paste theory" applied for the mix design of "sandless concrete". Although the workability of "sandless concrete" in terms of slump by both mix design approaches was reduced, it could still meet the requirement of ACI 211.1 design code.

b. "Sandless concrete" showed almost the same mechanical properties as normal concrete at various *w/c* ratios except the reduced modulus of elasticity. Also, it was found that the empirical formulas provided by ACI 318 would conservatively estimate the tensile strength for "sandless concrete". However, modulus of elasticity would be comprehended.

c. The influences of fly ash in "sandless concrete" were almost identical as in normal concrete. Up to 50% of cement content, fly ash would compromise early

age strengths but show comparable mechanical properties at later stage. Fly ash could effectively reduce drying shrinkage and enhance the resistance to chloride ion penetration at higher content, due to the densified microstructure by pozzolanic reaction.

5.3 Limitations of Study and Suggestions for Future Research

Some limitations and recommendations are presented for future research in the area of glass sand cementitious composites and "sandless concrete", from this study. They are:

1. All the results and analyses of this study are based on accelerated mortar-bar tests, which cannot reflect the real site condition well. ASR should be investigated in the long term under circumstances close to reality. With regard to the ASR test of concrete in long term, some existing standard methods, including ASTM C 1293, BS 812-123, and RILEM AAR-3, are available.

2. The different ASR reactivity of green and brown glass particles (larger than 0.6 mm) in the long term remains not clarified. The distribution and density of micro-cracks of glass sand caused by crushing should be studied, especially for clear glass which shows the highest alkali reactivity. ASR reaction gel should be investigated based on its chemical compositions, to better understand its expansion characteristics. SEM and EDS could provide such valuable information, to complement and help explain the test results. In addition, some other advanced techniques can also be employed in the study of ASR gel with respect to the morphology, such as soft X-ray microscopy, X-ray microtomography, neutron diffraction and texture analysis [Monteiro et al., 2009]. Furthermore, the

mechanical properties of ASR gel can be determined in the nano-scale (~10^{-9} m) which will be increasingly significant in future research in concrete, especially for durability. Nano-indentation has been successfully used to study the cement hydration product of CSH gel [Constantinides and Ulm, 2004]. The same rationale can be applied in the study of other detrimental mechanisms in concrete, which is beneficial for durability study. Lastly, a plausible explanation should be proposed to interpret the occurrence of pozzolanic reaction rather than ASR at glass particle surface, if micro-mechanical and morphology characteristics of ASR gel can be known.

3. More durability properties should be determined to complete the database of glass sand mortar and concrete, including resistance to wear, freeze-and-thawing, water permeability, etc. Nevertheless, such durability properties might not be significant compared to ASR.

4. This study is only an initial effort to propose the concept of "sandless concrete" and test its basic properties, through two different mix design approaches. A number of areas remain unexplored for its application. First, the mix design methods used in this study should be further optimized to yield satisfactory properties for structural construction, especially workability. In mix design Approach 2, the amount of excess paste should be more scientifically studied in future, which may show different performances for "sandless concrete". In addition, besides fly ash, other by-products or waste materials can also be included in "sandless concrete" as binding materials to increase its sustainability. More investigations on the durability properties of "sandless concrete" should also be considered in the future.

5. Fundamental aspects of “sandless concrete”, in terms of a two-phase composite, should be investigated, including the nature of interfacial zone between coarse aggregate particles and cement paste (microstructure, porosity, and permeability), the optimum packing of coarse aggregates (theoretically and experimentally), and the optimum amount of excess paste (including statistically measured thickness of paste coating on coarse aggregate particles and specific surface area of aggregate particles), etc. The engineering properties of “sandless concrete”, as reported in this study, should be linked with those basic material behaviors.

Table 5-1: Overview of the main contributions from the study

Studies	Contribution
Glass sand cementitious composites	1. Characterized fresh properties of mortar and concrete with up to 100% glass sand, which were not much affected except for the flowability of mortar; 2. Explored mechanical properties of mortar and concrete containing glass sand, which were compromised in case of mortar but enhanced for concrete; 3. Complemented durability properties of glass sand mortar and concrete, notably, the resistance to chloride ion penetration was found to significantly increase with glass sand.
Alkali-silica reaction for glass particles in cementitious composites	1. Determined the effect of glass color, content and particle size on ASR expansion; 2. Studied the mechanism of ASR for glass particles, which was found to form and cause cracks within glass particles, different from traditional ASR; 3. Investigated the efficiency and determined the optimum dosage of different ASR mitigation methods; 30% fly ash or 60% GGBS proved to be efficient and recommended for practical use.
"Sandless concrete"	1. Proposed two different concrete mix design approaches, which were both proved to be suitable; 2. Examined properties of "sandless concrete" at both fresh and hardened states, which were comparable to normal concrete except for the decreased workability; 3. Used fly ash as cement replacement in "sandless concrete", by which the cement content was significantly reduced.

References

ACI 211.1-91, *Standard Practice for Selecting Proportions for Normal, Heavyweight, and Mass Concrete (Reapproved 2002)*, American Concrete Institution, Farmington Hills, MI, 2002, 38 pp.

ACI 318-08, *Building Code Requirements for Structural Concrete (ACI 318-08) and Commentary*, American Concrete Institute, Farmington Hills, MI, 2008, 465 pp.

ACI 224R-01, *Control of Cracking in Concrete Structure*, American Concrete Institute, Farmington Hills, MI, 2001, 46 pp.

ACI 522R-10, *Report on Pervious Concrete*, American Concrete Institute, Farmington Hills, MI, 2010, 38 pp.

Ahn, N., and Fowler, D. W., *An Experimental Study on the Guidelines for Using Higher Contents of Aggregate Microfines in Portland Cement Concrete*, Report No. ICAR 102-1F, International Center for Aggregates Research, University of Texas, Austin, 2001, 435 pp.

Aldea, C. M.; Shah, S. P.; and Karr, A., "Effect of Cracking on Water and Chloride Permeability of Concrete," *Journal of Materials in Civil Engineering*, V. 11, No. 3, 1999, pp. 181-187.

Alexander, M.; Mindess, S.; Diamond, S.; and Qu, L., "Properties of Paste/Rock Interfaces and Their Influence on Composite Behavior," *Materials and Structures*, V. 28, No. 183, 1995, pp. 497-506.

Alexander, M., and Mindess, S., *Aggregates in Concrete*, First Edition, Taylor & Francis, 2005, 435 pp.

AS 3600, *Concrete Structures*, Australian Standard International, Sydney, 2001.

ASTM C 29/C 29M-97, *Standard Test Method for Bulk Density ("Unit Weight") and Voids in Aggregate*, ASTM International, West Conshohocken, PA, 2003, 4 pp.

ASTM C 33-03, *Standard Specification for Concrete Aggregates*, ASTM International, West Conshohocken, PA, 2003, 11 pp.

ASTM C 39/C 39M-05, *Standard Test Method for Compressive Strength of Cylindrical Concrete Specimens*, ASTM International, West Conshohocken, PA, 2005, 7 pp.

ASTM C 78-02, *Standard Test Method for Flexural Strength of Concrete (Using Simple Beam with Third-Point Loading)*, ASTM International, West Conshohocken, 2002, PA, 3 pp.

ASTM C 109/C 109M-05, *Standard Test Method for Compressive Strength of Hydraulic Cement Mortars (Using 2-in. or [50 mm] Cube Specimens)*, ASTM International, West Conshohocken, PA, 2005, 9 pp.

ASTM C 125-03, *Standard Terminology Relating to Concrete and Concrete Aggregates*, ASTM International, West Conshohocken, PA, 2003, 14 pp.

ASTM C 128-01, *Standard Test Method for Density, Relative Density (Specific Gravity), and Absorption of Fine Aggregate*, ASTM International, West Conshohocken, PA, 2007, 7 pp.

ASTM C 138/C 138M-01a, *Standard Test Method for Density (Unit Weight), Yield, and Air Content (Gravimetric) of Concrete*, ASTM International, West Conshohocken, PA, 2001, 4 pp.

ASTM C 143/C 143M-05a, *Standard Test Method for Sump of Hydraulic-Cement Concrete*, ASTM International, West Conshohocken, PA, 2005, 4 pp.

ASTM C 150-05, *Standard Specification for Portland Cement*, ASTM International, West Conshohocken, PA, 2005, 8 pp.

ASTM C 157/C 157M-06, *Standard Test Method for Length Change of Hardened Hydraulic-Cement Mortar and Concrete*, ASTM International, West Conshohocken, PA, 2006, 7 pp.

ASTM C 185-02, *Standard Test Method for Air Content of Hydraulic Cement Mortar*, ASTM International, West Conshohocken, PA, 2002, 3 pp.

ASTM C 215-08, *Standard Test Method for Fundamental Transverse, Longitudinal, and Torsional Resonant Frequencies of Concrete Specimens*, ASTM International, West Conshohocken, PA, 2008, 7 pp.

ASTM C 227-03, *Standard Test Method for Potential Alkali Reactivity of Cement-Aggregate Combinations (Mortar-Bar Method)*, ASTM International, West Conshohocken, PA, 2003, 5 pp.

ASTM C 231-03, *Standard Test Method for Air Content of Freshly Mixed Concrete by the Pressure Method*, ASTM International, West Conshohocken, PA, 2003, 9 pp.

ASTM C 267-01, *Standard Test Methods for Chemical Resistance for Mortars, Grouts, and Monolithic Surfacings and Polymer Concretes*, ASTM International, West Conshohocken, PA, 2006, 6 pp.

ASTM C 348-02, *Standard Test Method for Flexural Strength of Hydraulic-Cement Mortar*, ASTM International, West Conshohocken, PA, 2002, 6 pp.

ASTM C 403/C 403M-06, *Standard Test Method for Time of Setting of Concrete Mixtures by Penetration Resistance*, ASTM International, West Conshohocken, PA, 2006, 7 pp.

ASTM C 469-02, *Standard Test Method for Static Modulus of Elasticity and Poisson's Ratio of Concrete in Compressio*n, ASTM International, West Conshohocken, PA, 2002, 5 pp.

ASTM C 496/C 496M-04, *Standard Test Method for Splitting Tensile Strength of Cylindrical Concrete Specimens*, ASTM International, West Conshohocken, PA, 2004, 5 pp.

ASTM C 596-01, *Standard Test Method for Drying Shrinkage of Mortar Containing Hydraulic Cement*, ASTM International, West Conshohocken, PA, 2001, 3 pp.

ASTM C 618-08a, *Standard Specification for Coal Fly Ash and Raw or Calcined Natural Pozzolan for Use in Concrete*, ASTM International, West Conshohocken, PA, 2005, 3 pp.

ASTM C 1012/C 1012 M-10, *Standard Test Method for Length Change of Hydraulic-Cement Mortars Exposed to a Sulfate Solution*, ASTM International, West Conshohocken, PA, 2010, 7 pp.

ASTM C 1202-05, *Standard Test Method for Electrical Indication of Concrete's Ability to Resist Chloride Ion Penetration*, ASTM International, West Conshohocken, PA, 2005, 6 pp.

ASTM C 1260-07, *Standard Test Method for Potential Alkali Reactivity of Aggregates (Mortar-Bar Method)*, ASTM International, West Conshohocken, PA, 2007, 5 pp.

ASTM C 1293-01, *Standard Test Method for Determination of Length Change of Concrete Due to Alkali-Silica Reaction*, ASTM International, West Conshohocken, PA, 2001, 6 pp.

ASTM C 1437-01, *Standard Test Method for Flow of Hydraulic Cement Mortar*, ASTM International, West Conshohocken, PA, 2001, 2 pp.

ASTM C 1567-08, *Standard Test Method for Determining the Potential Alkali-Silica Reactivity of Combinations of Cementitious Materials and Aggregate (Accelerated Mortar-Bar Method),* ASTM International, West Conshohocken, PA, 2008, 6 pp.

Atis, C. D., "High-Volume Fly Ash Concrete with High Strength and Low Drying Shrinkage," *Journal of Materials in Civil Engineering*, V. 15, No. 2, 2003, pp. 153-156.

BACSD, "White Paper on Sustainable Development," *Concrete International*, V. 27, No. 2, 2005, pp. 19-21.

Bazant, Z. P., and Steffens, A., "Mathematical Model for Kinetics of Alkali-Silica Reaction in Concrete," *Cement and Concrete Research*, V. 30, No. 3, 2000, pp. 419-428.

Bazant, Z. P.; Zi, G.; and Meyer, C., "Fracture Mechanics of ASR in Concretes with Waste Glass Particles of Different Sizes," *Journal of Engineering Mechanics*, V. 126, No. 3, 2000, pp. 226-232.

Bentz, D. P., "Virtual Pervious Concrete: Microstructure, Percolation, and Permeability," *ACI Materials Journal,* V. 105, No. 3, 2008, pp. 297-301.

Berra, M.; Mangialardi, T.; and Paolini, A. E., "Application of the NaOH Bath Test Method for Assessing the Effectiveness of Mineral Admixtures against Reaction of Alkali with Artificial Siliceous Aggregate," *Cement and Concrete Composites*, V. 116, No., 3, 1994, pp. 207-218.

Berube, M. A.; Duchesne, J.; and Chouinard, D., "Why the Accelerated Mortar Bar Method ASTM C 1260 Is Reliable for Evaluating the Effectiveness of Supplementary Cementing Materials in Suppressing Expansion due to Alkali-Silica Reactivity," *Cement, Concrete and Aggregate*, V. 17, No. 1, 1995, pp. 26-34.

Bilodeau, A., and Malhotra, V. M., "High-Volume Fly Ash System: Concrete Solution for Sustainable Development," *ACI Materials Journal*, V. 97, No. 1, 2000, pp. 41-48.

BS 812-123, *Testing Aggregates - Method for Determination of Alkali-Silica Reactivity - Concrete Prism Method*, British Standard Institution, London, 1999, 18 pp.

BS 8500-2, *Concrete – Complementary British Standard to BS EN 206-1 Part 2: Specification for Constituent Materials and Concrete*, British Standards Institution, London, 2006, 46 pp.

BS DD 249, *Testing Aggregate - Method for the Assessment of Alkali-Silica Reactivity – Potential Accelerated Mortar-Bar Method*, British Standards Institution, London, 1999, 12 pp.

BS EN 12390-3, *Testing Hardened Concrete Part 3: Compressive Strength of Test Specimens*, British Standards Institution, London, 2009, 22 pp.

CCAA T60, *Guide to the Specification and Use of Manufactured Sand in Concrete*, Cement Concrete & Aggregates Australia, Sydney, 2008.

Chen, C. H.; Huang, R.; Wu, J. K.; and Yang, C. C., "Waste E-glass Particles Used in Cementitious Mixtures," *Cement and Concrete Research*, V. 36, No. 3, 2006, pp. 449-456.

Chen, H.; Soles, J. A.; and Malhotra, V. M., "Investigations of Supplementary Cementing Materials for Reducing Alkali-Aggregate Reactions," *Cement and Concrete Composites*, V. 15, No. 1-2, 1993, pp. 75-84.

Christensen, T. H., and Damaggard, A., Recycling of Glass, In Christensen, T. H., (Eds), *Solid Waste Technology & Management, Chapter 5.2*, John Wiley & Sons, Chichester, 2010.

Collins, C. L.; Idelker, J. H.; Willis, G. S.; and Kurtis, K. E., "Examination of the Effects of LiOH, LiCl, and $LiNO_3$ on Alkali-Silica Reaction," *Cement and Concrete Research*, V. 34, No. 8, 2004, pp. 1403-1415.

Constantinides, G., and Ulm, F. J., "The Effects of Two Types of C-S-H on the Elasticity of Cement-Based Materials: Results from Nanoindentation and Micromechanical Modeling," *Cement and Concrete Research*, V. 34, No. 1, 2004, pp. 67-80.

Dhir, R. K., and Jones, M. R., "Development of Chloride-Resisting Concrete Using Fly Ash," *Fuel*, V. 78, No. 2, 1999, pp. 137-142.

Dhir, R. K.; Dyer, T. D.; and Tang, M. C., "Alkali-Silica Reaction in Concrete Containing Glass," *Materials and Structures*, V. 42, No. 10, 2009, pp. 1451-1462.

Diamond, S., "Effects of Two Danish Flyashes on Alkali Contents of Pore Solutions of Cement-Flyash Pastes," *Cement and Concrete Research*, V. 11, No. 3, 1981, pp. 383-394.

Diamond, S., "Alkali-Silica Reaction – Some Paradoxes," *Cement and Concrete Composites*, V. 19, No. 5, 1997, pp. 391-401.

Dyer, T. D., and Dhir, R. K., "Chemical Reactions of Glass Cullet Used as Cement Component," *Journal of Materials in Civil Engineering*, V. 13, No. 6, 2001, pp. 412-417.

Edwards, A. G., "Shrinkage and Other Properties of Concrete Made with Crushed Rock Aggregates from Scottish Source," *BGWF Journal*, Autumn, 1966, pp. 23-41.

Feldman, R. F.; Chan, G. W.; Brousseau, R. J.; and Tumidajski, P. J., "Investigation of the Rapid Chloride Permeability Test," *ACI Materials Journal*, V. 91, No. 3, 1994, pp. 246-255.

Feng, X.; Thomas, M. D. A.; Bremner, T. W.; Balcom, B. J.; and Folliard, K. J., "Studies on Lithium Salts to Mitigate ASR Induced Expansion in New Concrete: A Critical Review," *Cement and Concrete Research*, V. 35, No. 9, 2005, pp. 1789-1796.

Figg, J. W., "Reaction between Cement and Artificial Glass in Concrete," *5th International Conference on Concrete Alkali Aggregate Reactions*, Cape Town, South Africa, 1981, pp. 252-257.

Ghafoori, N., and Dutta, S., "Development of No-fines Concrete Pavement Applications," *Journal of Transportation Engineering*, V. 121, No. 3, 1995a, pp. 283-288.

Ghafoori, N., and Dutta, S., "Building and Nonpavement Application of No-fines Concrete," *Journal of Materials in Civil Engineering*, V. 7, No. 4, 1995b, pp. 286-289.

Ghafoori, N., and Dutta, S., "Laboratory Investigation of Compacted No-fines Concrete for Paving Materials", *Journal of Materials in Civil Engineering*, V. 7, No. 3, 1995c, pp. 183-191.

Ghafoori, N., and Diawara, H., "Strength and Wear Resistance of Sand-Replaced Silica Fume Concrete," *ACI Materials Journal*, V. 104, No. 2, 2007, pp. 206-214.

Gilkey, H. J., "Water-Cement Ratio versus Strength- Another Look," *Journal of the American Concrete Institute*, V. 57, No. 10, 1961, pp. 1287-1312.

Hansen, T. C., *Recycling of Demolished Concrete and Masonry*, RILEM Report No. 6, Chapman and Hall, London, 1994.

Haselbach, L. M., and Freeman, R. M., "Vertical Porosity Distributions in Pervious Concrete Pavement," *ACI Materials Journal*, V. 103, No. 6, 2006, pp. 452-458.

Haselbach, L. M., and Liu, L., "Calcium Hydroxide Formation in Thin Cement Paste Exposed to Air," *ACI Materials Journal*, V.107, No. 4, 2010, pp. 365-371.

Hasparky, N. P.; Monteiro, P. J. M.; and Carasek, H., "Effect of Silica Fume and Rice Husk Ash on Alkali-Silica Reaction," *ACI Materials Journal*, V. 97, No. 4, 2000, pp. 486-492.

Helmuth, R., and Stark, D., "Alkali-Silica Reactivity Mechanisms," In J. P. Skalny (ed.) *Materials Science of Concrete III*, American Ceramic Society, Westerville, OH, 1992, pp. 131-208.

Helmuth, R., "Alkali-Silica Reactivity: An Overview of Research," SHRP-C-342, National Research Council, Washington, DC, 1993, pp. 1-11.

Heukamp, F. H.; Ulm, F. J.; and Germaine, J. T., "Poroplastic Properties of Calcium-Leached Cement-Based Materials," *Cement and Concrete Research*, V. 33, No. 8, 2003, pp. 1155-1173.

Hobbs, W., *Alkali-Silica Reaction in Concrete*, Telford, London, 1988.

Hudec, P. P., and Banahene, N. K., "Chemical Treatments and Admixtures for Controlling Alkali Reactivity," *Cement and Concrete Composites*, V. 15, No. 1-2, 1993, pp. 21-26.

Idir, R.; Cyr, M.; and Tagnit-Hamou, A., "Use of Fine glass as ASR Inhibitor in Glass Aggregate Mortars," *Construction and Building Materials*, V. 24, No. 7, 2010, pp. 1309-1312.

Ismail, Z. Z., and Al-Hashimi, E. A., "Recycling of Waste Glass as A Partial Replacement for Fine Aggregate in Concrete," *Waste Management*, V. 29, No. 2, 2009, pp. 655-659.

Jin, W.; Meyer, C.; and Baxter, S., "Glascrete"-Concrete with Glass Aggregate," *ACI Materials Journal*, V. 97, No. 2, 2000, pp. 208-213.

Kaplan, M. F., "Flexural and Compressive Strength of Concrete as Affected by the Properties of Coarse Aggregate," *ACI Journal* Proceedings, V. 55, 1959, pp. 1193-1207.

Kennedy, C. T., "The Design of Concrete Mixes," *ACI Journal* Proceedings, V. 36, No. 2, 1940, pp. 373-400.

Kou, S. C., and Poon, C. S., "Properties of Self-Compacting Concrete Prepared with Recycled Glass Aggregate," *Cement and Concrete Composites*, V. 31, No. 2, 2009, pp. 107-113.

Kumar, B.; Tike, G. K.; and Nanda, P. K., "Evaluation of Properties of High-Volume Fly-Ash Concrete for Pavements," *Journal of Materials in Civil Engineering*, V. 19, No. 10, 2007, pp. 906-911.

Limbachiya, M. C., "Bulk Engineering and Durability Properties of Washed Glass Sand Concrete," *Construction and Building Materials*, V. 23, No. 2, 2009, pp. 1078-1083.

Ling, T. C.; Poon, C. S.; and Kou, S. C., "Feasibility of Using Recycled Glass in Architectural Cement Mortar," *Cement and Concrete Composites*, V. 33, No. 8, 2011, pp. 848-854.

Mahboub, K. C.; Canler, J.; Rathbone, R.; Robl, T.; and Davis, B., "Pervious Concrete: Compaction and Aggregate Gradation," *ACI Materials Journal*, V. 106, No. 6, 2009, pp. 523-528.

Malhotra, V. M., "No-Fines Concrete – Its Properties and Applications," *ACI Journal* Proceedings, V. 73, No. 11, 1976, pp. 628-644.

Malhotra, V. M., "Making Concrete Greener with Fly Ash," *Concrete International*, V. 21, No. 5, 1999, pp. 61-66.

Malhotra, V. M., "High-Performance High-Volume Fly Ash Concrete," *Concrete International*, V. 24, No. 7, 2002, pp. 30-34.

Maraghechi, H.; Shafaatian, S. M. H.; Fischer, G.; and Rajabipour, F., "The Role of Residual Cracks on Alkali Reactivity of Recycled Glass Aggregates," *Cement and Concrete Composites*, V. 34, No. 1, 2012, pp. 41-47.

McCoy, W. J., and Caldwell, A. G., "New Approach to Inhibiting Alkali-Aggregate Expansion," *ACI Journal* Proceedings, V. 47, No. 5, 1951, pp. 693-706.

McLellan, G. W., and Shand, E. B., *Glass Engineering Handbook*, McGraw-Hill, New York, 1984.

Mehta, P. K., "Reducing the Environmental Impact of Concrete," *Concrete International*, V. 23, No. 10, 2001, pp. 61-66.

Mehta, P. K., "Greening of the Concrete Industry for Sustainable Development," *Concrete International*, V. 24, No. 7, 2002, pp. 23-28.

Mehta, P. K., and Monteiro, P. J. M.*; Concrete: Microstructure, Properties, and Materials*, third ed., McGraw-Hill, New York, 2006.

Meininger, R. C., "No-fines Pervious Concrete for Paving," *Concrete International*, V. 10, No. 8, 1998, pp. 20-27.

Meyer, C., and Baxter, S., *Use of Recycled Glass for Concrete Masonry Blocks*, Final Report to New York State Energy Research and Development Authority, Report No. 97-15, Albany, NY, 1997.

Meyer, C., and Baxter, S., *Use of Recycled Glass and Fly Ash for Precast Concrete*, Final Report to New York State Energy Research and Development Authority, Report No. 98-18, NY, 1998.

Meyer, C., "The Greening of the Concrete Industry," *Cement and Concrete Composites*, V. 31, No. 8, 2009, pp. 601-605.

Mindess, S.; Yong, J. F.; and Darwin, D., *Concrete*, 2nd edition, Prentice Hall, NJ, 2003.

Mitchell, L. D.; Beaudoin, J. J.; and Grattan-Bellew, P., "The Effects of Lithium Hydroxide Solution on Alkali Silica Reaction Gels Created with Opal," *Cement and Concrete Research*, V. 34, No. 4, 2004, pp. 641-649.

Monteiro, P. J. M.; Wang, K.; Sposito, G.; dos Santos, M. C.; de Andrade, W. P., "Influence of Mineral Admixtures on the Alkali-Aggregate Reaction," *Cement and Concrete Research*, V. 27, No. 12, 1997, pp. 1899-1909.

Monteiro, P. J. M.; Kirchheim, A. P.; Chae, S.; Fischer, P.; MacDowell, A. A.; Schaible, E.; and Wenk, H. R., "Characterizing the Nano and Micro Structure of Concrete to Improve Its Durability," *Cement and Concrete Composites*, V. 31, No. 8, 2009, pp. 577-584.

Naik, T., "Greener Concrete Using Recycled Materials," *Concrete International*, V. 24, No. 7, 2002, pp. 45-49.

Neville, A. M., *Properties of Concrete*, 4th edition, Longman, London, 1995.

NT BUILD 492, *Concrete, Mortar and Cement-Based Repair Materials: Chloride Migration Coefficient from Non-Steady-State Migration Experiments*, NORDTEST, Espoo, 1999, 8 pp.

Ostertage, C. P.; Yi, C.; and Monteiro, P. J. M., "Effect of Confinement on Properties and Characteristics of Alkali-Silica Reaction Gel," *ACI Materials Journal*, V. 104, No. 3, 2007, pp. 276-282.

Ozkan, O., and Yuksel, I., "Studies on Mortars Containing Waste Bottle Glass and Industrial By-Products," *Construction and Building Materials*, V. 22, No. 6, 2008, pp. 1288-1298.

Park, S. B., and Lee, B., "Studies on Expansion Properties in Mortar Containing with Waste Glass and Fibers," *Cement and Concrete Research*, V. 34, No. 7, 2004, pp. 1145-1152.

Park, S. B.; Lee, B. C.; and Kim, J. H., "Studies on Mechanical Properties of Concrete Containing Waste Glass Aggregate," *Cement and Concrete Research*, V. 34, No. 12, 2004, pp. 2181-2189.

Powers, T. C., *The Properties of Fresh Concrete*, John Wiley & Sons, New York, 1968.

Prezzi, M.; Monteiro, P. J. M.; and Sposito, G., "The Alkali-Silica Reaction, Part I: Use of the Double-Layer Theory to Explain the Behavior of Reaction-Product Gels," *ACI Materials Journal*, V. 94, No. 1, 1997, pp. 10-17.

Prezzi, M.; Monteiro, P. J. M.; and Sposito, G., "Alkali-Silica Reaction – Part 2: The Effect of Chemical Admixtures," *ACI Materials Journal*, V. 95, No. 1, 1998, pp. 3-10.

Ranc, R.; Isabelle, H.; Clement, J. Y.; and Sorrentino, D., "Limits of Application of the ASTM C 227 Mortar Bar Test. Comparison with Two Other Standards on Alkali Aggregate Reactivity," *Cement, Concrete and Aggregate*, V. 16, No. 1, 1994, pp. 63-72.

Rajabipour, F.; Maraghechi, H.; and Fischer, G., "Investigating the Alkali Silica Reaction of Recycled Glass Aggregates in Concrete Materials," *Journal of Materials in Civil Engineering*, V.22, No. 12, 2010, pp. 1201-1208.

Reinhardt, H.-W., and Jooss, M., "Permeability and Self-Healing of Cracked Concrete as A Function of Temperature and Crack Width," *Cement and Concrete Research*, V. 33. No. 7, 2003, pp. 981-985.

Richardson, I. G., "Tobermorite/Jennite- and Tobermorite/Calcium Hydroxide-based Models for the Structure of C-S-H: Applicability to Hardened Pastes of Tricalcium Silicate, β-Dicalcium Silicate, Portland Cement, and Blends of Portland Cement with Blast-Furnace Slag, Metakaolin, or Silica Fume," *Cement and Concrete Research*, V. 34, No. 9, 2004, pp. 1733-1777.

RILEM TC 106-AAR, "Recommendations of RILEM TC 106-AAR: Alkali Aggregate Reaction A. TC 106-2 - Detection of Potential Alkali-Reactivity of Aggregates – The Ultra-Accelerated Mortar-Bar Test B. TC 106-3 - Detection of Potential Alkali-Reactivity of Aggregates- Method for Aggregate Combinations Using Concrete Prisms," *Materials and Structures*, V. 33, No. 229, 2000, pp. 283-293.

Rogers, C.; Thomas, M. D. A.; and Hooton, R. D., "Prevention of Damage due to Alkali-Aggregate Reaction (AAR) in Concrete Construction-Canadian Approach," *Cement, Concrete and Aggregate*, V.19, No. 1, 1997, pp. 26-32.

Saccani, A., and Bignozzi, M. C., "ASR Expansion Behavior of Recycled Glass Fine Aggregates in Concrete," *Cement and Concrete Research*, V. 40, No. 4, 2010, pp. 531-536.

Sahmaran, M.; Li, V. C.; and Andrade, C., "Corrosion Resistance Performance of Steel-Reinforced Engineered Cementitious Composite Beams," *ACI Materials Journal*, V. 105, No. 3, 2008, pp. 243-250.

Scanlon, J. M., and Sherman, M. R., "Fly Ash Concrete: An Evaluation of Chloride Penetration Test Method," *Concrete International*, V. 18, No. 6, 1996, pp. 57-62.

Schaefer, V. R.; Wang, K.; Suleiman, M. T.; and Keveern, J. T., *Mix Design Development for Pervious Concrete in Cold Weather Climates*, Final Report, Report 2006-1, National Concrete Pavement Technology, Feb. 2006, 67 pp.

Schmidt, A., and Saia, W. H. F., "Alkali-aggregate Reaction Tests on Glass Used for Exposed Aggregate Wall Panel Work," *ACI Materials Journal*, V. 60, 1963, pp. 1235-1236.

Scholze, H., *Glass: Nature, Structure, and Properties*, Springer-Verlag, NY, 1990.

Shao, Y.; Lefor, T.; Moras, S.; and Rodriguez, D., "Studies on Concrete Containing Ground Waste Glass," *Cement and Concrete Research*, V. 30, No. 1, 2000, pp. 91-100.

Shayan, A., and Xu, A., "Value-Added Utilisation of Waste Glass in Concrete," *Cement and Concrete Research,* V. 34, No. 5, 2004, pp. 81-89.

Shi, C., "Effect of Mixing Proportions of Concrete on Its Electrical Conductivity and the Rapid Chloride Permeability Test (ASTM C1202 or AASHTO T277) Results," *Cement and Concrete Research*, V. 34, No. 3, 2004, pp. 537-545.

Shi, C.; Wu, Y.; Riefler, C.; and Wang, H., "Characteristics and Pozzolanic Reactivity of Glass Powders," *Cement and Concrete Research*, V. 35, No. 5, 2005, pp. 987-993.

Shi, C., and Zheng, K., "A Review on the Use of Waste Glasses in the Production of Cement and Concrete," *Resource, Conservation and Recycling*, V. 52, No. 2, 2007, pp. 234-247.

Shi, C., "Corrosion of Glasses and Expansion Mechanism of Concrete Containing Waste Glasses as Aggregates," *Journal of Materials in Civil Engineering*, V. 21, No. 10, 2009, pp. 529-534.

Siddique, R., "Performance Characteristics of High-Volume Class F Fly Ash Concrete," *Cement and Concrete Research,* V. 34, No. 3, 2004, pp. 487-493.

Siddique, R., *Waste Materials and By-Products in Concrete*, Springer, Berlin, 2008.

Stark, D. C., "Lithium Salt Admixtures – An Alternative Method to Prevent Expansive Alkali-Silica Reactivity," In: *Proceedings of the 9th International Conference on Alkali-Aggregate Reaction in Concrete*, London, 1992, pp. 1-7.

Stark, D.; Morgan, B.; and Okamoto, P., *Eliminating or Minimizing Alkali-Silica Reactivity*, National Research Council, Washington, D.C., 1993, pp. 75-93.

Sumanasooriya, M. S.; Bentz, D. P.; and Neithalath, N., "Planar Image-Based Reconstruction of Pervious Concrete Pore Structure and Permeability Prediction," *ACI Materials Journal*, V.107, No. 4, 2010, pp. 413-421.

Suwito, A.; Jin, W.; Xi, Y.; and Meyer, C., "A Mathematical Model for the Pessimum Size Effect of ASR in Concrete," *Concrete Science and Engineering (RILEM)*, V. 4, No. 13, 2002, pp. 23-34.

Swamy, R. N., and Al-Asali, M. M., "Engineering Properties of Concrete Affected by Alkali-Silica Reaction," *ACI Materials Journal*, V. 85, No. 5, 1988, pp. 367-374.

Taha, B., and Nounu, G., "Properties of Concrete Contains Mixed Colour Waste Recycled Glass as Sand and Cement Replacement," *Construction and Building Materials*, V. 22, No. 5, 2008, pp. 713-720.

Taha, B., and Nounu, G., "Utilizing Waste Recycled Glass as Sand/Cement Replacement in Concrete," *Journal of Materials in Civil Engineering*, V. 21, No. 12, 2009, pp. 709-721.

Tang, M. H.; Xu, Z.; and Han, S., "Alkali-Reactivity of Glass Aggregate," *Durability of Building Materials*, V. 4, No. 4, 1987, pp. 377-385.

Termkhajornkit, P.; Nawa, T.; Yamashiro, Y.; and Saito, T., "Self-Healing Ability of Fly Ash-Cement Systems," *Cement and Concrete Composites*, V. 31, No. 3, 2009, pp. 195-203.

Terro, M. J., "Properties of Concrete Made with Recycled Crushed Glass at Elevated Temperatures," *Building and Environment*, V. 41, No. 5, 2006, pp. 633-639.

Thomas, M. D. A, and Innis, F. A., "Use of the Accelerate Mortar Bar Test for Evaluating the Efficacy of Mineral Admixtures for Controlling Expansion due to Alkali-Silica Reaction," *Cement, Concrete and Aggregates*, V. 21, No. 2, 1999, pp. 157-164.

Thomas, M. D. A.; Fournier, B.; Folliard, K. J.; Ideker, J. H.; and Shehata, M., *Test Methods for Evaluating Preventive Measures for Controlling Expansive due to Alkali-Silica Reaction in Concrete*, Report No. ICAR 302-1, International Center for Aggregates Research, US, 2006, 57 pp.

Thomas, M. D. A.; Fournier, B.; Folliard, K. J.; Ideker, J. H.; and Rescendez, Y., *The Use of Lithium to Prevent or Mitigate Alkali-Silica Reaction in Concrete Pavement and Structures*, Report No. FHWA-HRT-06-133, Department of Transportation, US, 2007a.

Thomas, M. D. A.; Fournier, B.; Folliard, K. J.; Shehata, M. H.; Ideker, J. H.; and Rogers, C., "Performance Limits for Evaluating Supplementary Cementing Materials Using Accelerated Mortar Bar Test," *ACI Materials Journal*, V. 104, No. 2, 2007b, pp. 115-122.

Topcu, I. B., and Canbaz, M., "Properties of Concrete Containing Waste Glass," *Cement and Concrete Research,* V. 34, No. 2, 2004, pp. 267-274.

Topcu, I. B.; Boga, A. R.; and Bilir, T., "Alkali-Silica Reactions of Mortars Produced by Using Waste Glass as Fine Aggregate and Admixtures such as Fly Ash and Li_2CO_3," *Waste Management*, V. 28, No. 5, 2008, pp. 878-884.

Turanli, L.; Bektas, F.; and Monteiro, P. J. M., "Use of Ground Clay Brick as A Pozzolanic Material to Reduce the Alkali-Silica Reaction," *Cement and Concrete Research*, V. 33, No. 10, 2003, pp. 1539-1542.

Turanli, L.; Shomglin, K.; Ostertag, C. P.; and Monteiro, P. J. M., "Reduction in Alkali-Silica Expansion Due to Steel Microfibers," *Cement and Concrete Research*, V. 31, No. 5, 2001, pp. 825-827.

United Nations, *Report of the World Commission on Environment and Development*, Brundtland Commission, Brundtland, 1987.

Villalobos, S.; Lange, D. A.; and Roesler, J. R., *Evaluation, Testing and Comparison between Crushed Manufactured Sand and Natural Sand*, Technical Note, University of Illinois, Department of Civil & Environmental Engineering, Urbana, IL, 2005.

Wang, H., "A Study of the Effects of LCD Glass Sand on the Properties of Concrete," *Waste Management,* V. 29, No. 1, 2009, 335-341.

Wee, T. H.; Suryavanshi, A. K.; and Tin, S. S., "Evaluation of Rapid Chloride Permeability Test (RCPT) Results for Concrete Containing Mineral Admixtures," *ACI Materials Journal*, V. 97, No. 2, 2000, pp. 221-232.

Wigum, B. J., and Danielsen, S. W., *Production and Utilisation of Manufactured Sand*, COIN Project Report 12-2009, SINTEF Building and Infrastructure, Oslo, 2009.

Xie, Z., and Xi, Y., "Use of Recycled Glass as A Raw Material in the Manufacture of Portland Cement," *Materials and Structures*, V. 35, No. 8, 2002, pp. 510-515.

Xie, Z.; Xiang, W.; and Xi, Y., "ASR Potentials of Glass Aggregates in Water-Glass Activated Fly Ash and Portland Cement Mortars," *Journal of Materials in Civil Engineering*, V. 15, No. 1, 2003, pp 67-74.

Xu, G. J. Z.; Watt, D. F.; and Hudec, P. P., "Effectiveness of Mineral Admixtures in Reducing ASR Expansion," *Cement and Concrete Research*, V. 25, No. 6, 1995, pp. 1225-1236.

Yamada, K., and Ishiyama, S., *Maximum Dosage of Glass Cullet as Fine Aggregate Mortar*, London: Thomas Telford, 2005.

Yang, C. C.; Huang, R.; Yeih, W.; and Sue, I. C., "Aggregate Effect on Elastic Moduli of Cement-Based Composite Materials," *Journal of Marine Science and Technology*, V. 3, No. 1, 1995, pp. 5-10.

Yang, J., and Jiang, G., "Experimental Study on Properties of Pervious Concrete Pavement Materials," *Cement and Concrete Research*, V. 33, No. 3, 2003, pp. 381-386.

Yi, C. K., and Osertag, C. P., "Mechanical Approach in Mitigating Alkali-Silica Reaction," *Cement and Concrete Research*, V. 35, No. 1, 2005, pp. 67-75.

Yuksel, I.; Ozkan, O.; and Bilir, T., "Use of Granulated Blast-Furnace Slag in Concrete as Fine Aggregate," *ACI Materials Journal*, V. 103, No. 3, 2006, pp. 203-208.

Yuksel, I., and Genc, A., "Properties of Concrete Containing Nonground Ash and Slag as Fine Aggregate," *ACI Materials Journal*, V. 104, No. 4, 2007, pp. 397-403.

Zhu, H., and Byars, E. A., "Alkali-Silica Reaction of Recycled Glass in Concrete," In: *12th International Conference on Concrete Alkali Aggregate Reactions (ICAAR)*, Beijing, China, 2004, pp. 811-820.

Zhu, H.; Chen, W.; Zhou, W.; and Byars, E. A., "Expansion Behaviour of Glass Aggregates in Different Testing for Alkali-Silica Reactivity," *Materials and Structures*, V. 42, No. 4, 2009, pp. 485-494.